University of Cincinnati

Date: 5/23/2019

I, Katelyn M Melgar, hereby submit this original work as part of the requirements for the degree of Doctor of Philosophy in Immunology.

It is entitled:

A polypharmacologic strategy for overcoming adaptive therapy resistance in AML by targeting immune stress response pathways

Student's name: **Katelyn M Melgar**

This work and its defense approved by:

Committee chair: Daniel Starczynowski, Ph.D.

Committee member: H. Leighton Grimes, Ph.D.

Committee member: Ashish Kumar, M.D.

Committee member: Chandrashekhar Pasare

Committee member: William Seibel, Ph.D.

34154

A polypharmacologic strategy to overcome adaptive therapy resistance in AML by targeting immune stress response pathways

A dissertation submitted to the
Graduate School
of the University of Cincinnati
in partial fulfillment of the
requirements to the degree of

Doctor of Philosophy

In the Department of Immunology of the
College of Medicine

By

Katelyn Michelle Melgar

Dissertation Committee:
Daniel T. Starczynowski, PhD (Chair)
H. Leighton Grimes, PhD
Ashish Kumar, MD, PhD
Chandrashekhar Pasare, DVM, PhD
William Seibel, PhD

Abstract

Targeted inhibitors to oncogenic kinases demonstrate encouraging clinical responses early in the treatment course, however most patients will relapse due to target-dependent mechanisms that mitigate enzyme-inhibitor binding, or through target-independent mechanisms, such as alternate activation of survival and proliferation pathways, known as adaptive resistance. Here we describe mechanisms of adaptive resistance in FLT3 mutant acute myeloid leukemia (AML) by examining integrative in-cell kinase and gene regulatory network responses after oncogenic signaling blockade by FLT3 inhibitors (FLT3i). We identified activation of innate immune stress response pathways after treatment of FLT3-mutant AML cells with FLT3i and showed that innate immune pathway activation via the IRAK1/4 kinase complex contributes to adaptive resistance in FLT3-mutant AML cells. To overcome this acute adaptive resistance mechanism, we developed a small molecule that simultaneously inhibits FLT3 and IRAK1/4 kinases. The multi-kinase FLT3-IRAK1/4 inhibitor eliminated adaptively resistant FLT3-ITD AML cells in vitro and in vivo, and displayed superior efficacy as compared to current targeted FLT3 therapies. These findings uncover a polypharmacologic strategy for overcoming adaptive resistance to therapy in AML by targeting immune stress response pathways.

Preface

The work presented in this dissertation will be published in *Science Translational Medicine*

Melgar, K., Walker, M., Jones, L.M., Bolanos, L.C., Hueneman, K., Wunderlich, M., Jiang, J.K., Wilson, K., Zhang, X., Sutter, P., Wang, A., Xu, X., Choi, K., Tawa, G., Lorimer, D., Abendroth, J., O'Brien, E., Hoyt, S.B., Famulare, C.A., Mulloy, J.C., Levine, R., Perentesis, J.P., Thomas, C.J., Starczynowski, D.T. "Overcoming adaptive therapy resistance in AML by targeting immune response pathways."

Acknowledgements

I would first like to thank Dan for being an incredible mentor over the last 5 years. He has helped me grow tremendously as a scientist. I know his invaluable advice will help guide me for the rest of my career. I would also like to thank my committee for their insights and support. Additionally, I would like to extend a huge thank you to Craig Thomas and his team at NCATS for all of their outstanding contributions to this project, particularly the medicinal chemistry. They have been a joy to collaborate with. Next, this PhD process would not have been anywhere near as fun if not for the amazing “Star Lab”. Every single person in the lab is not merely a co-worker, but a friend. This group is unbelievably fun and supportive; they have set the bar impossibly high for my future work-places. They are truly stars. I’d also like to thank my friends and Eric for the many adventures, laughs, and love. Finally, I’d like to thank my family, Mom, Dad, Jen, and Chris, for always being there for me and making me feel at home even though I’m far away.

Table of Contents

List of Figures and Tables

Chapter 1

Chapter 2

Chapter 3

Chapter 1: Background and Introduction

Acute myeloid leukemia

Overview and classification

Acute myeloid leukemia (AML) is defined by the World Health Organization (WHO) as a disease of clonal expansion of myeloid blasts in the peripheral blood, bone marrow or other tissue with a blast percentage of at least 20% *(1)*. The worldwide incidence is 2.5 to 3 per 100,000 people per year and in the United States the incidence was reported to be 4.3 per 100,000 between 2011 and 2015 *(1, 2)*. The median age at diagnosis for AML is 65 years old and has a slight male predominance (1.4:1 male:female) *(1, 2)*. AMLs can arise de novo, as a transformation of a chronic hematopoietic disease such as Chronic Myeloid Leukemia (CML) or Myelodysplastic Syndrome (MDS), or can be a sequelae of previous therapy such as radiation or chemotherapy. AMLs are further classified by the WHO by various genetic and morphological abnormalities (**Table 1.1**). Genetic changes typically include both a mutation that blocks myeloid differentiation as well as a mutation that provides a survival and/or proliferative advantage *(1)*. The overall 5-year survival from 2008-2014 in the United States was 27.4%; however the survival rates between the various genetic subtypes are very variable *(2)*.

Another method of classifying AMLs is using the French-American-British (FAB) system which groups AMLs into eight classes (**Table 1.2**). This system is primarily based on cell morphology and flow cytometric markers. However, the simplicity of this system does not take into account prognostic factors thus the WHO classification system is more widely used.

Table 1.1: WHO Acute Myeloid Leukemia Subtypes *(3, 4)*.

AML Class	Subtype
Acute myeloid leukemia with recurrent genetic abnormalities	t(8;21)(q22;q22); Runx1-Runx1t1
	inv(16)(p13.1q22) or t(16:16)(p13.1;q22); CBFB-MYH11
	t(15;17)(q22;q12); PML-RARA
	t(9;11)(p22;q23); MLLT3-KMT2A
	t(6;9)(p23;q34); DEK-NUP214
	inv(3)(q21q26.2) or t(3;3)(q21;q26.2); RPN1-EVI1
	Megakaryoblastic with t(1;22)(p13;q13); RBM15-MKL1
	Mutated NPM1
	Mutated CEBPA
	BCR-ABL1
Acute myeloid leukemia with myelodysplasia-related changes	
Therapy-related myeloid neoplasms	
Acute myeloid leukemia, not otherwise specified (NOS)	With minimal differentiation
	Without maturation
	With maturation
	Acute myelomonocytic leukemia
	Acute monoblastic/monocytic leukemia
	Acute erythroid leukemia
	Acute megakaryoblastic leukemia
	Acute basophilic leukemia
	Acute basophilic leukemia
	Acute panmyelosis with myelofibrosis

Table 1.2: FAB AML Subtypes

FAB Subtype	Name
M0	Undifferentiatied acute myeloblastic leukemia
M1	Acute myeloblastic leukemia with minimal maturation
M2	Acute myeloblastic leukemia with maturation
M3	Acute promyelocytic leukemia
M4	Acute myelomonocytic leukemia
M4 eos	Acute myelomonocytic leukemia with eosinophils
M5	Acute monocytic leukemia
M6	Acute erythroid leukemia
M7	Acute megakaryoblastic leukemia

Genetics

AMLs typically require two mutations: one that blocks a step of myeloid differentiation and one that provides a survival or proliferation advantage. In addition to determining the subtype of AML, the genetic profile of an AML plays a large role in the prognosis and therapeutic strategy. Chromosomal abnormalities are very common in AML, present in about 60% of AML patients at diagnosis *(5, 6)*. Additionally, the presence of one of following three chromosomal rearrangements alone is enough to make a diagnosis of AML even if the blast count is below 20%: t(15;17), t(8;21), or inv(16) *(1)*. These are the most commonly found chromosomal abnormalities in AML, with each found in 5-15% of AML cases *(5–7)*. In addition to chromosomal changes, mutations in individual genes also contribute to patient prognosis and direction of treatment.

Although many factors contribute to prognosis, including patient age and comorbidities, genetic changes are the strongest indicators of prognosis. Table 1.3 lists genetic alterations that are associated with a poor prognosis in AML patients and have a frequency of >5% in de novo AML cases.

Table 1.3: Genetic alterations in AML with an unfavorable prognosis and a frequency of greater than 5%. Adapted from *The 2016 revision to the World Health Organization classification of myeloid neoplasms and acute leukemia* (Blood 2016) and *The Cancer Genome Atlas Research Network: Genomic and epigenomic landscapes of adult de novo AML* (NEJM 2013) *(4, 8)*.

Genetic Alteration	Frequency in TCGA de Novo AMLs	Additional factors required for poor prognosis	Functional class
FLT3-ITD	28%		Receptor tyrosine kinase
DNMT3A	26%	Normal karyotype	Epigenetic modification
IDH1 or IDH2	20%		Metabolism/epigenetic modification
RUNX1	10%		Transcription factor
TET2	8%	Normal karyotype	Epigenetic modification
TP53	8%	Complex karyotype (>= 3 abnormalities) or abnormalities in chromosomes 5, 7, or 17	Cell cycle
CEBPA	6%	Single allelic	Transcription factor
WT1	6%		Transcription factor

Treatment strategies

Induction Chemotherapy:

The traditional standard of care for AML is the "7 + 3" induction regimen which consists of 7 days of continuous intravenous cytarabine (araC) at 100 or 200 mg/m^2 per day along with single i.v. infusions of daunorubicin at 60 mg/m^2 on days 1 through 3, though doses may vary between instititutions *(9, 10)*. Both compounds work to inhibit cell cycling: Cytarabine is a pyrimidine analog that inhibits DNA synthesis and daunorubicin is an anthracycline antibiotic that inhibits topoisomerase *(11, 12)*. More recently, an alternative standard of care has been growing in popularity which combines high-dose araC (HiDAC; >1000 mg/m^2) with 2-3 nucleoside analogues *(13)*. The rational for this approach was that the efficacy of araC depends on its intracellular metabolism to ara-CTP. The presence of purine nucleoside analogues, such as cladrabine or fludarabine, inhibit ribonucleoside reductase, thus limiting dNTP production and increasing incorporation of ara-CTP *(13)*. Several clinical trials have shown an improved complete remission (CR) for patients receiving HiDAC with nucleoside doublets compared to the 7+3 regimen, however debate over the appropriate patient populations for each treatment regimen remains *(13–17)*. Many factors contribute to an individual's response to induction therapy, but overall the CR for induction therapy is 40-60%. Therefore, the main goal of induction therapy is to reduce the bulk leukemia population while physicians either wait for genetic profiling results which will direct more targeted therapy, or to prepare patients for allogeneic hematopoietic stem cell transplantation (HSCT) *(10)*.

Targeted therapy:

All-trans retinoic acid/arsenic trioxide

One of the first and most effective examples of targeted therapy in AML is all-trans retinoic acid (ATRA) and arsenic trioxide (ATO) to treat t(15;17) acute promyelocytic leukemia (APML). The t(15;17) translocation creates a fusion protein of promyelocytic leukemia (PML) and the

retinoic acid receptor α (RARα) which acts as a dominant negative block on differentiation *(18)*. APML patients treated with chemotherapy alone had a CR of 75-80% but the median remission was only 1-2 years and patients also suffered from chemotherapy-related morbidity and mortality *(19)*. ATRA/ATO act on the PML-ATRA fusion protein to lift the differentiation block. The introduction of these therapies into the clinic resulted in a dramatic increase in CR and 5-year disease free survival (both >90%) *(19)*. APML went from a fatal diagnosis to a very treatable disease because of this targeted treatment strategy.

Kinase Inhibitors

The amazing success of imatinib in treating BCR-ABL chronic myeloid leukemia (CML) has spawned a huge effort to develop targeted kinase inhibitors based on individualized patient genetics in many diseases. The more complicated genetic background of AMLs compared to CML has made finding an effective target in AML more complicated; however, significant advances have been made in the field in the last decade. FLT3 inhibitors are probably the class with the most progress in AML; they will be reviewed in detail in the next section.

Another target of interest is MAPK/ERK Kinase (MEK). Preclinical studies have shown activation of the mitogen activated protein kinase (MAPK) pathway in a variety of AMLs, particularly in those with aberrant RAS activation *(20, 21)*. Although MEK inhibitors have had efficacy in preclinical models, translation to clinical studies as single agents or in combination with chemotherapy has not matched expectations and several trials have been terminated due to lack of efficacy (NCT00957580, NCT01907815) *(22–26)*.

Another pathway of interest is the PI3K/AKT/mTOR pathway, which, like the MAPK pathway, shows increased activation in many AMLs and is important for leukemic cell survival *(27, 28)*. Preclinical studies of PI3K/AKT/mTOR inhibitors are promising, showing significant induction of apoptosis in vitro and prolonged cell survival in murine xenograft models *(29–32)*.

Multiple clinical trials for various PI3K/AKT/mTOR inhibitors are on-going and results have not been posted yet for most (NCT00710528, NCT01396499, NCT01756118). Unfortunately, two studies have been terminated for lack of efficacy (NCT02438761 and NCT01253447) *(33)*.

Cyclin-dependent kinase (CDKs) inhibitors are another growing class of compounds. CDKs regulate cell cycle progression and gene transcription and can be dysregulated in AML *(34–36)*. A number of CDK inhibitors have been evaluated in preclinical and clinical studies with a focus on CDK4, 6 and 9 *(34, 37–41)*. Because CDKs have a highly conserved ATP-binding pocket, most CDK inhibitors are not very selective for individual CDKs, but they can have slight differences in IC50 between them *(41)*. As certain CDKs are involved in cell cycle and others are involved in transcription, CDK inhibitors can have different or multiple mechanisms of action for cell death depending on which CDKs they target *(41)*. There has been some progress in moving CDK inhibitors into the clinic. A phase 2 randomized clinical trial of flavopiradol in combination with Ara-C induction showed an increase in CR, though the study was not large enough to detect a difference in overall survival *(42)*. Phase 1/2 studies of other CDK inhibitors, palbociclib (CDK4/6) and AZD4573, in relapsed/refractory AML are ongoing (NCT02310243, NCT03844997, NCT03263637).

Unfortunately, a common theme between all the kinase inhibitors seems to be effective preclinical studies followed by underwhelming clinical results highlighting the complex nature of AML *in vivo*.

Epigenetic modulators

As noted in **Table 1.3**, several of the most commonly mutated genes with poor prognosis in AML have a functional role in epigenetic modification. Thus, in recent years, compounds that inhibit the proteins responsible for these aberrant epigenetic changes have been developed. Inhibitors of several methyltransferases, such as mixed lineage leukemia (MLL) fusion products,

G9A/KMT1C, EZH2, and DOT1L, have shown efficacy against AML in preclinical studies *(43–49)*. EZH2 inhibitors are currently being studied in clinical trials of lymphoma but have yet to be applied to AML. The DOT1L inhibitor, pinometostat (EPZ-5676) has completed a phase I clinical trial in MLL-rearranged AML (NCT02141828, results not yet posted) and a phase 1b/2 study of pinometostat in combination with chemotherapy is currently enrolling (NCT03724084).

Alternatively, histone deacetaylases (HDAC) have been studied as therapeutic targets as well. In addition to inducing epigenetic modifications through their activity on histones, HDAC inhibitors also have antileukemic activity by preventing deacetylation of non-histone proteins such as HSP90 and by stimulating the immune reponse *(50–52)*. Vorinostat, romidepsin, and belinostat have been approved for T-cell lymphoma, and panabinostat has been approved for multiple myeloma. Belinostat, vorinostat, panobinostat, and entinostat are currently being investigated in multiple phase I and phase II clinical trials of AML, however the results that have been published so far have been underwhelming (NCT02381548, NCT00357032, NCT00878722, NCT01550224, NCT00656617, NCT01242774, NCT01463046, NCT00946647, NCT01305499, NCT01159301, NCT00015925).

A third approach to epigenetic modification is through IDH1/2 inhibitors in cancers with IDH1/2 mutations. IDH1/2 normally operate in the citric acid cycle to convert isocitrate to α-ketoglutarate (α-KG). Mutant IDH1/2 instead produce the oncometabolite 2-hydroxyglutarate (2-HG). TET2 is dependent on α-KG, therefore the accumulation of 2-HG inhibits TET2 demethylation activity and results in a differentiation block *(53, 54)*. Two IDH inhibitors were FDA-approved in recent years for relapsed/refractory AML. Enasidanib (AG-221), an IDH2 inhibitor, was FDA-approved in 2017 and several clinical studies are currently examining its use in newly diagnosed AML or other hematopoietic malignancies and in combination with various chemotherapy regimens (NCT01915498, NCT03173248, NCT02632708, NCT02677922, NCT02577406, NCT03839771) *(55)*. Similarly, ivosidenib (AG-120) is an IDH1 inhibitor that was

FDA-approved in 2018 for relapsed/refractory IDH1-mutant AML and several studies are ongoing to expand access to other patient populations and in combination with chemotherapy (NCT03245424, NCT02632708, NCT02677922, NCT03839771) *(56)*.

Pro-apoptotic agents

Another common class of genetic alterations in cancer in general is an imbalance between pro- and anti-apoptotic signaling that favors anti-apoptotic signals and thus maintains survival in cancer cells. B-cell lymphoma 2 (BCL-2) is an anti-apoptotic protein that is particularly important for normal hematopoietic cell survival and its overexpression has been implicated in chemoresistance in AML *(57, 58)*. Venetoclax (ABT-199) is an antagonist of BCL-2 and was FDA-approved in 2018 for AML in combination with low-dose chemotherapy in adults over 75 years old whose comorbidities preclude them from high-dose induction therapy *(59)*. This approval was partially based on the phase 1 clinical trial in which it was found that addition of venetoclax to induction therapy in older patients had a CR of 60%, which is a significant increase over previous studies which have shown a CR of 10-50% for older patients with azacytidine or decitabine monotherapy (NCT02203773) *(60)*.

Immune Therapies

Another treatment strategy to manipulate the immune system to direct an anti-tumor immune response. One method is monoclonal antibodies or bispecific T-cell engagers (BiTEs) against myeloid surface antigens such as CD33 and the interleukin-3 receptor alpha (CD123). AMLs have shown overexpression of CD33 and CD123 compared to normal hematopoietic progenitors, therefore they present targets that are relatively leukemia-specific *(61–63)*. The antibodies are conjugated to DNA-damaging agents such as an antibiotic or a DNA cross-linker resulting in cell death when the antibody is internalized *(64, 65)*. Gemtuzumab ozogamicin, a

CD33 antibody conjugated to the antibiotic calicheamicin, received FDA approval for relapsed/refractory AML in 2000 and then approval was expanded to newly diagnosed and pediatric patients (> 2 years old) in 2017. Gemtuzumab has seen the greatest benefit in patients who are not fit for chemotherapy: In several phase 2 trials of relapsed patients older than 60 years and ineligible for chemotherapy, there was a CR of about 30% and in a phase 2 trial of older patients ineligible for chemotherapy, there was a roughly 5 week improvement in overall survival compared to supportive care *(66–68)*. Multiple anti-CD123 antibodies are in development and a few phase I trials in AML are ongoing, however results have not been released yet *(69–71)*.

In a variation on traditional antibodies, BiTEs consist of two variable domains from different monoclonal antibodies linked together: one side binds CD3 and the other binds the tumor antigen of choice *(72)*. The binding of a T-cell to a tumor cell in this manner activates a targeted anti-tumor t-cell response regardless of the T-cell's innate antigen specificity *(72)*. For applications to AML, BiTEs have been made with anti-CD33 (AMG-330) or anti-CD123 (XmAb14045 and JNJ-6309178) domains *(73–75)*. Phase I trials for each BiTE are ongoing in relapsed/refractory AML (NCT02520427, NCT02730312, NCT02715011) and preliminary results from the XmAb14045 trial showed a CR of 23% as of 2018 *(76)*.

An additional strategy to activate an anti-tumor T-cell response is through chimeric antigen receptor T cells (CARTs). CARTs are allogeneic or autologous T cells that have been genetically engineered to express a T-cell receptor (TCR) that recognizes a surface antigen of choice as well as costimulatory molecules to allow the CARTs to act independently of traditional immune activation mechanisms *(77)*. The CARTs are then adoptively transferred into the patient and are able to find and kill any cell expressing the target. CARTs using CD19 as a target have had great success in B-cell lymphoma and were recently FDA approved *(78)*. Because of the efficacy of the CARTs eradicating any cell expressing the target antigen, if the target antigen is expressed on normal cells they must be an expendable population. Therefore, applications to AML have been difficult because AML protein expression is largely shared by hematopoietic stem and progenitor

cells which are necessary for survival *(79)*. CD33 and CD123 are being investigated as potential targets, however they both come with significant risk for myeloablation as well as on-target/off-tumor toxicity of endothelial cells (CD123) or hepatic cells (CD33) *(79–81)*. Despite these complications, several clinical trials are ongoing with CD123 and CD33 CARTs (NCT03126864, NCT03190278, NCT03473457). Additionally the search for better AML-specific targets is on-going, including one clinical trial investigating FLT3 CARTs in FLT3-mutant AML (NCT03904069) *(82–85)*.

The immune system has many mechanisms in place to limit inappropriate immune activation to promote self-tolerance and attenuate collateral damage of surrounding tissue. Cancers often take advantage of these pathways to protect themselves from anti-tumor immune responses. Therefore, another approach to immunotherapy is to inhibit the immune tolerance mechanisms employed by the cancer. These therapies, labeled checkpoint inhibitors, have had a lot of success in solid tumors and are now being studied in the context of hematologic neoplasms. Two of the most widely studied mechanisms are programmed cell death protein 1 (PD-1) and cytotoxic T-lymphocyte antigen 4 (CTLA-4). It has been shown across many different types of cancers, including AML, that cancer cells upregulate PD-1 surface expression which binds to PD-L1 on T-cells resulting in inhibition of T-cell activation *(86–88)*. Therefore, blocking the PD-1/PD-L1 interaction has been of great interest in the cancer research community and several blocking antibodies have been developed. The PD-1 inhibitors pembrolizumab and nivolumab have received FDA approval for a variety of solid tumors including non-small cell lung cancer (NSCLC), melanoma, renal cell carcinoma and lymphoma. Furthermore, pembrolizumab was recently designated as a first-line therapy in NSCLC. The application of these antibodies to AML are currently being investigated in multiple phase 1 and 2 clinical trials (NCT02845297, NCT02996474, NCT02708641, NCT02768792, NCT02532231, NCT02464657, NCT03417154, NCT02397720). CTLA-4 is expressed by T cells and inhibits T-cell activation by competing with

CD28 to bind the co-stimulator molecules CD80 and CD86 expressed by antigen presenting cells (APCs) *(89–91)*. While CD28:CD80/86 interaction promotes T-cell activation, CTLA-4:CD80/86 drives an inhibitory signal *(89–91)*. Ipilimumab, an anti-CTLA-4 antibody that blocks CTLA-4 from binding CD80/86, is FDA-approved for melanoma and is being tested in clinical trials for AML and other cancers (NCT01757639, NCT02890329). Although checkpoint inhibition seems to be a promising treatment strategy, there is a serious risk of potentially life-threatening autoimmunity against various organs because of the non-specific immune activation, particularly with CTLA-4 blockade more so than PD-1 blockade *(92, 93)*. Immune-related adverse events are very common, with rates usually around 25-50% but as high as 90% in some trials *(92)*. Therefore, patient fitness and ability of the medical team to manage autoimmune complications is an important consideration in deciding on checkpoint-inhibitor therapy.

Hematopoietic Stem Cell Transplantation (HSCT):

Ultimately, the treatment strategy with the best chance for preventing relapse is HSCT. HSCT involves conditioning the patient with cyclophosphamide and either busulfan or total body irradiation, followed by infusion of allogeneic HLA-matched donor HSCs, usually from a sibling *(94)*. In addition to replacing the diseased bone marrow, the donor graft also provides life-long anti-leukemic activity by surveilling for and killing remaining leukemic cells. However, there are limits to the availability and feasibility of HSCT in AML patients. For example, it can be difficult to find an HLA-matched donor. Additionally, because of the intensity of conditioning and the relatively high risk of treatment-related morbidities, such as graft-vs-host disease, HSCT is usually reserved for younger, fitter patients (<65 years old), although recent advancements in conditioning regimens have improved outcomes in older patients *(94–96)*. Furthermore, multiple studies have shown that HSCT provides a significant survival benefit for adverse and intermediate risk-groups, but not for patients with favorable cytogenetics (such as NPM1-mutant/FLT3-wild

type (WT)) *(97)*. Thus, development of alternative treatment strategies are needed for patients who would not benefit from HSCT.

FLT3-mutant Acute Myeloid Leukemia and Treatment Strategies

FLT3 Structure and Signaling

FLT3 is a transmembrane protein composed of an extracellular domain, a transmembrane helix, and an intracellular module. The intracellular module consists of the juxtamembranal domain, the kinase domain, and the C-terminal tail *(98)*. Glycosylation is required for targeting FLT3 to the extracellular membrane, where FLT3 ligand (FL) binds the extracellular domain of FLT3 *(99–101)*. Upon binding, the receptor dimerizes and the kinase domains autophosphorylate the JM segments, releasing the JM domain from its autoinhibitory conformation and stabilizing the active conformation *(98, 102)*. Once active, there is autophosphorylation of additional tyrosine residues which then serve to further stabilize the active conformation and also act as recruitment sites for downstream substrates, such as GRB2, SHC, and SHIP2 *(98, 102, 103)*. FLT3 activation plays a key role in normal hematopoietic development by promoting anti-apoptosis, pro-survival, and cell cycle pathways primarily via PI3K/AKT/mTOR, Ras, MAPK, and STAT pathways *(104)*.

FLT3 Mutations in AML

FLT3 mutations are one of the most common sites for mutation in AML and are associated with poor prognosis (**Table 1.3**). The most common type of FLT3 mutation is an internal tandem duplication (ITD) in the JM domain, occurring in roughly 25% of newly diagnosed adult AMLs and about 15% of pediatric AMLs *(8, 105–109)*. The ITDs in the JM domain prevent the protein from folding into its autoinhibitory conformation, resulting in constitutive activation *(98)*. The next most common class of FLT3 mutations are point mutations in the tyrosine kinase domain which occur in about 7% of AMLs *(105, 110, 111)*. These mutations typically occur at the D835 residue *(110,*

111). Rather than physically locking the protein in to its active state like the ITD mutations, these point mutations instead shift the equilibrium between active and inactive states toward the active state *(112)*.

In addition to an unregulated increase in normal FLT3 signaling (i.e. MAPK and PI3K/mTOR signaling), mutant FLT3 can aberrantly activate additional signaling pathways. Although wild-type and mutant FLT3 both result in STAT5 phosphorylation, only mutant FLT3 signaling induces phosphorylated STAT5 to bind to DNA *(113, 114)*. Furthermore, FLT3 overexpression can induce NFkB activity, providing an additional survival mechanism *(115, 116)*.

As FLT3 signaling promotes hematopoietic survival and proliferation, this mutation alone is not sufficient to induce leukemia, a second mutation blocking differentiation is required in combination, such as DNMT3a loss-of-function, or CEPBα, IDH1, or NPM1 mutations *(117–120)*.

Prognosis and Treatment of FLT3-mutant AML

In general, FLT3-ITD mutation confers a poor prognosis compared to wild-type FLT3. Multiple studies have demonstrated that FLT3-ITD AML patients have poorer CR, relapse rate (RR), and survival than FLT3-WT patients regardless of age: the overall survival ranges from 13-32% in FLT3-ITD patients compared to 44-50% in FLT3-WT patients *(106, 108, 121, 122)*. In addition to the presence of an ITD having prognostic significance, the characteristics of the ITD have prognostic significance as well. For example, the size of the duplication is a prognostic indicator *(107, 123)*. The ITDs typically occur in exons 14 and 15 and can range in size from a few nucleotides up to over 200 *(106–108, 123, 124)*. One study looking at the ITD size in 151 AML patients found that those with ITDs larger than 40 nucleotides had poorer CR (37%) and estimated 5-year survival (5YS) (13%) than patients with smaller ITDs (1-30 nucleotides) (CR 67%; 5YS 26%) or ITD-negative (CR 52%; 5YS 21%) *(123)*. Additionally, allelic burden is a significant prognostic factor. AML patients with a high ratio of FLT3-ITD compared to FLT3-WT have a significantly worse 5YS, disease-free survival, and RR compared to those with a low ratio

(107). This effect is further exaggerated when expression of FLT3-WT completely lost, with the median disease-free survival reaching as low as 4 months in those patients *(109)*.

With the strong prognostic significance of FLT3-ITD, high incidence in AML, as well as its inherent druggability as a tyrosine kinase, FLT3 has been extensively studied as a therapeutic target. All FLT3 inhibitors developed so far have been small molecules that competitively bind in the ATP binding pocket of FLT3 which contains a conserved Asp-Phe-Gly (DFG motif) that is flipped in or out depending on the active state of the kinase *(125)*. ATP-competitive kinase inhibitors are separated into two classes: type 1 and type 2. Type 1 inhibitors bind to the DFG-IN conformation, therefore binding preferentially to the active kinase. Type 2 inhibitors are the opposite, they bind the DFG-OUT conformation found in the inactive form of the kinase *(126)*. Currently available FLT3 inhibitors are summarized in **Table 1.4** and selected compounds are described in detail below.

Table 1.4: Targets and clinical status of currently available FLT3 inhibitors.

Inhibitor	Generation	Inhibitor type	Molecular Targets	Clinical Status
Midostaurin (PKC412)	1st	1	FLT3-WT, FLT3-ITD, FLT3-D835Y, JAK3, KIT, PDGFRβ, VEGFR-2, PKC*(127, 128)*	FDA approved in 2017 for newly diagnosed adult AML in combination with induction
Sunitinib (SU11248)	1st	1	FLT3, KIT, CSF-1R, PDGFRα/β, VEGFR1/2/3*(127, 129)*	FDA approved in renal cell carcinoma. Phase I and II studies show some efficacy in AML
Sorafinib	1st	2	FLT3-WT, FLT3-ITD, FLT3-D835Y, JNK3, KIT, CSK, PDGFRα/β, RET, TIE1, VEGFR2*(127, 130)*	Phase I and II clinical trials show efficacy as part of post-transplant maintenance therapy
Quizartinib (AC220)	2nd	1	FLT3-ITD, FLT3-WT RET, KIT, PDGFRα/β, CSFR*(131)*	Phase III and multiple phase I/II trials are ongoing
Crenolanib	2nd	1	FLT3-ITD, FLT3-D835Y, PDGFR*(132)*	Phase I and II trials are ongoing.
Gilteritinib (ASP2215)	2nd	1	FLT3-ITD, FLT3-D835Y, AXL, LTK, ALK*(125)*	FDA approved in 2018 for FLT3-mutant relapsed/refractory adult AML
TTT-3002	3rd	Not published	FLT3, FLT3-ITD, FLT3-D835Y. Full kinase profile not published.*(133)*	Preclinical
FF-10101	3rd	Covalently binds active and inactive forms	FLT3, FLT3-D835Y, FMS, KIT, MINK, KHS1, FGR, IRAK1, MELK, HGK*(134)*	Preclinical

Midostaurin

Midostaurin (PKC412), a staurosporine derivative, was originally developed as a protein kinase C (PKC) inhibitor for solid tumors *(135, 136)*. Midostaurin was later reported to have potent activity against FLT3 and subsequently showed activity against FLT3-mutant AML in preclinical models *(137–139)*. In early clinical studies, FLT3-mutant patients had no CR with midostaurin as a single agent, however they did have reduced peripheral blast counts indicating that midostuarin was having some biological effect *(140, 141)*. A later phase I study showed that midostaurin was well tolerated when combined with induction therapy *(142)*. A phase III study adding midostaurin to induction and consolidation regimens in over 700 newly-diagnosed FLT3-mutant AML patients showed a significant increase in 4-year OS in the midostaurin-treated group compared to chemotherapy alone (51.4% vs 44.3%) and an increase in median survival of 49.1 months *(143)*. The success of this trial led to FDA approval of midostaurin in combination with standard induction and consolidation chemotherapy in April 2017, making midostaurin the first approved drug for AML since 2000 *(138)*. The approval of midostaurin has been a great accomplishment for AML treatment; however, there is certainly room to improve CR, mitigate myelosuppression, and decrease relapse rates.

Quizartinib

Quizartinib (AC220) is one of several compounds that were specifically designed to inhibit FLT3 and improve selectivity compared to midostaurin and other first-generation FLT3 inhibitors *(144)*. Quizartinib was shown to have impressive efficacy against FLT3-mutant AML in multiple preclinical models including xenograft studies *(131, 145, 146)*. A phase I clinical study of relapse/refractory AML examining quizaritinib as a single agent showed an overall CR of 30%, with FLT3-mutant patients faring better than FLT3-WT patients (CR: 53% vs 14%) *(147)*. Next, a phase 2 study of quizartinib as monotherapy in relapsed/refractory AML showed a CR of 56% and 46% in two independent cohorts of FLT3-ITD positive patients *(148)*. A phase 2 study

comparing 30mg/day and 60mg/day quizartinib as a single agent in FLT3-mutant relapsed/refractory showed a CR of 47% in both groups and a median OS of 20.9 and 27.9 weeks respectively *(149)*. These lower doses had an improved safety profile (particularly QT-prolongation) compared to previous studies using 90 – 135 mg/day with no difference in CR which supported using lower doses moving forward. A phase III trial (QuANTUM-R, NCT02039726) is ongoing comparing quizartinib as a monotherapy to salvage chemotherapy in relapsed/refractory FLT3-mutant AML.

Gilteritinib

Gilteritinib (ASP2215) is another second generation FLT3 inhibitor specifically designed to target FLT3. Importantly, gilteritinb also inhibits FLT3 with mutations in the tyrosine kinase domain that confer resistance to other FLT3 inhibitors including midostaurin and quizartinib. The significance of these mutations will be further explored in the next section. Preclinical studies showed gilteritinib is potently effective against FLT3-mutant AML cell lines, mouse models, and patient xenograft models *(150, 151)*. Additionally, gilteritinib has a higher IC50 against KIT than midostaurin or quizartinib, suggesting that gilteritinib may result in fewer myelosuppressive adverse events than other FLT3 inhibitors *(150)*. A multicenter phase I/II dose escalation and expansion study of gilteritinib in relapsed/refractory AML showed a CR of 37% and median OS of 30 weeks in FLT3-mutant patients *(152)*. This study, in part, resulted in FDA approval for gilteritinib in FLT3-mutant relapsed/refractory AML in late 2018 *(153)*. A phase III study (ADMIRAL; NCT02421939) is currently ongoing comparing gilteritinib to salvage chemotherapy in relapsed/refractory FLT3-mutant AML. Early analysis has reported a significant increase in median OS (9.3 months vs 5.6 months) and one-year survival rates (37.1% vs 16.7%) in the patients receiving gilteritinib compared to salvage chemotherapy *(154)*. Multiple clinical studies examining gilteritinib in combination with other therapies such as induction or other targeted inhibitors are ongoing (NCT02752035, NCT02310321, NCT03625505, NCT03730012).

Mechanisms of Resistance to FLT3 inhibitors in FLT3-mutant AML

Although some FLT3 inhibitors have had promising clinical effects in patients, there are still a large portion of FLT3-mutant patients that are not responsive. Furthermore, even among responders, the remissions typically last no more than a few months *(140, 141, 143, 148, 152, 155)*. Clonal heterogeneity can certainly play a role in these relapses *(156)*. In cases with low allelic burden of the FLT3-mutation, the FLT3-mutant dominant clone is eliminated by FLT3-inhibitor treatment followed by expansion of a FLT3-WT clone that is not dependent on FLT3 signaling and therefore not responsive to FLT3 inhibtion *(157)*. However, in cases with a higher allelic burden it is common to find that a relapsed AML has retained the FLT3 mutation but has become resistant to the FLT3 inhibitor *(157, 158)*. The breadth of potential mechanisms that contribute to resistance to FLT3 inhibitors is quite astounding and further study is warranted to detangle their intricacies.

One of the most common mechanisms of resistance to FLT3-inhibitors is the acquisition of a mutation in the tyrosine kinase domain, usually in or near the ATP pocket, that results in steric hinderance, preventing compounds from binding *(159, 160)*. For example, Smith et al. (2012) sequenced 8 patients who relapsed after treatment with quizartinib and found all 8 of them had new mutations in the TK domain that were not detected before treatment. As has been supported in many other studies, these mutations were either at the D835 or F691 residues *(112, 161–163)*. Typically, at D835, which resides in the activation loop, the hydrophilic asparagine is mutated for a hydrophobic side chain, such as tyrosine, phenylalanine or valine. F691 is known as the "gatekeeper" and resides within the ATP-binding pocket. It was shown that F691 is a critical point of interaction for most FLT3 inhibitors and so the F691L mutation disrupts this interaction and weakens binding *(102, 162)*. These types of mutations account for about 20-50% of relapsed patients after FLT3-inhibitor treatment and can provide cross-resistance between FLT3 inhibitors *(158, 160, 163)*.

Another way that leukemias evade FLT3-inhibitors is through increased expression of FLT3 ligand and/or expression of FLT3-WT. It has been shown that patients can have increased FLT3L levels after chemotherapy *(164)*. Mutant FLT3 can remain responsive to FLT3L despite constitutive activation, therefore FLT3L can provide extrinsic support for FLT3 signaling dampening the effective concentration of FLT3 inhibitors *(165)*. Furthermore, it appears that the resistance provided by FLT3L could be acting through a FLT3-WT allele as Chen et al (2016) showed that FLT3L provided a greater protective effect when FLT3-WT was present as compared to two mutant alleles *(166)*.

In cases where FLT3 does not acquire a resistant mutation, patients may relapse due to a process called adaptive resistance. In adaptive resistance, alternative signaling mechanisms that promote cell survival and proliferation are activated to compensate for the loss of FLT3 activation. In these cases, the on-target effects of FLT3-inhibitors are maintained, FLT3 is inactivated; however, the cell's dependence on FLT3 signaling has been lifted *(167, 168)*. A large effort to identify mechanisms of resistance is underway as these pathways represent potential new targets for combination therapy with FLT3 inhibitors.

Many of the adaptive resistance pathways that have been identified so far are signaling cascades known to be downstream of FLT3, such as PI3K/AKT/mTOR or MAPKs. Aberrant activation of the PI3K pathway has been shown to play a role in hematologic malignancies, independent of FLT3 mutation status *(169)*. Furthermore, Lindblad et al (2016) demonstrated that AML cell lines exposed to sorafenib for 90 days were still able to show decreased FLT3 phosphorylation when treated with FLT3 inhibitors and there was no difference in mutational profile between sensitive and resistant cells; however, there was increased phosphorylation of mediators of the PI3K pathway such as AKT and ribosomal protein S6 kinase (S6K) as well as an enrichment in the mTOR transcriptional profile in the resistant cells *(170)*. They then showed that the resistant cell lines were sensitive to a PI3K/mTOR inhibitor, suggesting that this signaling pathway was important for survival in these cells. Furthermore, other groups have shown synergy

between targeting FLT3 and PI3K/AKT/mTOR, either with the combination of selective inhibitors or through the use of dual FLT3/AKT inhibitors *(171–173)*. Unfortunately, efforts to translate this treatment combination to the clinic appear to be lagging as only one trial combining a FLT3 inhibitor (midostaurin) and an mTOR inhibitor (everolimus) is listed on clinicaltrial.gov and no results have been posted since the study began in 2009 (NCT00819546).

Another well-characterized resistance pathway is the MEK/ERK/MAPK pathway. Like PI3K/AKT/mTOR, the MAPK pathway is downstream of FLT3 but can also be activated by many other receptors and plays an important function in cell survival and proliferation *(21)*. Additionally, the MAPK pathway has been shown to be upregulated in many types of cancer, particularly those with aberrant RAS activation *(20, 22)*. Several studies have demonstrated that many of the mediators of MAPK signaling, such as ERK, p38, and JNK, show increased phosphorylation in FLT3-inhibitor-resistant cell lines or as a rebound response during FLT3-inhibitor treatment *(167, 168, 174, 175)*. Importantly, Bruner et al (2017) showed that primary blasts taken from patients that were treated with sorafenib showed increased pERK 24 hours after treatment, suggesting that this MAPK response seen *in vitro* can translate *in vivo (175)*. Several groups have shown that MEK/ERK inhibition sensitizes AML cells to FLT3 inhibitors in vitro, either as a combination of selective inhibitors or with a dual FLT3/MEK inhibitor *(175–177)*. Zhang et al. (2016) showed significant survival in mice with human AML xenografts treated with the dual FLT3/MEK inhibitor, E6201 *(177)*. E6201 was moved into a phase I/II clinical trial of FLT3-mutant AML, however it was terminated early due to lack of efficacy during the phase I portion (NCT02418000).

Additionally, Pim-1 kinase has been found to directly interact with FLT3 and can stabilize FLT3 activation *(178)*. Green et al. (2015) showed that (1) patients that relapsed on sorafenib had increased expression of Pim-1 and Pim-2, (2) AML cell lines overexpressing Pim-2 were less sensitive to FLT3 inhibition, and (3) Pim inhibition or knockdown resensitized FLT3-inhibitor-resistance cells to quizartinib *(179)*. Several recent studies support these findings, showing

preclinical efficacy of combination of FLT3 and Pim inhibitors or novel dual FLT3/Pim inhibitors *(180–182)*.

Another potential contributor to FLT3-inhibitor resistance is Axl, a tyrosine kinase with a variety of functions including cell proliferation and survival. One study showed that Axl is required for FLT3 activation. The group later showed that Axl is upregulated in FLT3-inhibitor-resistant cells and that Axl inhibition resensitized those cells to FLT3 inhibitors *(183, 184)*. This was supported by a recent study which suggested that Axl expression may be induced by cytokines in the hematopoietic niche and/or hypoxia *(185)*. Axl is a known target of gilteritinib *(151)*. These findings may explain, in part, the clinical efficacy of gilteritinib in addition to its ability to inhibit FLT3-TK mutants.

Additionally, other pathways that are not associated with normal FLT3 signaling have been found to play a role in adaptive resistance to FLT3-inhibitors. For example, some studies have characterized metabolic changes in FLT3-inhibitor resistant cell lines. In a shRNA screen of a FLT3-ITD AML cell line, ataxia telangiectasia mutated (ATM) and glucose-6-phosphate dehydrogenase (G6PD) were found to be synthetic lethal with the early FLT3-inhibitor lestaurtinib *(186)*. These proteins are involved in responding to oxidative stress. Another study found that sorafenib-resistant FLT3-ITD cells had gene expression profiles consistent with mitochondrial dysfunction and displayed an increased dependence on glycolysis *(187)*. Furthermore, the resistant cells were more sensitive to glycolytic inhibitors than sorafenib-sensitive cells *(187)*. Metabolic proteins may present novel targets for combination with FLT3-inhibition.

Furthermore, a single study has suggested that runt related transcription factor 1 (RUNX1) may contribute to FLT3-inhibitor resistance *(188)*. Hirade et al. (2016) found that RUNX1 is upregulated in FLT3-ITD AML cells compared to FLT3-WT cells and was further induced in quizartinib-resistant cells compared to the parental sensitive cells in the absence of any mutational changes between the groups. Finally, they showed that shRNA knockdown of RUNX1 abrogated proliferation and tumor progression in *in vitro* and *in vivo* models.

Combination therapies may provide clues to other resistance mechanisms. One example is a few dual FLT3/cyclin dependent kinase (CDK) inhibitors have been shown to be effective in preclinical models of AML, however, no studies have specifically identified CDKs or other cell cycle regulators as mediators of adaptive resistance *(189–191)*. Although, there is some evidence that CDK6 is required for transformation in FLT3-ITD cells *(192)*. Another example is the dual FLT3/inhibitor of kappa B kinase (IKK) inhibitor, AS602868 *(193, 194)*. Again, no direct evidence of IKK or NFkB playing a role in FLT3-inhibitor resistance has been published yet.

It is important to note that the various resistance mechanisms are not mutually exclusive and can occur simultaneously within a single patient. As discussed above, Smith et al (2012) showed that 8 out of 8 patients that relapsed after quizartinib treatment had FLT3-TK mutations *(158)*. This group later performed single-cell RNA sequencing on these same samples and found that the TK mutations were only found in 20-50% of the cells within each patient, suggesting that the remaining 50-80% of cells without the mutations were surviving through some other resistance mechanism *(195)*.

Innate Immune Signaling in Hematopoietic Neoplasms

Selected sections were published in:

> Varney, M., **Melgar, K**., Niederkorn, M. Smith, M. A., Barreyro, L., and Starczynowski, D.T. Deconstructing innate immune signaling in myelodysplastic syndromes. *Experimental Hematology*, 43, 587-598 (2015).

Innate Immune Signaling

The innate immune system recognizes foreign pathogens by cell surface pattern recognition receptors (PRRs). These receptors recognize foreign pathogen components, termed pathogen-associated molecular patterns (PAMPs), as well as host cellular by-products, referred to as damage-associated molecular patterns (DAMPS). Among the first PRRs to be identified were Toll-like Receptors (TLRs). TLRs, together with the Interleukin-1 receptor (IL1R), form the interleukin-1 receptor/toll-like receptor (TIR) superfamily. All members of this family have in common a TIR domain. TLRs consist of a single-pass transmembrane protein with a leucine-rich ectodomain. There are currently 10 known human TLRs and 12 murine TLRs. The TLRs can be divided into two main groups based on subcellular location - extracellular (TLR1, TLR2, TLR4, TLR5, TLR6, and TLR11) and intracellular, or endosomal (TLR3, TLR7, TLR8, and TLR9). The location of the receptors, in turn, relates to their specific ligands. The intracellular receptors bind to features of pathogen nucleic acids - such as dsRNA, and CpG DNA; whereas the extracellular receptors bind to pathogen membrane components, the best characterized being TLR4 binding to lipopolysaccharide (LPS) of gram-negative bacteria.

Binding of a TLR to its ligand results in recruitment of a TIR domain-containing adaptor protein. There are two main TLR adaptor proteins which induce the activation of separate innate immune signaling pathways, MyD88 and TRIF. TLR3 is the only TLR that does not use MyD88 and exclusively recruits TRIF. Signaling through TRIF results in activation of IRF3 and MyD88-independent activation of NF-κB, leading to transcription of the same pro-inflammatory cytokines

as the MyD88 pathway with the addition of type 1 interferons. TLR4 is the only receptor that utilizes both MyD88 and TRIF *(203–205)*. All of the TLRs, with the exception of TLR3, use MyD88. MyD88 forms a large multi-unit complex with interleukin-1-receptor-associated-kinase-4 (IRAK4) via Death Domain (DD) interactions; this complex is called the myddosome *(196, 197)*. The myddosome recruits and phosphorylates additional proteins in the TLR/IL-1R signaling pathway, such as IRAK1 and IRAK2. Following IRAK4 activation, IRAK4 phosphorylates IRAK1, which allows IRAK1 to interact with TRAF6. TRAF6 subsequently K63 ubiquitinates IRAK1, producing a scaffold for interactions with additional downstream proteins *(198)*. Ultimately, the signal results in the activation of NF-κB and MAPK pathways, leading to transcription of pro-inflammatory cytokines, such as tumor necrosis factor alpha (TNF-α), interleukine-1 (IL-1) and IL-6. In addition to activating IRAK1, phosphorylation of IRAK1 by IRAK4 has been shown to induce degradation of IRAK1, providing a negative feedback mechanism for TLR signaling *(199)*. Originally it was thought that both IRAK2 and IRAK-M (or IRAK3) lacked kinase activity; however later studies have shown that IRAK2 can act as a kinase and plays a major role in TLR-induced NF-κB activation, particularly from TLR3, TLR4 and TLR8 *(200)*. IRAK-M is thought to be a negative regulator by competing with IRAK1 or IRAK2 for access to the myddosome; additionally, it has been proposed that that IRAK-M may have kinase-independent activity regulating alternative NF-κB activation *(201, 202)*.

Much of the early work to determine the function of IRAKs was done using knockout mice. IRAK knockout mice for each of the four IRAK family members have been generated. The knockout lines for IRAK1, 2, and 4 show poor response to both viral and bacterial infections, emphasizing their important role in immunity *(206–209)*. Alternatively, the IRAK-M knockout mice exhibit increased TLR-induced NF-κB and MAPK activity, highlighting the regulatory role of IRAK-M *(210)*. IRAK4 deficiency is the only IRAK family deficiency identified in humans at this time. Patients with IRAK4 deficiency show recurrent infections and poor inflammatory response *(211)*. Interestingly, the rate of infection decreases with age, presumably due to intact adaptive memory

responses, though further investigation is needed to determine an exact mechanism. Remarkably, there was recently a case study of one infant with loss of IRAK1 as part of a larger chromosomal deletion. This patient's peripheral blood mononuclear cells responded normally to TLR and IL1R stimulation *(212)*. However, interpretations of the role of IRAK1 in this context are complicated by the potential other genetic abnormalities in the chromosome deletion and the fact that this is a single patient.

Dysregulation and Targeting of Innate Immune Signaling in Hematopoietic Neoplasms

Dysregulation at multiple points along the innate immune signaling pathway have been implicated in disease pathogenesis of many disorders including autoinflammatory conditions as well as hematopoietic neoplasms, such as myelodysplastic syndrome (MDS) and AML. This pathway has been better described in MDS, which can transform to AML at a rate as high as 50% in some genetic subtypes *(213)*, therefore we will focus on both diseases in the following review.

TLR expression has been implicated in hematopoietic stem cell (HSC) development, suggesting that changes in TLR expression could lead to deregulated hematopoiesis *(214, 215)*. Several mouse studies have shown that chronic administration of low levels of LPS in vivo, meant to model chronic infection, result in loss of HSC quiescence, increased HSC numbers, myeloid skewing and decreased progenitor capacity *(216–218)*. Taken together, chronic TLR signaling impairs HSC function and alters normal hematopoiesis, which suggests a causal role in MDS and potential contribution to pro-leukemic conditions.

Indeed, overexpression or gain-of-function mutations in a subset of TLR have been described in this context. TLR4 was shown to be overexpressed at both the mRNA and protein levels in the CD34+ cells isolated from the bone marrow (BM) of MDS patients *(219)*. The overexpressed TLR4 exhibited normal functional capacity as assessed by ICAM-1 expression after LPS stimulation. TNF-α was shown to increase TLR4 expression in a dose-dependent manner and depletion of TNF with anti-TNF antibody treatment of MDS bone marrow cells

resulted in decreased TLR4 expression, suggesting that the TLR4 expression was TNF-α dependent. Additionally, Maratheftis et al. (2007) found a significant correlation between TLR4 expression and apoptosis in CD34+ MDS cells, providing evidence for a mechanism for TLR4 expression and development of MDS *(219)*. However, TLR4 expression within the total BM population did not differ from normal controls, nor was there correlation between TNF-α levels and TLR4 expression. Kuninaka et al. (2010) described TLR9 overexpression in MDS BM cells. TLR9 expression positively correlated with TNF-α levels *(220)*. Interestingly, TLR9 expression decreased once the MDS transformed to leukemia in these patients, further supporting the link between TLR expression and apoptosis in MDS, though through a TLR9 dependent pathway rather than TLR4 dependent. Both of these studies found evidence for TLR2 overexpression in MDS and through deep sequencing analysis, a later study found a TLR2-F217S gain-of-function variant in the CD34+ bone marrow cells of 11% of 149 MDS patients *(221)*. Additionally, in a study of 103 AML patients, TLR2, TLR4, and TLR9 mRNA expression was correlated with resistance to chemotherapy and shorter overall survival *(222)*.

Other mediators of the innate immune signaling pathway that show dysregulation in hematopoietic neoplasms are IRAK1 and IRAK4. Using gene expression data from two separate cohorts of MDS patient bone marrow *(223, 224)*, IRAK1 was found to be overexpressed in MDS patient samples compared with normal CD34+ bone marrow *(225, 226)*. This pattern of overexpression was also seen at the protein level, both in primary MDS patient samples and several MDS and AML cell lines *(225, 226)*. Not only was IRAK1 protein level increased, but phosphorylation of IRAK1 was also increased. IRAK1 inhibition, either through shIRAK1 knockdown or through the use of an IRAK1/4 inhibitor, resulted in delayed MDS-like disease and delayed mortality in a xenograft model of MDS *(225)*. Additionally, Smith et al (2019) recently showed that MDS and AML cell lines and patient samples preferentially expressed a longer isoform of IRAK4 compared to the short isoform expressed by normal hematopoietic stem cells *(227)*. Furthermore, they found that the long isoform was more efficient at conducting innate

immune signaling and that the long isoform-expressing cells were more sensitive to IRAK4 inhibition *(227)*.

These results suggest that IRAK inhibition could present a useful therapeutic target in the treatment of MDS and AML. As mentioned earlier, there is some evidence showing efficacy of targeting IKK, a downstream mediator of IRAK signaling, in combination with FLT3, suggesting a potential benefit of targeting this pathway in AML *(193, 194)*. Many IRAK4 and/or IRAK1 small molecule inhibitors are in development for the treatment of hematologic malignancies, particularly those with MyD88 gain-of-function mutations and a few examples in T-cell acute lymphocytic leukemia (T-ALL), however AML studies are lacking with newer compounds (**Table 1.5**) *(228–230)*. Furthermore, it has been reported that pacritinib has activity against IRAK1. Originally developed as a JAK inhibitor, Hosseini et al. (2018) showed that pacritinib can inhibit IRAK1 and that this activity may contribute to its anti-leukemic activity *(231)*. Together these studies present an exciting prospect for targeting innate immune signaling in the treatment of hematologic malignancies in the future.

Table 1.5: Currently available IRAK inhibitors.

Inhibitor	IRAK Selectivity	Other Targets	Clinical Status
IRAK1/4-inhibitor*(225, 229, 232)*	1 and 4	Not published	In vitro efficacy against AML/MDS cell lines, but not fit for clinical use
PF-06650833*(233)*	4	IRAK3, CK1γ, CK1δ/ε, PIPK2C	Phase I in healthy subjects and rheumatoid arthritis. No published data in AML.
Pacritinib*(234)*	1	JAK2, JAK3, FLT3, TYK2, TRKC, TNK1, ROS1, KIT, SRC, CSR1R, HIPK4	Phase I/II studies in AML. Phase III in myelofibrosis
CA-4948	4	Not published	Phase I in relapsed/refractory hematologic malignancies (Non-Hodgkin Lymphoma or AML)

References

1. S. H. Swerdlow, E. Campo, N. L. Harris, E. S. Jaffe, S. A. Pileri, H. Stein, J. Theile, J. W. Vardiman, *WHO Classification of Tumours of Haematopoietic and Lymphoid Tissues* (2008).
2. Cancer Stat Facts: Leukemia - Acute Myeloid Leukemia (AML)*NCI Surveillance, Epidemiaology, End Results Progr.* (2019) (available at https://seer.cancer.gov/statfacts/html/amyl.html).
3. J. W. Vardiman, J. Thiele, D. A. Arber, R. D. Brunning, M. J. Borowitz, A. Porwit, N. L. Harris, M. M. Le Beau, E. Hellström-Lindberg, A. Tefferi, C. D. Bloomfield, The 2008 revision of the World Health Organization (WHO) classification of myeloid neoplasms and acute leukemia: Rationale and important changes, *Blood* **114**, 937–951 (2009).
4. D. A. Arber, A. Orazi, R. Hasserjian, M. J. Borowitz, M. M. Le Beau, C. D. Bloomfield, M. Cazzola, J. W. Vardiman, T. Westergaard, P. K. Andersen, J. B. Pedersen, J. H. Olsen, M. Frisch, H. T. Sorensen, J. Wohlfahrt, M. Melbye, The 2016 revision to the World Health Organization classi fi cation of myeloid neoplasms and acute leukemia, *Blood* **127**, 2391–2406 (2016).
5. D. Grimwade, H. Walker, F. Oliver, K. Wheatley, C. Harrison, G. Harrison, J. Rees, I. Hann, R. Stevens, A. Burnett, A. Goldstone, The importance of diagnostic cytogenetics on outcome in AML: analysis of 1,612 patients entered into the MRC AML 10 trial. The Medical Research Council Adult and Children's Leukaemia Working Parties., *Blood* **92**, 2322–33 (1998).
6. D. Grimwade, R. K. Hills, A. V Moorman, H. Walker, S. Chatters, A. H. Goldstone, K. Wheatley, C. J. Harrison, A. K. Burnett, Refinement of cytogenetic classification in acute myeloid: determination of prognostic significance of rare recurring chromosomal abnormalities among 5876 younger adult patients treated in the United Kingdom Medical Research COuncil trials, *Blood* **116**, 354–366 (2010).
7. J. J. Yang, T. S. Park, T. S. K. Wan, in *Cancer Cytogenetics. Methods in Molecular Biology vol 1541*, T. S. K. Wan, Ed. (Humana Press, New York, NY, 2017), pp. 223–245.
8. The Cancer Genome Atlas Research Network: Genomic and Epigenomic Landscapes of Adult De Novo Acute Myeloid Leukemia, *N. Engl. J. Med.* **368**, 2059–2074 (2013).
9. H. Dombret, C. Gardin, An update of current treatments for adult acute myeloid leukemia, *Blood* **127**, 53–62 (2016).
10. G. Tamamyan, T. Kadia, F. Ravandi, G. Borthakur, J. Cortes, E. Jabbour, N. Daver, M. Ohanian, H. Kantarjian, M. Konopleva, Frontline treatment of acute myeloid leukemia in adults, *Crit. Rev. Oncol. Hematol.* **110**, 20–34 (2017).
11. Daunorubicin*Natl. Cent. Biotechnol. Information. PubChem Database* (2019) (available at https://pubchem.ncbi.nlm.nih.gov/compound/daunorubicin).
12. Cytarabine*Natl. Cent. Biotechnol. Information. PubChem Database.* (2019) (available at https://pubchem.ncbi.nlm.nih.gov/compound/cytarabine).
13. T. M. Kadia, F. Ravandi, S. O'Brien, J. Cortes, H. M. Kantarjian, Progress in acute myeloid leukemia, *Clin. Lymphoma, Myeloma Leuk.* **15**, 139–151 (2015).
14. A. K. Burnett, N. H. Russell, R. K. Hills, A. E. Hunter, L. Kjeldsen, J. Yin, B. E. S. Gibson, K. Wheatley, D. Milligan, Optimization of chemotherapy for younger patients with acute myeloid leukemia: Results of the medical research council AML15 trial, *J. Clin. Oncol.* **31**, 3360–3368 (2013).
15. R. Willemze, S. Suciu, G. Meloni, B. Labar, J. P. Marie, C. J. M. Halkes, P. Muus, M. Mistrik, S. Amadori, G. Specchia, F. Fabbiano, F. Nobile, M. Sborgia, A. Camera, D. L. D. Selleslag, F. Lefrerè, D. Magro, S. Sica, N. Cantore, M. Beksac, Z. Berneman, X. Thomas, L. Melillo, J. E. Guimaraes, P. Leoni, M. Luppi, M. E. Mitra, D. Bron, G. Fillet, E. W. A. Marijt, A. Venditti, A. Hagemeijer, M. Mancini, J. Jansen, D. Cilloni, L. Meert, P. Fazi, M. Vignetti, S. M. Trisolini, F. Mandelli, T. De Witte, High-Dose cytarabine in induction treatment improves the outcome of adult patients younger than age 46 years with acute myeloid leukemia: Results of the EORTC-

GIMEMA AML-12 trial, *J. Clin. Oncol.* **32**, 219–228 (2014).
16. J. Holowiecki, S. Grosicki, T. Robak, S. Kyrcz-Krzemien, S. Giebel, A. Hellmann, A. Skotnicki, W. W. Jedrzejczak, L. Konopka, K. Kuliczkowski, B. Zdziarska, A. Dmoszynska, B. Marianska, A. Pluta, K. Zawilska, M. Komarnicki, J. Kloczko, K. Sulek, O. Haus, B. Stella-Holowiecka, W. Baran, B. Jakubas, M. Paluszewska, A. Wierzbowska, M. Kielbinski, K. Jagoda, Addition of cladribine to daunorubicin and cytarabine increases complete remission rate after a single course of induction treatment in acute myeloid leukemia. Multicenter, phase III study, *Leukemia* **18**, 989–997 (2004).
17. J. Holowiecki, S. Grosicki, S. Giebel, T. Robak, S. Kyrcz-Krzemien, K. Kuliczkowski, A. B. Skotnicki, A. Hellmann, K. Sulek, A. Dmoszynska, J. Kloczko, W. W. Jedrzejczak, B. Zdziarska, K. Warzocha, K. Zawilska, M. Komarnicki, M. Kielbinski, B. Piatkowska-Jakubas, A. Wierzbowska, M. Wach, O. Haus, Cladribine, but not fludarabine, added to daunorubicin and cytarabine during induction prolongs survival of patients with acute myeloid leukemia: A multicenter, randomizedphase III study, *J. Clin. Oncol.* **30**, 2441–2448 (2012).
18. B. J. V Raelson, C. Nervi, A. Rosenauer, L. Benedetti, Y. Monczak, M. Pearson, P. G. Pelicci, W. H. Miller Jr, The PML/RARa oncoprotein is a direct molecular target of retinoic acid in acute promyelocytic leukemia cells, *Blood* **88**, 2826–2832 (1996).
19. W. Z., C. Z., Acute promyelocytic leukemia: from highly fatal to highly curable, *Blood* **111**, 2505–2515 (2008).
20. M. E. M. Van Meter, E. Díaz-Flores, J. A. Archard, E. Passegué, J. M. Irish, N. Kotecha, G. P. Nolan, K. Shannon, B. S. Braun, K-RasG12D expression induces hyperproliferation and aberrant signaling in primary hematopoietic stem/progenitor cells, *Blood* **109**, 3945–3952 (2007).
21. Y. Sun, W. Z. Liu, T. Liu, X. Feng, N. Yang, H. F. Zhou, Signaling pathway of MAPK/ERK in cell proliferation, differentiation, migration, senescence and apoptosis, *J. Recept. Signal Transduct.* **35**, 600–604 (2015).
22. M. Milella, S. M. Kornblau, Z. Estrov, B. Z. Carter, H. Lapillonne, D. Harris, M. Konopleva, S. Zhao, E. Estey, M. Andreeff, Therapeutic targeting of the MEK/MAPK signal transduction module in acute myeloid leukemia, *J. Clin. Invest.* **108**, 851–859 (2001).
23. J. Wu, W. W. L. Wong, F. Khosravi, M. D. Minden, L. Z. Penn, Blocking the Raf/MEK/ERK pathway sensitizes acute myelogenous leukemia cells to lovastatin-induced apoptosis, *Cancer Res.* **64**, 6461–6468 (2004).
24. N. Jain, E. Curran, N. M. Iyengar, E. Diaz-Flores, R. Kunnavakkam, L. Popplewell, M. H. Kirschbaum, T. Karrison, H. P. Erba, M. Green, X. Poire, G. Koval, K. Shannon, P. L. Reddy, L. Joseph, E. L. Atallah, P. Dy, S. P. Thomas, S. E. Smith, A. Doyle, W. M. Stadler, R. A. Larson, W. Stock, O. Odenike, Phase 2 study of the oral MEK inhibitor selumetinib in advanced acute myelogenous leukemia: A university of chicago phase 2 consortium trial, *Clin. Cancer Res.* **20**, 490–498 (2014).
25. A. Maiti, K. Naqvi, T. M. Kadia, G. Borthakur, K. Takahashi, P. Bose, N. G. Daver, A. Patel, Y. Alvarado, M. Ohanian, C. D. DiNardo, J. E. Cortes, E. J. Jabbour, G. Garcia-Manero, H. M. Kantarjian, F. Ravandi, Phase II Trial of MEK Inhibitor Binimetinib (MEK162) in RAS-mutant Acute Myeloid Leukemia, *Clin. Lymphoma, Myeloma Leuk.* **19**, 142-148.e1 (2019).
26. C. R. Wei, X. F. Ge, Y. Wang, X. R. Li, MEK inhibitor CI-1040 induces apoptosis in acute myeloid leukemia cells in vitro, *Eur. Rev. Med. Pharmacol. Sci.* **20**, 1961–1968 (2016).
27. Q. Xu, S. E. Simpson, T. J. Scialla, A. Bagg, M. Carroll, Survival of acute myeloid leukemia cells requires PI3 kinase activation, *Blood* **102**, 972–980 (2003).
28. A. M. Martelli, M. Nyåkern, G. Tabellini, R. Bortul, P. L. Tazzari, C. Evangelisti, L. Cocco, Phosphoinositide 3-kinase/ Akt signaling pathway and its therapeutical implications for human acute myeloid leukemia, *Leukemia* **20**, 911–928 (2006).
29. N. Sandhöfer, K. H. Metzeler, M. Rothenberg, T. Herold, S. Tiedt, V. Groiß, M. Carlet, G. Walter, T. Hinrichsen, O. Wachter, M. Grunert, S. Schneider, M. Subklewe, A. Dufour, S.

Fröhling, H. G. Klein, W. Hiddemann, I. Jeremias, K. Spiekermann, Dual PI3K/mTOR inhibition shows antileukemic activity in MLL-rearranged acute myeloid leukemia, *Leukemia* **29**, 828–838 (2015).
30. J. Bertacchini, N. Heidari, L. Mediani, S. Capitani, M. Shahjahani, A. Ahmadzadeh, N. Saki, Targeting PI3K/AKT/mTOR network for treatment of leukemia, *Cell. Mol. Life Sci.* **72**, 2337–2347 (2015).
31. J. Bertacchini, C. Frasson, F. Chiarini, D. D'Avella, B. Accordi, L. Anselmi, P. Barozzi, F. Foghieri, M. Luppi, A. M. Martelli, G. Basso, S. Najmaldin, A. Khosravi, F. Rahim, S. Marmiroli, Dual inhibition of PI3K/mTOR signaling in chemoresistant AML primary cells, *Adv. Biol. Regul.* **68**, 2–9 (2018).
32. L. Deng, L. Jiang, X. H. Lin, K. F. Tseng, Y. Liu, X. Zhang, R. H. Dong, Z. G. Lu, X. J. Wang, The PI3K/mTOR dual inhibitor BEZ235 suppresses proliferation and migration and reverses multidrug resistance in acute myeloid leukemia, *Acta Pharmacol. Sin.* **38**, 382–391 (2017).
33. M. Y. Konopleva, R. B. Walter, S. H. Faderl, E. J. Jabbour, Z. Zeng, G. Borthakur, X. Huang, T. M. Kadia, P. P. Ruvolo, J. B. Feliu, H. Lu, L. K. Debose, J. A. Burger, M. Andreeff, W. Liu, K. A. Baggerly, S. M. Kornblau, L. A. Doyle, E. H. Estey, H. M. Kantarjian, Preclinical and early clinical evaluation of the oral AKT inhibitor, MK-2206, for the treatment of acute myelogenous leukemia, *Clin. Cancer Res.* **20**, 2226–2235 (2014).
34. S. Boffo, A. Damato, L. Alfano, A. Giordano, CDK9 inhibitors in acute myeloid leukemia, *J. Exp. Clin. Cancer Res.* **37**, 1–10 (2018).
35. G. Romano, Deregulations in the Cyclin-Dependent Kinase-9-Related Pathway in Cancer: Implications for Drug Discovery and Development, *ISRN Oncol.* **2013**, 1–14 (2013).
36. T. Placke, K. Faber, A. Nonami, S. L. Putain, H. R. Salih, F. H. Heidel, A. Kramer, D. E. Root, D. A. Barbie, A. V. Krivtsov, S. A. Armstrong, W. C. Hahn, B. J. Huntly, S. M. Sykes, M. D. Milsom, C. Scholl, S. Frohling, Requirement for CDK6 in MLL-rearranged acute myeloid leukemia, *Blood* **122**, 13–23 (2014).
37. A. Baker, G. P. Gregory, I. Verbrugge, L. Kats, J. J. Hilton, E. Vidacs, E. M. Lee, R. B. Lock, J. Zuber, J. Shortt, R. W. Johnstone, The CDK9 inhibitor dinaciclib exerts potent apoptotic and antitumor effects in preclinical models of MLL-rearranged acute myeloid Leukemia, *Cancer Res.* **76**, 1158–1169 (2016).
38. A.-M. Duchemin, R. Briesewitz, T. Liu, D. F. Kusewitt, J. Wang, M. A. Caligiuri, L. Wang, B. W. Blaser, Pharmacologic inhibition of CDK4/6: mechanistic evidence for selective activity or acquired resistance in acute myeloid leukemia, *Blood* **110**, 2075–2083 (2007).
39. E. Walsby, M. Lazenby, C. Pepper, A. K. Burnett, The cyclin-dependent kinase inhibitor SNS-032 has single agent activity in AML cells and is highly synergistic with cytarabine, *Leukemia* **25**, 411–419 (2011).
40. S. Xie, H. Jiang, X. W. Zhai, F. Wei, S. D. Wang, J. Ding, Y. Chen, Antitumor action of CDK inhibitor LS-007 as a single agent and in combination with ABT-199 against human acute leukemia cells, *Acta Pharmacol. Sin.* **37**, 1481–1489 (2016).
41. G. Mariaule, P. Belmont, Cyclin-dependent kinase inhibitors as marketed anticancer drugs: Where are we now? A short survey, *Molecules* **19**, 14366–14382 (2014).
42. J. F. Zeidner, M. C. Foster, A. L. Blackford, M. R. Litzow, L. E. Morris, S. A. Strickland, J. E. Lancet, P. Bose, M. Yair Levy, R. Tibes, I. Gojo, C. D. Gocke, G. L. Rosner, R. F. Little, J. J. Wright, L. Austin Doyle, B. Douglas Smith, J. E. Karp, Randomized multicenter phase II study of flavopiridol (alvocidib), cytarabine, and mitoxantrone (FLAM) versus cytarabine/daunorubicin (7+3) in newly diagnosed acute myeloid leukemia, *Haematologica* **100**, 1172–1179 (2015).
43. F. Cao, E. C. Townsend, H. Karatas, J. Xu, L. Li, S. Lee, L. Liu, Y. Chen, P. Ouillette, J. Zhu, J. L. Hess, P. Atadja, M. Lei, Z. S. Qin, S. Malek, S. Wang, Y. Dou, Targeting MLL1 H3K4 Methyltransferase Activity in Mixed-Lineage Leukemia, *Mol. Cell* **53**, 247–261 (2014).
44. S. He, T. J. Senter, J. Pollock, C. Han, S. K. Upadhyay, T. Purohit, R. D. Gogliotti, C. W. Lindsley, T. Cierpicki, S. R. Stauffer, J. Grembecka, High-affinity small molecule inhibitors of the

menin-Mixed Lineage Leukemia (MLL) interaction closely mimic a natural protein-protein interaction., *J. Med. Chem.* **57**, 1542–1556 (2014).
45. M. Vedadi, D. Barsyte-Lovejoy, F. Liu, S. Rival-Gervier, A. Allali-Hassani, V. Labrie, T. J. Wigle, P. A. Dimaggio, G. A. Wasney, A. Siarheyeva, A. Dong, W. Tempel, S. C. Wang, X. Chen, I. Chau, T. J. Mangano, X. P. Huang, C. D. Simpson, S. G. Pattenden, J. L. Norris, D. B. Kireev, A. Tripathy, A. Edwards, B. L. Roth, W. P. Janzen, B. A. Garcia, A. Petronis, J. Ellis, P. J. Brown, S. V. Frye, C. H. Arrowsmith, J. Jin, A chemical probe selectively inhibits G9a and GLP methyltransferase activity in cells, *Nat. Chem. Biol.* **7**, 566–574 (2011).
46. W. Qi, H. Chan, L. Teng, L. Li, S. Chuai, R. Zhang, J. Zeng, M. Li, H. Fan, Y. Lin, J. Gu, O. Ardayfio, J.-H. Zhang, X. Yan, J. Fang, Y. Mi, M. Zhang, T. Zhou, G. Feng, Z. Chen, G. Li, T. Yang, K. Zhao, X. Liu, Z. Yu, C. X. Lu, P. Atadja, E. Li, Selective inhibition of Ezh2 by a small molecule inhibitor blocks tumor cells proliferation, *Proc. Natl. Acad. Sci.* **109**, 21360–21365 (2012).
47. K. D. Konze, A. Ma, F. Li, D. Barsyte-Lovejoy, T. Parton, C. J. MacNevin, F. Liu, C. Gao, X. P. Huang, E. Kuznetsova, M. Rougie, A. Jiang, S. G. Pattenden, J. L. Norris, L. I. James, B. L. Roth, P. J. Brown, S. V. Frye, C. H. Arrowsmith, K. M. Hahn, G. G. Wang, M. Vedadi, J. Jin, An orally bioavailable chemical probe of the lysine methyltransferases EZH2 and EZH1, *ACS Chem. Biol.* **8**, 1324–1334 (2013).
48. S. R. Daigle, E. J. Olhava, C. A. Therkelsen, A. Basavapathruni, L. Jin, P. A. Boriack-Sjodin, C. J. Allain, C. R. Klaus, A. Raimondi, M. P. Scott, N. J. Waters, R. Chesworth, M. P. Moyer, R. A. Copeland, V. M. Richon, R. M. Pollock, Potent inhibition of DOT1L as treatment of MLL-fusion leukemia, *Blood* **122**, 1017–1025 (2013).
49. R. E. Rau, B. A. Rodrigues, M. Luo, M. Jeong, A. Rosen, J. H. Rogers, C. T. Campbell, S. R. Daigle, L. Deng, Y. Song, S. Sweet, T. Chevassut, M. Andreeff, S. M. Kornblau, W. Li, M. A. Goodell, DOT1L as a therapeutic target for the treatment of DNMT3A-mutant acute myeloid leukemia, *Blood* **128**, 971–981 (2016).
50. P. Bali, M. Pranpat, J. Bradner, M. Balasis, W. Fiskus, F. Guo, K. Rocha, S. Kumaraswamy, S. Boyapalle, P. Atadja, E. Seto, K. Bhalla, Inhibition of histone deacetylase 6 acetylates and disrupts the chaperone function of heat shock protein 90: A novel basis for antileukemia activity of histone deacetylase inhibitors, *J. Biol. Chem.* **280**, 26729–26734 (2005).
51. M. R. Shakespear, M. A. Halili, K. M. Irvine, D. P. Fairlie, M. J. Sweet, Histone deacetylases as regulators of inflammation and immunity, **32**, 335–343 (2011).
52. A. C. West, S. R. Mattarollo, J. Shortt, L. A. Cluse, A. J. Christiansen, M. J. Smyth, R. W. Johnstone, An intact immune system is required for the anticancer activities of histone deacetylase inhibitors, *Cancer Res.* **73**, 7265–7276 (2013).
53. M. E. Figueroa, O. Abdel-Wahab, C. Lu, P. S. Ward, J. Patel, A. Shih, Y. Li, N. Bhagwat, A. Vasanthakumar, H. F. Fernandez, M. S. Tallman, Z. Sun, K. Wolniak, J. K. Peeters, W. Liu, S. E. Choe, V. R. Fantin, E. Paietta, B. Löwenberg, J. D. Licht, L. A. Godley, R. Delwel, P. J. M. Valk, C. B. Thompson, R. L. Levine, A. Melnick, Leukemic IDH1 and IDH2 Mutations Result in a Hypermethylation Phenotype, Disrupt TET2 Function, and Impair Hematopoietic Differentiation, *Cancer Cell* **18**, 553–567 (2010).
54. L. M. Gagné, K. Boulay, I. Topisirovic, M. É. Huot, F. A. Mallette, Oncogenic Activities of IDH1/2 Mutations: From Epigenetics to Cellular Signaling, *Trends Cell Biol.* **27**, 738–752 (2017).
55. K. Yen, J. Travins, F. Wang, M. D. David, E. Artin, K. Straley, A. Padyana, S. Gross, B. Delabarre, E. Tobin, Y. Chen, R. Nagaraja, S. Choe, L. Jin, Z. Konteatis, G. Cianchetta, J. O. Saunders, F. G. Salituro, C. Quivoron, P. Opolon, O. Bawa, V. Saada, A. Paci, S. Broutin, O. A. Bernard, S. De Botton, B. S. Marteyn, M. Pilichowska, Y. Xu, C. Fang, F. Jiang, W. Wei, S. Jin, L. Silverman, W. Liu, H. Yang, L. Dang, M. Dorsch, V. Penard-Lacronique, S. A. Biller, S. S. Michael Su, AG-221, a first-in-class therapy targeting acute myeloid leukemia harboring oncogenic IDH2 mutations, *Cancer Discov.* **7**, 478–493 (2017).
56. J. Popovici-Muller, R. M. Lemieux, E. Artin, J. O. Saunders, F. G. Salituro, J. Travins, G.

Cianchetta, Z. Cai, D. Zhou, D. Cui, P. Chen, K. Straley, E. Tobin, F. Wang, M. D. David, V. Penard-Lacronique, C. Quivoron, V. Saada, S. De Botton, S. Gross, L. Dang, H. Yang, L. Utley, Y. Chen, H. Kim, S. Jin, Z. Gu, G. Yao, Z. Luo, X. Lv, C. Fang, L. Yan, A. Olaharski, L. Silverman, S. Biller, S. S. M. Su, K. Yen, Discovery of AG-120 (Ivosidenib): A First-in-Class Mutant IDH1 Inhibitor for the Treatment of IDH1 Mutant Cancers, *ACS Med. Chem. Lett.* **9**, 300–305 (2018).
57. S. Ogilvy, D. Metcalf, C. G. Print, M. L. Bath, A. W. Harris, J. M. Adams, Constitutive Bcl-2 expression throughout the hematopoietic compartment affects multiple lineages and enhances progenitor cell survival, *Proc. Natl. Acad. Sci.* **96**, 14943–14948 (2002).
58. M. Konopleva, S. Zhao, W. Hu, S. Jiang, V. Snell, D. Weidner, C. E. Jackson, X. Zhang, R. Champlin, E. Estey, J. C. Reed, M. Andreeff, The anti-apoptotic genes Bcl-XL and Bcl-2 are over-expressed and contribute to chemoresistance of non-proliferating leukaemic CD34+ cells, *Br. J. Haematol.* **118**, 521–534 (2002).
59. J. Kale, E. J. Osterlund, D. W. Andrews, BCL-2 family proteins: Changing partners in the dance towards death, *Cell Death Differ.* **25**, 65–80 (2018).
60. C. D. DiNardo, K. Pratz, V. Pullarkat, B. A. Jonas, M. Arellano, P. S. Becker, O. Frankfurt, M. Konopleva, A. H. Wei, H. M. Kantarjian, T. Xu, W.-J. Hong, B. Chyla, J. Potluri, D. A. Pollyea, A. Letai, Venetoclax combined with decitabine or azacitidine in treatment-naive, elderly patients with acute myeloid leukemia, *Blood* **133**, 7–17 (2019).
61. I. Jilani, E. Estey, Y. Huh, Y. Joe, T. Manshouri, M. Yared, F. Giles, H. Kantarjian, J. Cortes, D. Thomas, M. Keating, E. Freireich, M. Albitar, Differences in CD33 intensity between various myeloid neoplasms, *Am. J. Clin. Pathol.* **118**, 560–566 (2002).
62. L. Munoz, J. F. Nomdedeu, O. Lopez, C. <aria J., M. Bellido, A. Aventin, S. Brunet, J. Sierra, Interleukin-3 receptor alpha chain (CD123) is widely expressed in hematological malignancies, *Haematologica* **86**, 1261–1269 (2001).
63. U. Testa, R. Riccioni, S. Militi, E. Coccia, E. Stellacci, P. Samoggia, G. Mariani, A. Rossini, A. Battistini, F. Lo-coco, C. Peschle, Elevated expression IL-3alpha in acute myelogenous leukemia is associated with enhanced blast proliferation, increased cellularity, and poor prognosis, *Blood* **100**, 2980–2988 (2002).
64. N. K. Damle, P. Frost, Antibody-targeted chemotherapy with immunoconjugates of calicheamicin, *Curr. Opin. Pharmacol.* **3**, 386–390 (2003).
65. J. G. Drachman, R. P. Lyon, I. Stone, L. Westendorf, S. C. Jeffrey, D. R. Benjamin, K. Klussman, K. H. Harrington, P. D. Senter, C. Yu, D. Sussman, R. B. Walter, D. Meyer, M. C. Ryan, M. S. Kung Sutherland, J. A. McEarchern, P. J. Burke, H. Kostner, W. Zeng, I. D. Bernstein, SGN-CD33A: a novel CD33-targeting antibody-drug conjugate using a pyrrolobenzodiazepine dimer is active in models of drug-resistant AML, *Blood* **122**, 1455–1463 (2013).
66. E. L. Sievers, R. A. Larson, E. A. Stadtmauer, E. Estey, B. Löwenberg, H. Dombret, C. Karanes, M. Theobald, J. M. Bennett, M. L. Sherman, M. S. Berger, C. B. Eten, M. R. Loken, J. J. M. Van Dongen, I. D. Bernstein, F. R. Appelbaum, Efficacy and safety of gemtuzumab ozogamicin in patients with CD33-positive acute myeloid leukemia in first relapse, *J. Clin. Oncol.* **19**, 3244–3254 (2001).
67. R. A. Larson, E. L. Sievers, E. A. Stadtmauer, B. Löwenberg, E. H. Estey, H. Dombret, M. Theobald, D. Voliotis, J. M. Bennett, M. Richte, L. H. Leopold, M. S. Berger, M. L. Sherman, M. R. Loken, J. J. M. Van Dongen, I. D. Bernstein, F. R. Appelbaum, Final report of the efficacy and safety of gemtuzumab ozogamicin (Mylotarg) in patients with CD33-positive acute myeloid leukemia in first recurrence, *Cancer* **104**, 1442–1452 (2005).
68. S. Amadori, S. Suciu, D. Selleslag, F. Aversa, G. Gaidano, M. Musso, L. Annino, A. Venditti, M. T. Voso, C. Mazzone, D. Magro, P. De Fabritiis, P. Muus, G. Alimena, M. Mancini, A. Hagemeijer, F. Paoloni, M. Vignetti, P. Fazi, L. Meert, S. M. Ramadan, R. Willemze, T. de Witte, F. Baron, Gemtuzumab Ozogamicin Versus Best Supportive Care in Older Patients With Newly

Diagnosed Acute Myeloid Leukemia Unsuitable for Intensive Chemotherapy: Results of the Randomized Phase III EORTC-GIMEMA AML-19 Trial, *J. Clin. Oncol.* **34**, 972–979 (2016).
69. B. Li, W. Zhao, X. Zhang, J. Wang, X. Luo, S. D. Baker, C. T. Jordan, Y. Dong, Design, synthesis and evaluation of anti-CD123 antibody drug conjugates, *Bioorganic Med. Chem.* **24**, 5855–5860 (2016).
70. Y. Kovtun, G. E. Jones, S. Adams, L. Harvey, C. A. Audette, A. Wilhelm, C. Bai, L. Rui, R. Laleau, F. Liu, O. Ab, Y. Setiady, N. C. Yoder, V. S. Goldmacher, R. V. J. Chari, J. Pinkas, T. Chittenden, A CD123-targeting antibody-drug conjugate, IMGN632, designed to eradicate AML while sparing normal bone marrow cells, *Blood Adv.* **2**, 848–858 (2018).
71. L. Han, J. L. Jorgensen, C. Brooks, C. Shi, Q. Zhang, G. M. Nogueras Gonzalez, A. Cavazos, R. Pan, H. Mu, S. A. Wang, J. Zhou, G. Ai-Atrash, S. O. Ciurea, M. Rettig, J. F. Dipersio, J. Cortes, X. Huang, H. M. Kantarjian, M. Andreeff, F. Ravandi, M. Konopleva, Antileukemia efficacy and mechanisms of action of SL-101, a novel anti-CD123 antibody conjugate, in acute myeloid leukemia, *Clin. Cancer Res.* **23**, 3385–3395 (2017).
72. P. A. Baeuerle, C. Reinhardt, Bispecific T-cell engaging antibodies for cancer therapy, *Cancer Res.* **69**, 4941–4944 (2009).
73. C. Krupka, P. Kufer, R. Kischel, G. Zugmaier, J. Bögeholz, T. Köhnke, F. S. Lichtenegger, S. Schneider, K. H. Metzeler, M. Fiegl, K. Spiekermann, P. A. Baeuerle, W. Hiddemann, G. Riethmüller, M. Subklewe, CD33 target validation and sustained depletion of AML blasts in long-term cultures by the bispecific T-cell-engaging antibody AMG 330, *Blood* **123**, 356–365 (2014).
74. M. Friedrich, A. Henn, T. Raum, M. Bajtus, K. Matthes, L. Hendrich, J. Wahl, P. Hoffmann, R. Kischel, M. Kvesic, J. W. Slootstra, P. A. Baeuerle, P. Kufer, B. Rattel, Preclinical Characterization of AMG 330, a CD3/CD33-Bispecific T-Cell-Engaging Antibody with Potential for Treatment of Acute Myelogenous Leukemia, *Mol. Cancer Ther.* **13**, 1549–1557 (2014).
75. S. Y. Chu, E. Pong, H. Chen, S. Phung, E. W. Chan, N. A. Endo, R. Rashid, C. Bonzon, I. W. L. Leung, U. S. Muchhal, G. L. Moore, M. j. Bernett, D. E. Szymkowski, J. R. Desjarlais, Immunotherapy with long-lived anti-CD123 x anti-CD3 bispecific antibodies stimulates potent t cell-mediated killing of human AML cell lines and of CD123+ cells in monkeys: A potential therapy for acute myelogenous leukemia, *Blood* **123**, 2316 (2014).
76. F. Ravandi, A. Bashey, J. M. Foran, W. Stock, R. Mawad, W. Blum, M. W. Saville, C. M. Johnson, G. J. Vanasse, T. Ly, H. M. Kantarjian, B. Bhatnagar, K. Takahashi, A. S. Mims, Complete responses in relapsed/refractory acute myeloid leukemia (AML) patients on a weekly dosing schedule of XmAb14045, a CD123 x CD3 T cell-engaging bispecific antibody: Initial results of a phase 1 study, *Blood* **132**, 763 (2018).
77. M. L. Schubert, J. M. Hoffmann, P. Dreger, C. Müller-Tidow, M. Schmitt, Chimeric antigen receptor transduced T cells: Tuning up for the next generation, *Int. J. Cancer* **142**, 1738–1747 (2018).
78. YESCARTA (axicabtagene ciloleucel) (2018) (available at https://www.fda.gov/vaccines-blood-biologics/cellular-gene-therapy-products/yescarta-axicabtagene-ciloleucel).
79. S. Gill, Chimeric antigen receptor T cell therapy in AML: How close are we?, *Best Pract. Res. Clin. Haematol.* **29**, 329–333 (2016).
80. S. Gill, S. K. Tasian, M. Ruella, O. Shestova, Y. Li, D. L. Porter, M. Carroll, G. Danet-Desnoyers, J. Scholler, S. A. Grupp, C. H. June, M. Kalos, Preclinical targeting of human acute myeloid leukemia and myeloablation using chimeric antigen receptor-modified T cells, *Blood* **123**, 2343–2354 (2014).
81. S. S. Kenderian, M. Ruella, O. Shestova, M. Klichinsky, V. Aikawa, J. J. D. Morrissette, J. Scholler, D. Song, D. L. Porter, M. Carroll, C. H. June, S. Gill, CD33-specific chimeric antigen receptor T cells exhibit potent preclinical activity against human acute myeloid leukemia, *Leukemia* **29**, 1637–1647 (2015).
82. M. Fan, M. Li, L. Gao, S. Geng, J. Wang, Y. Wang, Z. Yan, L. Yu, Chimeric antigen receptors for adoptive T cell therapy in acute myeloid leukemia, *J. Hematol. Oncol.* **10**, 1–14

(2017).
83. L. Chen, H. Mao, J. Zhang, J. Chu, S. Devine, M. A. Caligiuri, J. Yu, Targeting FLT3 by chimeric antigen receptor T cells for the treatment of acute myeloid leukemia, *Leukemia* **31**, 1830–1834 (2017).
84. R. C. Lynn, M. Poussin, A. Kalota, Y. Feng, P. S. Low, D. S. Dimitrov, D. J. Powell, Targeting of folate receptor β on acute myeloid leukemia blasts with chimeric antigen receptor-expressing T cells, *Blood* **125**, 3466–3476 (2015).
85. H. Tashiro, T. Sauer, T. Shum, K. Parikh, M. Mamonkin, B. Omer, R. H. Rouce, P. Lulla, C. M. Rooney, S. Gottschalk, M. K. Brenner, Treatment of Acute Myeloid Leukemia with T Cells Expressing Chimeric Antigen Receptors Directed to C-type Lectin-like Molecule 1, *Mol. Ther.* **25**, 2202–2213 (2017).
86. L. Zhang, T. F. Gajewski, J. Kline, PD-1/PD-L1 interactions inhibit anti-tumor immune responses in a murine acute myeloid leukemia model, *Blood* **114**, 1545–1553 (2009).
87. M. Dail, L. Yang, C. Green, C. Ma, A. Robert, E. E. Kadel, H. Koeppen, J. Adamkewics, J. Byon, J. Woodard, S. J. Rodig, J. M. Venstrom, Distinct patterns of PD-L1 and PD-L2 expression by tumor and non-tumor cells in patients with MM, MDS, and AML, *Blood* **128**, 1340 (2016).
88. A. V. Balar, J. S. Weber, PD-1 and PD-L1 antibodies in cancer: current status and future directions, *Cancer Immunol. Immunother.* **66**, 551–564 (2017).
89. J. C. D. Schwartz, X. Zhang, A. A. Fedorov, S. G. Nathenson, S. C. Almo, Structural basis for co-stimulation by the human CTLA-4/B7-2 complex, *Nature* **410**, 604–608 (2001).
90. B. Rowshanravan, N. Halliday, D. M. Sansom, CTLA-4: A moving target in immunotherapy, *Blood* **131**, 58–67 (2018).
91. C. E. Rudd, A. Taylor, H. Schneider, CD28 and CTLA-4 coreceptor expression and signal transduction, *Immunol. Rev.* **229**, 12–26 (2009).
92. K. A. Marrone, W. Ying, J. Naidoo, Immune-Related Adverse Events From Immune Checkpoint Inhibitors, *Clin. Pharmacol. Ther.* **100**, 242–251 (2016).
93. B. El Osta, F. Hu, R. Sadek, R. Chintalapally, S. C. Tang, Not all immune-checkpoint inhibitors are created equal: Meta-analysis and systematic review of immune-related adverse events in cancer trials, *Crit. Rev. Oncol. Hematol.* **119**, 1–12 (2017).
94. B. Gyurkocza, H. M. Lazarus, S. Giralt, Allogeneic hematopoietic cell transplantation in patients with AML not achieving remission: Potentially curative therapy, *Bone Marrow Transplant.* **52**, 1083–1090 (2017).
95. Y. S. Jethava, S. Sica, B. Savani, F. Socola, M. Jagasia, M. Mohty, A. Nagler, A. Bacigalupo, Conditioning regimens for allogeneic hematopoietic stem cell transplants in acute myeloid leukemia, *Bone Marrow Transplant.* **52**, 1504–1511 (2017).
96. D. Modi, A. Deol, S. Kim, L. Ayash, A. Alavi, M. Ventimiglia, D. Bhutani, V. Ratanatharathorn, J. P. Uberti, Age does not adversely influence outcomes among patients older than 60 years who undergo allogeneic hematopoietic stem cell transplant for AML and myelodysplastic syndrome, *Bone Marrow Transplant.* **52**, 1530–1536 (2017).
97. A. K. Burnett, K. Wheatley, A. H. Goldstone, R. F. Stevens, I. M. Hann, J. H. K. Rees, G. Harrison, The value of allogeneic bone marrow transplant in patients with acute myeloid leukaemia at differing risk of relapse: results of the UK MRC AML 10 trial, *Br. J. Haematol.* **118**, 385–400 (2002).
98. J. Griffith, J. Black, C. Faerman, L. Swenson, M. Wynn, F. Lu, J. Lippke, K. Saxena, W. Street, The Structural Basis for Autoinhibition of FLT3 by the Juxtamembrane Domain, *Mol. Cell* **13**, 169–178 (2004).
99. A. B. Williams, L. Li, B. Nguyen, P. Brown, M. Levis, D. Small, Fluvastatin inhibits FLT3 glycosylation in human and murine cells and prolongs survival of mice with FLT3/ITD leukemia, *Blood* **120**, 3069–3079 (2012).
100. S. D. Lyman, L. James, T. V. Bos, P. de Vries, K. Brasel, B. Gilniak, L. T. Hollingsworth, K.

S. Picha, H. J. McKenna, R. R. Splett, F. A. Fletcher, E. Maraskovsky, T. Farrah, D. Foxworthe, D. E. Williams, M. P. Beckmann, Molecular cloning of a ligand for the flt3/flk2 tyrosine kinase receptor: A proliferative factor for primitive hematopoietic cells, *Cell* **75**, 1157–1167 (1993).
101. S. D. Lyman, L. James, J. Zappone, P. R. Sleath, M. P. Beckmann, T. Bird, Characterization of the protein encoded by the flt3 (flk2) receptor-like tyrosine kinase gene, *Oncogene1* **8**, 8150822 (1993).
102. J. A. Zorn, Q. Wang, E. Fujimura, T. Barros, J. Kuriyan, Crystal Structure of the FLT3 Kinase Domain Bound to the Inhibitor Quizartinib (AC220), *PLoS One* , 1–15 (2015).
103. S. R. Hubbard, Juxtamembrane autoinhibition in receptor tyrosine kinases, *Nat. Rev. Mol. Cell Biol.* **5**, 464–470 (2004).
104. T. Grafone, M. Palmisano, C. Nicci, S. Storti, C. Giovanni, P. Ii, M. Medicine, An overview on the role of FLT3-tyrosine kinase receptor in acute myeloid leukemia : biology and treatment, *Oncol. Rev.* **6**, 64–74 (2012).
105. C. Thiede, C. Steudel, B. Mohr, M. Schaich, U. Scha, U. Platzbecker, M. Wermke, M. Bornha, M. Ritter, A. Neubauer, G. Ehninger, T. Illmer, Analysis of FLT3-activating mutations in 979 patients with acute myelogenous leukemia : association with FAB subtypes and identification of subgroups with poor prognosis, *Blood* **99**, 4326–4336 (2002).
106. P. D. Kottaridis, R. E. Gale, M. E. Frew, G. Harrison, S. E. Langabeer, A. A. Belton, H. Walker, K. Wheatley, D. T. Bowen, A. K. Burnett, A. H. Goldstone, D. C. Linch, The presence of a FLT3 internal tandem duplication in patients with acute myeloid leukemia (AML) adds important prognostic information to cytogenetic risk group and response to the first cycle of chemotherapy : analysis of 854 patients from the United K, *Blood* **98**, 1752–1760 (2001).
107. R. E. Gale, C. Green, C. Allen, A. J. Mead, A. K. Burnett, R. K. Hills, The impact of FLT3 internal tandem duplication mutant level, number, size, and interaction with NPM1 mutations in a large cohort of young adult patients with acute myeloid leukemia, *Blood* **111**, 2776–2785 (2008).
108. S. Meshinchi, W. G. Woods, D. L. Stirewalt, D. a. Sweetser, J. D. Buckley, T. K. Tjoa, I. D. Bernstein, J. P. Radich, Prevalence and prognostic significance of Flt3 internal tandem duplication in pediatric acute myeloid leukemia, *Blood* **97**, 89–94 (2001).
109. S. P. Whitman, K. J. Archer, L. Feng, C. Baldus, B. Becknell, B. D. Carlson, A. J. Carroll, K. Mro, J. W. Vardiman, S. L. George, J. E. Kolitz, R. A. Larson, C. D. Bloomfield, M. A. Caligiuri, Absence of the Wild-Type Allele Predicts Poor Prognosis in Adult de Novo Acute Myeloid Leukemia with Normal Cytogenetics and the Internal Tandem Duplication of FLT3 : A Cancer and Leukemia Group B Study 1, *Cancer Res.* **61**, 7233–7239 (2001).
110. Y. Yamamoto, H. Kiyoi, Y. Nakano, R. Suzuki, Y. Kodera, S. Miyawaki, N. Asou, K. Kuriyama, F. Yagasaki, C. Shimazaki, H. Akiyama, K. Saito, M. Nishimura, T. Motoji, K. Shinagawa, A. Takeshita, H. Saito, R. Ueda, R. Ohno, T. Naoe, Activating mutation of D835 within the activation loop of FLT3 in human hematologic malignancies, *Blood* **97**, 2434–2439 (2001).
111. F. M. Abu-Duhier, A. C. Goodeve, G. A. Wilson, R. S. Care, I. R. Peake, J. T. Reilly, Identification of novel FLT-3 Asp835 mutations in adult acute myeloid leukaemia., *Br. J. Haematol.* **113**, 983–8 (2001).
112. L. R. Klug, J. D. Kent, M. C. Heinrich, Structural and clinical consequences of activation loop mutations in class III receptor tyrosine kinases, *Pharmacol. Ther.* **191**, 123–134 (2018).
113. C. Choudhary, C. Brandts, J. Schwable, L. Tickenbrock, B. Sargin, A. Ueker, F.-D. Böhmer, W. E. Berdel, C. Müller-Tidow, H. Serve, Activation mechanisms of STAT5 by oncogenic Flt3-ITD., *Blood* **110**, 370–4 (2007).
114. M. Mizuki, J. Schwa, C. Steur, C. Choudhary, S. Agrawal, I. Matsumura, Y. Kanakura, F. D. Bo, Suppression of myeloid transcription factors and induction of STAT response genes by AML-specific Flt3 mutations, **101**, 3164–3173 (2003).
115. S. Takahashi, H. Harigae, K. Kumura Ishii, M. Inomata, T. Fujiwara, H. Yokoyama, K.

Ishizawa, J. Kameoka, J. D. Licht, T. Sasaki, M. Kaku, Over-expression of Flt3 induces NF-kB pathway and increases the expression of IL-6, *Leuk. Res.* **29**, 893–899 (2005).
116. J. Grosjean-Raillard, L. Adès, S. Boehrer, M. Tailler, C. Fabre, T. Braun, S. De Botton, A. Israel, P. Fenaux, G. Kroemer, Flt3 receptor inhibition reduces constitutive NFkappaB activation in high-risk myelodysplastic syndrome and acute myeloid leukemia., *Apoptosis* **13**, 1148–61 (2008).
117. S. E. Meyer, T. Qin, D. E. Muench, K. Masuda, M. Venkatasubramanian, E. Orr, L. Suarez, S. D. Gore, R. Delwel, E. Paietta, M. S. Tallman, H. Fernandez, A. Melnick, M. M. Le Beau, S. Kogan, N. Salomonis, M. E. Figueroa, H. L. Grimes, DNMT3A Haploinsufficiency Transforms FLT3 ITD Myeloproliferative Disease into a Rapid, Spontaneous, and Fully Penetrant Acute Myeloid Leukemia, *Cancer Discov.* (2016), doi:10.1158/2159-8290.CD-16-0008.
118. A. Fasan, C. Haferlach, T. Alpermann, S. Jeromin, V. Grossmann, C. Eder, S. Weissmann, F. Dicker, A. Kohlmann, S. Schindela, W. Kern, T. Haferlach, S. Schnittger, The role of different genetic subtypes of CEBPA mutated AML, *Leukemia* **28**, 794–803 (2014).
119. K. P. Patel, F. Ravandi, D. Ma, A. Paladugu, B. A. Barkoh, L. J. Medeiros, R. Luthra, Acute Myeloid Leukemia With IDH1 or IDH2 Mutation, *Am. J. Clin. Pathol.* **135**, 35–45 (2011).
120. J. L. Patel, J. A. Schumacher, K. Frizzell, S. Sorrells, W. Shen, A. Clayton, R. Jattani, T. W. Kelley, Coexisting and cooperating mutations in NPM1-mutated acute myeloid leukemia, *Leuk. Res.* **56**, 7–12 (2017).
121. S. Fröhling, R. F. Schlenk, J. Breitruck, A. Benner, S. Kreitmeier, K. Tobis, H. Döhner, K. Döhner, Prognostic significance of activating FLT3 mutations in younger adults (16 to 60 years) with acute myeloid leukemia and normal cytogenetics: A study of the AML study group Ulm, *Blood* **100**, 4372–4380 (2002).
122. L.-Y. Shih, T. Lin, P. Wang, J. Wu, P. Dunn, M. Kuo, C. Huang, Internal Tandem Duplication of fms -Like Tyrosine Kinase 3 Is Associated with Poor Outcome in Patients with Myelodysplastic Syndrome, *Cancer* **101**, 989–998 (2004).
123. D. L. Stirewalt, K. J. Kopecky, S. Meshinchi, J. H. Engel, E. L. Pogosova-agadjanyan, J. Linsley, M. L. Slovak, C. L. Willman, J. P. Radich, Size of FLT3 internal tandem duplication has prognostic significance in patients with acute myeloid leukemia, *Blood* **107**, 3724–3727 (2006).
124. S. Kayser, R. F. Schlenk, M. C. Londono, F. Breitenbuecher, K. Wittke, J. Du, S. Groner, D. Spa, A. Ganser, H. Do, T. Fischer, K. Do, Insertion of FLT3 internal tandem duplication in the tyrosine kinase domain-1 is associated with resistance to chemotherapy and inferior outcome, *Blood* **114**, 2386–2393 (2016).
125. M. Larrosa-Garcia, M. R. Baer, FLT3 Inhibitors in Acute Myeloid Leukemia: Current Status and Future Directions, *Mol. Cancer Ther.* **16**, 991–1001 (2017).
126. R. Roskoski, Classification of small molecule protein kinase inhibitors based upon the structures of their drug-enzyme complexes, *Pharmacol. Res.* **103**, 26–48 (2016).
127. M. Hassanein, M. H. Almahayni, S. O. Ahmed, S. Gaballa, R. El Fakih, FLT3 Inhibitors for Treating Acute Myeloid Leukemia, *Clin. Lymphoma, Myeloma Leuk.* , 1–7 (2016).
128. P. W. Manley, G. Caravatti, P. Furet, J. Roesel, P. Tran, T. Wagner, M. Wartmann, Comparison of the Kinase Profile of Midostaurin (Rydapt) with That of Its Predominant Metabolites and the Potential Relevance of Some Newly Identified Targets to Leukemia Therapy, *Biochemistry* **57**, 5576–5590 (2018).
129. R. Roskoski, Sunitinib: A VEGF and PDGF receptor protein kinase and angiogenesis inhibitor, *Biochem. Biophys. Res. Commun.* **356**, 323–328 (2007).
130. M. W. Karaman, S. Herrgard, D. K. Treiber, P. Gallant, C. E. Atteridge, B. T. Campbell, K. W. Chan, P. Ciceri, M. I. Davis, P. T. Edeen, R. Faraoni, M. Floyd, J. P. Hunt, D. J. Lockhart, Z. V. Milanov, M. J. Morrison, G. Pallares, H. K. Patel, S. Pritchard, L. M. Wodicka, P. P. Zarrinkar, A quantitative analysis of kinase inhibitor selectivity, *Nat. Biotechnol.* **26**, 127–132 (2008).
131. Q. Chao, K. G. Sprankle, R. M. Grotzfeld, A. G. Lai, T. a. Carter, A. M. Velasco, R. N. Gunawardane, M. D. Cramer, M. F. Gardner, J. James, P. P. Zarrinkar, H. K. Patel, S. S.

Bhagwat, Identification of N-(5-tert-butyl-isoxazol-3-yl)-N???-{4-[7-(2- morpholin-4-yl-ethoxy)imidazo-[2,1-b][1,3]benzothiazol-2-yl]phenyl}urea dihydrochloride (AC220), a uniquely potent, selective, and efficacious FMS-like tyrosine kinase-3 (FLT3) inhibitor, *J. Med. Chem.* **52**, 7808–7816 (2009).
132. C. C. Smith, E. A. Lasater, K. C. Lin, Q. Wang, M. Quino, W. K. Stewart, L. E. Damon, A. E. Perl, G. R. Jeschke, M. Sugita, M. Carroll, S. C. Kogan, J. Kuriyan, N. P. Shah, Crenolanib is a selective type I pan-FLT3 inhibitor, *PNAS* **111**, 5319–5324 (2014).
133. H. Ma, B. Nguyen, L. Li, S. Greenblatt, A. Williams, M. Zhao, M. Levis, M. Rudek, A. Duffield, D. Small, TTT-3002 is a novel FLT3 tyrosine kinase inhibitor with activity against FLT3-associated leukemias in vitro and in vivo, *Blood* **123**, 1525–1535 (2014).
134. T. Yamaura, T. Nakatani, K. Uda, H. Ogura, W. Shin, N. Kurokawa, K. Saito, N. Fujikawa, T. Date, M. Takasaki, D. Terada, A. Hirai, A. Akashi, F. Chen, Y. Adachi, Y. Ishikawa, F. Hayakawa, S. Hagiwara, T. Naoe, H. Kiyoi, A novel irreversible FLT3 inhibitor, FF-10101, shows excellent efficacy against AML cells with FLT3 mutations, *Blood* **131**, 426–438 (2018).
135. D. Propper, A. McDonald, A. Man, P. Thavasu, F. Balkwill, J. Baybrooke, F. Caponigro, P. Graf, C. Dutreix, R. Blackie, S. Kaye, T. Ganesan, D. Talbot, A. Harris, C. Twelves, Phase I and pharmacokinetic study of PKC412, an inhibitor of protein kinase C., *J. Clin. Oncol.* **19**, 1485–1492 (2001).
136. M. R. Jirousek, P. G. Goekjian, Protein kinase C inhibitors as novel anticancer drugs, *Expert Opin. Investig. Drugs* **10**, 2117–2140 (2001).
137. E. Weisberg, C. Boulton, L. M. Kelly, P. Manley, D. Fabbro, T. Meyer, D. G. Gilliland, J. D. Griffin, Inhibition of mutant FLT3 receptors in leukemia cells by the small molecule tyrosine kinase inhibitor PKC412., *Cancer Cell* **1**, 433–43 (2002).
138. M. Levis, Midostaurin approved for FLT3-mutated AML, *Blood* **129**, 3403–3406 (2017).
139. Y. Furukawa, H. A. Vu, M. Akutsu, T. Odgerel, T. Izumi, S. Tsunoda, Y. Matsuo, K. Kirito, Y. Sato, H. Mano, Y. Kano, Divergent cytotoxic effects of PKC412 in combination with conventional antileukemic agents in FLT3 mutation-positive versus -negative leukemia cell lines, *Leukemia* **21**, 1005–1014 (2007).
140. T. Fischer, R. M. Stone, D. J. DeAngelo, I. Galinsky, E. Estey, C. Lanza, E. Fox, G. Ehninger, E. J. Feldman, G. J. Schiller, V. M. Klimek, S. D. Nimer, D. G. Gilliland, C. Dutreix, A. Huntsman-Labed, J. Virkus, F. J. Giles, Phase IIB trial of oral midostaurin (PKC412), the FMS-like tyrosine kinase 3 receptor (FLT3) and multi-targeted kinase inhibitor, in patients with acute myeloid leukemia and high-risk myelodysplastic syndrome with either wild-type or mutated FLT3, *J. Clin. Oncol.* **28**, 4339–4345 (2010).
141. R. M. Stone, D. J. Deangelo, V. Klimek, I. Galinsky, E. Estey, S. D. Nimer, W. Grandin, D. Lebwohl, Y. Wang, P. Cohen, E. A. Fox, D. Neuberg, J. Clark, D. G. Gilliland, J. D. Griffin, W. Dc, R. M. Stone, D. J. Deangelo, V. Klimek, I. Galinsky, E. Estey, S. D. Nimer, W. Grandin, D. Lebwohl, Patients with acute myeloid leukemia and an activating mutation in FLT3 respond to a small-molecule FLT3 tyrosine kinase inhibitor , PKC412, *Blood* **105**, 54–60 (2005).
142. R. M. Stone, T. Fischer, R. Paquette, G. Schiller, C. A. Schiffer, G. Ehninger, J. Cortes, H. M. Kantarjian, D. J. Deangelo, A. Huntsman-Labed, C. Dutreix, A. Del Corral, F. Giles, Phase IB study of the FLT3 kinase inhibitor midostaurin with chemotherapy in younger newly diagnosed adult patients with acute myeloid leukemia, *Leukemia* **26**, 2061–2068 (2012).
143. R. M. Stone, S. J. Mandrekar, B. L. Sanford, K. Laumann, S. Geyer, C. D. Bloomfield, C. Thiede, T. W. Prior, K. Döhner, G. Marcucci, F. Lo-Coco, R. B. Klisovic, A. Wei, J. Sierra, M. A. Sanz, J. M. Brandwein, T. de Witte, D. Niederwieser, F. R. Appelbaum, B. C. Medeiros, M. S. Tallman, J. Krauter, R. F. Schlenk, A. Ganser, H. Serve, G. Ehninger, S. Amadori, R. A. Larson, H. Döhner, Midostaurin plus Chemotherapy for Acute Myeloid Leukemia with a *FLT3* Mutation, *N. Engl. J. Med.* **377**, 454–464 (2017).
144. P. P. Zarrinkar, R. N. Gunawardane, M. D. Cramer, M. F. Gardner, D. Brigham, B. Belli, M. W. Karaman, K. W. Pratz, G. Pallares, Q. Chao, K. G. Sprankle, H. K. Patel, M. Levis, R. C.

Armstrong, J. James, S. S. Bhagwat, AC220 is a uniquely potent and selective inhibitor of FLT3 for the treatment of acute myeloid leukemia (AML), *Blood* **114**, 2984–2993 (2009).
145. P. P. Zarrinkar, R. N. Gunawardane, M. D. Cramer, M. F. Gardner, D. Brigham, B. Belli, M. W. Karaman, K. W. Pratz, G. Pallares, Q. Chao, K. G. Sprankle, H. K. Patel, M. Levis, R. C. Armstrong, J. James, S. S. Bhagwat, AC220 is a uniquely potent and selective inhibitor of FLT3 for the treatment of acute myeloid leukemia (AML)., *Blood* **114**, 2984–92 (2009).
146. K. M. Kampa-Schittenhelm, M. C. Heinrich, F. Akmut, H. Döhner, K. Döhner, M. M. Schittenhelm, Quizartinib (AC220) is a potent second generation class III tyrosine kinase inhibitor that displays a distinct inhibition profile against mutant-FLT3, -PDGFRA and -KIT isoforms, *Mol. Cancer* **12**, 1–15 (2013).
147. J. E. Cortes, H. Kantarjian, J. M. Foran, D. Ghirdaladze, M. Zodelava, G. Borthakur, G. Gammon, D. Trone, R. C. Armstrong, J. James, M. Levis, Phase I Study of Quizartinib Administered Daily to Patients With Relapsed or Refractory Acute Myeloid Leukemia Irrespective of FMS-Like Tyrosine Kinase 3 – Internal Tandem Duplication Status, *J. Clin. Oncol.* **31**, 3681–3687 (2013).
148. J. Cortes, A. E. Perl, H. Döhner, H. Kantarjian, G. Martinelli, T. Kovacsovics, P. Rousselot, B. Steffen, H. Dombret, E. Estey, S. Strickland, J. K. Altman, C. D. Baldus, A. Burnett, A. Krämer, N. Russell, N. P. Shah, C. C. Smith, E. S. Wang, N. Ifrah, G. Gammon, D. Trone, D. Lazzaretto, M. Levis, Quizartinib, an FLT3 inhibitor, as monotherapy in patients with relapsed or refractory acute myeloid leukaemia: an open-label, multicentre, single-arm, phase 2 trial, *Lancet Oncol.* **19**, 889–903 (2018).
149. J. E. Cortes, M. S. Tallman, G. J. Schiller, D. Trone, G. Gammon, S. L. Goldberg, A. E. Perl, J.-P. Marie, G. Martinelli, H. M. Kantarjian, M. J. Levis, Phase 2b study of two dosing regimens of quizartinib monotherapy in FLT3-ITD mutated, relapsed or refractory AML, *Blood* **132**, blood-2018-01-821629 (2018).
150. L. Y. Lee, D. Hernandez, T. Rajkhowa, S. C. Smith, J. R. Raman, B. Nguyen, D. Small, M. Levis, Preclinical studies of gilteritinib, a next-generation FLT3 inhibitor, *Blood* **129**, 257–260 (2017).
151. M. Mori, N. Kaneko, Y. Ueno, M. Yamada, R. Tanaka, R. Saito, I. Shimada, K. Mori, S. Kuromitsu, Gilteritinib, a FLT3/AXL inhibitor, shows antileukemic activity in mouse models of FLT3 mutated acute myeloid leukemia, *Invest. New Drugs* **35**, 556–565 (2017).
152. A. E. Perl, J. K. Altman, J. Cortes, C. Smith, M. Litzow, M. R. Baer, D. Claxton, H. P. Erba, S. Gill, S. Goldberg, J. G. Jurcic, R. A. Larson, C. Liu, E. Ritchie, G. Schiller, A. I. Spira, S. A. Strickland, R. Tibes, C. Ustun, E. S. Wang, R. Stuart, C. Röllig, A. Neubauer, G. Martinelli, E. Bahceci, M. Levis, Selective inhibition of FLT3 by gilteritinib in relapsed or refractory acute myeloid leukaemia: a multicentre, first-in-human, open-label, phase 1–2 study, *Lancet Oncol.* **18**, 1061–1075 (2017).
153. FDA approves gilteritinib for relapsed or refractory acute myeloid leukemia (AML) with a FLT3 mutation*FDA* (2018) (available at https://www.fda.gov/drugs/fda-approves-gilteritinib-relapsed-or-refractory-acute-myeloid-leukemia-aml-flt3-mutatation).
154. Gilteritinib improved survival for patients with acute myeloid leukemia*AACR* (2019) (available at https://www.aacr.org/Newsroom/Pages/News-Release-Detail.aspx?ItemID=1295).
155. W. Fiedler, S. Kayser, M. Kebenko, M. Janning, J. Krauter, M. Schittenhelm, K. Götze, D. Weber, G. Göhring, V. Teleanu, F. Thol, M. Heuser, K. Döhner, A. Ganser, H. Döhner, R. F. Schlenk, A phase I/II study of sunitinib and intensive chemotherapy in patients over 60 years of age with acute myeloid leukaemia and activating FLT3 mutations, *Br. J. Haematol.* **169**, 694–700 (2015).
156. L. Ding, T. J. Ley, D. E. Larson, C. A. Miller, D. C. Koboldt, J. S. Welch, J. K. Ritchey, M. A. Young, T. Lamprecht, M. D. Mclellan, J. F. Mcmichael, J. W. Wallis, C. Lu, D. Shen, C. C. Harris, D. J. Dooling, R. S. Fulton, L. L. Fulton, K. Chen, H. Schmidt, J. Kalicki-veizer, V. J. Magrini, L. Cook, S. D. Mcgrath, T. L. Vickery, M. C. Wendl, S. Heath, M. A. Watson, D. C. Link,

M. H. Tomasson, W. D. Shannon, J. E. Payton, S. Kulkarni, P. Westervelt, M. J. Walter, T. A. Graubert, E. R. Mardis, R. K. Wilson, J. F. Dipersio, Clonal evolution in relapsed acute myeloid leukaemia revealed by whole-genome sequencing, *Nat. Med.* **481**, 506–509 (2012).
157. K. W. Pratz, T. Sato, K. M. Murphy, A. Stine, T. Rajkhowa, M. Levis, FLT3-mutant allelic burden and clinical status are predictive of response to FLT3 inhibitors in AML, *Blood* **115**, 1425–1432 (2010).
158. C. C. Smith, Q. Wang, C.-S. Chin, S. Salerno, L. E. Damon, M. J. Levis, A. E. Perl, K. J. Travers, S. Wang, J. P. Hunt, P. P. Zarrinkar, E. E. Schadt, A. Kasarskis, J. Kuriyan, N. P. Shah, Validation of ITD mutations in FLT3 as a therapeutic target in human acute myeloid leukaemia., *Nature* **485**, 260–3 (2012).
159. J. Cools, N. Mentens, P. Furet, D. Fabbro, J. J. Clark, J. D. Griffin, P. Marynen, D. G. Gilliland, Prediction of resistance to small molecule FLT3 inhibitors: Implications for molecularly targeted therapy of acute leukemia, *Cancer Res.* **64**, 6385–6389 (2004).
160. Y. Alvarado, H. M. Kantarjian, R. Luthra, F. Ravandi, G. Borthakur, G. Garcia-Manero, M. Konopleva, Z. Estrov, M. Andreeff, J. E. Cortes, Treatment with FLT3 inhibitor in patients with FLT3-mutated acute myeloid leukemia is associated with development of secondary FLT3-tyrosine kinase domain mutations, *Cancer* **120**, 2142–2149 (2014).
161. C. C. Smith, K. Lin, A. Stecula, A. Sali, N. P. Shah, FLT3 D835 mutations confer differential resistance to type II FLT3 inhibitors, *Leukemia* **29**, 2390–2392 (2015).
162. C. C. Smith, C. Zhang, K. C. Lin, E. A. Lasater, Y. Zhang, E. Massi, L. E. Damon, M. Pendleton, A. Bashir, R. Sebra, A. Perl, A. Kasarskis, R. Shellooe, G. Tsang, H. Carias, B. Powell, E. A. Burton, B. Matusow, J. Zhang, W. Spevak, P. N. Ibrahim, M. H. Le, H. H. Hsu, G. Habets, B. L. West, G. Bollag, N. P. Shah, Characterizing and Overriding the Structural Mechanism of the Quizartinib-Resistant FLT3 " Gatekeeper " F691L Mutation with PLX3397, *Cancer Discov.* (2015), doi:10.1158/2159-8290.CD-15-0060.
163. A. B. Williams, B. Nguyen, L. Li, P. Brown, M. Levis, D. Leahy, D. Small, Mutations of FLT3 / ITD confer resistance to multiple tyrosine kinase inhibitors, *Leukemia* **27**, 48–55 (2013).
164. M. Levis, F. Ravandi, E. S. Wang, M. R. Baer, A. Perl, S. Coutre, H. Erba, R. K. Stuart, M. Baccarini, L. D. Cripe, M. S. Tallman, G. Meloni, L. a Godley, A. a Langston, S. Amadori, I. D. Lewis, A. Nagler, R. Stone, K. Yee, A. Advani, D. Douer, W. Wiktor-Jedrzejczak, G. Juliusson, M. R. Litzow, S. Petersdorf, M. Sanz, H. M. Kantarjian, T. Sato, L. Tremmel, D. M. Bensen-Kennedy, D. Small, B. D. Smith, Results From a Randomized Trial of Salvage Chemotherapy Followed by Lestaurtinib for FLT3 Mutant AML Patients in First Relapse, *Blood* **117**, 3294–3300 (2011).
165. X. Yang, B. D. Smith, S. Knapper, T. Sato, M. Levis, P. White, S. Galkin, A. Burnett, D. Small, FLT3 ligand impedes the efficacy of FLT3 inhibitors in vitro and in vivo, *Blood* **117**, 3286–3293 (2011).
166. F. Chen, Y. Ishikawa, A. Akashi, T. Naoe, H. Kiyoi, Co-expression of wild-type FLT3 attenuates the inhibitory effect of FLT3 inhibitor on FLT3 mutated leukemia cells, *Oncotarget* **7**, 47018–47032 (2016).
167. O. Piloto, M. Wright, P. Brown, K. T. Kim, M. Levis, D. Small, Prolonged exposure to FLT3 inhibitors leads to resistance via activation of parallel signaling pathways, *Blood* **109**, 1643–1652 (2007).
168. E. Siendones, N. Barbarroja, L. Torres, P. Buendı, F. Velasco, E. Siendones, N. Barbarroja, L. Arı, Inhibition of Flt3-activating mutations does not prevent constitutive activation of ERK / Akt / STAT pathways in some AML cells : a possible cause for the limited effectiveness of monotherapy with small-molecule inhibitors, *Hematol. Oncol.* **25**, 30–37 (2007).
169. W. Kolch, M. Halasz, M. Granovskaya, B. N. Kholodenko, The dynamic control of signal transduction networks in cancer cells, *Nat. Rev. Cancer* **15**, 515–527 (2015).
170. O. Lindblad, E. Cordero, A. Puissant, L. Macaulay, A. Ramos, N. N. Kabir, J. Sun, K. Haraldsson, M. T. Hemann, Å. Borg, F. Levander, K. Stegmaier, K. Pietras, L. Rönnstrand, J. U.

Kazi, Aberrant activation of the PI3K / mTOR pathway promotes resistance to sorafenib in AML, *Oncogene* **35**, 5119–5131 (2016).
171. E. Weisberg, Q. Liu, X. Zhang, E. Nelson, M. Sattler, F. Liu, M. Nicolais, J. Zhang, C. Mitsiades, R. W. Smith, R. Stone, I. Galinsky, A. Nonami, J. D. Griffin, N. Gray, Selective Akt Inhibitors Synergize with Tyrosine Kinase Inhibitors and Effectively Override Stroma-Associated Cytoprotection of Mutant FLT3-Positive AML Cells, *PLoS One* **8** (2013), doi:10.1371/journal.pone.0056473.
172. A. Wang, H. Wu, C. Chen, C. Hu, Z. Qi, K. Yu, X. Liu, F. Zou, Z. Zhao, J. Wu, J. Liu, F. Liu, L. Wang, R. M. Stone, I. A. Galinksy, D. Griffin, S. Zhang, E. L. Weisberg, J. Liu, Q. Liu, Dual inhibition of AKT / FLT3-ITD by A674563 overcomes FLT3 ligand-induced drug resistance in FLT3-ITD positive AML, *Oncotarget* **7** (2016), doi:10.18632/oncotarget.8675.
173. M. G. Mohi, C. Boulton, T.-L. Gu, D. W. Sternberg, D. Neuberg, J. D. Griffin, D. G. Gilliland, B. G. Neel, Combination of rapamycin and protein tyrosine kinase (PTK) inhibitors for the treatment of leukemias caused by oncogenic PTKs, *Proc. Natl. Acad. Sci.* **101**, 3130–3135 (2004).
174. E. Weisberg, A. Ray, E. Nelson, S. Adamia, R. Barrett, M. Sattler, C. Zhang, J. F. Daley, D. Frank, E. Fox, J. D. Griffin, Reversible Resistance Induced by FLT3 Inhibition : A Novel Resistance Mechanism in Mutant FLT3-Expressing Cells, *PLoS One* **6** (2011), doi:10.1371/journal.pone.0025351.
175. J. K. Bruner, H. S. Ma, L. Li, A. C. R. Qin, M. A. Rudek, R. J. Jones, M. J. Levis, K. W. Pratz, C. A. Pratilas, D. Small, Adaptation to TKI treatment reactivates ERK signaling in tyrosine kinase-driven leukemias and other malignancies, *Cancer Res.* , canres.2593.2016 (2017).
176. C. Nishioka, T. Ikezoe, J. Yang, A. Takeshita, A. Taniguchi, N. Komatsu, K. Togitani, H. Koeffler, A. Yokoyama, Blockade of MEK / ERK signaling enhances sunitinib-induced growth inhibition and apoptosis of leukemia cells possessing activating mutations of the FLT3 gene, *Leuk. Res.* **32**, 865–872 (2008).
177. W. Zhang, G. Borthakur, C. Gao, Y. Chen, H. Mu, V. R. Ruvolo, K. Nomoto, N. Zhao, M. Konopleva, M. Andreeff, The Dual MEK / FLT3 Inhibitor E6201 Exerts Cytotoxic Activity against Acute Myeloid Leukemia Cells Harboring Resistance-Conferring FLT3 Mutations, *Cancer Res.* **76**, 1528–1537 (2016).
178. K. Natarajan, Y. Xie, M. Burcu, D. E. Linn, Y. Qiu, M. R. Baer, Pim-1 Kinase Phosphorylates and Stabilizes 130 kDa FLT3 and Promotes Aberrant STAT5 Signaling in Acute Myeloid Leukemia with FLT3 Internal Tandem Duplication, *PLoS One* **8** (2013), doi:10.1371/journal.pone.0074653.
179. A. S. Green, T. T. Maciel, M.-A. Hospital, C. Yin, F. Mazed, E. C. Townsend, S. Pilorge, M. Lambert, E. Paubelle, A. Jacquel, F. Zylbersztejn, J. Decroocq, L. Poulain, P. Sujobert, N. Jacque, K. Adam, J. C. C. So, O. Kosmider, P. Auberger, O. Hermine, D. M. Weinstock, C. Lacombe, P. Mayeux, G. J. Vanasse, A. Y. Leung, I. C. Moura, D. Bouscary, J. Tamburini, Pim kinases modulate resistance to FLT3 tyrosine kinase inhibitors in FLT3-ITD acute myeloid leukemia, *Sci. Adv.* **1**, e1500221–e1500221 (2015).
180. S. Kapoor, K. Natarajan, P. R. Baldwin, K. A. Doshi, R. G. Lapidus, T. J. Mathias, M. Scarpa, R. Trotta, E. Davila, M. Kraus, D. Huszar, A. E. Tron, D. Perrotti, M. R. Baer, Concurrent inhibition of Pim and FLT3 kinases enhances apoptosis of FLT3-ITD acute myeloid leukemia cells through increased Mcl-1 proteasomal degradation, *Clin. Cancer Res.* **24**, 234–247 (2018).
181. N. Puente-Moncada, P. Costales, I. Antolín, L.-E. Núñez, P. Oro, M. A. Hermosilla, J. Pérez-Escuredo, N. Ríos-Lombardía, A. M. Sanchez-Sanchez, E. Luño, C. Rodríguez, V. Martín, F. Morís, Inhibition of FLT3 and PIM Kinases by EC-70124 Exerts Potent Activity in Preclinical Models of Acute Myeloid Leukemia, *Mol. Cancer Ther.* **17**, 614–624 (2018).
182. W. Czardybon, R. Windak, A. Gołas, M. Gałęzowski, A. Sabiniarz, I. Dolata, M. Salwińska, P. Guzik, M. Zawadzka, E. Gabor-Worwa, B. Winnik, M. Żurawska, E. Kolasińska, E. Wincza,

M. Bugaj, M. Danielewicz, E. Majewska, M. Mazan, G. Dubin, M. Noyszewska-Kania, E. Jabłońska, M. Szydłowski, T. Sewastianik, B. Puła, A. Szumera-Ciećkiewicz, M. Prochorec-Sobieszek, E. Mądro, E. L.- Marańda, K. Warzocha, J. Tamburini, P. Juszczyński, K. Brzózka, A novel, dual pan-PIM/FLT3 inhibitor SEL24 exhibits broad therapeutic potential in acute myeloid leukemia, *Oncotarget* **9**, 16917–16931 (2018).
183. I. K. Park, A. Mishra, J. Chandler, S. P. Whitman, G. Marcucci, M. A. Caligiuri, Inhibition of the receptor tyrosine kinase Axl impedes activation of the FLT3 internal tandem duplication in human acute myeloid leukemia: Implications for Axl as a potential therapeutic target, *Blood* **121**, 2064–2073 (2013).
184. I. K. Park, B. Mundy-Bosse, S. P. Whitman, X. Zhang, S. L. Warner, D. J. Bearss, W. Blum, G. Marcucci, M. A. Caligiuri, Receptor tyrosine kinase Axl is required for resistance of leukemic cells to FLT3-targeted therapy in acute myeloid leukemia, *Leukemia* **29**, 2382–2389 (2015).
185. P.-Y. Dumas, C. Naudin, S. Martin-Lannerée, B. Izac, L. Casetti, O. Mansier, B. Rousseau, A. Artus, M. Dufossée, A. Giese, P. Dubus, A. Pigneux, V. Praloran, A. Bidet, A. Villacreces, A. V Guitart, N. Milpied, O. Kosmider, I. Vigon, V. Desplat, I. Dusanter-Fourt, J.-M. Pasquet, Hematopoietic niche drives FLT3-ITD acute myeloid leukemia resistance to quizartinib via STAT5- and hypoxia- dependent up-regulation of AXL., *Haematologica* , haematol.2018.205385 (2019).
186. M. A. Gregory, A. D. Alessandro, F. Alvarez-calderon, J. Kim, T. Nemkov, ATM / G6PD-driven redox metabolism promotes FLT3 inhibitor resistance in acute myeloid leukemia, *PNAS* , 6669–6678 (2016).
187. A. Huang, H. Ju, K. Liu, G. Zhan, D. Liu, S. Wen, G. Garcia-manero, P. Huang, Y. Hu, Metabolic alterations and drug sensitivity of tyrosine kinase inhibitor resistant leukemia cells with a FLT3 / ITD mutation, *Cancer Lett.* **377**, 149–157 (2016).
188. T. Hirade, M. Abe, C. Onishi, T. Taketani, Internal tandem duplication of FLT3 deregulates proliferation and differentiation and confers resistance to the FLT3 inhibitor AC220 by Up - regulating RUNX1 expression in hematopoietic cells, *Int. J. Hematol.* **103**, 95–106 (2016).
189. K. Keegan, C. Li, Z. Li, J. Ma, M. Ragains, S. Coberly, D. Hollenback, J. Eksterowicz, L. Liang, M. Weidner, J. Huard, X. Wang, G. Alba, J. Orf, M.-C. Lo, S. Zhao, R. Ngo, A. Chen, L. Liu, T. Carlson, C. Quéva, L. R. McGee, J. Medina, A. Kamb, D. Wickramasinghe, K. Dai, Preclinical evaluation of AMG 925, a FLT3/CDK4 dual kinase inhibitor for treating acute myeloid leukemia., *Mol. Cancer Ther.* **13**, 880–9 (2014).
190. C. Li, L. Liu, L. Liang, Z. Xia, Z. Li, X. Wang, L. R. McGee, K. Newhall, A. Sinclair, A. Kamb, D. Wickramasinghe, K. Dai, AMG 925 Is a Dual FLT3/CDK4 Inhibitor with the Potential to Overcome FLT3 Inhibitor Resistance in Acute Myeloid Leukemia, *Mol. Cancer Ther.* **14**, 375–383 (2015).
191. Y. Wang, Y. Zhi, Q. Jin, S. Lu, G. Lin, H. Yuan, T. Yang, Z. Wang, C. Yao, J. Ling, H. Guo, T. Li, J. Jin, B. Li, L. Zhang, Y. Chen, T. Lu, Discovery of 4-((7H-Pyrrolo[2,3-d]pyrimidin-4-yl)amino)-N-(4-((4-methylpiperazin-1-yl)methyl)phenyl)-1H-pyrazole-3-carboxamide (FN-1501), an FLT3- and CDK-Kinase Inhibitor with Potentially High Efficiency against Acute Myelocytic Leukemia, *J. Med. Chem.* **61**, 1499–1518 (2018).
192. S. Lopez, E. Voisset, J. C. Tisserand, C. Mosca, T. Prebet, D. Santamaria, P. Dubreuil, P. De Sepulveda, An essential pathway links FLT3-ITD, HCK and CDK6 in acute myeloid leukemia, *Oncotarget* **7**, 51163–51173 (2016).
193. E. Griessinger, V. Imbert, P. Lagadec, N. Gonthier, P. Dubreuil, a Romanelli, M. Dreano, J.-F. Peyron, AS602868, a dual inhibitor of IKK2 and FLT3 to target AML cells., *Leukemia* **21**, 877–85 (2007).
194. E. Griessinger, C. Frelin, N. Cuburu, V. Imbert, C. Dageville, M. Hummelsberger, N. Sirvent, M. Dreano, J.-F. Peyron, Preclinical targeting of NF-kB and FLT3 pathways in AML cells, *Leukemia* **22**, 1466–1469 (2008).

195. C. C. Smith, A. Paguirigan, G. R. Jeschke, K. C. Lin, E. Massi, T. Tarver, C. Chin, S. Asthana, A. Oldshen, K. J. Travers, S. Wang, M. J. Levis, A. E. Perl, J. P. Radich, N. P. Shah, Heterogeneous Resistance to Quizartinib in Acute Myeloid Leukemia (AML) Revealed by Single Cell Analysis, *Blood* **130**, 48–59 (2017).
196. P. Motshwene, M. Moncrieffe, J. Grossmann, C. Kao, M. Ayaluru, A. Sandercock, An oligomeric signaling platform formed by the Toll-like receptor signal transducers MyD88 and IRAK-4, *J. Biol. Chem.* **284**, 25404–25411 (2009).
197. S. Lin, Y. Lo, H. Wu, Helical assembly in the MyD88 – IRAK4 – IRAK2 complex in TLR/IL-1R signalling, *Nature* **465**, 885–890 (2010).
198. M. Windheim, M. Stafford, M. Peggie, P. Cohen, Interleukin-1 (IL-1) induces the Lys63-linked polyubiquitination of IL-1 receptor-associated kinase 1 to facilitate NEMO binding and the activation of IkappaBalpha kinase, *Mol. Cell. Biol.* **38**, 1783–1791 (2008).
199. M. Kubo-Murai, K. Hazeki, K. Nigorikawa, T. Omoto, N. Inoue, O. Hazeki, IRAK-4-dependent Degradation of IRAK-1 is a Negative Feedback Signal for TLR-mediated NF-kB Activation, *J. Biochem.* **143**, 295–302 (2008).
200. S. E. Keating, G. M. Maloney, E. M. Moran, A. G. Bowie, IRAK-2 Participates in Multiple Toll-like Receptor Signaling Pathways to NFkB via Activation of TRAF6 Ubiquitination, *J. Biol. Chem.* **282**, 33435–33443 (2007).
201. J. Su, T. Zhang, J. Tyson, L. Li, The Interleukin-1 Receptor-Associated Kinase M Selectively Inhibits the Alternative, Instead of the Classical NFkB Pathway, *J. Innate Immun.* **1**, 1640174 (2009).
202. K. Kobayashi, L. D. Hernandes, J. E. Galan, C. A. Janeway Jr, R. Medzhitov, R. A. Flavell, IRAK-M Is a Negative Regulator of Toll-like Receptor Signaling, *Cell* **110**, 191–202 (2002).
203. S. Akira, K. Takeda, Toll-like receptor signalling., *Nat. Rev. Immunol.* **4**, 499–511 (2004).
204. T. Kawai, S. Akira, The role of pattern-recognition receptors in innate immunity: update on Toll-like receptors., *Nat. Immunol.* **11**, 373–384 (2010).
205. E. M. Y. Moresco, D. LaVine, B. Beutler, Toll-like receptors, *Curr. Biol.* **21**, R488–R493 (2011).
206. J. Thomas, J. Allen, M. Tsen, T. Dubnicoff, J. Danao, X. Liao, Z. Cao, S. Wasserman, Impaired cytokine signaling in mice lacking the IL-1 receptor-associated kinase, *J. Immunol.* **163**, 978–984 (1999).
207. T. Kawagoe, S. Sato, K. Matsushita, H. Kato, K. Matsui, Y. Kumagai, T. Saitoh, T. Kawai, O. Takeuchi, S. Akira, Sequential control of Toll-like receptor-dependent responses by IRAK1 and IRAK2, *Nat. Immunol.* **9**, 684–691 (2008).
208. N. Suzuki, S. Suzuki, G. Duncan, D. MIllar, T. Wada, C. Mirtsos, H. Takada, A. Wakeham, A. Itie, S. Li, J. Penninger, H. Wesche, P. Ohashi, T. Mak, W. Yeh, Severe impairment of interleukin-1 and Toll-like receptor signaling in mice lacking IRAK-4, *Nature* **416**, 750–756 (2002).
209. E. Meylan, J. Tschopp, IRAK2 takes its place in TLR signaling, *Nat. Immunol.* **9**, 581–582 (2008).
210. M. Seki, S. Kohno, M. Newstead, X. Zeng, U. Bhan, N. Lukacs, S. Kunkel, T. Standiford, Critical role of IL-1 receptor-associated kinase-M in regulating chemokine-dependent deleterious inflammation in murine influenza pneumonia, *J. Immunol.* **184**, 1410–1418 (2010).
211. C. Picard, H. von Bernuth, P. Ghandil, M. Chrabieh, O. Levy, P. Arkwright, D. McDonald, R. Geha, H. Takada, J. Krause, C. B. Creech, C.-L. Ku, S. Ehl, L. Marodi, S. Al-Muhsen, S. Al-Hajjar, J. Gallin, H. Chapel, D. Speert, C. Rodrigues-Gallego, E. Colino, B.-Z. Garty, C. Roifman, T. Hara, H. Yoshikawa, S. Nonoyama, J. Domachowski, A. Issekutz, M. Tang, J. Smart, S. Zitnik, C. Hoarau, D. Kumararatne, A. Thrasher, E. G. Davies, C. Bathune, N. Sirvent, D. de Ricaud, Y. Camcioglu, J. Vasconcelos, M. Guedes, A. Vitor, C. Rodrigo, F. AlmaYan, M. Mendes, J. I. Arostegui, L. Alsina, C. Fortuny, J. Reichenbach, J. W. Verbsky, X. Bossuyt, R. Doffinger, L. Abel, A. Puel, J.-L. Casanova, Clinical Features and Outcomes of Patients with

IRAK-4 and MyD88 Deficiency, *Medicine (Baltimore).* **89**, 403–425 (2010).
212. E. Della Mina, A. Borghesi, H. Zhou, S. Bougarn, S. Boughorbel, L. Israel, I. Meloni, M. Chrabieh, Y. Ling, Y. Itan, A. Renieri, I. Mazzucchelli, S. Basso, P. Pavone, R. Falsaperla, R. Ciccone, R. M. Cerbo, M. Stronati, C. Picard, O. Zuffardi, L. Abel, D. Chaussabel, N. Marr, X. Li, J.-L. Casanova, A. Puel, Inherited human IRAK-1 deficiency selectively impairs TLR signaling in fibroblasts, *PNAS* **114**, E514–E523 (2017).
213. A. Tefferi, J. w. Vardiman, Myelodysplastic syndromes., *N. Engl. J. Med.* **361**, 1872–1875 (2009).
214. J. R. Boiko, L. Borghesi, Hematopoiesis sculpted by pathogens: Toll-like receptors and inflammatory mediators directly activate stem cells, *Cytokine* **57**, 1–8 (2012).
215. M. Sioud, Y. Fløisand, TLR agonists induce the differentiation of human bone marrow CD34+ progenitors into CD11c+ CD80/86+ DC capable of inducing a Th1-type response, *Eur. J. Immunol.* **37**, 2834–2846 (2007).
216. H. Takizawa, R. R. Regoes, C. S. Boddupalli, S. Bonhoeffer, M. G. Manz, Dynamic variation in cycling of hematopoietic stem cells in steady state and inflammation, *J. Exp. Med.* **208**, 273–284 (2011).
217. B. L. Esplin, T. Shimazu, R. S. Welner, K. P. Garrett, L. Nie, Q. Zhang, M. B. Humphrey, Q. Yang, L. a Borghesi, P. W. Kincade, Chronic exposure to a TLR ligand injures hematopoietic stem cells., *J. Immunol.* **186**, 5367–5375 (2011).
218. Y. Zhao, F. Ling, H. C. Wang, X. H. Sun, Chronic TLR Signaling Impairs the Long-Term Repopulating Potential of Hematopoietic Stem Cells of Wild Type but Not Id1 Deficient Mice, *PLoS One* **8** (2013), doi:10.1371/journal.pone.0055552.
219. C. I. Maratheftis, E. Andreakos, H. M. Moutsopoulos, M. Voulgarelis, Toll-like receptor-4 is up-regulated in hematopoietic progenitor cells and contributes to increased apoptosis in myelodysplastic syndromes, *Clin. Cancer Res.* **13**, 1154–1160 (2007).
220. N. Kuninaka, M. Kurata, K. Yamamoto, S. Suzuki, S. Umeda, S. Kirimura, A. Arai, Y. Nakagawa, K. Suzuki, M. Kitagawa, Expression of Toll-like receptor 9 in bone marrow cells of myelodysplastic syndromes is down-regulated during transformation to overt leukemia, *Exp. Mol. Pathol.* **88**, 293–298 (2010).
221. Y. Wei, S. Dimicoli, C. Bueso-Ramos, R. Chen, H. Yang, D. Neuberg, S. Pierce, Y. Jia, H. Zheng, H. Wang, X. Wang, M. Nguyen, S. a Wang, B. Ebert, R. Bejar, R. Levine, O. Abdel-Wahab, M. Kleppe, I. Ganan-Gomez, H. Kantarjian, G. Garcia-Manero, Toll-like receptor alterations in myelodysplastic syndrome., *Leukemia* **27**, 1832–40 (2013).
222. J. Rybka, A. Butrym, T. Wróbel, B. Jaźwiec, E. Stefanko, O. Dobrzyńska, R. Poreba, K. Kuliczkowski, The expression of Toll-like receptors in patients with acute myeloid leukemia treated with induction chemotherapy, *Leuk. Res.* **39**, 318–322 (2015).
223. W. Hofmann, S. de Vos, M. Komor, D. Howlzer, W. Wachsman, H. Koeffler, Characterization of gene expression of CD34+ cells from normal and myelodysplastic bone marrow, *Blood* **100**, 3553–60 (2002).
224. A. Pellagatti, M. Cazzola, A. Giagounidis, J. Perry, L. Malcovati, M. Della Porta, M. Jadersten, S. Killick, A. Verma, C. Norbury, E. Hellstrom-Lindberg, J. Wainscoat, J. Boultwood, Deregulated gene expression pathways in myelodysplastic syndrome hematopoietic stem cells, *Leukemia* **24**, 756–764 (2010).
225. G. W. Rhyasen, L. Bolanos, J. Fang, A. Jerez, M. Wunderlich, C. Rigolino, L. Mathews, M. Ferrer, N. Southall, R. Guha, J. Keller, C. Thomas, L. J. Beverly, A. Cortelezzi, E. N. Oliva, M. Cuzzola, J. P. Maciejewski, J. C. Mulloy, D. T. Starczynowski, Targeting IRAK1 as a Therapeutic Approach for Myelodysplastic Syndrome, *Cancer Cell* **24**, 90–104 (2013).
226. G. W. Rhyasen, L. Bolanos, D. T. Starczynowski, Differential IRAK signaling in hematologic malignancies, *Exp. Hematol.* **41**, 1005–1007 (2013).
227. M. A. Smith, G. S. Choudhary, A. Pellagatti, K. Choi, L. C. Bolanos, T. D. Bhagat, S. Gordon-mitchell, D. Von Ahrens, K. Pradhan, V. Steeples, S. Kim, U. Steidl, M. Walter, I. D. C.

Fraser, A. Kulkarni, N. Salomonis, K. Komurov, J. Boultwood, A. Verma, D. T. Starczynowski, U2AF1 mutations induce oncogenic IRAK4 isoforms and activat innate immune pathways in myeloid malignancies, *Nat. Cell Biol.* **21**, 640–650 (2019).
228. D. Chaudhary, S. Robinson, D. L. Romero, Recent Advances in the Discovery of Small Molecule Inhibitors of Interleukin - 1 Receptor-Associated Kinase 4 (IRAK4) as a Therapeutic Target for Inflammation and Oncology Disorders, *J. Med. Chem.* **58**, 96–110 (2015).
229. C. Dussiau, L. Lhermitte, A. Trinquand, M. Simonin, A. Cieslak, N. Bedjaoui, P. Villarese, H. Dombret, N. Ifrah, E. Macintyre, V. Asnafi, Targeting IRAK1 in T-Cell Acute Lymphoblastic Leukemia, *Oncotarget* **6**, 18956–18965 (2015).
230. Z. Li, K. Younger, R. Gartenhaus, A. M. Joseph, F. Hu, M. R. Baer, P. Brown, E. Davila, Inhibition of IRAK1 / 4 sensitizes T cell acute lymphoblastic leukemia to chemotherapies, *J. Clin. Invest.* , 1–17 (2015).
231. M. M. Hosseini, S. E. Kurtz, S. Abdelhamed, S. Mahmood, M. A. Davare, A. Kaempf, J. Elferich, J. E. McDermott, T. Liu, S. H. Payne, U. Shinde, K. D. Rodland, M. Mori, B. J. Druker, J. W. Singer, A. Agarwal, Inhibition of interleukin-1 receptor-associated kinase-1 is a therapeutic strategy for acute myeloid leukemia subtypes, *Leuk. 2018* **32**, 1 (2018).
232. J. P. Powers, S. Li, J. C. Jaen, J. Liu, N. P. C. Walker, Z. Wang, H. Wesche, Discovery and initial SAR of inhibitors of interleukin-1 receptor-associated kinase-4, *Bioorganic Med. Chem. Lett.* **16**, 2842–2845 (2006).
233. K. L. Lee, C. M. Ambler, D. R. Anderson, B. P. Boscoe, A. G. Bree, J. I. Brodfuehrer, J. S. Chang, C. Choi, S. Chung, K. J. Curran, J. E. Day, C. M. Dehnhardt, K. Dower, S. E. Drozda, R. K. Frisbie, L. K. Gavrin, J. A. Goldberg, S. Han, M. Hegen, D. Hepworth, H. R. Hope, S. Kamtekar, I. C. Kilty, A. Lee, L. L. Lin, F. E. Lovering, M. D. Lowe, J. P. Mathias, H. M. Morgan, E. A. Murphy, N. Papaioannou, A. Patny, B. S. Pierce, V. R. Rao, E. Saiah, I. J. Samardjiev, B. M. Samas, M. W. H. Shen, J. H. Shin, H. H. Soutter, J. W. Strohbach, P. T. Symanowicz, J. R. Thomason, J. D. Trzupek, R. Vargas, F. Vincent, J. Yan, C. W. Zapf, S. W. Wright, Discovery of Clinical Candidate 1-{[(2S,3S,4S)-3-Ethyl-4-fluoro-5-oxopyrrolidin-2-yl]methoxy}-7-methoxyisoquinoline-6-carboxamide (PF-06650833), a Potent, Selective Inhibitor of Interleukin-1 Receptor Associated Kinase 4 (IRAK4), by Fragment-Based Drug De, *J. Med. Chem.* **60**, 5521–5542 (2017).
234. J. W. Singer, S. Al-Fayoumi, H. Ma, R. S. Komrokji, R. Mesa, S. Verstovsek, Comprehensive kinase profile of pacritinib, a nonmyelosuppressive janus kinase 2 inhibitor, *J. Exp. Pharmacol.* **8**, 11–19 (2016).

Chapter 2: Innate immune stress response pathways contribute to adaptive resistance in AML

The work in Chapters 2 and 3 will be published in *Science Translation Medicine*:

Overcoming adaptive therapy resistance in AML by targeting immune response pathways

Authors:

Katelyn Melgar[1,2], MacKenzie Walker[3], LaQuita M. Jones[4], Lyndsey C. Bolanos[1], Kathleen Hueneman[1], Mark Wunderlich[1], Jiang-Kang Jiang[3], Kelli Wilson[3], Xiaohu Zhang[3], Patrick Sutter[3], Amy Wang[3], Xin Xu[3]. Kwangmin Choi[1], Gregory Tawa[3], Donald Lorimer[4], Jan Abendroth[4], Eric O'Brien[5], Scott B. Hoyt[3], Ellin Berman[6], Christopher A. Famulare[7], James C. Mulloy[1], Ross L. Levine[6,7,8], John P. Perentesis[5], Craig J. Thomas*[3,9], and Daniel T. Starczynowski*[1,10].

Affiliations:

1. Division of Experimental Hematology and Cancer Biology, Cincinnati Children's Hospital Medical Center, Cincinnati, OH 45229
2. Immunology Graduate Program, Cincinnati Children's Hospital Medical Center and the University of Cincinnati College of Medicine, Cincinnati, OH 45229
3. Division of Preclinical Innovation, National Center for Advancing Translational Sciences, National Institutes of Health, Bethesda, MD 20892
4. UCB Bainbridge, Bainbridge Island, WA 98110
5. Division of Oncology, Cincinnati Children's Hospital Medical Center, Cincinnati, OH 45229
6. Leukemia Service, Department of Medicine, Memorial Sloan Kettering Cancer Center, New York, NY
7. Center for Hematologic Malignancies, Memorial Sloan Kettering Cancer Center, New York, NY 10065
8. Human Oncology and Pathogenesis Program, Memorial Sloan Kettering Cancer Center, New York, NY 10065
9. Lymphoid Malignancies Branch, Center for Cancer Research, National Cancer Institute, National Institutes of Health, Bethesda, MD 20829
10. Department of Cancer Biology, University of Cincinnati College of Medicine, Cincinnati, OH 45267

***Correspondence:**

Craig J. Thomas
Division of Preclinical Innovation, NIH Chemical Genomics Center, National Center for Advancing Translational Sciences,
Bethesda, MD, USA
301-827-1798
craigt@mail.nih.gov

Daniel T. Starczynowski
Division of Experimental Hematology and Cancer Biology, Cincinnati Children's Hospital Medical Center, Cincinnati, OH, USA
513-803-5317
Daniel.Starczynowski@cchmc.org

Abstract

Targeted inhibitors to oncogenic kinases demonstrate encouraging clinical responses early in the treatment course, however most patients will relapse due to target-dependent mechanisms that mitigate enzyme-inhibitor binding, or through target-independent mechanisms, such as alternate activation of survival and proliferation pathways, known as adaptive resistance. Here we describe mechanisms of adaptive resistance in FLT3 mutant acute myeloid leukemia (AML) by examining integrative in-cell kinase and gene regulatory network responses after oncogenic signaling blockade by FLT3 inhibitors (FLT3i). We identified activation of innate immune stress response pathways after treatment of FLT3-mutant AML cells with FLT3i and showed that innate immune pathway activation via the IRAK1/4 kinase complex contributes to adaptive resistance in FLT3-mutant AML cells.

Introduction

The identification of oncogenic kinases and small molecules designed to target active, functionally relevant kinases have revolutionized cancer treatment. Frustratingly, although many of these targeted inhibitors initially demonstrate encouraging clinical responses, most patients relapse as a result of primary or acquired resistance. Therapy resistance occurs through target-dependent mechanisms resulting from point mutations in the kinase domain that mitigate enzyme-inhibitor binding or through target-independent mechanisms, such as alternate activation of survival and proliferation pathways (*1, 2*). One example involves the FMS-like receptor tyrosine kinase (FLT3). Activating mutations of FLT3 result in its autophosphorylation and initiation of intracellular signaling pathways, which induce abnormal survival and proliferation of leukemic cells (*3-6*). One of the most common mutations in acute myeloid leukemia (AML) involves the internal tandem duplication (ITD) of FLT3, which occurs in ~25% of all cases of newly diagnosed AML and confers a particularly poor prognosis (*4, 7-10*). FLT3 inhibitors (FLT3i) evaluated in clinical studies as monotherapy and combination therapies have shown good initial response rates; however, patients eventually relapse with FLT3i-resistant disease (*11-20*). The absence of durable remission in patients treated with potent and selective FLT3i highlights the need to identify resistance mechanisms and develop additional treatment strategies. Several mechanisms contribute to resistance to selective FLT3i, including mutations in the tyrosine kinase domain of FLT3 (20–50%) or activation of parallel signaling mechanisms that bypass FLT3 signaling, referred to as adaptive resistance (30–50%) (*21-23*). Furthermore, it is possible for both mechanisms to simultaneously occur in different leukemic populations within a single patient (*23*). Adaptive resistance of FLT3-ITD AML cells to FLT3i had been attributed to alternate activation of survival and proliferation pathways (*1, 24-30*). However, combined inhibition of Ras/MAPK or PI3K signaling alongside FLT3 signaling blockade has not been sufficiently effective at eliminating resistant FLT3-ITD AML cells, implicating additional and/or broader mechanisms of adaptive resistance (*31-42*). Moreover, multi-drug combination regimens present challenges, including

synchronized drug exposure and/or cumulative toxicity, which often prevents dosing to therapeutically-optimal exposures (*43*). Therefore, identification of adaptive resistance mechanisms and development of therapies that concomitantly target the primary oncogenic signaling pathway and the relevant adaptive resistance mechanism will likely yield the best clinical outcomes.

Results

FLT3 inhibitors induce adaptive resistance in FLT3-ITD AML.

To investigate adaptive resistance to FLT3i in FLT3-ITD AML, we cultured an engineered primary $CD34^+$ human cell line expressing MLL-AF9 and FLT3-ITD (MLL-AF9;FLT3-ITD) and a FLT3-ITD AML cell line (MV4;11) in the presence of cytokines overexpressed in AML patient bone marrow (BM), including interleukin 3 (IL-3), interleukin 6 (IL-6), stem cell factor (SCF), thrombopoietin (TPO), and FLT3 ligand (FL) (*44-53*). This experimental design explored primary adaptive resistance mechanisms occurring immediately after FLT3i treatment. This approach avoids the possibility of subclones acquiring on-target mutations in FLT3, as observed after chronic exposure to FLT3i (*54-56*). The FLT3-ITD AML cell lines were treated with increasing concentrations of AC220 (quizartinib), a selective inhibitor of FLT3 currently in phase 3 clinical evaluation (NCT02668653), for 72 hours and then examined for leukemic cell recovery (**Fig. 2.1A**). Quizartinib treatment at the indicated doses decreased the viability of FLT3-ITD AML cell lines relative to control-treated (DMSO) cells as measured by AnnexinV staining (**Fig. 2.1B**). Although the FLT3-ITD AML cell lines were initially sensitive to quizartinib, FLT3-ITD AML cell lines rapidly proliferated after 3 days of quizartinib treatment (**Fig. 2.1B**). To determine whether the leukemic potential of the resistant FLT3-ITD AML cell lines is affected by quizartinib treatment, we examined leukemic progenitor function in vitro and leukemia in vivo. Adaptively resistant FLT3-ITD AML cell lines recovered 10 days after quizartinib exposure, as demonstrated by formation of leukemic cell colonies in methylcellulose (**Fig. 2.1C**). At the highest dose of quizartinib, the

leukemic progenitor function was decreased, which is likely the result of more robust on-target inhibition of FLT3 as well as potential off-target effects of quizartinib. Furthermore, resistant MLL-AF9;FLT3-ITD cells that recovered after 30 days of repeated quizartinib exposure rapidly developed leukemia in xenografted NOD.*Rag1*$^{-/-}$;□c^{null} (NRG) mice expressing human IL-3, granulocyte/macrophage-stimulating factor (GM-CSF), and steel factor (SF) (NRGS) at a comparable rate to parental MLL-AF9;FLT3-ITD cells (**fig. S2.1A**). Repeated exposure of the FLT3-ITD AML cell lines to quizartinib for 30 days revealed a diminished sensitivity to FLT3 inhibition at concentrations sufficient to induce cell death of parental cells (**fig. S2.1B**). FLT3 and NRAS resequencing confirmed the absence of second-site mutations (F691 and D835) in FLT3 or activating mutations (G12 and G13) in NRAS in the FLT3-ITD AML cell lines resistant to quizartinib treatment, indicating that these cell populations were relying on adaptive signaling resistance mechanisms, rather than acquired mutations (**fig. S2.1C**). Parallel studies in FLT3-ITD AML cell lines cultured under standard conditions exhibited a similar outgrowth and leukemic potential, suggesting that the presence of cytokines was not the sole mediator of the adaptive resistance (**figs. S2.1D,E**). FLT3-ITD AML cell lines cultured under standard conditions or in the presence of cytokines remained sensitive to blockade of FLT3 signaling after treatment with quizartinib (**fig. S2.1F**), suggesting that the cellular basis of adaptive resistance to FLT3 inhibitors is mediated by an alternate (non-FLT3-mediated) cell-intrinsic mechanism. Exposure of FLT3-ITD AML cells to the next generation FLT3i gilteritinib also resulted in cells with competent outgrowth potential, indicating that adaptive resistance is not specific to quizartinib (**fig. S2.1G**). These findings are consistent with eventual failure of FLT3 inhibitors in the clinic without evidence of acquired FLT3 mutations.

FLT3 inhibitors induce compensatory innate immune stress responses in FLT3-ITD AML.

Resistance of FLT3-ITD AML cells to FLT3i has been attributed to point mutations at or near the ATP-binding domain of FLT3 and to alternate activation of survival and proliferation

pathways (*1, 2, 22-27, 29, 30*). However, global approaches to delineate the alternate pathways contributing to adaptive resistance in FLT3-ITD AML are lacking. To define mechanisms of adaptive resistance, we examined in-cell kinase activity and gene regulatory networks in adaptively resistant FLT3-ITD AML cells (**Fig. 2.1A**). To identify active signaling cascades in adaptively resistant cells, we subjected protein lysates from MLL-AF9;FLT3-ITD and MV4;11 cells treated with quizartinib (IC_{10}; 0.3 nM) for 6 and 12 hours in biological duplicates to peptide phosphorylation profiling using commercially available serine/threonine kinase PamChip arrays. This concentration of quizartinib was selected because it blocks FLT3-ITD signaling and results in adaptively resistant FLT3-ITD AML cells without evidence of cell death, permitting analysis of adaptive responses to FLT3 signaling blockade in the absence of detectable cytotoxic effects. The PamChip arrays generate a dataset of relative phosphorylation propensity of synthetic peptides containing known substrate recognition sites of serine/threonine kinases in the presence and absence of inhibitor. Unsupervised hierarchical clustering analysis using these data identified two major signaling profiles based upon the identification of peptides with a relative decrease or increase in phosphorylation after quizartinib treatment for 6 and 12 hours in MLL-AF9;FLT3-ITD and MV4;11 cells (**Fig. 2.1D, fig. S2.2A**). The in-cell active kinases were inferred based on the combination of distinct phosphorylated peptides using the database of serine/threonine kinase-substrate pairs from PhosphoNet (https://www.phosphonet.ca) (**table S2.1**). Using a cut-off ($\tau > 3 \times 10^{-3}$), forty-six kinases were activated in both FLT3-mutant AML cell lines after 6 and 12 hours of quizartinib exposure (**Fig. 2.1E, table S2.2**). To identify the compensatory signaling networks associated with adaptive resistance to FLT3i, we performed functional annotation of the inferred active kinases common to both FLT3-mutant AML cell lines after 6 and 12 hours of quizartinib exposure (**table S2.2**). Using Panther, we identified known compensatory and stress signaling pathways, such as MAPK signaling and dopamine signaling, and several other signaling pathways, including Toll-like receptor activation (“innate immune signaling”), that have not

previously been implicated in FLT3i adaptive resistance mechanisms to therapy (**Fig. 2.1F**) (*25, 26, 57*).

In parallel, we performed RNA sequencing on MLL-AF9;FLT3-ITD cells treated with quizartinib (IC_{10}; 0.3 nM) for 6 and 12 hours. The compensatory transcriptional response involved sets of genes that increased in relative expression after quizartinib treatment for 6 hours (n = 1286; LogFC > 2, P < 0.05) and 12 hours (n = 1281; LogFC > 2, P < 0.05) in MLL-AF9;FLT3-ITD cells (**table S2.3**). The differentially overexpressed genes at 12 hours were enriched in Gene Ontology (GO) pathways related to innate immune signaling **(Fig. 2.1G)**, suggesting that compensatory activation of innate immune stress pathways provides a cytoprotective role after FLT3i treatment in FLT3-mutant AML.

Among the critical signaling elements within the innate immune pathway are the IL-1 receptor associated kinase 1 (IRAK1) and IRAK4, which are upstream of all signaling effectors within the innate immune pathway and are amenable to therapeutic inhibition (*58-69*). A more granular examination of the STK array outcomes highlights that MLL-AF9;FLT3-ITD and MV4;11 cells treated with quizartinib have increased phosphorylation of IRAK1/4-specific peptides (**Fig. 2.2A**). Orthogonal validation via immunoblotting confirmed increased phosphorylation of IRAK4 at threonine-345/serine-346 after inhibition of FLT3-ITD in MLL-AF9;FLT3-ITD or MV4;11 cells by quizartinib (**Fig. 2.2B and C**). Phosphorylation of IRAK4 was also observed after treatment with the next generation FLT3i, gilteritinib, in MLL-AF9;FLT3-ITD cells (**Fig. 2.2D**). In these experiments, although the majority of FLT3 signaling is inhibited (as indicated by reduced pFLT3 and pSTAT5)(**Fig. 2.2B, fig. S2.1F**), >95% of quizartinib-treated FLT3-ITD AML cells remained viable (AnnexinV-negative), strongly suggesting that IRAK1/4 activation is an adaptive survival mechanism. The activation state of IRAK1/4 is durable, and we observed phosphorylated IRAK4 after 72 hours of quizartinib treatment in MV4;11 cells (**fig. S2.2B**). To determine whether this is an adaptive response based primarily on FLT3 blockade, the isogenic AML cell line MLL-AF9;$NRAS^{G12D}$, which does not depend on FLT3-ITD oncogenic signaling, was treated with

quizartinib at the same dose and time points as the FLT3-ITD line. The NRAS-mutant cells did not exhibit phosphorylation of IRAK4 when treated with quizartinib, suggesting that a dependence on FLT3 signaling is needed to elicit this adaptive response (**fig. S2.2C**). These observations were extended to FLT3-ITD AML patients enrolled in a study evaluating the efficacy of gilteritinib (Study ID: 2215-CL-9100; **table S2.4**). As compared to peripheral blood mononuclear cells (PBMCs) obtained at diagnosis, PMBCs from two patients treated with gilteritinib for 27 and 39 days exhibited increased phosphorylated and total IRAK4 protein at comparable amounts to gilteritinib-treated cells in vitro (**Fig. 2.2D**). As an indication of active IRAK4 signaling, we observed phosphorylated IRAK1 in MV4;11 cells after treatment with quizartinib (**fig. S2.2D**), a patient after gilteritinib treatment (**fig. S2.2E**), and BaF3 cells transduced with FLT3-ITD and treated with quizartinib (**fig. S2.2F**). These findings strongly suggest that FLT3i induce compensatory IRAK1/4 activation in FLT3-ITD AML cells in vitro and in vivo.

To explore a potential mechanism of IRAK1/4 activation in FLT3i-treated FLT3-ITD AML cells, we examined RNA expression after quizartinib treatment of MLL-AF9;FLT3-ITD cells (**Fig. 2.1G**). Because IRAK1/4 is downstream of the TLR superfamily, we compared the expression of all TLRs before and after 6-hour quizartinib treatment. Although 6 of 8 TLRs exhibited increased expression in MLL-AF9;FLT3-ITD cells after quizartinib treatment, only TLR9 was significantly overexpressed at 6 hours and remained elevated at 12 hours ($P = 0.019$, adjusted)(**fig. S2.3A,B**). Immunoblotting of MLL-AF9;FLT3-ITD cells treated with quizartinib revealed that inhibition of FLT3-ITD increases the expression of cleaved TLR9, which has been associated with its active state (**fig. S2.3C**)(*70, 71*). To establish whether increased TLR9 expression and activation in quizartinib-treated FLT3-ITD AML cells results in IRAK1/4 activation, we treated MLL-AF9;FLT3-ITD simultaneously with quizartinib and a TLR9 antagonist (30 nM; ODN-INH-18). In the presence of the TLR9 antagonist, quizartinib-mediated activation of IRAK4 was suppressed as compared to MLL-AF9;FLT3-ITD cells treated only with quizartinib (**fig. S2.3D**). Increased expression of

TLRs, such as TLR9, on FLT3i-treated AML cells may account for the activation of innate immune pathways in adaptively resistant FLT3-ITD AML cells.

Innate immune signaling via IRAK1/4 is required for adaptive resistance of FLT3-ITD AML to FLT3i.

We next investigated whether IRAK1/4 activation is a functionally required element of adaptive resistance of FLT3-ITD AML to FLT3i. Several published inhibitors of IRAK1/4 exist, providing key tools to assess the role of IRAK1/4 in adaptive diseases (*69, 72, 73*). We first evaluated a pairwise matrix combination of quizartinib and a commercially-available IRAK1/4 inhibitor (IRAK-Inh) in MLL-AF9;FLT3-ITD cells (*74*). This experiment used a 48-hour CellTiter-Glo assay format to demonstrate that the combination of quizartinib and IRAK-Inh is synergistically cytotoxic in MLL-AF9;FLT3-ITD cells (**Fig. 2.2E**). Even at low doses of quizartinib (0.3 nM or 0.4 nM), inhibition of IRAK1/4 decreased MLL-AF9;FLT3-ITD cell viability more than would be expected as an additive response (**Fig. 2.2E, fig. S2.4A**). To further confirm that inhibition of IRAK1/4 can suppress adaptive resistance to FLT3i in FLT3-ITD AML cells, we used AnnexinV staining in MLL-AF9;FLT3-ITD and MV4;11 cells treated with quizartinib (0.5 μM), IRAK-Inh (10 μM), or the combination of quizartinib and IRAK-Inh. These studies show that the combination-treated cells had significantly suppressed outgrowth of adaptively resistant FLT3-ITD AML cells as compared to quizartinib or IRAK-Inh treatment alone (2.1% vs 71.8% or 75.3% AnnexinV-negative cells; P = 0.003)(**Fig. 2.2F, fig. S2.4B**). MLL-AF9;FLT3-ITD cells recovered 10 days after inhibitor exposure were also plated in methylcellulose to assess leukemic cell potential. Adaptively resistant MLL-AF9;FLT3-ITD cells treated with quizartinib or IRAK-Inh alone formed significantly more leukemic colonies as compared to parental cells (P < 0.0001)(**Fig. 2.2G**). In contrast, the MLL-AF9;FLT3-ITD cells recovered after treatment with quizartinib and IRAK-Inh did not form leukemic colonies (**Fig. 2.2G**). Inhibition of IRAK1/4 with IRAK-Inh or a potent IRAK4 inhibitor (PF-066) alone did not affect the leukemic cell viability, leukemic progenitor

activity in methylcellulose, or outgrowth of leukemic cells in liquid culture (**fig. S2.4B-E**), indicating that targeting IRAK1/4 alone does not confer cytotoxicity in FLT3-mutant AML. To reinforce that these outcomes implicate IRAK1/4 signaling as the primary driver of adaptive resistance, we expressed shRNA targeting IRAK4 (shIRAK4-MV4;11) or a non-targeting control shRNA (shControl-MV4;11) in MV4;11 cells (**Fig. 2.2H**, right panel). After treatment with quizartinib (1 nM and 50 nM), the proportion of shIRAK4-MV4;11 cells was significantly reduced relative to DMSO-treated shIRAK4-MV4;11 cells (1 nM: $P = 0.0035$; 50 nM: $P = 0.0169$) or quizartinib-treated shControl-MV4;11 cells (1 nM: $P = 0.0002$, 50 nM: $P < 0.0143$)(**Fig. 2.2H,** left panel). Conversely, we also examined the consequences of IRAK4 overexpression on mediating adaptive resistance of MV4;11 cells to FLT3i (**Fig. 2.2I,** right panel). After treatment with quizartinib (1 nM and 50 nM), the relative proportion of IRAK4-overexpressing MV4;11 cells was significantly increased relative to DMSO-treated IRAK4-overexpressing MV4;11 cells (50 nM: $P = 0.029$) or quizartinib-treated control MV4;11 cells (empty vector)(50 nM: $P = 0.029$)(**Fig. 2.2I,** left panel). Taken together, these studies suggest that IRAK1/4 signaling is required for adaptive resistance in FLT3-mutant AML immediately after inhibition of FLT3 and that inhibition of IRAK1/4 signaling creates a synthetic lethality when combined with FLT3i.

Discussion

Targeted inhibitors to oncogenic kinases initially demonstrate encouraging clinical responses, however, most patients relapse due to target-dependent and target-independent mechanisms. Monotherapy and combination therapies have shown good initial response rates to FLT3 inhibitors in clinical studies for FLT3-mutant leukemia; however, patients eventually relapse with FLT3i-resistant clones (*11-20*). The absence of durable remission in FLT3-mutant leukemia patients treated with potent and selective FLT3i establishes the need to identify resistance mechanisms and develop additional treatment strategies. Here we identified mechanisms of adaptive resistance to targeted inhibitors in AML associated with activating FLT3 mutations. Our

results suggest that FLT3i adaptive resistance occurs through compensatory activation of innate immune stress pathways in FLT3-mutant AML and that inhibition of IRAK1/4 with FLT3i targets the emergence of adaptively resistant mutant clones. Specifically, activation of IRAK1/4 in FLT3i-treated AML restored Ras/MAPK signaling along with NF-κB, which represents a major mechanism of resistance after tyrosine kinase inhibition (*1, 24-26, 78*).

Cellular stress responses are survival mechanisms activated by cells. Although stress pathways have been extensively characterized, recent studies have shown that proteins in cellular stress responses interact with and regulate signaling intermediates involved in the activation of immune-related pathways (*79*). Although we report that FLT3i treatment resulted in TLR9 overexpression and IRAK1/4 activation, the precise mechanism of innate immune signaling and specifically IRAK1/4 activation after targeted therapy is not resolved and may involve various cellular stress response pathways. Cellular stresses associated with FLT3i treatment, such as oxidative stress, heat shock, unfolded protein, and DNA damage responses have been independently shown to activate innate immune signaling, albeit by distinct mechanisms (*67, 80-87*). In addition to overexpression of certain TLRs, gene expression analysis of FLT3i-treated cells also revealed overexpression of TLR ligands and inflammatory cytokines. In such conditions, fractional cell death and/or cellular stress after FLT3i treatment can result in the release of inflammatory mediators that subsequently induce innate immune signaling and IRAK1/4 activation, such as via TLR9. Therefore, one potential mechanism of compensatory activation of the innate immune stress pathway in FLT3i-resistant AML subclones is through paracrine and autocrine activation of IRAK1/4. We also observed a modest, yet consistent, increase in IRAK4 expression after prolonged FLT3i treatment of FLT3-mutant AML cells in vitro and in vivo. Consistent with the idea that increased IRAK4 expression correlates with adaptive resistance, retroviral overexpression of IRAK4 decreased the sensitivity of FLT3-ITD AML cells to FLT3i. Thus, another potential mechanism of compensatory activation of the innate immune stress pathway in FLT3i-resistant AML subclones may occur as a result of IRAK1/4 overexpression.

There are ongoing efforts to suppress activation of parallel signaling pathways, such as MEK and ERK, after prolonged exposure to targeted therapies (*31-33, 36, 37, 42, 88*). Ras/MAPK signaling is responsible for adaptively resistant FLT3-mutant AML, however, targeting only a single arm of the signaling cascade has yielded limited clinical benefit (NCT02418000). Because IRAK1/4 complex is upstream of Ras/MAPK and NF-□B (*58*), we posit that targeting IRAK1/4 will yield more durable inhibition of bypass signaling cascades, prevent adaptive resistance, and result in improved therapeutic efficacy in FLT3-mutant AML. Although IRAK1 or IRAK4 inhibition has been explored in myelodysplastic syndrome, AML, T-ALL, and lymphoma, albeit with limited efficacy, we present evidence that innate immune pathway activation via IRAK1 and IRAK4 is essential for adaptive resistance to therapy (*64, 66, 69, 73, 89, 90*).

Figures

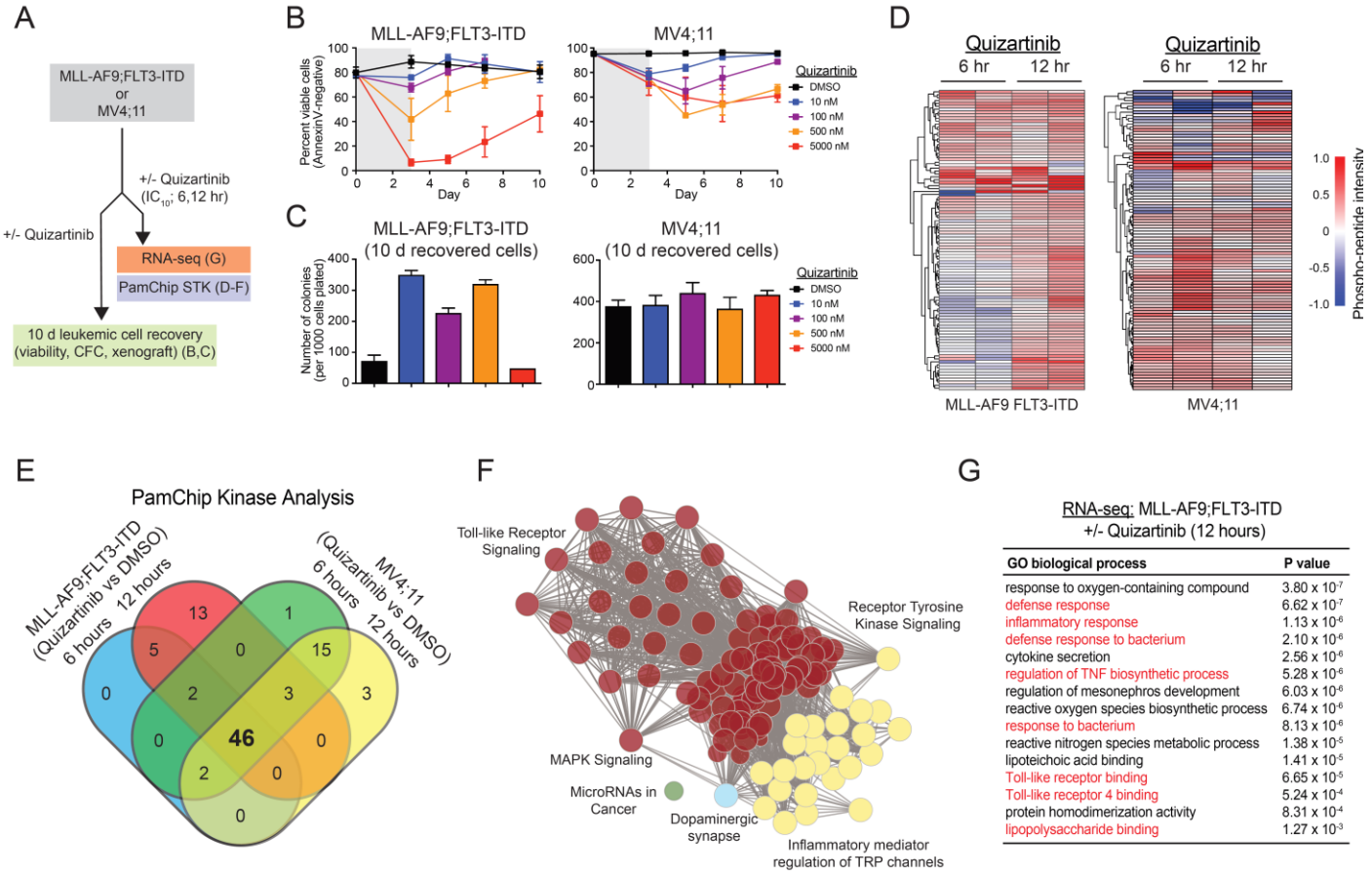

GO biological process	P value
response to oxygen-containing compound	3.80×10^{-7}
defense response	6.62×10^{-7}
inflammatory response	1.13×10^{-6}
defense response to bacterium	2.10×10^{-6}
cytokine secretion	2.56×10^{-6}
regulation of TNF biosynthetic process	5.28×10^{-6}
regulation of mesonephros development	6.03×10^{-6}
reactive oxygen species biosynthetic process	6.74×10^{-6}
response to bacterium	8.13×10^{-6}
reactive nitrogen species metabolic process	1.38×10^{-5}
lipoteichoic acid binding	1.41×10^{-5}
Toll-like receptor binding	6.65×10^{-5}
Toll-like receptor 4 binding	5.24×10^{-4}
protein homodimerization activity	8.31×10^{-4}
lipopolysaccharide binding	1.27×10^{-3}

Figure 2.1. FLT3-ITD AML develop adaptive resistance and activate innate immune pathways after FLT3i treatment. (A) Overview of experimental design to evaluate adaptive resistance. **(B)** MLL-AF9;FLT3-ITD cells or MV4;11 cells were cultured with quizartinib for 3 days, re-plated in fresh medium, and then cell viability was measured by AnnexinV staining (n = 2 per group). **(C)** After 10 days in liquid culture (from panel B), the remaining viable cells were plated in methylcellulose and colony formation was determined after 7 days (n = 4 per condition). Values are expressed as means +/- s.e.m. from 3 biological replicates. *, P < 0.05 (unpaired two-tailed t-test). **(D)** Serine-Threonine Kinase (STK) PamChip analysis was performed on protein lysates isolated from MLL-AF9;FLT3-ITD and MV4;11 cells treated with quizartinib (0.3 nM) for 6 and 12

hours. Hierarchical clustering analysis was performed on differentially phosphorylated peptides in the indicated groups relative to DMSO (2 biological replicates) (PamGene, Kwangmin Choi) **(E)** In-cell active kinases inferred from the phosphorylated peptides (STK PamChip) are shown for each of the indicated conditions. **(F)** Pathway enrichment of differential in-cell kinase activity in MLL-AF9;FLT3-ITD and MV4;11 cells treated with quizartinib for 6 and 12 hours was determined using Panther. **(G)** Pathway enrichment of differentially expressed genes (>2-fold; $P < 0.05$) in MLL-AF9;FLT3-ITD cells treated with quizartinib for 12 hours was determined using Toppgene (n = 3 per group). *, $P < 0.05$ (unpaired two-tailed t-test).

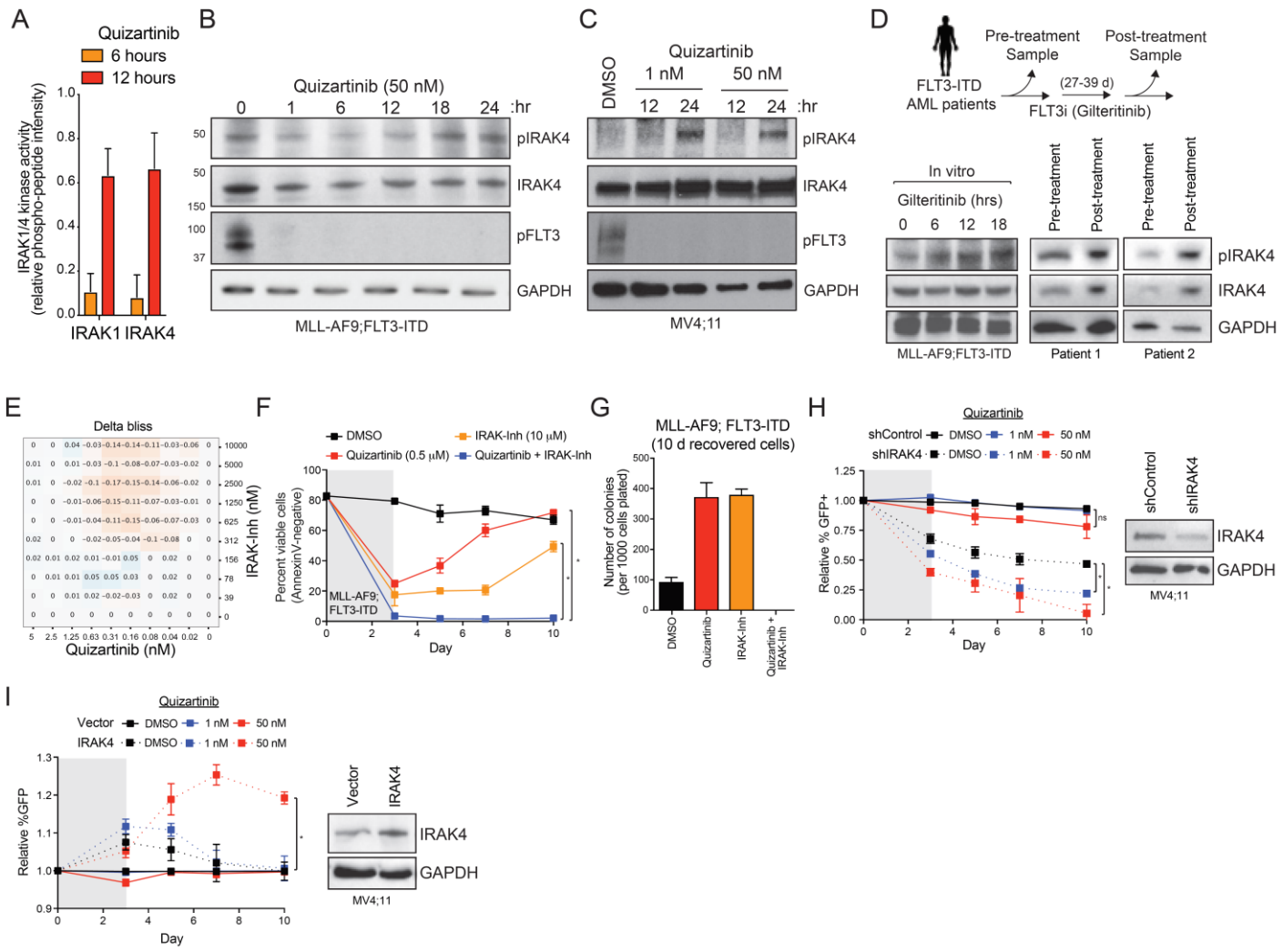

Figure 2.2. Innate immune signaling via IRAK1/4 mediates adaptive resistance to FLT3i. (A) IRAK1 and IRAK4 in-cell activity in MLL-AF9;FLT3-ITD cells treated with quizartinib for 6 and 12 hours is shown based on the relative phosphorylation of the indicated peptides on the STK PamChip array (summary of 4 or 3 independent peptides, respectively, from 2 biological replicates). **(B)** Immunoblotting of pFLT3 and pIRAK4 in MLL-AF9;FLT3-ITD cells treated with quizartinib for the indicated times. **(C)** Immunoblotting of pFLT3 and pIRAK4 in MV4;11 cells treated with quizartinib for the indicated times. **(D)** Immunoblotting of pIRAK4 and total IRAK4 in MLL-AF9;FLT3-ITD cells treated in vitro with gilteritinib (10 nM), or from the peripheral blood of FLT3-ITD AML patients treated with gilteritinib for the indicated number of days. **(E)** Delta Bliss

score of MLL-AF9;FLT3-ITD cells treated with the indicated concentrations of quizartinib and IRAK-Inh for 48 hours based on the cellular metabolic activity using CellTiter-Glo (Thomas Lab). **(F)** Viability of MLL-AF9;FLT3-ITD cells treated for 3 days with DMSO (vehicle control), quizartinib (0.5 μM), IRAK-Inh (10 μM), or quizartinib and IRAK-Inh. Values are expressed as means +/- s.d. from 3 biological replicates. **(G)** After 10 days in liquid culture (from panel F), the remaining viable cells were plated in methylcellulose and colony formation was determined after 7 days. Values are expressed as means +/- s.e.m from 4 biological replicates. **(H)** MV4;11 cells expressing control shRNA (shControl-GFP) or shRNAs targeting IRAK4 (shIRAK4-GFP) were treated with DMSO or quizartinib (1 nM or 50 nM) for 3 days. The proportion of GFP+ cells over 10 days in culture is shown relative to Day 0. Values are expressed as means +/- s.d. from 2 biological replicates. **(I)** MV4;11 cells expressing an empty GFP vector (vector) or a GFP vector with IRAK4 (IRAK4) were treated with DMSO or quizartinib (1 nM or 50 nM) for 3 days. The proportion of GFP+ cells over 10 days in culture is shown relative to Day 0. Values are expressed as means +/- s.e.m. from 4 biological replicates. *, P = 0.029 Mann-Whitney.

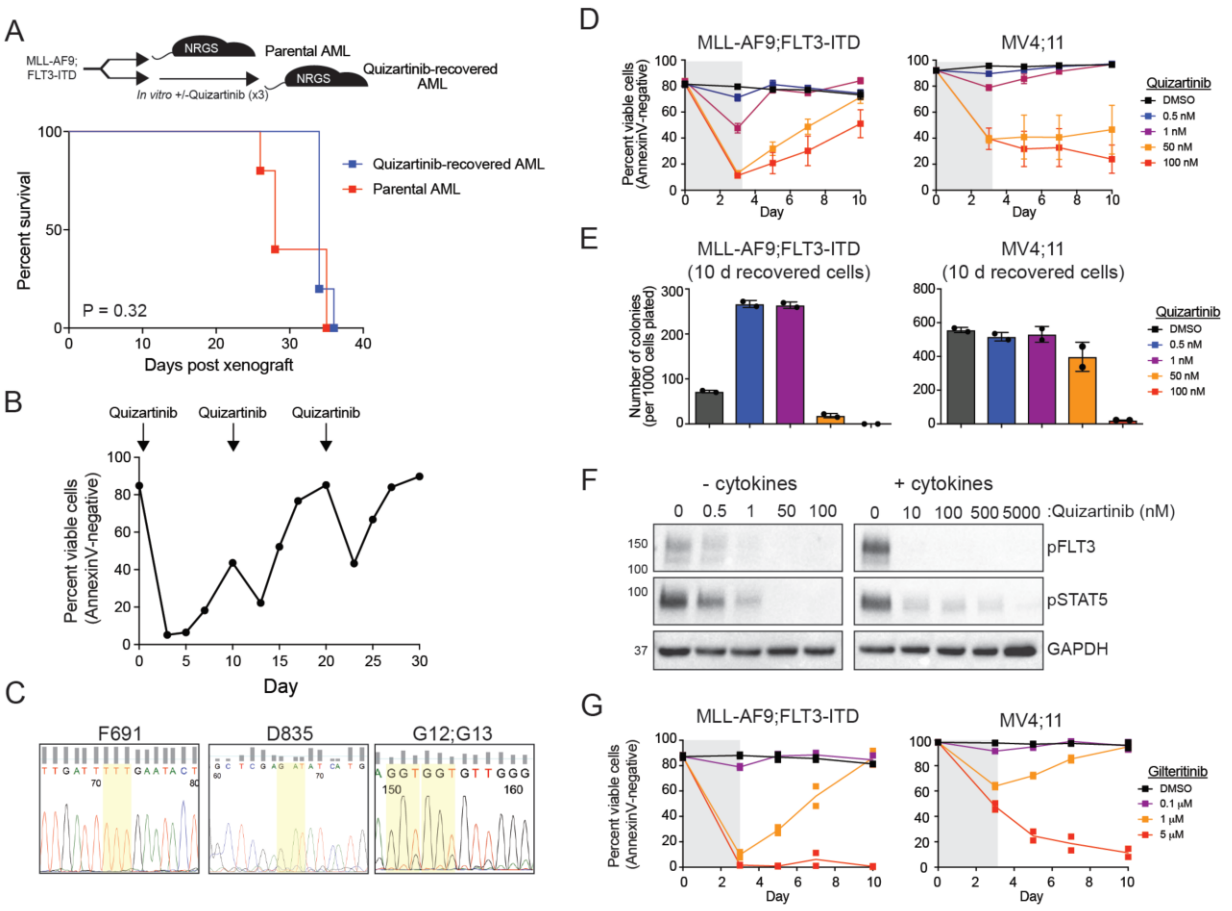

Supplemental Figure 2.1. FLT3+AML develop adaptive resistance to FLT3i. (A) Quizartinib-recovered MLL-AF9;FLT3-ITD cells (from panel B) or parental MLL-AF9;FLT3-ITD cells (n = 5 mice per group) were transplanted into NRGS mice (n = 5 mice per group). Disease free survival shown via Kaplan-Meier curve. P = 0.32, Mantel-Cox test. **(B)** MLL-AF9;FLT3-ITD cells were cultured with quizartinib (5 μM) for 3 days and re-plated in fresh medium. After 7 days, cells were treated with quizartinib (5 μM) for 3 days and re-plated in fresh medium. AnnexinV staining was used to measure cell viability. **(C)** Genomic DNA from quizartinib-recovered MLL-AF9;FLT3-ITD cells (from panel B) was sequenced at the FLT3 F691 and D835 loci and NRAS G12 and G13 loci. **(D)** MLL-AF9;FLT3-ITD cells or MV4;11 cells were cultured in standard medium without cytokines and then treated with quizartinib for 3 days, re-plated in fresh medium, and then cell viability was measured by AnnexinV staining. **(E)** After 10 days in liquid culture (from panel D),

the remaining viable cells were plated in methylcellulose and colony formation was determined after 7 days (n = 2 per condition). Values are expressed as means +/- s.e.m. from biological replicates. **(F)** Immunoblotting of MLL-AF9;FLT3-ITD cells grown with and without IL-3, IL-6, SCF, TPO, and FL (10 ng/mL) and treated with quizartinib for 24 hours. **(G)** MLL-AF9;FLT3-ITD cells or MV4;11 cells were cultured with gilteritinib for 3 days, re-plated in fresh medium, and then cell viability was measured by AnnexinV staining. Values are expressed as means +/- s.e.m from 2 biological replicates.

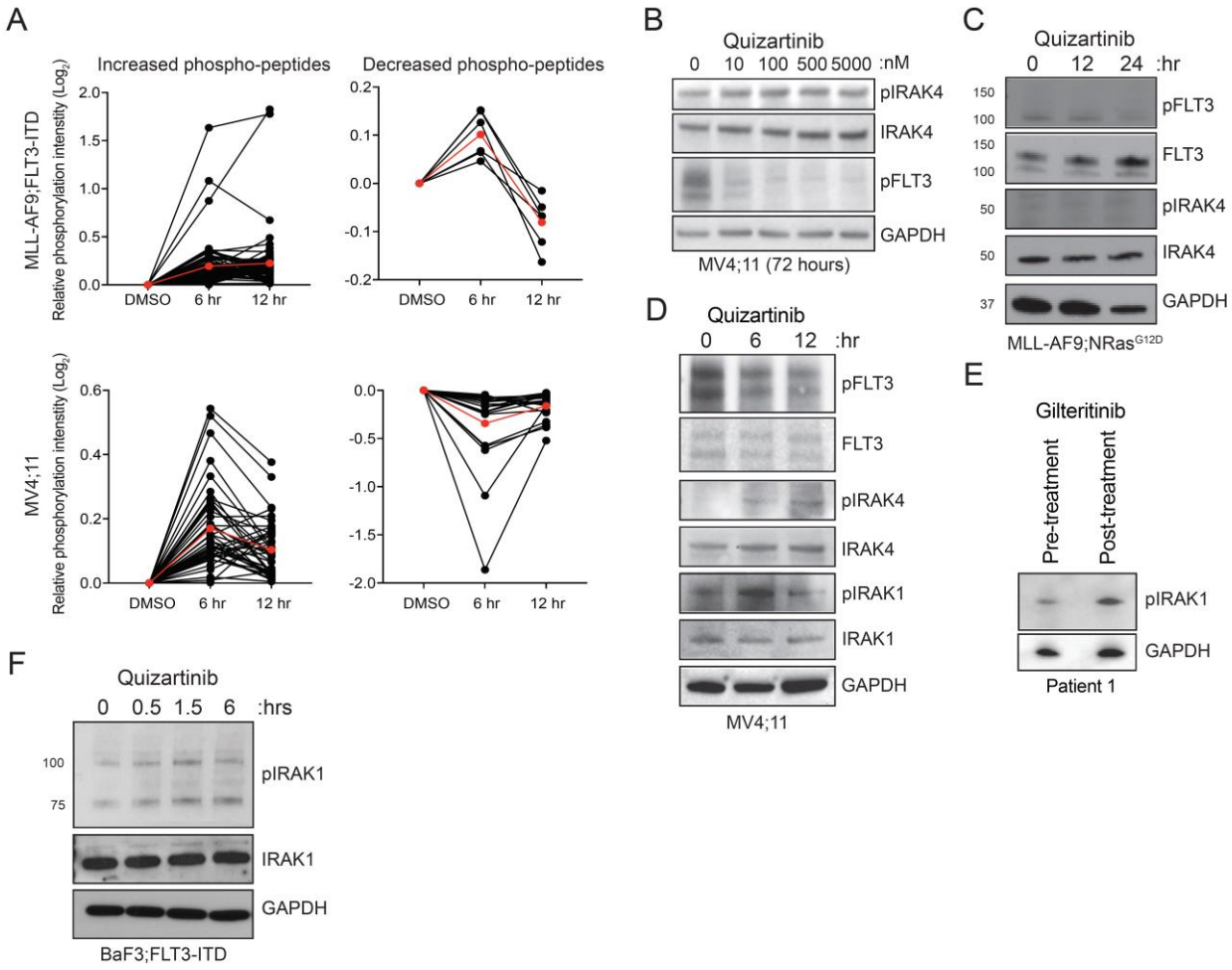

Supplemental Figure 2.2. Adaptively resistant FLT3+AML exhibit increased IRAK1/4 activation. (A) MLL-AF9;FLT3-ITD or MV4;11 cells treated with quizartinib showed two distinct patterns of peptide phosphorylation in the STK PamChip. Red line indicates the average phosphorylation within each group. **(B)** Immunoblotting of MV4;11 cells treated with quizartinib for 72 hours. **(C)** Immunoblotting of MLL-AF9;NRAS^{G12D} cells treated with quizartinib (50 nM). **(D)** Immunoblotting of the indicated proteins in MV4;11 cells treated with quizartinib (0.3 nM) for the indicated times. **(E)** Immunoblotting of pIRAK1 and GAPDH from the peripheral blood of a FLT3-ITD AML patient treated with quizartinib (50 nM) for the indicated times.

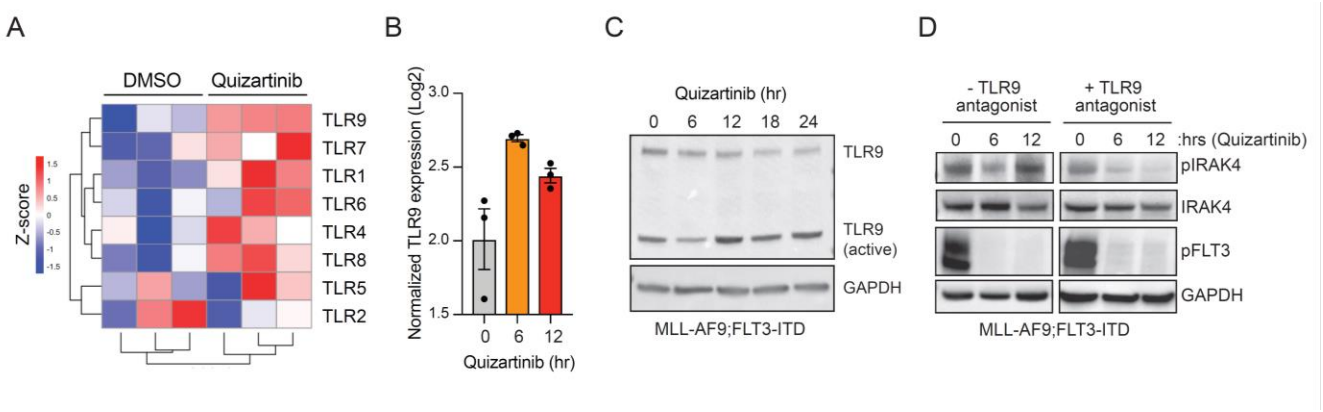

Supplemental Figure 2.3. Quizartinib induces TLR9-mediated activation of IRAK4. (A) RNA expression of the indicated TLRs in MLL-AF9;FLT3-ITD cells following 6 hour treatment with quizartinib. **(B)** RNA expression of TLR9 in MLL-AF9;FLT3-ITD cells following treatment with 0.3 nM quizartinib for 6 hours. **(C)** Immunoblotting of TLR9 in MLL-AF9;FLT3-ITD cells following treatment with 10 nM quizartinib for the indicated time points. **(D)** Immunoblotting of the indicated proteins in MLL-AF9;FLT3-ITD cells after treatment with 10 nM quizartinib and 30 nM of the TLR9 antagonist (ODN-INH-18) for the indicated time points.

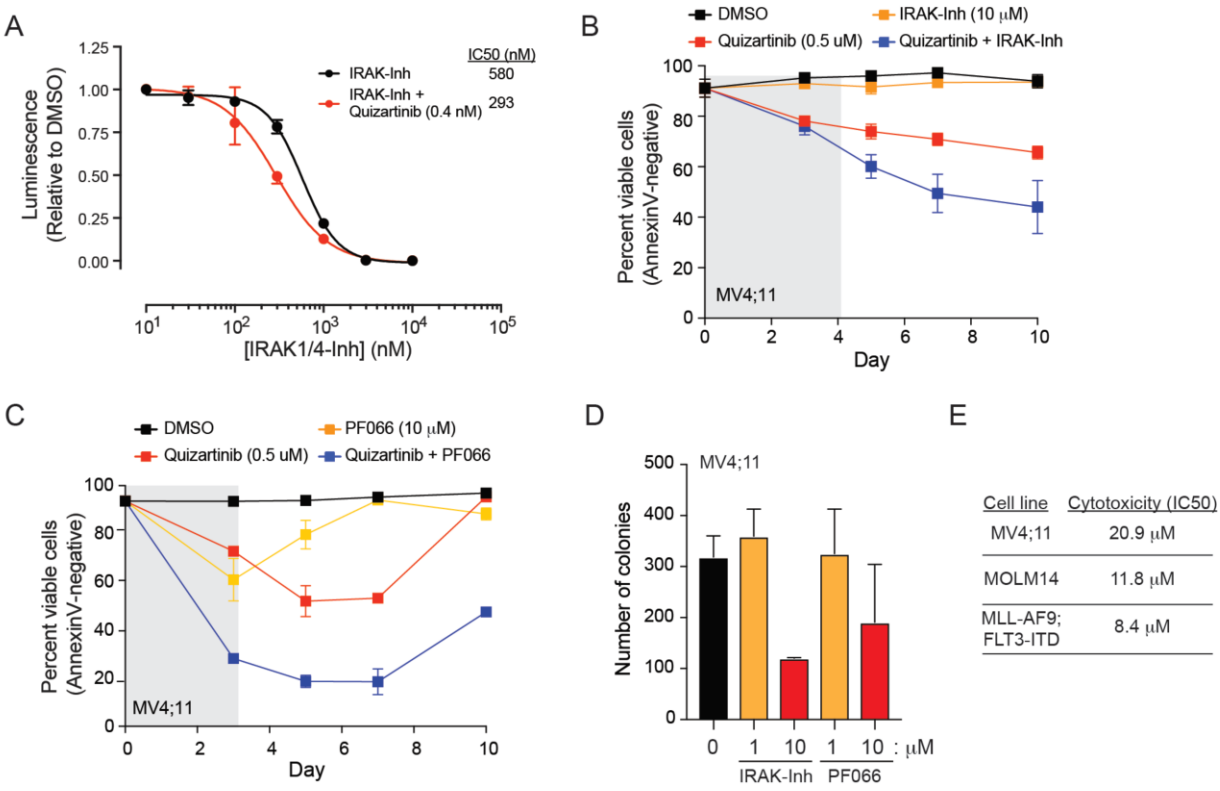

Supplemental Figure 2.4. Inhibition of IRAK1/4 sensitizes FLT3+ AML to quizartinib. (A) CellTiter-Glo was used to measure metabolic activity of MLL-AF9;FLT3-ITD cells treated with IRAK-Inh alone or with IRAK-Inh and quizartinib (0.4 nM). **(B)** MV4;11 cells were treated with DMSO, quizartinib (0.5 μM), IRAK-Inh (10 μM), or quizartinib and IRAK-Inh for 3 days, and then viability was evaluated every 2 days by AnnexinV staining. **(C)** MV4;11 cells were treated with DMSO, quizartinib (0.5 μM), PF06650833 (PF066) (10 μM), or quizartinib and PF066 for 3 days, and then viability was evaluated every 2 days by AnnexinV staining. **(D)** MV4;11 cells were treated with IRAK-Inh or PF066 in methylcellulose and then colonies were evaluated after 10 days. **(E)** CellTiter-Glo was used to measure metabolic activity of the indicated cell lines treated with 10 doses of the IRAK4 inhibitor, PF066 (Thomas Lab).

Supplemental Tables

Supplemental Table 2.1. Peptide phosphorylation in the PamChip Serine/Threonine in-cell kinase array

MLL-AF9;FLT3-ITD + quizartinib (0.3 nM) Log2 FC				
	6hr Replicate 1	6hr Replicate 2	12hr Replicate 1	12hr Replicate 2
ACM1_421_433	0.0235	0.30810118	0.21861601	-0.2318478
ACM1_444_456	0.70535708	0.4122467	0.22781897	0.0887
ACM4_456_468	0.12968302	-0.00734	0.22178078	0.27560043
ACM5_494_506	0.224329	0.10125542	0.10182667	0.21042538
ACM5_498_510	0.38423824	0.28599644	0.11578608	0.21242523
ADDB_696_708	-0.0685	0.12478066	0.2388463	0.22988176
ADDB_706_718	0.4594965	0.15941715	0.20844698	0.45226193
ADRB2_338_350	-0.1694632	-0.1051025	0.22102118	0.41425514
ANDR_785_797	-0.0103	-0.0232	0.22136164	0.35687208
ANXA1_209_221	-0.1503787	0.10134745	0.19214916	0.35755205
ART_025_CXGLRRWSLGGLRRWSL	-0.00746	-0.0846	0.25256538	0.48837137
BAD_112_124	0.37207413	0.47468758	0.54480028	0.4808569
BAD_69_81	0.61700058	0.23146629	0.38439226	0.43748379
BAD_93_105	0.36096001	0.11069298	0.21698618	0.36795998
BCKD_45_57	0.19977856	0.34081125	0.24199867	0.46583748
CA2D1_494_506	-0.0682	0.43646431	0.3266201	0.43652391
CAC1C_1974_1986	0.0234	-0.0424	0.26640701	0.51337338
CD27_212_224	0.82131338	0.49030924	0.49915171	1.07391787
CDC2_154_169	-0.2449923	0.0313	0.009	0.52934599
CDK7_163_175	0.15229511	0.284096	1.10509157	1.17280173
CDN1A_139_151	0.20919895	0.22308826	-0.00492	0.16717911
CENPA_1_14	0.57374191	0.11243725	0.32189751	0.35172558
CFTR_730_742	-0.0944	-0.1497641	0.34185743	0.45256996
CFTR_761_773	-0.0575	-0.0136	0.13493347	0.35540104
CGHB_109_121	-0.2747254	-0.2743487	0.21055889	0.65486479
CREB1_126_138	-0.0696	-0.171073	0.30056191	0.31225586
CSF1R_701_713	0.20988703	0.12465096	0.21135473	0.39986563
DCX_49_61	-0.1658585	0.0384	0.42067981	0.30882931
DESP_2842_2854	-0.0298	-0.2190018	0.46030235	0.39051771
E1A_ADE05_212_224	-0.2592916	-0.3977861	0.0964	0.3637495
EPB42_241_253	-0.07	-0.1542797	0.22856951	0.2875557
ERBB2_679_691	0.0335	0.1799593	0.21910095	0.48744583
ESR1_160_172	-0.2729049	-0.3741293	0.0189	0.26903296
F263_454_466	-0.0877	-0.1714249	0.18445587	0.38827515
FIBA_569_581	0.34138489	0.6149087	0.89522767	-0.0443
FOXO3_25_37	0.2221303	0.36363459	0.21089268	0.19380331
FRAP_2443_2455	0.22664356	0.51525831	0.30393362	0.44707489
GBRB2_427_439	-0.0152	-0.1803856	0.2121315	0.25789452
GPR6_349_361	0.38623095	0.40098858	0.0282	0.32296372
GPSM2_394_406	0.34795141	-0.0633	0.18736219	0.29295778
GRIK2_708_720	-0.00304	-0.131485	0.22306347	0.32380009
GSUB_61_73	0.29524326	0.45022154	-0.0866	0.26340485
GYS2_1_13	0.17285109	0.21060896	0.0205	0.33693123
H2B1B_ 27_40	0.27668619	0.20196724	0.038	0.20256138
H32_3_18	0.000212	0.22241974	0.1038065	0.57520437
IF4E_203_215	-0.1065507	0.52307224	0.21183848	1.37005019
K6PL_766_778	0.27413178	0.17172241	0.18990612	0.35819531
KAP2_92_104	-0.0805	0.0268	0.25025368	0.44789696
KAP3_107_119	-0.1162329	-0.0579	0.12879849	0.40597534
KAPCG_192_206	0.0178	0.11117601	0.20868349	0.62787199
KCC2G_278_289	0.6325469	0.0374	0.73718405	0.0761
KCNA1_438_450	0.24355698	-0.3300743	0.36829066	0.49901128
KCNA2_442_454	0.19557142	0.25340223	0.19149494	0.44811916
KCNA3_461_473	0.0202	0.1113801	0.25994635	0.48681879
KCNA6_504_516	-0.0121	-0.0895	0.1062994	0.30417252
KIF2C_105_118_S106G	0.095	0.18023968	0.10180855	0.40790653
KPB1_1011_1023	0.0307	-0.0446	0.38555288	0.55832005
KPCB_19_31_A25S	0.24399853	0.26969624	0.45933342	0.61329079
KS6A1_374_386	-0.3325114	-0.0641	-0.1147456	0.6958127
LIPS_944_956	0.17486382	0.0898	0.23136425	0.33646917
LMNB1_16_28	0.0867	0.067	0.2357614	0.17214966
MARCS_152_164	-0.1518979	0.18451214	0.0863	0.11785698
MARCS_160_172	0.31954193	0.2072854	0.10575342	0.26687956
MBP_222_234	0.44508505	0.0743	0.11387396	0.46269035
MP2K1_287_299	0.53155661	0.3178153	-0.044	0.52010393
MPIP1_172_184	0.13354683	0.0751	0.21541691	0.49359369
MYPC3_268_280	-0.0103	-0.036	0.33742237	0.44913292

MV4;11 + quizartinib (0.3 nM) Log2 FC				
	6hr Replicate 1	6hr Replicate 2	12hr Replicate 1	12hr Replicate 2
ACM1_421_433	0.0504	-0.5528867	0.28883076	0.13215256
ACM1_444_456	0.16789675	-0.2850809	0.0829	0.14009523
ACM4_456_468	0.0294	-0.2314944	0.18639088	0.18867588
ACM5_494_506	0.0729	0.12873125	0.0707	0.24529171
ACM5_498_510	0.11436892	-0.1408958	0.17108774	0.33868742
ADDB_696_708	-0.1905899	-0.0474	0.0991	0.5812974
ADDB_706_718	0.25695419	0.0406	0.0982	0.36468363
ADRB2_338_350	0.3089633	0.13791323	0.0674	-0.1007967
ANDR_785_797	-0.4003816	-0.2665048	0.0193	0.27781677
ANXA1_209_221	-0.1176591	-0.038	0.00902	0.11792564
ART_025_CXGLRRWSLGGLRRWSL	0.13192844	0.0779	0.0198	-0.1929441
BAD_112_124	0.53257608	0.55416441	0.41172171	0.3411746
BAD_69_81	0.12029409	0.0874	0.0421	0.0496
BAD_93_105	0.0407	0.1850462	0.0321	0.0597
BCKD_45_57	-0.0141	-0.2087307	-0.0707	0.0197
CA2D1_494_506	-0.05	0.26211882	-0.00856	0.0745
CAC1C_1974_1986	0.0553	0.0896	0.13786888	-0.0616
CD27_212_224	-0.1445036	0.0274	-0.0375	0.0614
CDC2_154_169	-0.0987	0.0301	-0.3416276	0.35485911
CDK7_163_175	-0.5576472	0.15200329	0.67226481	-0.6336231
CDN1A_139_151	-0.0723	0.24405098	-0.1699152	-0.0599
CENPA_1_14	0.0203	0.16924	-0.0405	0.0659
CFTR_730_742	0.0946	0.0585	0.21339798	0.0797
CFTR_761_773	0.0343	0.0879	0.0751	-0.0757
CGHB_109_121	0.53216839	-0.4199619	-0.178267	-0.2966447
CREB1_126_138	-0.1514368	-0.0676	0.0608	-0.1755972
CSF1R_701_713	0.0448	0.31238365	0.1512599	0.20309973
DCX_49_61	-0.4275129	0.25616598	-0.051	-0.0361
DESP_2842_2854	-0.0821	0.5081172	0.17848539	-0.1938748
E1A_ADE05_212_224	-0.3313961	-0.1165981	0.0777	-0.1868043
EPB42_241_253	-0.1855383	0.36222649	0.27725363	-0.0165
ERBB2_679_691	0.00979	0.5124855	0.18517208	0.20413876
ESR1_160_172	-0.3962922	0.22809792	0.00538	0.36538029
F263_454_466	-0.0371	0.0559	0.14489174	-0.0723
FIBA_569_581	-3.6135318	-0.1130257	-0.3930724	-0.6487775
FOXO3_25_37	0.0408	0.45835161	0.0183	0.0472
FRAP_2443_2455	-0.0405	0.25353527	0.0817	0.27016974
GBRB2_427_439	-0.3559952	0.0207	0.14110947	-0.1231298
GPR6_349_361	-0.1059885	0.25444841	-0.0714	0.12223434
GPSM2_394_406	-0.3082666	0.31186199	0.17611647	0.16171265
GRIK2_708_720	0.23452091	0.0589	0.10818481	-0.1399088
GSUB_61_73	0.0411	0.37112331	0.1287899	0.28869724
GYS2_1_13	0.16404009	0.76962519	0.19520807	0.27571964
H2B1B_ 27_40	0.31115723	0.47011948	-0.0365	-0.00562
H32_3_18	0.0803	0.36688137	0.036	0.27265978
IF4E_203_215	0.35804725	0.68274164	0.17402911	0.48604727
K6PL_766_778	0.19536972	0.39942408	-0.0642	0.06
KAP2_92_104	0.31376743	0.11146736	0.012	-0.1688633
KAP3_107_119	0.0536	0.18764591	0.1129694	-0.046
KAPCG_192_206	-0.0908	0.2742939	0.0876	-0.0679
KCC2G_278_289	-0.1666427	-0.1167836	-0.1949759	-0.0794
KCNA1_438_450	0.0142	-0.338285	-0.096	0.0986
KCNA2_442_454	-0.0367	0.39249134	0.0402	0.12838316
KCNA3_461_473	-0.5387611	0.0611	0.0351	0.16794491
KCNA6_504_516	0.074	0.16548538	0.0904	-0.05
KIF2C_105_118_S106G	-0.0462	0.52997017	0.10392952	0.063
KPB1_1011_1023	0.0962	0.0683	0.19685173	-0.00884
KPCB_19_31_A25S	0.25400925	0.50743723	0.23685932	-0.0181
KS6A1_374_386	-0.0289	0.33034706	0.17911291	-0.1388187
LIPS_944_956	0.14463568	0.52087975	0.054	0.1516757
LMNB1_16_28	-0.4271829	-0.74066	-0.00744	0.62227941
MARCS_152_164	0.10186005	0.46796942	-0.1724381	0.21227646
MARCS_160_172	0.18186379	-0.1774445	0.0923	-0.1163139
MBP_222_234	-0.028	0.24581432	0.0425	-0.1834621
MP2K1_287_299	0.0799	0.47260714	-0.058	-0.0762
MPIP1_172_184	0.0477	0.47534132	0.19476414	-0.0196
MYPC3_268_280	0.0978	0.1133461	0.21673775	0.0061

NCF1_296_308	-0.0123	-0.1776838	0.095	0.22075939
NCF1_321_333	-0.041	-0.190527	0.28134441	0.31953716
NEK2_172_184	0.13857508	0.0856	0.18675709	0.22873926
NEK3_158_170	-0.44506	0.00881	0.63923192	0.78749657
NFKB1_330_342	-0.0725	0.12194395	0.1547575	0.42376089
NMDZ1_890_902	0.14416504	-0.0452	0.32211399	0.33479023
NOS3_1171_1183	-0.0207	0.17490101	0.19026852	0.29502678
NR4A1_344_356	0.25683928	0.1733141	0.31073332	0.39354897
P53_308_323	0.0355	0.0908	0.20872212	0.26303482
PLEK_106_118	0.10362816	0.22149086	0.38739014	0.28584576
PLM_76_88	0.39102745	1.48266387	0.51834488	4.96730757
PP2AB_297_309	0.0278	0.10327506	0.66034436	0.47549629
PPR1A_28_40	0.0325	0.17288113	0.0909	0.19388676
PRKDC_2618_2630	0.30829239	-0.3487768	0.70406699	0.3517437
PTK6_436_448	-0.115427	-0.0276	0.16954708	0.39393234
PTN12_32_44	-0.0339	-0.2131739	0.16601467	0.24049568
PYGL_8_20	0.52917051	4.37405539	0.14771915	0.92119837
RADI_559_569	-1.8419352	2.30651283	1.51872897	-0.2093623
RAF1_253_265	0.38379908	0.16921425	0.078	0.25524235
RAP1B_172_184	0.0498	0.0488	0.0712	0.17468309
RBL2_655_667	-0.1099477	0.061	0.28018045	0.38844109
RB_242_254	0.0597	-0.00628	0.17577648	-0.2984653
RB_350_362	0.78988934	0.14761925	0.70510674	-0.2015753
RB_803_815	0.0845	0.24909687	0.16220236	0.19301176
REL_260_272	0.00865	0.0163	0.071	0.34058523
RS6_228_240	-0.0811	-0.1353865	0.30468941	0.18024826
RYR1_4317_4329	-0.1960201	-0.295929	0.10412884	0.15400791
SCN7A_898_910	0.0789	-0.1410546	0.41175556	0.50277233
STK6_283_295	-0.2936344	0.0647	0.0711	0.55671692
STMN2_90_102	-1.160773	-0.193651	0.27673912	0.29938555
TOP2A_1463_1475	-0.0948	-0.1224556	0.0584	0.12687683
TY3H_65_77	-0.0805	-0.1411505	0.15616703	0.46357822
VASP_150_162	-0.063	-0.2817707	0.18026733	0.30617762
VASP_271_283	-0.1129246	-0.1728306	0.0497	0.1809473
VTNC_390_402	-0.0925	-0.1181393	0.12088871	0.34496117

NCF1_296_308	-0.3215046	-0.0204	0.0657	-0.1639643
NCF1_321_333	-0.0511	0.0882	0.0806	-0.071
NEK2_172_184	-0.1038194	-0.0157	-0.3170786	0.00132
NEK3_158_170	0.77070785	0.30433416	-0.4709706	-0.4742963
NFKB1_330_342	0.13580418	0.12654114	0.19785738	-0.0663
NMDZ1_890_902	0.25656986	0.23143196	0.031	-0.1122417
NOS3_1171_1183	0.1633358	0.21518803	0.0913	-0.1436853
NR4A1_344_356	-0.0648	0.11140728	-0.1205816	0.013
P53_308_323	-0.00294	0.11341858	0.16491079	0.15858889
PLEK_106_118	0.3845253	-0.0731	-0.103075	-0.249773
PLM_76_88	-0.3800898	0.19959259	0.21823216	-0.4834437
PP2AB_297_309	0.42432928	-0.3149416	-0.4326673	-0.2049606
PPR1A_28_40	-0.0271	-0.0599	-0.1513348	-0.3117142
PRKDC_2618_2630	-0.3185773	-0.3643065	-0.3025627	0.46424151
PTK6_436_448	-0.0264	0.11028004	0.10338402	0.14941883
PTN12_32_44	-0.3853312	0.0442	0.0613	-0.2682447
PYGL_8_20	-0.3198509	-0.8500056	-0.7844481	0.0157
RADI_559_569	0.21069837	-2.3954847	-0.8952646	0.57908583
RAF1_253_265	-0.1493258	-0.1749063	0.10522556	-0.0788
RAP1B_172_184	0.12002945	0.0469	0.18074703	0.12388754
RBL2_655_667	-0.0712	-0.3703637	0.0695	-0.1193876
RB_242_254	0.0742	0.22642803	0.26788187	-0.0781
RB_350_362	-0.1678162	-1.0744467	-0.4612274	-0.2583337
RB_803_815	-0.1352062	-0.0347	0.20621538	0.0741
REL_260_272	0.0995	0.0952	-0.1395426	-0.0334
RS6_228_240	-0.0224	0.0281	-0.0761	-0.1311016
RYR1_4317_4329	-0.5554276	-0.5893259	-0.2839718	-0.3666506
SCN7A_898_910	0.14711475	0.21801424	0.1494751	-0.0152
STK6_283_295	0.29301167	0.21700954	0.0711	-0.0223
STMN2_90_102	-0.0235	-0.2147932	-0.0268	-0.1299443
TOP2A_1463_1475	-0.3706141	-0.1113634	-0.0416	-0.1703453
TY3H_65_77	0.0472	0.21745586	0.13320351	-0.0794
VASP_150_162	-0.2666388	0.11897469	0.10963726	-0.2155046
VASP_271_283	-0.3108759	-0.1849675	-0.1701279	-0.2424726
VTNC_390_402	0.16150188	0.20618725	0.0812	-0.0606

Supplemental Table 2.2. Top active kinases inferred from the PamChip in-cell kinase array.

MLL-AF9;FLT3-ITD + quizartinib (0.3 nM) 6 hr				
Kinase	tau.spec	tau.sig	score.sum	tau
SGK1	0.954677	3.30103	4.255707	7.18121
RPS6KA6	0.838632	3.30103	4.139862	10.24839
SGK1	0.61261	3.30103	3.91364	6.002851
MAPKAPK2	0.595166	3.30103	3.898196	7.002454
MAPKAPK3	0.581699	3.30103	3.882729	7.002454
RPS6KA3	0.559878	3.30103	3.860908	6.543916
PRKCG	0.559091	3.30103	3.860121	4.529762
PRKCQ	0.559091	3.30103	3.860121	4.529762
PRKCD	0.555966	3.30103	3.856996	4.529762
PRKCH	0.547447	3.30103	3.848477	4.529762
PRKCE	0.538361	3.30103	3.839391	4.676927
RPS6KA1	0.526513	3.30103	3.827543	6.543916
NPR1	0.519275	3.30103	3.820305	3.401272
PRKCA	0.510745	3.30103	3.811775	5.062956
PRKY	0.509339	3.30103	3.810369	3.401272
PRKCB1	0.490126	3.30103	3.791156	5.062956
SGK2	0.482804	3.30103	3.783834	5.135524
PIM1	0.451611	3.30103	3.752641	5.803434
RPS6KA2	0.410609	3.30103	3.711639	5.590577
Pim3	0.390907	3.30103	3.691937	5.503164
CDKL5	0.37366	3.30103	3.67469	2.809923
CDK7	0.367543	3.30103	3.668573	2.809923
GSK3A	0.364014	3.30103	3.665044	2.809923
MAPK3	0.355561	3.30103	3.656591	4.940148
MAPK1	0.350178	3.30103	3.651209	4.940148
PIM2	0.338187	3.30103	3.639217	3.777386
PRKG1	0.334518	3.30103	3.635548	4.037136
PRKACB	0.284414	3.30103	3.585444	3.227924
PRKX	0.240332	3.30103	3.541362	3.683644
PRKG2	0.232473	3.30103	3.533503	3.46038
RPS6KA5	0.221126	3.30103	3.522156	3.132577
AKT2	0.203079	3.30103	3.504109	2.75573
AKT3	0.193142	3.30103	3.494172	2.75573
PRKACA	0.192803	3.30103	3.493833	2.908573
CHEK2	0.146302	3.30103	3.447332	1.556169
MYLK3	0.140862	3.30103	3.441892	1.556169
RPS6KB2	0.112102	3.30103	3.413132	2.231764
MAPK7	0.099906	3.30103	3.400936	1.84646
MAPK11	0.092857	3.30103	3.393887	1.816902
AKT1	0.088044	3.30103	3.389074	1.721549
CDK13	0.083809	3.30103	3.384839	1.691212
MAPK14	0.08148	3.30103	3.38251	1.834805
CDK2	0.050854	3.30103	3.351884	1.751012
RPS6KB1	0.049635	3.30103	3.350665	1.736465
MAPK13	0.043112	3.30103	3.344142	1.831681
MAPK9	0.030351	3.30103	3.331381	1.5056
MTOR	0.027334	3.30103	3.328364	1.193302
MAPK8	0.00811	3.30103	3.30914	1.272325
MAPK10	0.003707	3.30103	3.304737	1.272325
CDK3	0.033389	0.182104	0.215493	0.572501
CDK4	0.034563	0.180127	0.21469	0.572501
CDK5	0.030584	0.183759	0.214343	0.572501
CDK6	0.032686	0.165261	0.197948	0.572501
NEK4	0.018634	0.175874	0.194509	0.515991
MAP3K14	0.017277	0.176852	0.194129	0.515991

MLL-AF9;FLT3-ITD + quizartinib (0.3 nM) 12 hr				
Kinase	tau.spec	tau.sig	score.sum	tau
RPS6KA5	1.823909	3.30103	5.124939	9.121294
AKT1	1.782516	3.30103	5.083546	10.82754
PIM1	1.610834	3.30103	4.911864	7.018828
PIM2	1.425969	3.30103	4.726999	8.207689
Pim3	1.376751	3.30103	4.677781	6.186124
RPS6KB2	1.327902	3.30103	4.628932	8.381042
AKT3	1.283997	3.30103	4.585027	8.018864
AKT2	1.211125	3.30103	4.512155	8.018864
MYLK3	0.941195	3.30103	4.242225	10.94627
CHEK2	0.941195	3.30103	4.242225	10.94627
MAP3K14	0.720105	3.30103	4.021135	4.909969
RPS6KB1	0.716699	3.30103	4.017729	6.213503
NEK4	0.708863	3.30103	4.009893	4.909969
PRKG2	0.694649	3.30103	3.995679	5.089753
PRKX	0.645862	3.30103	3.946922	4.783427
PRKCB	0.525058	3.30103	3.826098	4.925746
PRKCA	0.497573	3.30103	3.798603	4.925746
MTOR	0.476964	3.30103	3.777934	3.471551
PRKG1	0.437707	3.30103	3.738737	4.179198
MAPKAPK3	0.423083	3.30103	3.724113	4.152788
MAPKAPK2	0.414539	3.30103	3.715569	4.152788
RPS6KA6	0.40618	3.30103	3.70719	4.137224
RPS6KA1	0.347754	3.30103	3.648764	3.847563
RPS6KA3	0.335359	3.30103	3.636368	3.847563
RPS6KA2	0.235077	3.30103	3.536107	3.202841
PRKCE	0.232102	3.30103	3.533132	1.717594
PRKACA	0.21254	3.30103	3.51357	2.340745
SGK1	0.210067	3.30103	3.511097	1.600121
MAPK7	0.20621	3.30103	3.50724	1.6813
PRKCC	0.196853	3.30103	3.467883	1.033673
PRKCQ	0.186216	3.30103	3.457246	1.033673
PRKCH	0.183676	3.30103	3.454706	1.033673
PRKCD	0.159864	3.30103	3.430924	1.033673
MAPK1	0.150561	3.30103	3.421611	2.339862
MAPK3	0.141764	3.30103	3.412794	2.339862
PRKACB	0.134304	3.30103	3.405334	1.558295
SGK3	0.118615	3.30103	3.389645	0.798727
SGK2	0.079355	3.30103	3.350385	1.185812
MAPK9	0.059733	3.30103	3.330763	1.113943
MAPK14	0.031984	3.30103	3.303014	0.86972
MAPK13	0.028724	3.30103	3.329754	0.984657
CDK2	0.024799	3.30103	3.325828	0.815666
MAPK10	0.011887	3.30103	3.312917	0.789724
MAPK8	0.008996	3.30103	3.310026	0.789724
CDK13	0.007667	3.30103	3.308697	0.206933
MAPK11	0.007005	3.30103	3.308035	0.788014
GSK3A	0.07443	0.178814	0.253244	0.566798
CDKL5	0.077015	0.175874	0.252889	0.566798
CDK7	0.072373	0.18077	0.241143	0.566798
PRKY	0.054531	0.178486	0.233018	0.357195
NPR1	0.052611	0.172631	0.225242	0.357195
CDK6	0.040959	0.180456	0.221415	-0.18293
CDK4	0.038579	0.174574	0.213153	0.18293
CDK5	0.031984	0.175224	0.207208	0.18293
CDK3	0.036212	0.170053	0.206265	-0.18293
AKT3	0.759451	3.30103	4.060481	4.709442
RPS6KA3	0.55752	3.30103	3.85855	3.845263
RPS6KA1	0.516413	3.30103	3.817443	3.72529
CDKL4	0.487449	3.30103	3.788479	3.659455
PRKACA	0.477558	3.30103	3.778586	3.809531
SGK2	0.467248	3.30103	3.768276	3.597336
PRKG1	0.440093	3.30103	3.741123	3.886083
PRKG2	0.438302	3.30103	3.739332	3.682099
PRKX	0.437113	3.30103	3.738143	3.617099
RPS6KA6	0.433563	3.30103	3.734593	3.462809
PRKACB	0.420788	3.30103	3.721818	3.54742
RPS6KA2	0.390408	3.30103	3.691436	3.402654
MAPK12	0.3711	3.30103	3.67213	2.350004
MAPK10	0.359022	3.30103	3.660052	3.00473
CDK1	0.357041	3.30103	3.658071	3.00473
MAPK8	0.355069	3.30103	3.656099	3.00473
MAPK9	0.355069	3.30103	3.656099	3.00473
MAPK11	0.354087	3.30103	3.655117	3.00473
MAPK3	0.353106	3.30103	3.654136	3.00473
MAPK13	0.353106	3.30103	3.654136	2.350004
MAPK1	0.348239	3.30103	3.649269	3.00473
MAPK14	0.344862	3.30103	3.645892	3.00473
SCYL2	0.331149	3.30103	3.632178	2.324665
AKT2	0.319211	3.30103	3.620241	3.152006
STK38L	0.293282	3.30103	3.594312	2.221832
CDK4	0.291164	3.30103	3.592194	2.221832
AURKC	0.28948	3.30103	3.59049	2.221832
SGK1	0.274497	3.30103	3.575507	2.772146
DCLK1	0.269218	3.30103	3.570248	1.989966
ATR	0.245652	3.30103	3.546682	1.861798
RPS6KB1	0.24527	3.30103	3.5463	2.637399
PRKCA	0.231732	3.30103	3.532762	2.996925
MAPKAPK3	0.222211	3.30103	3.523241	3.033639
PRKCB	0.216089	3.30103	3.517126	2.996925
RPS6KB2	0.173925	3.30103	3.474965	2.889694
PRKY	0.169091	3.30103	3.470121	2.46264
PRKCQ	0.162412	3.30103	3.463442	2.701489
MYLK	0.156767	3.30103	3.457797	1.520703
RPS6KA5	0.150689	3.30103	3.451918	2.91373
MAPKAPK2	0.139662	3.30103	3.440892	2.686109
PRKACG	0.136083	3.30103	3.437113	1.425537
AKT1	0.114074	3.30103	3.415104	2.466588
PRKCE	0.109869	3.30103	3.410899	2.403358
Pim3	0.091247	3.30103	3.392277	2.91622
PRKCD	0.090444	3.30103	3.391474	2.183251
SGK3	0.089109	3.30103	3.390139	1.593419
NPR1	0.077275	3.30103	3.378305	1.865875
PRKCH	0.061981	3.30103	3.363011	2.015034
MTOR	0.056753	3.30103	3.357783	1.079565
PIM1	0.056258	3.30103	3.357288	2.736055
PRKCG	0.04624	3.30103	3.34727	1.784233
CAMK4	0.027566	3.30103	3.328596	1.58093
COQ8A	0.027334	3.30103	3.328364	0.813964
PIM2	0.02618	3.30103	3.32721	2.344396
RPS6KL1	0.025028	3.30103	3.326058	0.813964
CHEK2	0.005023	3.30103	3.306053	1.267051
DCLK2	0.003928	3.30103	3.304956	1.414498

MV4;11 + quizartinib (0.3 nM) 6 hr				
Kinase	tau.spec	tau.sig	score.sum	tau
PKG2 (PRKG2)	2.522879	3.30103	5.823909	5.82521
PKG1 (PRKG1)	2.30103	3.30103	5.60206	5.565708
PKACb PRKACB	2.046757	3.30103	5.346787	5.617756
PKACa (PRKACA)	1.732828	3.30103	5.033858	5.280763
MAPKAPK2	1.371611	3.30103	4.672641	4.846896
MAPKAPK3	1.296709	3.30103	4.597739	4.259883
MSK1 (RPS6KA5)	0.987183	3.30103	4.288193	3.742414
PRKX	0.924453	3.30103	4.225463	3.905925
NEK4 (STK2)	0.917215	3.30103	4.218225	4.464689
NIK (MAP3K14)	0.908333	3.30103	4.209363	4.464689
DCAMKL1	0.756992	3.30103	4.057992	2.998838
ANPa (NPR1)	0.609065	3.30103	3.910095	2.524148
mTOR/FRAP	0.599482	3.30103	3.900492	2.61359
Pim3 (AL549548)	0.59176	3.30103	3.89279	2.945983
PIM1	0.578398	3.30103	3.879428	2.947728
PRKY	0.55752	3.30103	3.85855	2.484109
SGK3 (SGKL)	0.533874	3.30103	3.834904	2.324294
DCAMKL3 (KIAA1765	0.530178	3.30103	3.831208	1.614082
AMPKa1 (PRKAA1)	0.526956	3.30103	3.826986	1.614082
CHK2 (CHEK2)	0.497573	3.30103	3.798603	2.289924
PKACg (PRKACG)	0.493495	3.30103	3.794525	1.612096
CDK9	0.456553	3.30103	3.757583	1.396432
RSK2 (RPS6KA3)	0.454893	3.30103	3.755723	2.603911
CDK5	0.452841	3.30103	3.753671	1.396432
RSK4 (RPS6KA6)	0.430941	3.30103	3.731771	2.373049
RSK1 (RPS6KA2)	0.398493	3.30103	3.699513	2.44819
AKT2	0.384676	3.30103	3.685696	2.358648
DCAMKL2 (BI035543)	0.381429	3.30103	3.682459	1.910719
SGK2	0.376234	3.30103	3.677264	2.078324
RSK3 (RPS6KA1)	0.354087	3.30103	3.655117	2.291739
SGK	0.327902	3.30103	3.628932	1.765676
p70S6K (RPS6KB1)	0.287771	3.30103	3.588801	1.862084
CHED (CDC2L5)	0.286539	3.30103	3.587539	1.120863
PIM2	0.268009	3.30103	3.569039	2.118041
p38b MAPK (MAPK11	0.234331	3.30103	3.535361	0.972933
caMLCK (MLCK)	0.212894	3.30103	3.513924	0.921084
p70S6Kb (RPS6KB2)	0.131356	3.30103	3.432386	1.356762
AurC (STK13)	1.004305	0.484126	1.488491	4.745124
NDR2 (KIAA0965)	1	0.473015	1.473015	4.745124
CDK4	0.753255	0.484789	1.238044	3.070778
PKCI (PRKCQ)	0.589223	0.478862	1.068085	3.209317
PKCb (PRKCB1)	0.590913	0.460924	1.051837	3.208588
PKCa (PRKCA)	0.576754	0.455932	1.032686	3.208588
AKT1	0.462811	0.475604	0.938415	2.651027
PKCe (PRKCE)	0.442493	0.480829	0.923321	2.408176
PKCg (PRKCG)	0.335826	0.487448	0.823277	1.649015
PKCd (PRKCD)	0.331148	0.482804	0.813952	1.649015
AKT3	0.336299	0.46916	0.805459	1.809795
PKCh (PRKCH)	0.269218	0.457797	0.727015	1.539886
CAMK4	0.239955	0.475604	0.715559	1.175944
CHK1 (CHEK1)	0.193142	0.476904	0.670046	0.671374
p38d MAPK (MAPK13	0.04624	0.50307	0.549311	0.637686
CDK1 (CDC2)	0.041814	0.484126	0.52604	0.262
JNK2 (MAPK9)	0.057248	0.462811	0.520059	0.585784
ERK2 (MAPK1)	0.028724	0.473661	0.502385	0.545844
JNK1 (MAPK8)	0.014349	0.481486	0.495835	0.424033
ERK1	0.026949	0.465974	0.491923	0.625091
JNK3 (MAPK10)	0.014125	0.476254	0.490378	0.424033
CDK2	0.02641	0.454693	0.481103	0.563466
PSKH1 (HUMPSKB)	0.266402	0.182765	0.449167	0.94388
CDKL5 (STK9)	0.235077	0.191114	0.426191	0.845293
GSK3A	0.227678	0.172631	0.400309	0.845293
CDK7	0.20621	0.182765	0.388975	0.845293
RSKL2	0.08066	0	0.08066	0.355387
ADCK3 (LOC56997)	0.077794	0	0.077794	0.355387
p38a MAPK (MAPK14	0.022605	0	0.022605	0.396873
CDK3	0.014798	0	0.014798	0.100532
p38g MAPK (MAPK12	0.007005	0	0.007005	-0.0474
ERK5 (MAPK7)	0.005803	0	0.005803	-0.19099

MV4;11 + quizartinib (0.3 nM) 12 hr				
Kinase	tau.spec	tau.sig	score.sum	tau
CHK1 (CHEK1)	3.30103	3.30103	6.60206	36.18351
CDK1 (CDC2)	2.259637	3.30103	5.560667	18.84191
p38a MAPK (MAPK14	1.468521	3.30103	4.769552	7.783707
NEK4 (STK2)	1.323306	3.30103	4.624336	8.645559
CDK2	1.305396	3.30103	4.606425	6.551068
NIK (MAP3K14)	1.29243	3.30103	4.59346	8.645559
JNK2 (MAPK9)	1.289193	3.30103	4.590223	8.933557
p38d MAPK (MAPK13	1.247952	3.30103	4.548982	7.467368
JNK1 (MAPK8)	1.229148	3.30103	4.530178	8.2704
JNK3 (MAPK10)	1.167491	3.30103	4.468521	8.2704
PSKH1 (HUMPSKB)	1.088842	3.30103	4.389872	4.833544
ERK2 (MAPK1)	1.024568	3.30103	4.326598	5.669874
ERK1	0.98457	3.30103	4.2856	4.870352
AMPKa1 (PRKAA1)	0.945004	3.30103	4.246034	3.788447
mTOR/FRAP	0.943095	3.30103	4.244125	4.102222
DCAMKL3 (KIAA1765	0.897909	3.30103	4.198939	3.788447
GSK3A	0.697886	3.30103	3.998916	1.602612
CDKL5 (STK9)	0.692982	3.30103	3.994012	1.602612
CDK7	0.666591	3.30103	3.967621	1.602612
DCAMKL1	0.630784	3.30103	3.931814	1.550147
PRKY	0.438899	3.30103	3.739929	1.15929
AKT3	0.431798	3.30103	3.732828	1.277027
CHED (CDC2L5)	0.421361	3.30103	3.722391	0.995241
CDK3	0.390406	3.30103	3.691436	0.944088
AKT1	0.220764	3.30103	3.521794	0.858018
PKACb PRKACB	0.163993	3.30103	3.465023	0.676663
PKACa (PRKACA)	0.139962	3.30103	3.440992	0.640388
PKCg (PRKCG)	0.130768	3.30103	3.431798	-0.34424
PKCd (PRKCD)	0.125808	3.30103	3.426838	-0.34424
caMLCK (MLCK)	0.087188	0.460782	1.179971	2.208059
CHK2 (CHEK2)	0.440692	0.496209	0.936901	1.191142
p38b MAPK (MAPK11	0.370381	0.517841	0.887922	0.837918
p38g MAPK (MAPK12	0.336296	0.465074	0.802273	0.788762
AKT2	0.291154	0.489455	0.780609	0.996143
RSK2 (RPS6KA3)	0.317655	0.460924	0.778779	1.024161
PKG2 (PRKG2)	0.28735	0.485452	0.772803	1.295533
RSK3 (RPS6KA1)	0.230623	0.467246	0.697868	0.826892
RSK1 (RPS6KA2)	0.210067	0.473661	0.683728	0.811845
p70S6Kb (RPS6KB2)	0.130083	0.500313	0.630396	0.529193
DCAMKL2 (BI035543)	0.131944	0.489455	0.621399	0.392464
PKG1 (PRKG1)	0.119045	0.476254	0.594299	0.603995
PKCb (PRKCB1)	0.102098	0.481486	0.583584	0.346925
PKCe (PRKCE)	0.081707	0.485452	0.56716	0.296783
PKCa (PRKCA)	0.098096	0.467246	0.563342	0.346925
PIM2	0.052076	0.482804	0.53488	0.341507
PRKX	0.039528	0.49147	0.531	0.262578
MSK1 (RPS6KA5)	0.040958	0.482804	0.523763	0.340759
PKCh (PRKCH)	0.02641	0.476254	0.502664	-0.09095
CDK5	0.211125	0.175874	0.386999	0.38787
NDR2 (KIAA0965)	0.197568	0.176852	0.37442	0.369452
AurC (STK13)	0.18809	0.178814	0.366904	0.369452
CDK6	0.192465	0.171985	0.36445	0.38787
CDK4	0.164309	0.169411	0.333721	0.378661
SGK3 (SGKL)	0.097453	0	0.097453	-0.24111
ERK5 (MAPK7)	0.092857	0	0.092857	0.262753
CAMK4	0.064746	0	0.064746	-0.14703
ADCK3 (LOC56997)	0.060231	0	0.060231	0.089582
ANPa (NPR1)	0.053302	0	0.053302	0.123229
RSKL2	0.051098	0	0.051098	0.089582
RSK4 (RPS6KA6)	0.048724	0	0.048724	-0.15822
p70S6K (RPS6KB1)	0.024798	0	0.024798	0.094445
MAPKAPK3	0.021591	0	0.021591	0.168278
SGK2	0.020907	0	0.020907	0.074882
MAPKAPK2	0.016825	0	0.016825	-0.09358
SGK	0.007446	0	0.007446	-0.02546
PKACg (PRKACG)	0.005683	0	0.005683	-0.00281
PKCI (PRKCQ)	0.004804	0	0.004804	0.019384
Pim3 (AL549548)	0.003926	0	0.003926	0.123436
PIM1	0.003269	0	0.003269	0.116068

Supplemental Table 2.3. Gene expression analysis of FLT3-ITD AML-treated with FLT3i.

RNA-seq: MLL-AF9;FLT3-ITD + quizartinib (0.3 nM, 6 hr) Log FC (P < 0.05)						
Gene	LogFC	AveExpr	t	P.Value	Adj.P.Val	B
S100A9	15.21	3.012	40.96	1.57E-17	9.19E-16	27.36
PRTN3	14.83	2.044	54.57	1.70E-19	6.18E-17	29.64
S100A8	14.47	1.868	57.19	8.11E-20	4.03E-17	29.95
CES1	14.34	1.801	53.77	2.15E-19	6.55E-17	29.54
LPPR3	14.1	1.679	47.84	1.36E-18	1.69E-16	28.67
CYBB	13.57	1.942	44.78	3.85E-18	3.42E-16	28.14
FLT3	13.52	2.974	45.38	3.13E-18	2.95E-16	28.25
CD9	13.14	2.501	40.82	1.66E-17	9.39E-16	27.32
BEX1	13.08	1.168	51.56	4.17E-19	8.80E-17	29.23
PSAT1	12.84	1.052	47.52	1.51E-18	1.80E-16	28.61
EPB41L3	12.79	1.024	47.7	1.43E-18	1.74E-16	28.64
TGFBI	12.78	1.794	31.27	1.09E-15	1.89E-14	24.6
CEACAM6	12.66	1.489	39.79	2.48E-17	1.24E-15	27.08
ST14	12.57	0.9182	48.83	9.86E-19	1.44E-16	28.82
LPL	12.5	0.8829	48.8	9.95E-19	1.44E-16	28.82
PLBD1	12.39	0.8235	48.33	1.16E-18	1.57E-16	28.74
LILRB4	12.38	0.8195	48.53	1.09E-18	1.53E-16	28.77
IGF2BP1	12.35	0.8085	47.97	1.30E-18	1.67E-16	28.68
TLR2	12.06	0.6605	45.48	3.02E-18	2.89E-16	28.25
EMC10	12.05	0.6542	47	1.80E-18	2.03E-16	28.51
BASP1	12.04	0.6492	46.66	2.02E-18	2.21E-16	28.46
LAMP5	11.77	0.5171	45.87	2.64E-18	2.61E-16	28.31
GAL	11.76	1.286	31.75	8.55E-16	1.56E-14	24.77
MNDA	11.69	1.002	37.99	5.14E-17	2.07E-15	26.63
PADI2	11.56	0.4079	44.57	4.15E-18	3.62E-16	28.07
ANXA5	11.46	0.3608	43.96	5.16E-18	4.38E-16	27.95
DEFB1	11.42	0.3413	43.1	7.03E-18	5.43E-16	27.78
FUCA2	11.39	1.096	30.14	1.93E-15	2.99E-14	24.18
TIFAB	11.31	0.8099	32.42	6.18E-16	1.22E-14	24.99
B3GNT7	11.29	1.825	30.47	1.63E-15	2.61E-14	24.31
IL13RA1	11.25	0.2553	42.1	1.02E-17	6.83E-16	27.57
HNMT	11.25	0.2542	42.9	7.59E-18	5.73E-16	27.73
B4GALT2	11.21	0.2337	43.64	5.78E-18	4.67E-16	27.88
PROK2	11.14	0.2015	43.63	5.81E-18	4.67E-16	27.88
AP1S1	11.08	0.169	41.6	1.23E-17	7.75E-16	27.46
NT5DC2	11.05	2.679	34.38	2.46E-16	6.24E-15	25.63
EIF4E3	11	0.1322	42.13	1.01E-17	6.83E-16	27.57
DNAJC15	10.98	0.1221	41.44	1.31E-17	8.02E-16	27.42
TREM2	10.96	0.1073	39.37	2.93E-17	1.40E-15	26.95
PTGFRN	10.92	0.08714	40.74	1.71E-17	9.50E-16	27.26
SCOC	10.79	0.02118	40.97	1.57E-17	9.19E-16	27.31
EBF3	10.78	0.02281	42.44	8.97E-18	6.34E-16	27.63
ALDH3A2	10.73	-0.006122	41.3	1.38E-17	8.35E-16	27.38
BTBD6	10.67	-0.03369	41.76	1.16E-17	7.48E-16	27.48
MPEG1	10.64	0.7242	28.42	4.82E-15	6.25E-14	23.49
KCNJ12	10.58	-0.07973	41.09	1.50E-17	8.92E-16	27.33
GRAMD1B	10.57	-0.07955	37.92	5.28E-17	2.09E-15	26.58
CLEC5A	10.51	0.9417	35.31	1.62E-16	4.52E-15	25.89
CHI3L1	10.49	-0.1303	37.91	5.31E-17	2.09E-15	26.57
ZDHHC2	10.44	-0.1532	39.98	2.30E-17	1.18E-15	27.07
SASH1	10.4	-0.1721	40.56	1.83E-17	9.97E-16	27.2
IGFBP2	10.35	2.324	31.05	1.21E-15	2.05E-14	24.52
GLB1L2	10.33	0.3249	29.57	2.60E-15	3.81E-14	23.94
GPR125	10.3	0.3081	29.17	3.22E-15	4.51E-14	23.78
MRAS	10.24	-0.2468	39.71	2.55E-17	1.26E-15	27
NDNF	10.2	-0.2695	37.61	6.02E-17	2.25E-15	26.48
LRIG1	10.19	0.2543	33.31	4.04E-16	8.91E-15	25.26
XK	10.16	-0.2837	37.67	5.86E-17	2.21E-15	26.5
PDGFD	10.12	-0.3146	35.75	1.33E-16	3.99E-15	25.97
SDC2	10.11	-0.3139	39.59	2.69E-17	1.31E-15	26.96
PSMD5-AS1	10.11	-0.317	36.51	9.60E-17	3.12E-15	26.18
ATP6V0E2	10.09	-0.322	38.72	3.80E-17	1.68E-15	26.76
AZU1	10.08	1.908	34.82	2.02E-16	5.32E-15	25.75
MYBPH	10.06	-0.3485	27.81	6.77E-15	8.13E-14	23.2
PSMD5	10.03	1.109	26.31	1.61E-14	1.62E-13	22.56
HSD11B1	10.01	-0.3663	38.38	4.37E-17	1.86E-15	26.67

MLL-AF9;FLT3-ITD + quizartinib (0.3 nM) 12 hr - RNASeq LogFC >+2, P<0.05						
Gene	logFC	AveExpr	t	P.Value	adj.P.Val	B
S100A9	15.21	3.014	35.25	2.07E-14	9.09E-13	19.87
PRTN3	14.89	2.082	46.27	5.96E-16	8.00E-14	21.32
S100A8	14.54	1.908	45.89	6.64E-16	8.65E-14	21.29
CES1	14.39	1.831	45.41	7.61E-16	9.46E-14	21.24
LPPR3	14.21	1.743	45.08	8.38E-16	1.03E-13	21.2
CYBB	13.6	1.968	35.43	1.94E-14	8.73E-13	19.9
FLT3	13.47	2.958	36.18	1.48E-14	7.19E-13	20.03
CD9	13.22	2.552	34.91	2.36E-14	9.97E-13	19.81
BEX1	13.01	1.145	41.98	2.12E-15	1.94E-13	20.85
EPB41L3	12.84	1.055	40.94	2.95E-15	2.46E-13	20.72
TGFBI	12.84	1.831	26.13	1.01E-12	1.34E-11	17.69
PSAT1	12.76	1.019	38.56	6.44E-15	4.12E-13	20.39
ST14	12.64	0.9551	40.34	3.58E-15	2.81E-13	20.64
CEACAM6	12.63	1.48	33.98	3.34E-14	1.23E-12	19.63
LPL	12.49	0.8822	36.25	1.44E-14	7.09E-13	20.03
LILRB4	12.45	0.8629	39.65	4.47E-15	3.25E-13	20.54
PLBD1	12.43	0.8532	37.9	8.06E-15	4.66E-13	20.29
IGF2BP1	12.36	0.8195	38.23	7.20E-15	4.38E-13	20.34
BASP1	12.12	0.6987	39.18	5.23E-15	3.67E-13	20.48
TLR2	12.06	0.6651	38.24	7.19E-15	4.38E-13	20.34
EMC10	12	0.6392	35.42	1.95E-14	8.73E-13	19.88
LAMP5	11.89	0.5807	34.58	2.67E-14	1.07E-12	19.73
GAL	11.69	1.256	28.16	3.83E-13	6.61E-12	18.29
PADI2	11.61	0.442	33.2	4.52E-14	1.51E-12	19.46
MNDA	11.57	0.9526	32.12	6.96E-14	2.06E-12	19.24
ANXA5	11.52	0.4003	34.36	2.89E-14	1.13E-12	19.69
FUCA2	11.39	1.108	27.35	5.61E-13	8.69E-12	18.05
DEFB1	11.38	0.3272	34.83	2.42E-14	1.02E-12	19.77
TIFAB	11.34	0.8376	30.73	1.23E-13	2.99E-12	18.93
HNMT	11.3	0.2884	34.71	2.54E-14	1.03E-12	19.75
B3GNT7	11.3	1.837	27.72	4.70E-13	7.62E-12	18.17
IL13RA1	11.27	0.2721	30.87	1.17E-13	2.90E-12	18.96
PROK2	11.2	0.2387	30.48	1.37E-13	3.21E-12	18.87
B4GALT2	11.17	0.2245	34.36	2.89E-14	1.13E-12	19.68
NT5DC2	11.1	2.703	27.61	4.96E-13	7.92E-12	18.18
AP1S1	11.06	0.1656	31.3	9.74E-14	2.55E-12	19.05
EIF4E3	11.03	0.1523	35.14	2.16E-14	9.32E-13	19.82
DNAJC15	10.92	0.0964	29	2.62E-13	4.98E-12	18.5
EBF3	10.9	0.08567	34.83	2.43E-14	1.02E-12	19.76
TREM2	10.81	0.0425	29.32	2.27E-13	4.55E-12	18.58
MPEG1	10.81	0.8197	24.11	2.85E-12	2.93E-11	17
PTGFRN	10.79	0.03372	28.8	2.87E-13	5.31E-12	18.44
KCNJ12	10.78	0.02543	34.14	3.14E-14	1.18E-12	19.63
SCOC	10.77	0.02421	32.44	6.12E-14	1.91E-12	19.29
ALDH3A2	10.69	-0.01711	30.94	1.13E-13	2.85E-12	18.96
BTBD6	10.62	-0.05274	33.44	4.12E-14	1.43E-12	19.49
SASH1	10.47	-0.1278	32	7.29E-14	2.11E-12	19.19
GRAMD1B	10.46	-0.133	30.64	1.29E-13	3.08E-12	18.89
CHI3L1	10.44	-0.1448	27.35	5.59E-13	8.69E-12	18.03
ZDHHC2	10.41	-0.1568	31.24	9.99E-14	2.60E-12	19.02
GPR125	10.4	0.3662	25.12	1.68E-12	1.97E-11	17.35
CLEC5A	10.39	0.8862	28.12	3.92E-13	6.71E-12	18.27
MRAS	10.32	-0.2012	32.63	5.67E-14	1.81E-12	19.32
IGFBP2	10.29	2.299	24.42	2.42E-12	2.59E-11	17.15
NAPSB	10.27	0.3032	28.11	3.93E-13	6.72E-12	18.25
GLB1L2	10.25	0.2893	24.02	2.99E-12	3.04E-11	16.96
PDGFD	10.24	-0.24	25.34	1.50E-12	1.82E-11	17.41
LRIG1	10.18	0.2541	27.86	4.40E-13	7.23E-12	18.18
MYBPH	10.17	-0.2756	31.73	8.16E-14	2.27E-12	19.13
AZU1	10.14	1.942	19.08	5.69E-11	3.15E-10	14.82
PSMD5-AS1	10.13	-0.2986	27.79	4.55E-13	7.41E-12	18.15
NDNF	10.12	-0.3033	31.98	7.36E-14	2.11E-12	19.18
HMX2	10.12	-0.3014	31.6	8.59E-14	2.33E-12	19.1
XK	10.05	-0.3356	30.76	1.22E-13	2.97E-12	18.91
SDC2	10.03	-0.3449	30.48	1.37E-13	3.21E-12	18.84
DOCK1	10.02	-0.3533	32.05	7.16E-14	2.09E-12	19.19

DOCK1	9.996	-0.3702	38.52	4.13E-17	1.77E-15	26.7
ARHGEF39	9.986	0.1513	29.07	3.39E-15	4.70E-14	23.74
HMX2	9.983	-0.3813	37.11	7.41E-17	2.59E-15	26.34
CBX1	9.966	1.198	21.66	3.24E-13	1.97E-12	20.09
LRRC4	9.953	-0.3914	38.22	4.66E-17	1.94E-15	26.63
NAPSB	9.902	0.1095	31.97	7.67E-16	1.44E-14	24.81
GALNT14	9.885	-0.4239	36.23	1.08E-16	3.45E-15	26.1
KLF4	9.877	-0.4328	37.36	6.68E-17	2.41E-15	26.4
IRF8	9.872	3.481	42.36	9.27E-18	6.48E-16	28.82
PON2	9.857	-0.4474	28.73	4.07E-15	5.44E-14	23.58
GPR27	9.812	-0.4631	37.96	5.19E-17	2.08E-15	26.55
S100A10	9.806	-0.472	35.49	1.49E-16	4.27E-15	25.88
PBK	9.805	-0.4656	35.62	1.41E-16	4.12E-15	25.92
KIAA1598	9.799	-0.4763	34.48	2.35E-16	5.98E-15	25.59
HOXA11	9.793	-0.4722	37.72	5.73E-17	2.18E-15	26.49
GPR88	9.791	0.301	25.65	2.39E-14	2.24E-13	22.24
NR2F2	9.757	-0.4856	35.64	1.40E-16	4.09E-15	25.92
S100A6	9.749	0.804	28.06	5.90E-15	7.32E-14	23.33
SIX2	9.715	-0.5124	37.37	6.64E-17	2.40E-15	26.39
TRIP6	9.712	1.776	24.94	3.68E-14	3.18E-13	21.91
FAM64A	9.705	-0.5149	37.56	6.13E-17	2.28E-15	26.44
TMEM246	9.677	-0.5326	36.18	1.10E-16	3.49E-15	26.07
FAIM	9.648	-0.547	37.27	6.92E-17	2.48E-15	26.36
CCR2	9.618	3.46	42.38	9.17E-18	6.45E-16	28.91
ARL4C	9.603	-0.5698	34.01	2.91E-16	7.06E-15	25.43
AGT	9.59	-0.04473	29.92	2.17E-15	3.29E-14	24.06
CCDC50	9.562	-0.5858	36.75	8.65E-17	2.90E-15	26.22
GNAI1	9.544	-0.6008	36.35	1.03E-16	3.29E-15	26.11
FAM83G	9.544	-0.5946	36.22	1.09E-16	3.45E-15	26.07
GAS6	9.536	-0.07655	29.81	2.30E-15	3.46E-14	24.01
GPD2	9.524	-0.07975	31.3	1.07E-15	1.87E-14	24.56
BBS7	9.524	-0.6072	36.7	8.84E-17	2.94E-15	26.2
PYGO1	9.496	-0.6175	35.42	1.54E-16	4.36E-15	25.85
C10orf118	9.496	-0.6228	36.9	8.12E-17	2.75E-15	26.25
CTC-276P9.1	9.48	-0.628	36.55	9.42E-17	3.08E-15	26.16
NEBL	9.455	-0.644	34.24	2.62E-16	6.56E-15	25.49
MCOLN2	9.382	-0.6776	36.12	1.14E-16	3.52E-15	26.03
IFI27L2	9.382	-0.6798	32.03	7.47E-16	1.41E-14	24.78
SLC22A15	9.373	0.3732	30.14	1.93E-15	2.99E-14	24.15
ALDH1L2	9.365	0.08752	25.51	2.59E-14	2.39E-13	22.16
CKAP4	9.36	0.895	35.53	1.47E-16	4.25E-15	25.94
C3orf14	9.353	-0.6883	33.28	4.09E-16	8.98E-15	25.19
MPO	9.346	3.135	42.62	8.40E-18	6.12E-16	28.81
CDA	9.329	-0.7087	35.38	1.57E-16	4.42E-15	25.82
KLRG2	9.306	-0.1922	28.94	3.65E-15	4.97E-14	23.66
HOXA13	9.29	-0.7244	34.91	1.94E-16	5.16E-15	25.68
MT1E	9.261	-0.7431	34.07	2.84E-16	6.94E-15	25.43
RNF175	9.26	-0.7492	31.59	9.24E-16	1.65E-14	24.62
LGR4	9.257	0.8075	25.46	2.67E-14	2.45E-13	22.15
THSD7A	9.24	-0.747	35.58	1.44E-16	4.17E-15	25.87
GSTM4	9.207	-0.2415	27.44	8.33E-15	9.60E-14	23.03
EMP2	9.161	0.9209	24.73	4.19E-14	3.53E-13	21.79
HP	9.112	-0.2879	29.24	3.10E-15	4.41E-14	23.77
KCNN2	9.111	-0.2871	29.76	2.36E-15	3.52E-14	23.97
HLA-DQB1	9.095	-0.04873	24.99	3.58E-14	3.11E-13	21.9
RPS6KL1	9.09	-0.8286	33.88	3.09E-16	7.41E-15	25.36
NID1	9.088	-0.8344	31.01	1.24E-15	2.09E-14	24.4
ANXA6	9.071	3.035	38.68	3.87E-17	1.69E-15	27.8
HOMER1	9.066	-0.8307	33.32	4.02E-16	8.91E-15	25.18
CD14	9.036	0.736	34.25	2.61E-16	6.53E-15	25.55
CPNE7	9.03	-0.08278	18.15	4.85E-12	2.04E-11	17.69
CPEB2	9.018	-0.3251	25.22	3.10E-14	2.77E-13	22
RNASE3	8.996	-0.3488	27.95	6.25E-15	7.64E-14	23.24
SLC22A16	8.992	0.06169	19.58	1.53E-12	7.46E-12	18.72
CD163L1	8.992	-0.3435	29.18	3.20E-15	4.50E-14	23.74
C9orf64	8.964	-0.896	31.48	9.76E-16	1.72E-14	24.56
GLT1D1	8.945	-0.9033	32.3	6.52E-16	1.28E-14	24.84

CBX1	9.989	1.217	19.51	4.30E-11	2.50E-10	15.04
HSD11B1	9.977	-0.3745	31.78	7.99E-14	2.24E-12	19.13
PSMD5	9.971	1.087	23.41	4.17E-12	3.92E-11	16.74
KLF4	9.962	-0.3819	29.79	1.85E-13	3.93E-12	18.67
LRRC4	9.961	-0.3812	31.64	8.46E-14	2.31E-12	19.1
ARHGEF39	9.96	0.1452	24.16	2.77E-12	2.88E-11	17.01
IRF8	9.952	3.527	37.05	1.08E-14	5.81E-13	21.8
GPR27	9.948	-0.3886	30.96	1.12E-13	2.83E-12	18.95
ATP6V0E2	9.946	-0.3908	31.11	1.05E-13	2.70E-12	18.98
KIAA1598	9.906	-0.4092	29.69	1.94E-13	4.04E-12	18.64
GPR88	9.865	0.3448	22.83	5.76E-12	4.99E-11	16.51
HOXA11	9.864	-0.428	25.92	1.12E-12	1.45E-11	17.59
NR2F2	9.83	-0.4456	27.86	4.40E-13	7.23E-12	18.16
PBK	9.788	-0.467	27.3	5.73E-13	8.80E-12	18
S100A6	9.784	0.8325	24.32	2.55E-12	2.70E-11	17.07
PON2	9.782	-0.4734	29.83	1.82E-13	3.89E-12	18.67
FAIM	9.773	-0.4739	28.63	3.09E-13	5.59E-12	18.37
GALNT14	9.761	-0.4824	30.59	1.31E-13	3.10E-12	18.86
FAM64A	9.749	-0.4889	30.02	1.68E-13	3.67E-12	18.72
SIX2	9.741	-0.4901	28.37	3.48E-13	6.08E-12	18.3
TRIP6	9.735	1.795	21.79	1.05E-11	8.02E-11	16.1
ARL4C	9.666	-0.5268	25.7	1.25E-12	1.58E-11	17.51
TMEM246	9.654	-0.5345	30.2	1.55E-13	3.49E-12	18.76
CTC-276P9.1	9.654	-0.5343	29.14	2.46E-13	4.78E-12	18.5
CCR2	9.648	3.481	38.21	7.26E-15	4.38E-13	22.15
CCDC50	9.643	-0.5383	27.2	6.00E-13	9.13E-12	17.97
GNAI1	9.634	-0.5438	29.4	2.19E-13	4.46E-12	18.56
MCOLN2	9.63	-0.5487	29.37	2.22E-13	4.48E-12	18.55
NEBL	9.616	-0.5544	30.86	1.17E-13	2.91E-12	18.91
S100A10	9.592	-0.5668	29.52	2.08E-13	4.27E-12	18.59
GAS6	9.58	-0.04454	24.5	2.32E-12	2.52E-11	17.12
AGT	9.518	-0.07534	26.37	8.98E-13	1.24E-11	17.73
BBS7	9.499	-0.6149	26.17	9.88E-13	1.33E-11	17.65
FAM83G	9.471	-0.6291	27.11	6.26E-13	9.41E-12	17.93
SLC22A15	9.454	0.4199	26.16	9.93E-13	1.33E-11	17.68
GPD2	9.435	-0.1172	26.27	9.44E-13	1.28E-11	17.7
PYGO1	9.415	-0.654	29.75	1.88E-13	3.97E-12	18.64
C10orf118	9.408	-0.66	29.08	2.52E-13	4.89E-12	18.47
MPO	9.377	3.155	35.63	1.81E-14	8.34E-13	21.4
HOXA13	9.372	-0.6737	26.45	8.61E-13	1.19E-11	17.73
KLRG2	9.36	-0.1559	25.01	1.78E-12	2.07E-11	17.29
ALDH1L2	9.342	0.08266	22.38	7.41E-12	6.08E-11	16.32
CDA	9.339	-0.6933	29.81	1.83E-13	3.90E-12	18.65
IFI27L2	9.332	-0.698	27.47	5.28E-13	8.36E-12	18.03
RNF175	9.322	-0.7019	29.22	2.38E-13	4.68E-12	18.5
CKAP4	9.293	0.8688	28.97	2.65E-13	5.02E-12	18.49
HLA-DQB1	9.283	0.05293	22.05	8.99E-12	7.11E-11	16.18
AC018470.4	9.26	-0.7439	14.15	2.45E-09	7.85E-09	11.66
NID1	9.219	-0.748	22.98	5.29E-12	4.68E-11	16.53
THSD7A	9.198	-0.7684	24.1	2.87E-12	2.94E-11	16.95
GSTM4	9.191	-0.2399	23.82	3.34E-12	3.31E-11	16.87
MT1E	9.185	-0.773	25.74	1.23E-12	1.57E-11	17.5
LGR4	9.18	0.7755	20.11	2.91E-11	1.83E-10	15.33
C3orf14	9.167	-0.7756	25.9	1.13E-12	1.46E-11	17.55
ANXA6	9.144	3.076	34.24	3.03E-14	1.17E-12	21.12
MLPH	9.108	-0.8051	25.55	1.35E-12	1.68E-11	17.44
CPNE7	9.098	-0.04883	11.86	2.12E-08	5.43E-08	9.715
RPS6KL1	9.096	-0.8159	22.71	6.16E-12	5.25E-11	16.42
KCNN2	9.092	-0.2872	24.76	2.02E-12	2.26E-11	17.2
EMP2	9.089	0.8919	20.68	2.05E-11	1.38E-10	15.59
SLC22A16	9.085	0.115	17.49	1.72E-10	7.98E-10	13.92
ADD2	9.05	2.032	28.79	2.88E-13	5.32E-12	18.73
CPEB2	9.046	-0.3131	20.69	2.04E-11	1.37E-10	15.58
GLT1D1	9.043	-0.8428	25.18	1.63E-12	1.93E-11	17.31
HOMER1	9.038	-0.8431	28.18	3.80E-13	6.57E-12	18.21
SLPI	9.006	-0.8628	26.33	9.15E-13	1.25E-11	17.68
EDA2R	9.004	-0.8614	27.2	6.02E-13	9.13E-12	17.93

ADD2	8.936	1.968	34.07	2.84E-16	6.94E-15	25.68
ISL2	8.929	-0.9045	34.1	2.79E-16	6.89E-15	25.41
DYNLT3	8.926	-0.9123	33.2	4.26E-16	9.19E-15	25.13
HTATIP2	8.925	-0.9064	34.52	2.31E-16	5.91E-15	25.53
EDA2R	8.922	-0.9063	33.07	4.53E-16	9.63E-15	25.09
SLPI	8.909	-0.9189	33.62	3.49E-16	8.08E-15	25.26
MTX3	8.897	-0.9124	31.49	9.72E-16	1.72E-14	24.56
MLPH	8.887	-0.9283	33.13	4.40E-16	9.41E-15	25.1
PTPN14	8.873	1.669	29.84	2.26E-15	3.41E-14	24.09
AC018470.4	8.867	-0.9417	26.28	1.63E-14	1.64E-13	22.47
LY86	8.855	0.3547	25.41	2.75E-14	2.52E-13	22.11
ISOC1	8.837	-0.9503	33.36	3.95E-16	8.82E-15	25.17
CIDEB	8.834	1.409	28.14	5.65E-15	7.10E-14	23.37
RP11-742N3.1	8.812	3.119	34.53	2.29E-16	5.88E-15	26.62
ANKRD18B	8.805	-0.9713	31.78	8.44E-16	1.55E-14	24.65
FZD3	8.799	0.3369	25.67	2.35E-14	2.21E-13	22.24
HOXA7	8.781	-0.9678	29.43	2.80E-15	4.06E-14	23.79
RGAG4	8.735	-0.4754	27.1	1.02E-14	1.12E-13	22.86
TRIM59	8.734	1.235	32.72	5.34E-16	1.10E-14	25.07
CDC42BPB	8.707	-0.4878	28.2	5.45E-15	6.93E-14	23.33
ANKRD22	8.702	0.2834	25.79	2.19E-14	2.08E-13	22.29
ZNF532	8.683	0.5199	25.29	2.96E-14	2.67E-13	22.06
CCDC112	8.654	-1.049	32.06	7.35E-16	1.40E-14	24.73
PRLR	8.639	-1.042	28.12	5.70E-15	7.14E-14	23.26
GSTM1	8.628	-0.5236	24.36	5.31E-14	4.27E-13	21.55
VWDE	8.611	-1.071	28.09	5.80E-15	7.25E-14	23.24
PHLDA3	8.601	0.2369	23.29	1.06E-13	7.60E-13	21.01
GCHFR	8.593	-1.074	32.96	4.77E-16	9.99E-15	25.01
NCS1	8.588	0.472	24.89	3.80E-14	3.25E-13	21.86
ARHGEF10L	8.568	-0.3093	22.35	2.00E-13	1.31E-12	20.46
KCNA3	8.564	-1.084	32.6	5.66E-16	1.15E-14	24.9
HOXB7	8.522	-0.5745	26.74	1.25E-14	1.32E-13	22.69
FAM111B	8.519	-1.113	32.02	7.49E-16	1.42E-14	24.7
SLC7A2	8.496	-1.113	30.33	1.75E-15	2.74E-14	24.11
ANKRD18A	8.476	-1.121	26.59	1.36E-14	1.41E-13	22.58
ARSD	8.474	-1.13	32.09	7.23E-16	1.39E-14	24.72
SIRPB2	8.473	0.5771	20	1.10E-12	5.63E-12	19.02
ABCA5	8.465	-1.144	25.71	2.30E-14	2.17E-13	22.17
HRH2	8.394	0.1338	25.29	2.97E-14	2.68E-13	22.04
NOS2	8.387	-0.406	22.13	2.34E-13	1.49E-12	20.33
RP11-84C10.2	8.376	1.742	22.03	2.51E-13	1.59E-12	20.4
SLC8A1	8.354	1.445	23.68	8.22E-14	6.16E-13	21.27
FAM127A	8.338	-1.203	31.24	1.10E-15	1.90E-14	24.41
3-Sep	8.332	0.8759	30.61	1.52E-15	2.48E-14	24.32
FAM127B	8.318	-1.215	28.76	4.00E-15	5.37E-14	23.48
KCNQ3	8.284	-1.228	30.73	1.43E-15	2.34E-14	24.22
LRRK2	8.277	-1.231	29.22	3.13E-15	4.43E-14	23.66
CPM	8.275	1.889	24.86	3.86E-14	3.30E-13	22.04
ADRB2	8.274	-1.236	30.77	1.40E-15	2.32E-14	24.23
FAM50B	8.273	-1.236	29.16	3.24E-15	4.53E-14	23.64
SLC2A5	8.272	0.475	22.29	2.09E-13	1.35E-12	20.45
LRRCC1	8.263	0.4671	21.06	5.02E-13	2.87E-12	19.7
LOXHD1	8.246	-0.7207	23.15	1.16E-13	8.21E-13	20.89
SERPING1	8.241	-0.7324	24.19	5.90E-14	4.65E-13	21.44
SGSH	8.234	-1.253	31.29	1.08E-15	1.87E-14	24.41
PRDM5	8.231	-1.253	31.24	1.10E-15	1.90E-14	24.4
QPCT	8.187	-0.7509	25.27	3.00E-14	2.71E-13	21.98
1-Mar	8.175	-1.287	29.59	2.57E-15	3.78E-14	23.79
CITED4	8.168	1.112	23.89	7.15E-14	5.45E-13	21.35
ADAMTS5	8.162	-1.288	29.22	3.12E-15	4.43E-14	23.65
SLITRK4	8.156	-1.299	29.41	2.83E-15	4.10E-14	23.72
SERPINA1	8.141	0.249	23.24	1.09E-13	7.81E-13	20.98
TMEM233	8.131	-1.307	30.55	1.56E-15	2.52E-14	24.14
ZBTB38	8.084	0.2557	17.89	6.05E-12	2.48E-11	17.49
CES1P1	8.078	-1.332	30.56	1.56E-15	2.52E-14	24.13
HMX3	8.064	-0.5625	19.33	1.86E-12	8.84E-12	18.52

RNASE3	8.984	-0.3426	24.76	2.03E-12	2.26E-11	17.19
ISL2	8.966	-0.8815	25.29	1.54E-12	1.84E-11	17.34
HOXA7	8.96	-0.8797	26.4	8.85E-13	1.22E-11	17.69
HP	8.952	-0.3565	23.3	4.43E-12	4.12E-11	16.66
CD14	8.949	0.6963	28.15	3.86E-13	6.65E-12	18.26
C9orf64	8.939	-0.8928	28.56	3.20E-13	5.73E-12	18.3
CD163L1	8.937	-0.3653	24.54	2.27E-12	2.48E-11	17.11
LY86	8.932	0.4063	23.25	4.54E-12	4.20E-11	16.67
PTPN14	8.891	1.681	20.17	2.81E-11	1.78E-10	15.42
CIDEB	8.884	1.438	24.06	2.93E-12	2.99E-11	16.98
DYNLT3	8.88	-0.9228	27.93	4.27E-13	7.13E-12	18.13
HTATIP2	8.87	-0.9246	25.01	1.77E-12	2.06E-11	17.25
RP11-742N3.1	8.788	3.116	26.49	8.48E-13	1.18E-11	18.92
MTX3	8.757	-0.9854	27.44	5.35E-13	8.41E-12	17.99
VWDE	8.72	-1.008	21.97	9.43E-12	7.40E-11	16.1
ZNF532	8.719	0.5444	21.82	1.03E-11	7.93E-11	16.09
ISOC1	8.718	-1.003	24.99	1.80E-12	2.08E-11	17.23
CDC42BPB	8.685	-0.4929	23.54	3.88E-12	3.71E-11	16.74
GCHFR	8.682	-1.023	26.94	6.80E-13	9.99E-12	17.84
TRIM59	8.67	1.211	24.33	2.54E-12	2.69E-11	17.07
ABCA5	8.666	-1.033	24.97	1.82E-12	2.09E-11	17.22
ANKRD18B	8.665	-1.028	26.35	9.06E-13	1.24E-11	17.66
ARSD	8.655	-1.033	24.43	2.41E-12	2.58E-11	17.03
FZD3	8.618	0.2494	22.12	8.63E-12	6.87E-11	16.21
CCDC112	8.61	-1.057	27.24	5.91E-13	9.04E-12	17.92
GSTM1	8.609	-0.5311	20.87	1.82E-11	1.25E-10	15.64
KCNA3	8.592	-1.064	24.35	2.51E-12	2.67E-11	17
ARHGEF10L	8.585	-0.2956	19.81	3.54E-11	2.14E-10	15.15
SLC7A2	8.552	-1.085	25.42	1.44E-12	1.77E-11	17.36
RGAG4	8.544	-0.5606	22.01	9.18E-12	7.24E-11	16.14
HOXB7	8.528	-0.5692	22.57	6.66E-12	5.58E-11	16.36
NCS1	8.527	0.4486	20.03	3.08E-11	1.91E-10	15.28
SIRPB2	8.516	0.604	16.37	3.96E-10	1.61E-09	13.24
FAM111B	8.494	-1.115	24.82	1.96E-12	2.21E-11	17.15
PRLR	8.478	-1.12	23.71	3.53E-12	3.43E-11	16.77
ANKRD22	8.463	0.17	20.5	2.28E-11	1.50E-10	15.5
KCNQ3	8.437	-1.142	25.99	1.08E-12	1.41E-11	17.53
HRH2	8.416	0.1487	21.74	1.08E-11	8.21E-11	16.05
3-Sep	8.402	0.9143	25.34	1.50E-12	1.82E-11	17.41
ANKRD18A	8.397	-1.165	26.51	8.37E-13	1.17E-11	17.69
NOS2	8.366	-0.4038	19.37	4.71E-11	2.69E-10	14.93
ADRB2	8.36	-1.182	25.43	1.44E-12	1.77E-11	17.35
RP11-84C10.2	8.329	1.717	19.06	5.79E-11	3.20E-10	14.98
FAM127A	8.323	-1.203	25.51	1.38E-12	1.72E-11	17.37
FAM50B	8.314	-1.205	25.87	1.15E-12	1.48E-11	17.48
LRRCC1	8.302	0.497	17.57	1.63E-10	7.61E-10	13.97
SLC2A5	8.3	0.4968	19.37	4.70E-11	2.69E-10	14.95
CITED4	8.281	1.177	21.92	9.70E-12	7.55E-11	16.14
SLC8A1	8.278	1.409	21.05	1.63E-11	1.14E-10	15.84
PHLDA3	8.276	0.07706	18.23	1.02E-10	5.12E-10	14.34
FAM127B	8.275	-1.223	23.45	4.08E-12	3.85E-11	16.65
SERPING1	8.263	-0.7023	21.98	9.36E-12	7.35E-11	16.11
CDC42EP1	8.245	-1.238	23.79	3.39E-12	3.34E-11	16.77
LRRK2	8.235	-1.245	24.29	2.59E-12	2.73E-11	16.95
CPM	8.233	1.882	21.03	1.65E-11	1.16E-10	16.05
LOXHD1	8.23	-0.7242	18.17	1.06E-10	5.30E-10	14.28
TMEM233	8.207	-1.265	22.26	7.94E-12	6.43E-11	16.19
CES1P1	8.201	-1.266	23.59	3.77E-12	3.63E-11	16.7
SGSH	8.158	-1.285	25.29	1.54E-12	1.84E-11	17.28
ADAMTS5	8.148	-1.286	24.22	2.68E-12	2.81E-11	16.92
ARHGAP12	8.142	-0.3587	16.34	4.06E-10	1.65E-09	13.2
HMX3	8.121	-0.5277	17.15	2.21E-10	9.78E-10	13.7
PRDM5	8.12	-1.305	23.78	3.40E-12	3.35E-11	16.76
43525	8.11	-1.306	24.12	2.84E-12	2.92E-11	16.88
SLAIN1	8.103	-1.31	24.82	1.96E-12	2.21E-11	17.12
NKX2-3	8.068	-1.327	23.11	4.90E-12	4.44E-11	16.51

Supplemental Table 2.4. AML patients treated with gilteritinib in Study ID: 2215-CL-910

Patient ID	FLT3i	FLT3 status	Difference between collection date and treatment start (days)	Blast (pre/post-treatment)
Patient -1	Gilteritinib	FLT3-TKD	27	11% - 4%
Patient -2	Gilteritinib	FLT3-ITD	39	24% - 4%

Chapter 3: Targeting innate immune pathways to overcome adaptive resistance in AML using a novel polypharmacologic inhibitor

The work in Chapters 2 and 3 will be published in *Science Translation Medicine.*

Abstract

To overcome the innate immune adaptive resistance mechanism described in Chapter 2, we developed a small molecule that simultaneously inhibits FLT3 and IRAK1/4 kinases. The multi-kinase FLT3-IRAK1/4 inhibitor, NCGC1481, eliminated adaptively resistant FLT3-ITD AML cells in vitro and in vivo, and displayed superior efficacy as compared to current targeted FLT3 therapies. These findings uncover a polypharmacologic strategy for overcoming adaptive resistance to therapy in AML by targeting immune stress response pathways.

Results

Small-molecule inhibitors were generated to simultaneously target IRAK1/4 and FLT3.

The immediate nature of IRAK1/4 activation in adaptively resistant FLT3-ITD AML cells requires concomitant inhibition of these targets to avoid compensatory signaling and cell survival. Achieving optimal multi-drug combination regimens that yield extended overlapping exposure while avoiding unwanted toxicities is challenging. Therefore, we desired a small molecule inhibitor that simultaneously targeted the FLT3 and IRAK1/4 kinases to eradicate adaptively resistant FLT3-ITD AML. Inhibition of FLT3 is a common 'off-target' pharmacology for many advanced kinases inhibitors (e.g. cabozantinib, sorafenib and ponatinib). We therefore considered previously reported IRAK1/4 inhibitors as potential starting points for the optimization of a dual FLT3/IRAK inhibitor. Among the more promising candidates were a series of 3-(pyridin-2-yl)imidazo[1,2-a]pyridines that were previously reported as selective IRAK4 inhibitors and appeared to be attractive chemical starting points for optimization as dual FLT3/IRAK inhibitors (*72*). Structure activity relationship exploration around this core scaffold yielded a series of small molecules that potently targeted IRAK1, IRAK4, and FLT3. In a functional biochemical assay, three of these agents (NCGC2376, NCGC2327, and NCGC1410) inhibited FLT3 at subnanomolar concentrations (IC_{50} < 0.5 nM), and IRAK1 and IRAK4 at low nanomolar concentrations (**Fig. 3.1A,B**). Whereas the three compounds were equipotent FLT3 inhibitors (IC_{50} < 0.5 nM), their relative efficacies at inhibiting FLT3-ITD AML cell viability correlated with their IRAK1/4 inhibitory potencies (**Fig. 3.1B,C**). Thus, the most potent IRAK1/4 inhibitor NCGC2327 (IRAK1 IC_{50} = 1.6 nM, IRAK4 IC_{50} <0.5 nM) was the most efficacious at inhibiting MLL-AF9;FLT3-ITD cell growth, and the weakest IRAK1/4 inhibitor NCGC1410 (IRAK1 IC_{50} = 636 nM, IRAK4 IC_{50} 8.7 nM) was correspondingly less efficacious (**Fig. 3.1C**). Moreover, NCGC2327 and NCGC2376 were more effective at suppressing MLL-AF9;FLT3-ITD leukemic cell recovery relative to NCGC1410, as measured by AnnexinV staining (**Fig. 3.1D**), suggesting that potency against IRAK1/4 is a driving element for suppressing adaptively resistant FLT3-ITD AML cells. Given that NCGC1410 retained

potency against IRAK4, yet was less effective at suppressing MLL-AF9;FLT3-ITD AML cells than NCGC2376, which inhibits IRAK1 and IRAK4, argues that targeting both kinases is necessary to achieve optimal suppression of FLT3-mutant AML. NCGC2327 also effectively suppressed FLT3-ITD signaling and compensatory activation of IRAK4 in MLL-AF9;FLT3-ITD cells and was more effective at preventing compensatory activation of IRAK4 as compared to simultaneously inhibiting FLT3 and IRAK1/4 with a combination of quizartinib and IRAK-Inh (**Fig. 3.1E**). These findings indicate that the efficacy of suppressing FLT3-ITD AML with a FLT3i correlates with concomitant targeting of IRAK1 and IRAK4.

Continued optimization of these agents led to the identification of NCGC1481, which retained strong biochemical potency versus FLT3, IRAK1, and IRAK4 while also displaying acceptable pharmacokinetic properties in mice (**Fig. 3.2A, fig. S3.1**). NCGC1481 exhibited potent binding affinity for IRAK1 (K_D = 2.9 nM), IRAK4 (K_D = 0.3 nM), and FLT3 (K_D = 0.3 nM), as well as potent functional inhibition of IRAK1 (IC_{50} = 22.6 nM), IRAK4 (IC_{50} = 0.8 nM), and FLT3 (IC_{50} = <0.5 nM)(**Fig. 3.2A**). To gain insight into the structure-activity relationship of this agent, we obtained a high-resolution (2.1 Å) crystal structure of the NCGC1481-IRAK4 complex (PDB: 6MOM, **Fig. 3.2B**), which demonstrates that NCGC1481 binds as a type I inhibitor (ATP-competitive binding to the active state) with excellent shape complementarity at the ATP-binding pocket. Key hydrogen bonds are established between the NCGC1481 imidazole nitrogen and a hinge domain (Met265) amide and the NCGC1481 pyrrolidine and Asp329 and Ala315 (**Fig. 3.2B**). Consistent with our data that NCGC1481 also inhibits FLT3, we have obtained a crystal structure of the NCGC1481-FLT3 complex (PDB: 6IL3). Sequence alignment and two dimensional (2D) interaction diagrams derived from these structures highlight conserved binding elements between IRAK4 and FLT3, and that the FLT3 ATP-binding domain is relatively more permissive, which is consistent with the fact that FLT3 is routinely found as an 'off-target' pharmacology for multiple kinase inhibitors (**fig. S3.2**). When profiled against 369 kinases using Reaction Biology biochemical inhibition assays, NCGC1481 demonstrated modest selectivity (10-

fold or greater selectivity versus more than 80% of tested kinases relative to IRAK1, IRAK4, and FLT3) with strong activity noted versus Src-family kinases and selected classes of receptor tyrosine kinases (**Fig. 3.2C, table S3.1**). Given the known caveats of relying on biochemical assays to decipher kinome selectivity, we felt it was critical to establish the in situ kinome selectivity for this class of agents in relevant cells (*75*). We therefore submitted NCGC1481 to the KiNativ in situ kinase profiling platform. Examination of NCGC1481 in MV4;11 revealed a higher kinase selectivity in situ relative to the selectivity observed in biochemical assays using purified, active proteins (**Fig. 3.2D,E, table S3.2**). Of the 259 expressed and active kinases in MV4;11 cells, only 12 were inhibited with an IC_{50} value of less than 250 nM (**Fig. 3.2E**). We next sought to delineate which of these kinase targets contribute to the cytotoxicity of NCGC1481. For this we generated a series of analogs of NCGC1481 with varying potency against the 12 top kinase targets based on biochemical inhibition assays and then evaluated each analog's cytotoxicity in MV4;11 cells (**Fig. 3.2F**). Based on this analysis, the more highly correlated contributing targets to the cytotoxicity of MV4;11 cells are FLT3 (R^2 = 0.79), IRAK4 (R^2 = 0.70), and LYN (R^2 = 0.87). IRAK1 also shows correlation between potency and cytotoxicity, but the potency decline between NCGC2376 and NCGC1410 is ~35-fold, whereas the cytotoxicity decline between these two analogs is only 2-fold. Although LYN was inhibited by NCGC1481 in the biochemical assays, NCGC1481 exhibited only moderate effects on the phosphorylation status of LYN at the doses at which FLT3 and IRAK1/4 were inhibited in MV4;11 cells (**fig. S3.3A**), suggesting that inhibition of FLT3 and IRAK4 primarily contributes to the cytotoxicity of NCGC1481. Notwithstanding, most small molecule kinase inhibitors target more than one kinase and it is often the collective inhibition of multiple signaling nodes that contributes to the broad biological effects of a kinase inhibitor. Additional assays further demonstrated that NCGC1481 inhibited phosphorylation of FLT3 and IRAK4 and IRAK1/4-mediated NF-κB transcriptional activation in a time- and dose-dependent manner (**fig. S3.3B,C**). Moreover, NCGC1481 exhibits attractive physical properties, including

good aqueous solubility, cell permeability, metabolic stability, and low activity in selected in vitro-based toxicity-associated target assay (**fig. S3.1A,B**).

To demonstrate that NCGC1481 is selective for AML cells dependent on FLT3 signaling, we measured proliferation of isogenic AML cells lines derived from primary $CD34^+$ human cord blood cells transduced with MLL-AF9 and then transduced with $NRAS^{G12D}$ or FLT3-ITD (*45*). MLL-AF9;FLT3-ITD cells were highly sensitive to NCGC1481 (IC_{50} = 0.1 nM), whereas MLL-AF9;$NRAS^{G12D}$ cells were less responsive to NCGC1481 (IC_{50} = 573 nM)(**Fig. 3.2G**). The parental MLL-AF9 cells exhibited an intermediate sensitivity to NCGC1481 (IC_{50} = 4.9 nM) because these cells are dependent on wild-type FLT3 signaling (**Fig. 3.2G**)(*45*). As expected, NCGC1481 suppressed the short-term proliferation of MLL-AF9;FLT3-ITD, MV4;11, and MOLM13 cells (**fig. S3.3D**). In a panel of 13 primary AML patient samples, NCGC1481 was primarily effective against FLT3-mutant AML, while exhibiting minimal activity against FLT3-wild type AML (**Fig. 3.2H, table S3.3**). Collectively these data demonstrate 1) the importance of concomitant in vitro and in situ kinase target profiling; 2) that NCGC1481 is highly effective at targeting FLT3, IRAK1, and IRAK4 in FLT3-ITD mutant AML cells; and 3) that inhibition of these targets correlates with the cytotoxicity of NCGC1481.

NCGC1481 inhibits IRAK1/4 and compensatory innate immune signaling in FLT3-ITD AML cells.

The systems-level differences associated with simultaneous IRAK1/4 and FLT3 inhibition versus selective inhibition of FLT3 were next examined in FLT3-ITD AML cells. We first confirmed, via immunoblotting for pIRAK4 and pFLT3, that NCGC1481 simultaneously inhibited IRAK4 and FLT3, whereas quizartinib induced activation of IRAK4 upon inhibition of FLT3 in the appropriate cell models (MLL-AF9;FLT3-ITD and MV4;11)(**Fig. 3.3A, fig. S3.3B**). We thereafter collected protein lysates from MLL-AF9;FLT3-ITD and MV4;11 cells treated with NCGC1481 (0.1 nM; IC_{10}) for 6 and 12 hours and subjected these samples to PamChip peptide phosphorylation profiling.

Our ability to contrast these outcomes with the data generated in the same cells after quizartinib treatment (**Fig. 2.1**) offered insight into the divergent cellular response to these agents (**table S3.4**). Notably, the set of peptides with increased phosphorylation intensity after 12 hours of quizartinib treatment showed decreased phosphorylation in NCGC1481-treated MLL-AF9;FLT3-ITD and MV4;11 cells (**Fig. 3.3B**). Inspection of the IRAK1/4-specific peptides revealed that IRAK1 and IRAK4 activation was also inhibited after 6 and 12 hours of NCGC1481 treatment as compared to quizartinib (**Fig. 3.3C**). We next compared the effects of NCGC1481 and quizartinib on global gene expression in FLT3-ITD AML cells at 6 and 12 hours (**Fig. 3.3D, tables S2.3 and S3.5**). Gene expression profiling by RNA-sequencing in MLL-AF9;FLT3-ITD cells treated with NCGC1481 (0.1 nM), quizartinib (0.3 nM), or DMSO showed that genes upregulated by quizartinib, but not NCGC1481, at 12 hours were enriched for interleukin ($P = 0.0021$) and inflammation signaling ($P = 0.030$) by ToppGene analysis (**Fig. 3.3E**). Because quizartinib induced genes and kinases associated with immune signaling pathway activation, we determined whether MAPKs, which are implicated as compensatory pathways in FLT3i-treated AML cells, are regulated by IRAK1/4. Based on the in-cell kinase analysis, quizartinib-treated MLL-AF9;FLT3-ITD cells exhibited compensatory activation of Ras/MAPK as well as PI3K/AKT pathways (**Fig. 3.3F**). In contrast, NCGC1481-treated MLL-AF9;FLT3-ITD cells did not reactivate these kinases (**Fig. 3.3F**). To confirm these downstream signaling consequences, we used immunoblotting to show that quizartinib treatment resulted in increased phosphorylation of JNK and p38 at 12 hours in MLL-AF9;FLT3-ITD cells. This is approximately the same time point at which phosphorylation of IRAK4 is detected (**Fig. 2.2B, Fig. 3.3A**). In contrast, NCGC1481-treated FLT3-ITD AML cells did not exhibit phosphorylated JNK and p38 (**Fig. 3.3G**), suggesting that IRAK1/4 activation mediates immune signaling in part via MAPKs after FLT3i treatment of FLT3-ITD AML cells. Collectively these findings confirm that NCGC1481 inhibits compensatory IRAK1/4 activation and downstream immune pathways in FLT3-ITD AML.

NCGC1481 prevents adaptive resistance of FLT3-ITD AML in vitro.

We next investigated whether NCGC1481 can suppress adaptive resistance of FLT3-ITD AML in vitro. NCGC1481 treatment of MLL-AF9;FLT3-ITD, MV4;11, or FLT3-ITD AML patient-derived cells abolished the outgrowth of adaptively resistant FLT3-ITD AML cells as compared to quizartinib (**Fig. 3.4A**). NCGC1481 treatment did not inhibit the viability and progenitor function of normal $CD34^+$ BM cells after 72 hours of treatment and seven days of recovery (**Fig. 3.4B,C**). MLL-AF9;FLT3-ITD and MV4;11 cells recovered 10 days after inhibitor exposure were plated in methylcellulose to assess leukemic cell potential. The recovered MLL-AF9;FLT3-ITD and MV4;11 cells treated with NCGC1481 did not form any leukemic colonies, whereas quizartinib-treated recovered cells maintained their leukemic potential (**Fig. 3.4D**). In a direct comparison to gilteritinib, NCGC1481 was more effective at suppressing adaptively resistant MV4;11 cells (**fig. S3.4A,B**). We also noted that the leukemic cell potential of parental FLT3-ITD AML cells was diminished by NCGC1481 relative to quizartinib or DMSO (**fig. S3.4C**), which coincided with drug-stimulated induction of apoptosis (**fig. S3.4D**). NCGC1481 did not affect colony formation of healthy cord blood (CB) $CD34^+$ cells or adult $CD34^+$ BM cells at equivalent or even higher concentrations (**fig. S3.4E**).

Given the efficacy of NCGC1481 in suppressing adaptive resistance in naïve FLT3-ITD AML cells, we asked whether NCGC1481 remained effective at inhibiting adaptively resistant FLT3-ITD AML cells after treatment with quizartinib. Prior exposure of MV4;11 cells to quizartinib for 3 days followed by 7 days of recovery in fresh medium resulted in diminished sensitivity to re-exposure with quizartinib even at increased concentrations (IC_{50} = not achieved) (**Fig. 3.4E**). In contrast, NCGC1481 remained effective at eliminating adaptively resistant FLT3-ITD AML cells after primary exposure to quizartinib (IC_{50} = 230 nM)(**Fig. 3.4E**). This effect was mediated by inhibition of FLT3 and IRAK1/4, and the IRAK-Inh alone was insufficient for suppressing the viability of adaptively resistant FLT3-ITD AML (**Fig. 3.4E**). As an orthogonal approach, after three

days of exposure to quizartinib (5 μM) followed by seven days of recovery, MLL-AF9;FLT3-ITD cells were either exposed to quizartinib (5 μM) or NCGC1481 (5 μM). After 10 days, the recovered MLL-AF9;FLT3-ITD cells were treated again with quizartinib or with NCGC1481. Although repeated exposure of MLL-AF9;FLT3-ITD cells to quizartinib resulted in diminished sensitivity to quizartinib at concentrations sufficient to induce cell death of parental cells, NCGC1481 remained effective at eliminating adaptively resistant FLT3-ITD AML cells in culture after the primary or secondary exposure to quizartinib (**Fig. 3.4F**). To assess if a similar effect of NCGC1481 was observed in FLT3-ITD AML patient-derived cells, we treated primary FLT3-ITD AML cells with quizartinib (5 μM), which resulted in an acute drop in viable cells that began to recover after day three. After seven days, the recovered FLT3-ITD AML cells were treated again with quizartinib (5 μM) or with NCGC1481 (5 μM). In this setting, primary FLT3-ITD AML cells were moderately sensitive (relative to vehicle-treated cells) to quizartinib re-treatment, whereas treatment with NCGC1481 significantly reduced the number of viable FLT3-ITD AML cells (P = 0.027)(**Fig. 3.4G**).

NCGC1481 effectively targets resistant FLT3-ITD AML xenografts.

Finally, we assessed the in vivo anti-leukemic activity of NCGC1481. NCGC1481 exhibits suitable pharmacokinetic properties in mice for once-daily intraperitoneal (IP) dosing and does not result in hematologic toxicity (**fig. S31C-E**). The anti-leukemic activity of NCGC1481 was initially assessed on parental and quizartinib-refractory MLL-AF9;FLT3-ITD cells intravenously (i.v.) injected into NRGS mice, which develop aggressive disseminated AML (**Fig. 3.4H**) (*76, 77*). After 48 hours, phosphorylated IRAK4 and FLT3 were lower in MLL-AF9;FLT3-ITD cells isolated from mice treated with NCGC1481 (30 mg/kg/d) as compared to mice receiving vehicle (**Fig. 3.4I**). At the same dose, NCGC1481 administration significantly extended the overall median survival of mice xenografted with parental MLL-AF9;FLT3-ITD cells from 40 days to 49 days (P = 0.0026)(**Fig. 3.4J**). NCGC1481 also significantly extended the overall median survival of mice xenografted with quizartinib-recovered MLL-AF9;FLT3-ITD cells from 34 days to 53 days (P =

0.0068)(**Fig. 3.4J**). Mice were sacrificed when they exhibited physical symptoms of leukemia such as reduced motility, rough coat, and hunched posture. At the time of sacrifice, leukemic burden (percent GFP) in the BM (88.4 ± 5.7% versus 70.1 ± 12.8%) and spleen (79.3 ± 8.2% versus 51.4 ± 19%) was reduced after treatment with NCGC1481 as compared to vehicle-treated mice (**fig. S3.5A**). In a second approach, we compared the anti-leukemic effects of NCGC1481 and quizartinib using FLT3-mutant AML cells from patients with refractory leukemia (AML-174 and AML-019). NSGS mice were i.v. xenografted with AML-174 or AML-019 cells, then dosed with NCGC1481 (30 mg/kg/d), quizartinib (15 mg/kg/d), or vehicle (**Fig. 3.4K**). These doses were chosen to correct for the disparity in exposure concentration and half-life (NCGC1481: AUClast = 6750 hr*ng/mL, $T_{1/2}$ = 4.2 hr; quizartinib: AUClast = 155 hr*µg/mL, $T_{1/2}$ = 5.7 hr; **fig. S3.1C**). After confirming engraftment of AML-174 cells (day 0) and then after 14 days of treatment, NCGC1481 afforded a 38% and 48% reduction in leukemic burden in the BM as compared to mice receiving vehicle or quizartinib, respectively (**Fig. 3.4L**). After 28 days of treatment, mice that were treated with NCGC1481 exhibited a 66% and 50% reduction in leukemic burden in the BM as compared to mice receiving vehicle or quizartinib, respectively (**Fig. 3.4L**). Moreover, the frequency of $CD34^+$ AML cells in the BM (P = 0.0011) and spleen (P = 0.00016) was significantly reduced after NCGC1481 administration as compared to control mice (**fig. S3.5B**), indicating that NCGC1481 has an effect on disease-propagating AML cells. In this model, NCGC1481 significantly extended the overall median survival to 90 days compared to 66.5 days for mice receiving vehicle (P = 0.0016) or to 76 days for mice receiving quizartinib (P = 0.0097)(**Fig. 3.4M**). For mice xenografted with AML-019 cells, NCGC1481 administration also significantly extended the overall median survival of mice (P = 0.0021)(**Fig. 3.4N**). As compared to vehicle (median survival = 57 d) or quizartinib (median survival = 64 d), most of the mice treated with NCGC1481 did not succumb to leukemia beyond 94 days of treatment, at which time the experiment was terminated (**Fig. 3.4N**). Lastly, we wanted to determine whether NCGC1481 can reduce the leukemic burden of mice treated with quizartinib. NSGS mice were i.v. xenografted with AML-174 cells then dosed

with quizartinib (15 mg/kg/d) for 43 days and then either continued on quizartinib or switched to NCGC1481 for an additional 14 days (**fig. S3.6A**). After 43 days of quizartinib treatment, the leukemic burden in the mice was approximately 18% (**fig. S3.6B**). For the mice that continued on quizartinib treatment, the leukemic burden in the BM increased from 18% to 54% (**fig. S3.6B**), whereas for the mice that were switched to NCGC1481, the leukemic burden increased only from 17% to 43% (**fig. S3.6B**). The mice that were switched to NCGC1481 also exhibited a decrease in the $CD34^+$ leukemic stem cell population as compared to mice that continued on quizartinib treatment ($P = 0.12$)(**fig. S3.6C**).

Discussion

To overcome the current limitations of FLT3 inhibitors, we report a polypharmacologic strategy and a multi-target small molecule with potent activity against the IRAK1/4 complex and FLT3, which suppresses adaptive resistance to therapy in FLT3-mutant AML by targeting inflammatory stress response pathways.

Given the restrictions of using patient-derived samples for functional studies, it was necessary to confirm the adaptive resistance mechanism via innate immune pathway activation and validate NCGC1481 in independent FLT3-mutant AML cell lines. However, cell lines may not accurately represent the complexity of adaptive resistance mechanisms to FLT3i in patients, arguing for cautious interpretation of these data. Further, the current experimental design is limited to adaptive resistance mechanisms occurring immediately after FLT3i treatment, and it should be noted that adaptive resistance mechanisms after prolonged FLT3i treatment may differ.

Here, we identified activation of innate immune stress response pathways after treatment of FLT3-mutant AML cells with FLT3i. Although further studies are needed, our study demonstrates that therapies that simultaneously inhibit FLT3 signaling and compensatory IRAK1/4 activation have the potential to improve the therapeutic efficacy in patients with FLT3-mutant AML. We demonstrate that inflammatory stress response pathways contribute to adaptive

resistance in FLT3-mutant AML and propose that this mechanism may extend to other malignant cells undergoing a stress-induced response to therapy.

Figures

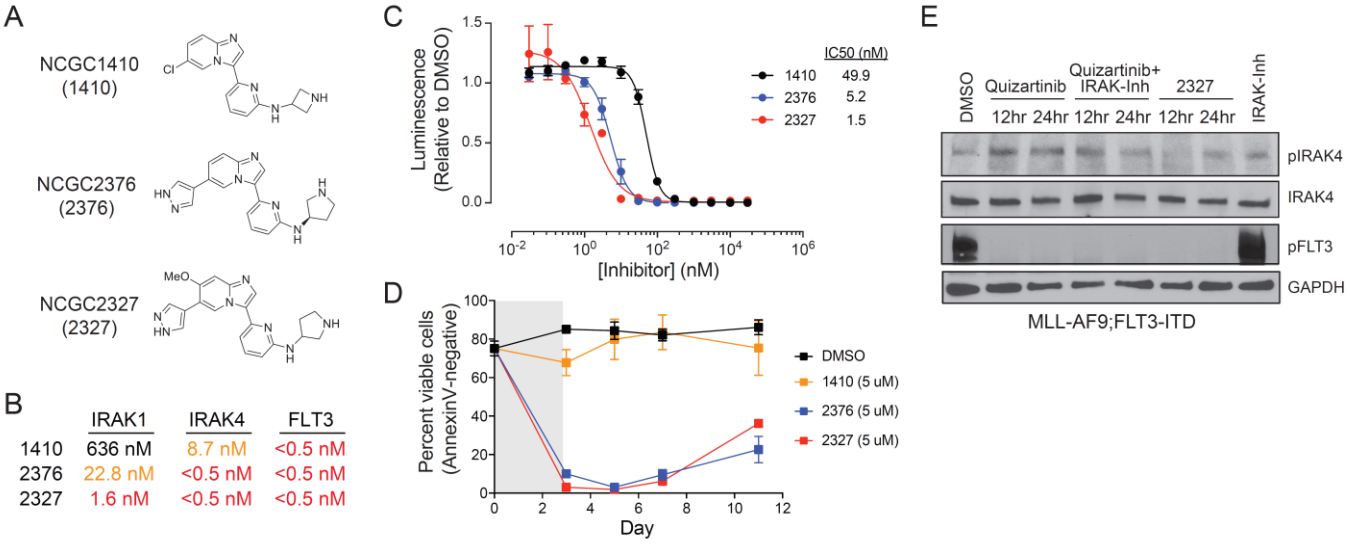

Figure 3.1. Structure activity relationship of small molecule inhibitors reveals the importance of targeting IRAK1/4 and FLT3 in FLT3+AML. (A) Chemical structures of NCGC1410, NCGC2376, and NCGC2327 (Thomas Lab). **(B)** The half maximal inhibitory concentration (IC50) for NCGC1410, NCGC2376, and NCGC2327 on IRAK1, IRAK4, and FLT3 activity (Reaction Biology). **(C)** Metabolic activity of MLL-AF9;FLT3-ITD cells treated with NCGC1410, NCGC2376, and NCGC2327 for 72 hours as measured by CellTiter-Glo. Values are expressed as means +/- s.e.m. from 3 biological replicates. **(D)** Viability of MLL-AF9;FLT3-ITD cells treated for 3 days with DMSO (vehicle control), NCGC1410, NCGC2376, or NCGC2327. Values are expressed as means +/- s.d. from 2 biological replicates. **(E)** Immunoblotting of MLL-AF9;FLT3-ITD cells treated with quizartinib (50 nM), quizartinib and IRAK-Inh (10 μM), NCGC2327 (50 nM), or IRAK-Inh.

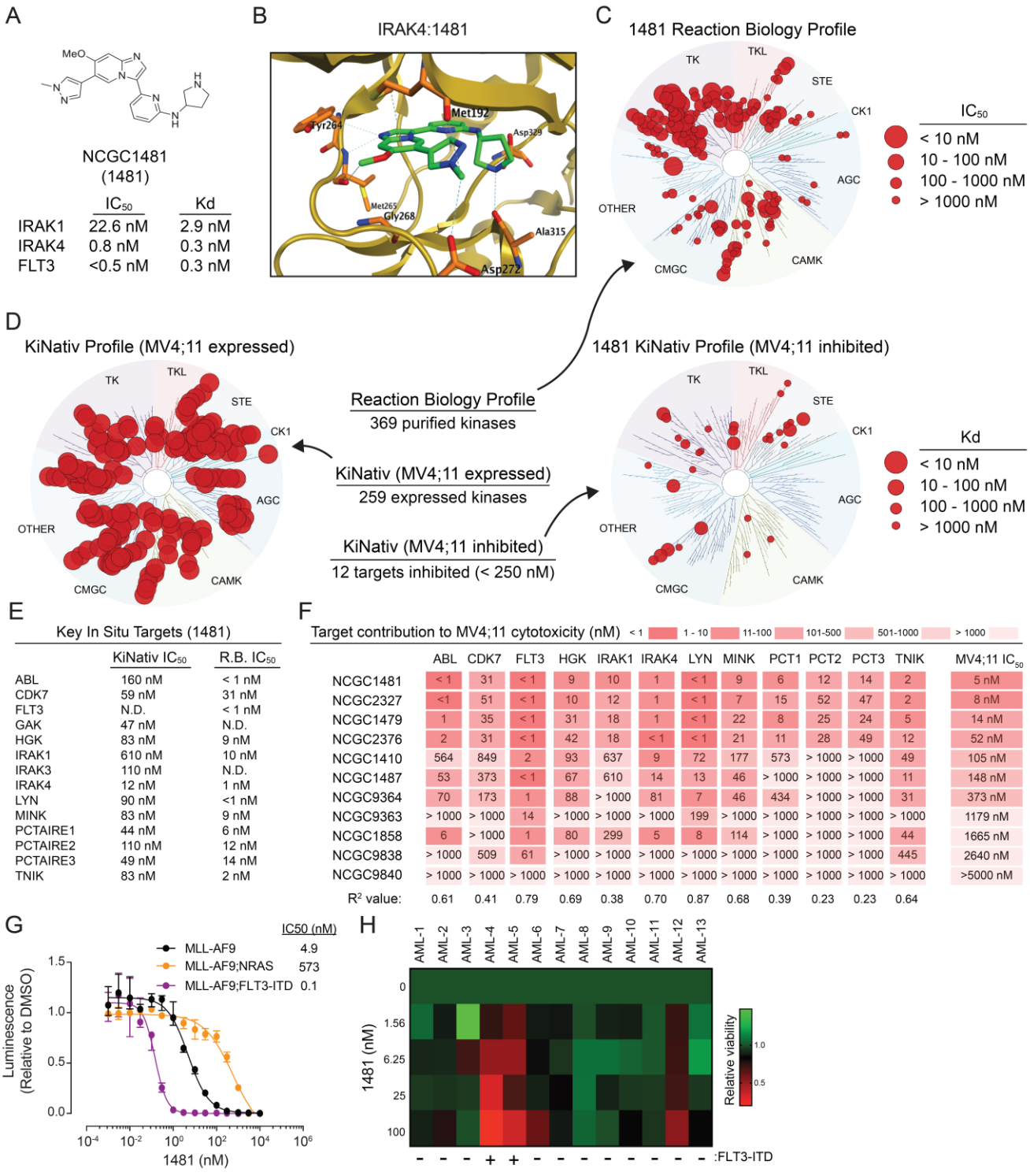

Figure 3.2. NCGC1481 is a potent of small molecule inhibitor of FLT3 and IRAK1/4. (A) Chemical structure of NCGC1481 (1481). The half maximal inhibitory concentration (IC_{50}) and equilibrium dissociation constant (K_d) for NCGC1481 with IRAK1, IRAK4, and FLT3 is shown

below the structure (Thomas Lab). **(B)** NCGC1481-binding pocket of IRAK4 from NCGC1481-IRAK4 crystal structure. IRAK4 is shown as a ribbon structure along with contact residues. NCGC1481 is shown in green and blue (Beryllium Discovery). **(C)** Reaction Biology kinome map showing selectivity of NCGC1481 across 369 purified and active kinases (Reaction Biology; Thomas Lab). **(D)** KiNative in situ kinome profile of NCGC1481 in MV4;11 cells showing the expressed and active kinases (left dendrogram) and these inhibited by NCGC1481 (right dendrogram) (KiNative; Thomas Lab). **(E)** Top kinases (listed in alphabetical order) inhibited by NCGC1481 as determined by the KiNative in situ kinome profile and the corresponding IC_{50} value for NCGC1481 as determined versus purified, active kinases at Reaction Biology (KiNative; Reaction Biology; Thomas Lab). **(F)** Table of kinase inhibitory activity (Reaction Biology, IC50 values) for top kinase targets for selected NCGC1481 analogs with variable cytotoxicity (far right column) versus MV4;11 cells (Reaction Biology; Thomas Lab). **(G)** Proliferation of MLL-AF9, MLL-AF9;FLT3-ITD, and MLL-AF9;NRAS cells treated with the indicated concentration of NCGC1481 for 72 hours. Values are expressed as means +/- s.e.m. from 3 biological replicates. **(H)** Viability of primary AML cells from 13 patients was determined in the presence of NCGC1481 for 48 hours by Trypan blue exclusion. The FLT3-ITD status of the patients is indicated below the heatmap (**table S3.3**) (Eric O'Brien).

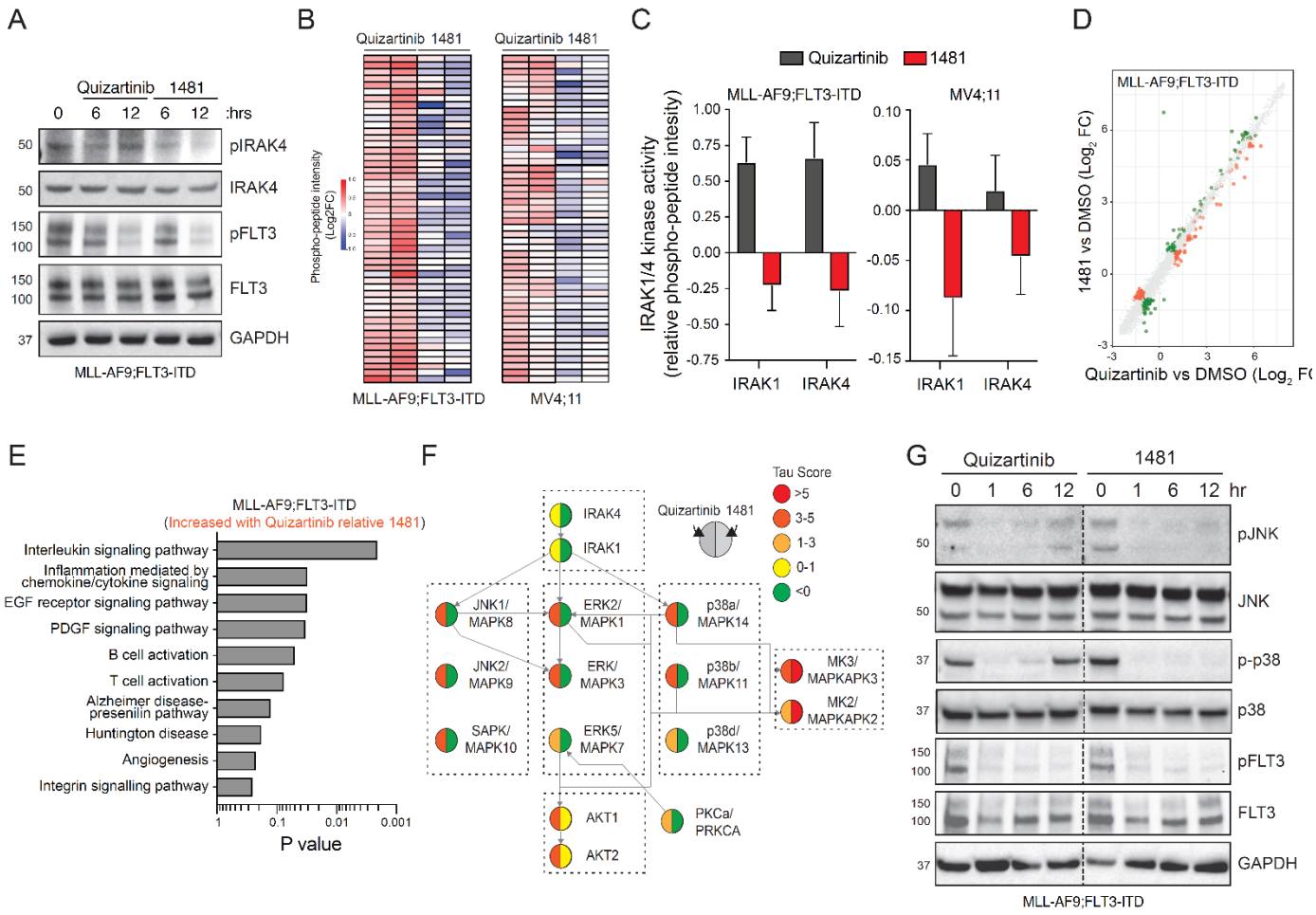

Figure 3.3. NCGC1481 inhibits compensatory IRAK1/4 signaling in FLT3-ITD AML cells. (A) Immunoblotting of pFLT3 and pIRAK4 in MLL-AF9;FLT3-ITD and MV4;11 cells treated with IC_{10} of quizartinib or NCGC1481 for 6 and 12 hours. **(B)** STK PamChip analysis was performed on protein lysates isolated from MLL-AF9;FLT3-ITD and MV4;11 cells treated with IC_{10} of quizartinib or NCGC1481 for 12 hours (PamGene, Kwangmin Choi). **(C)** IRAK1 and IRAK4 in-cell activity in MLL-AF9;FLT3-ITD and MV4;11 cells treated with IC_{10} of quizartinib or NCGC1481 for 12 hours. Values are expressed as means +/- s.d. from 2 biological duplicate samples using 4 or 3 independent peptides, respectively. **(D)** Differential gene expression of MLL-AF9;FLT3-ITD treated with IC_{10} of quizartinib or NCGC1481 for 12 hours. Summary from biological triplicate samples (Kwangmin Choi). **(E)** Pathway enrichment of differential gene expression (RNA-

sequencing) in MLL-AF9;FLT3-ITD cells treated with quizartinib for 12 hours was determined using Toppgene. **(F)** Network map of in-cell active kinases in MLL-AF9-FLT3-ITD cells treated with quizartinib for 12 hours. Tau (τ) scores indicate activity inferred from the phosphorylated peptides (STK PamChip). The left half of the circle represents data from quizartinib-treated cells. The right half of the circle represents data from NCGC1481-treated cells. **(G)** Immunoblotting of MLL-AF9;FLT3-ITD cells treated with 1 nM quizartinib or NCGC1481 for the indicated times.

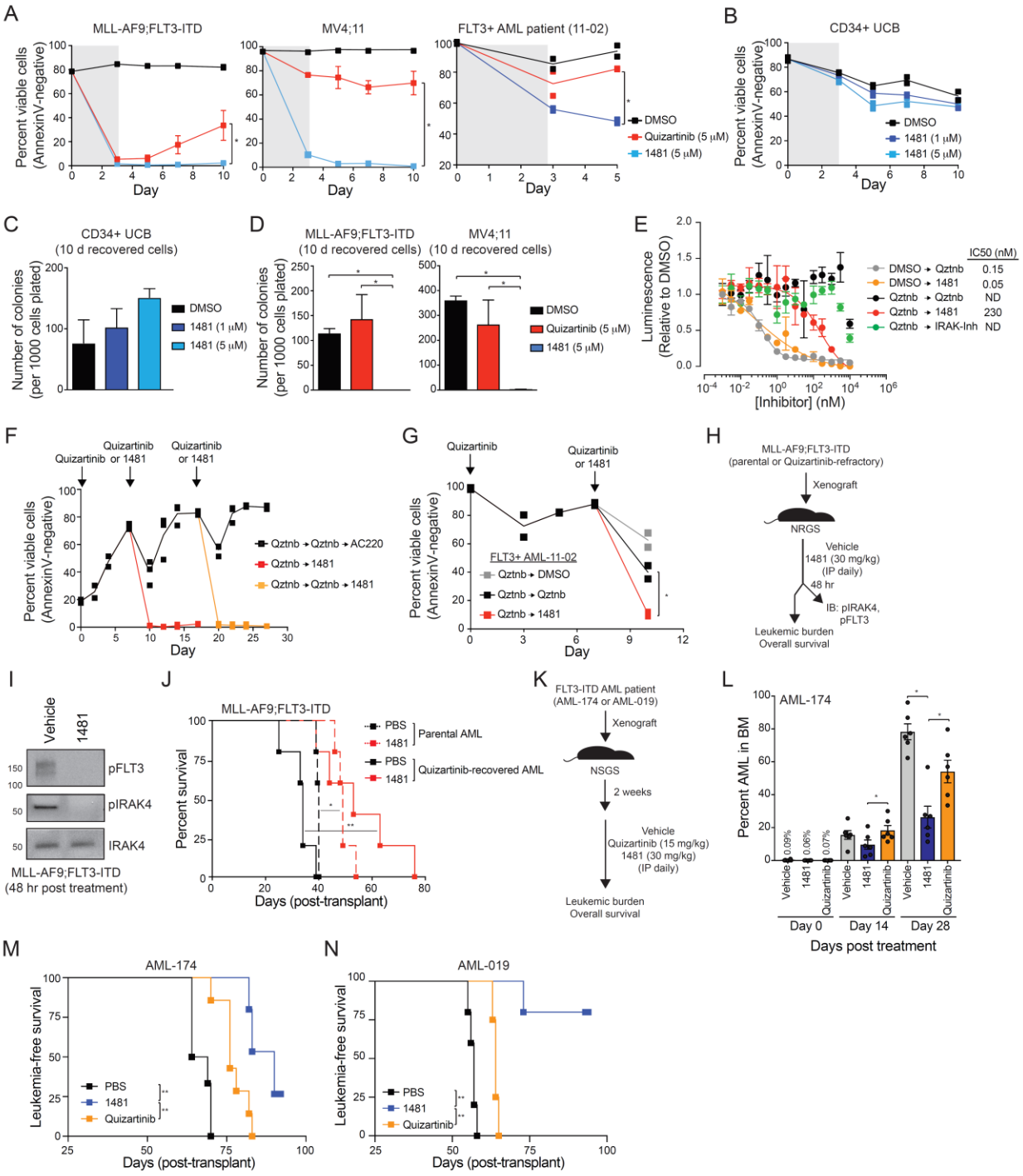

Figure 3.4. NCGC1481 prevents adaptive resistance in FLT3-ITD AML cells in vitro and prolongs survival in vivo. (A) MLL-AF9;FLT3-ITD, MV4;11, or FLT3-ITD AML patient-derived cells were cultured with quizartinib or NCGC1481 for 3 days, re-plated in fresh media, and then

cell viability was measured by AnnexinV staining. Values are expressed as means +/- s.d. from 4 biological replicates for cell lines and 2 replicates for the patient sample. *, $P < 0.05$ (unpaired two-tailed t-test). **(B)** Healthy human CD34+ umbilical cord blood cells were treated with 1481 (1 μM or 5 μM) for 3 days and re-plated in fresh media. Cell viability was measured by AnnexinV staining. Values are expressed as means +/- s.e.m. from biological duplicates. **(C)** After 10 days in liquid culture (from panel B), the remaining viable CD34+ cells were plated in methylcellulose and colony formation was determined after 14 days. Values are expressed as means +/- s.e.m. from 4 biological replicates. **(D)** After 10 days in liquid culture (from panel A), the remaining viable cells were plated in methylcellulose and colony formation was determined after 7 days. Values are expressed as means +/- s.e.m. from 4 biological replicates. *, $P < 0.05$ (unpaired two-tailed t-test). **(E)** MV4;11 cells were cultured with quizartinib (5 μM) for 3 days, plated in fresh media and then cell proliferation was determined after treatment with the indicated concentration of NCGC1481 or quizartinib (Qztnb) for 72 hours. Values are expressed as means +/- s.d. from a representative experiment from 2 independent experiments each done in technical triplicate. **(F)** MLL-AF9;FLT3-ITD cells were cultured with quizartinib (5 μM) for 3 days, plated in fresh media (Day 0 and 7) and then re-plated in media containing quizartinib (Qztnb; 5 μM) or NCGC1481 (5 μM) at days 7 and 17. Cell viability was measured by AnnexinV staining. Values are expressed as means +/- s.d. from 2 biological replicates. **(G)** FLT3-ITD AML patient-derived cells were cultured with quizartinib (Qztnb; 5 μM) for 3 days, plated in fresh media and then re-plated in media containing DMSO, quizartinib (Qztnb; 5 μM), or NCGC1481 (5 μM) at day 7. Cell viability was measured by AnnexinV staining. Values are expressed as means +/- s.d. from 2 technical replicates from the same donor cells. **(H)** Overview of experimental design of xenograft studies. Parental or quizartinib -refractory (from panel E) MLL-AF9;FLT3-ITD cells were i.v. injected in NRGS mice. On Day 10 post-transplant, the mice were treated i.p. with NCGC1481 (30 mg/kg) or vehicle control daily (n = 5 mice per condition). **(I)** After 48 hours of treatment with NCGC1481,

MLL-AF9;FLT3-ITD (GFP+) cells were isolated from the BM for immunoblot analysis. **(J)** Disease-free survival of NRGS mice xenografted with parental or quizartinib-refractory MLL-AF9;FLT3-ITD cells and treated with NCGC1481 or vehicle (n = 5 mice per condition). *, $P < 0.05$; **, $P < 0.01$ (Mantel-Cox test). **(K)** Overview of experimental design of xenograft studies using FLT3-ITD AML cells obtained from a patient (FLT3+AML-174). FLT3-ITD AML cells were i.v. injected into NSGS mice. Two weeks post-transplant, mice were treated with vehicle control, quizartinib (15 mg/kg), or NCGC1481 (30 mg/kg) i.p. daily. **(L)** Bone marrow aspirates were analyzed for leukemic burden on days 0, 14, and 28 post-treatment (n = 6 mice per condition). Values are expressed as means +/- s.e.m. from individual mice. *, $P < 0.05$ (unpaired two-tailed t-test) (Mark Wunderlich). **(M)** Leukemia-free survival of NRGS mice xenografted with AML-174 patient cells and treated with quizartinib, NCGC1481, or vehicle (n = 6 mice per group). **, $P < 0.005$ (Mantel-Cox test) (Mark Wunderlich). **(N)** Leukemia-free survival of NRGS mice xenografted with AML-019 patient cells and treated with quizartinib, NCGC1481, or vehicle (n = 4-5 mice per group). **, $P < 0.005$ (Mantel-Cox test) (LaQuita Jones, Katie Hueneman).

Supplemental Figures

A

NCGC1481	
MW	389.46
tPSA	76.85
CLogP	2.19

B

Assay	Result
Microsomal $t_{1/2}$ (r/m/h, min)	>120 / 13 / >120
Solublity @ pH 7.4 (μM)	>58
CYP3A4/2C9/2D6 IC50 (μM)	4.8 / 9.4 / 0.09
hERG/Nav1.5/Cav2.2 (% inh. @ 10μM)	1% / 0% / 11%

C

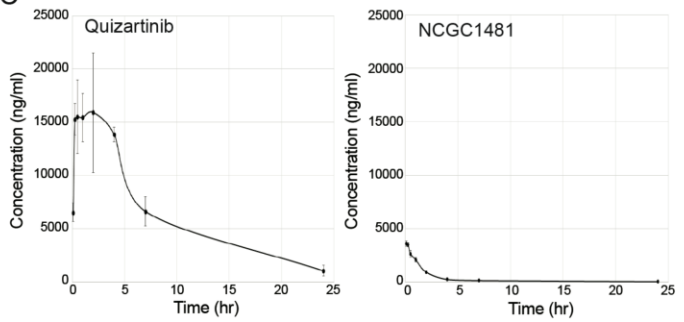

Parameter	Units	Quizartinib	NCGC1481
Dose	mg/kg	30	30
AUClast	hr*ng/ml	155000	6750
SE AUClast	hr*ng/ml	9700	226
AUCINF/D	hr*kg*ng/ml/mg	5440	227
T1/2	hr	5.7	4.2
Tmax	hr	2	0.083
Cmax	ng/ml	15900	3570
Cmax/D	kg*ng/ml/mg	530	119

D

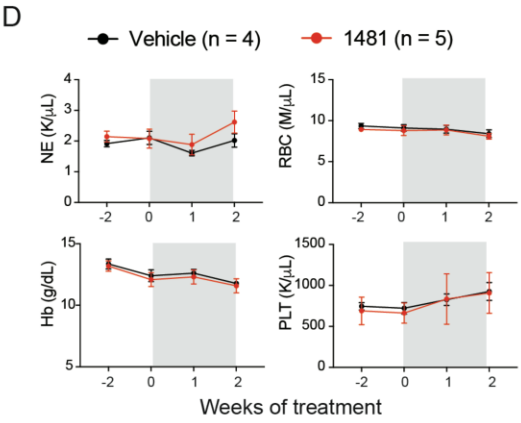

E

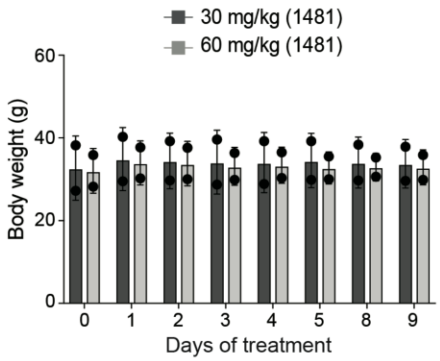

Supplemental Figure 3.1. NCGC1481 exhibits promising physicochemical, selected ADME, and in vivo pharmacokinetic properties. (A) Molecular weight, tPSA, cLogP for NCGC1481 (Thomas Lab). **(B)** Microsomal stability (rat, mouse, human), aqueous solubility, CYP inhibition (3A4, 2C9, 2D6), ion channel inhibition (nERG, Nav1.5, Cav2.2) for NCGC1481. All assays measured at a 10 μM concentration NCGC1481 (Thomas Lab). **(C)** Plasma levels of quizartinib and NCGC1481 in mice measured at the indicated time points over 24 hours. Three mice per time point were evaluated (Thomas lab). **(D)** Blood counts performed at the indicated time points on mice treated daily with 30 mg/kg IP of NCGC1481 (Lyndsey Bolanos). **(E)** Body weight

measurements of NRGS mice treated with 30 or 60 mg/kg of NCGC1481 for the indicated number of days. Data shown as s.d. (n=2 mice per time point) (Katie Hueneman, Katelyn Melgar).

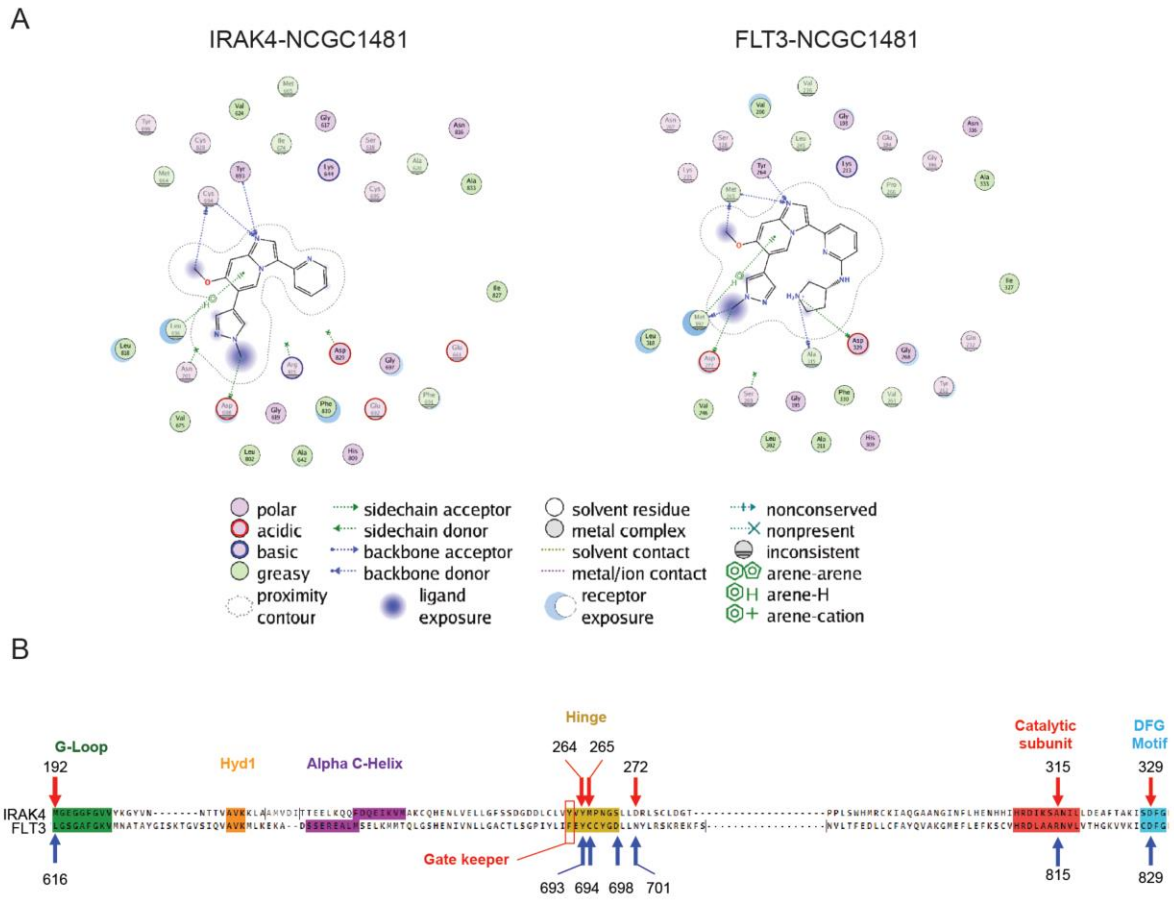

Supplemental Figure 3.2. 2-dementional interaction diagrams for NCGC1491 bound to IRAK4 and FLT3. (A) The crystal structure coordinates of the NCGC1481-IRAK4 complext (left) and the NCGC1481-FLT3 complex (right) are shown as a 2-dimentional interaction diagram. The elements of the 2-dimentional image are illustrated in the legend below (Thomas Lab). **(B)** Alignment of IRAK4 and FLT3 amino acid sequences and associated sequence annotation (Thomas Lab).

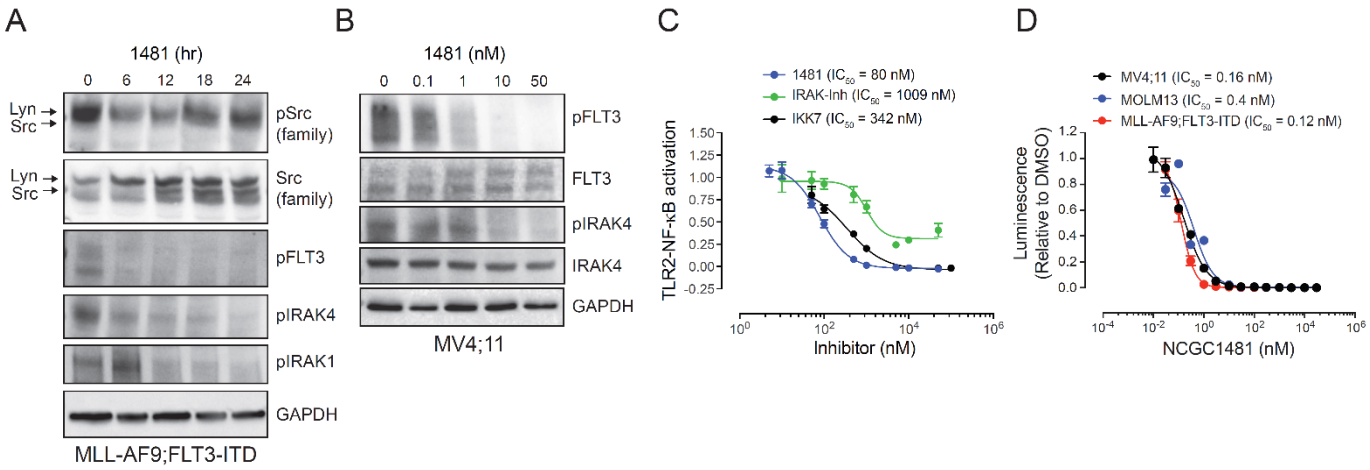

Supplemental Figure 3.3. NCGC1481 inhibits compensatory IRAK1/4 activation and adaptive resistance to FLT3-ITD AML. (A) Immunoblotting of MLL-AF9;FLT3-ITD cells treated with 10 nM NCGC1481 for the indicated hours. **(B)** Immunoblotting of MV4;11 cells treated with NCGC1481 for 24 hours. **(C)** Relative NF-κB activity in Pam3CSK4-stimulated THP1-NF-κB reporter cells treated with NCGC1481, IKK7, or IRAK-Inh for 24 hours was measured via QuantiBlue Reagent. Values are expressed as means +/- s.e.m. from 3 biological replicate samples. **(D)** Proliferation of MLL-AF9;FLT3-ITD, MV4;11, and MOLM13 cells treated with NCGC1481 for 72 hours as measured by CellTiter-Glo. Values are expressed as means +/- s.e.m. from 3 biological replicates.

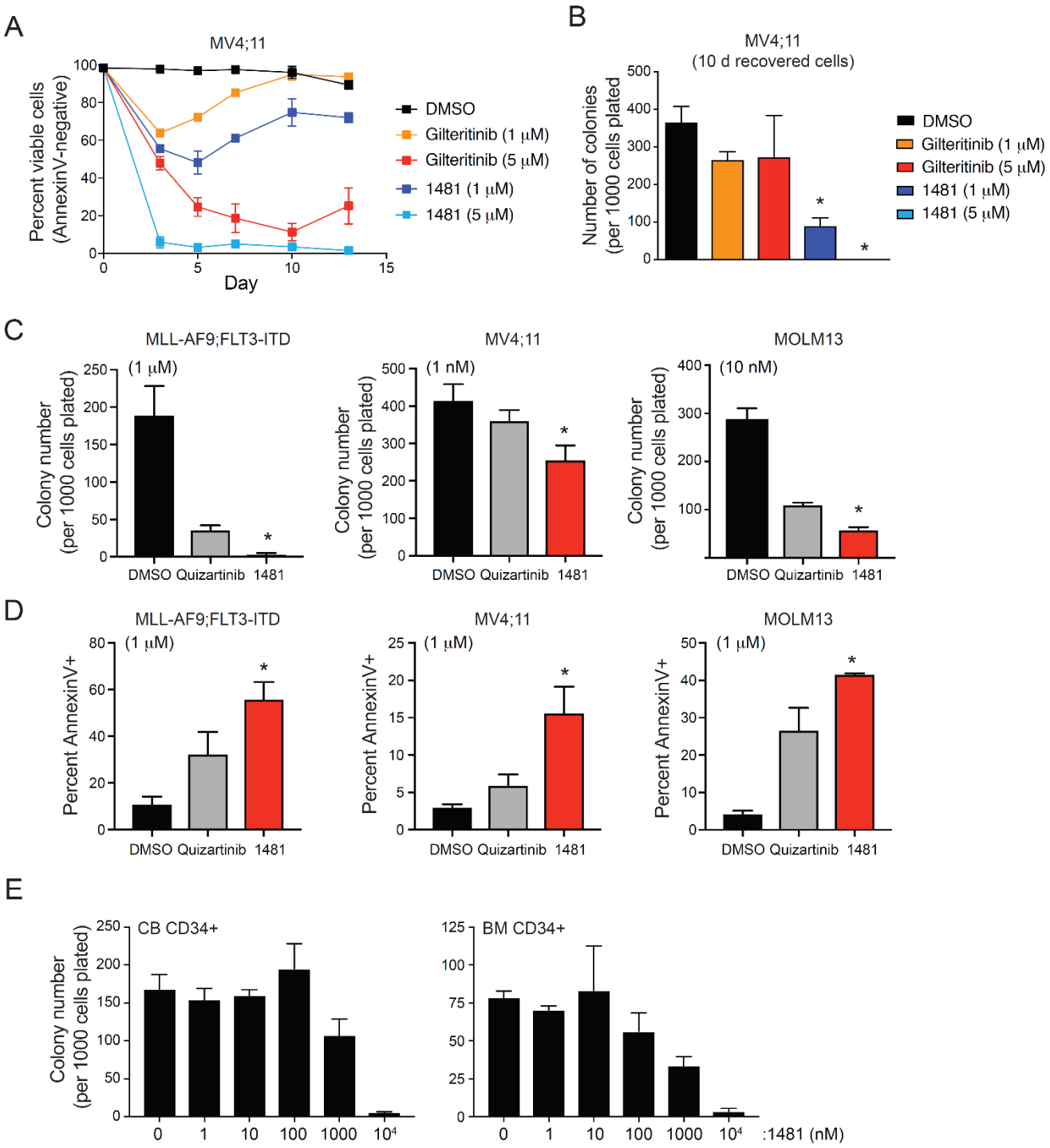

Supplemental Figure 3.4. NCGC1481 prevents adaptive resistance of FLT3-ITD AML in vitro and has minimal effects on normal hematopoietic cells. (A) MV4;11 cells were cultured with

gilteritinib or NCGC1481 for 3 days, re-plated in fresh medium and then cell viability was measured by AnnexinV staining. Values are expressed as measns +/- s.d. from 2 biological replicates. **(B)** After 10 days in liquid culture (from panel A), the remaining viable cells were plated in methylcellulose and colony formation was determined after 7 days (n = 4 per condition). *, $P < 0.05$ (unapired, two-tailed t-test). **(C)** MLL-AF9;FLT3-ITD, MV4;11, and MOLM13 cells were plated in methylcellulose and treated with DMSO, quizartinib, or NCGC1481 at the indicated concentrations. Colony formation was determined after 7 days (n = 3 per condition). *, $P < 0.05$ (unpaired, two-tailed t-test). **(D)** MLL-AF9;FLT3-ITD (n = 4), MV4;11 (n = 2), and MOLM13 (n = 2) cells were treated with DMSO, quizartinib, or 1481 for 3 days and cell death was measured using AnnexinV. *, $P < 0.05$. **(E)** Normal human CD34+ cord blood (CB) cells or normal human CD34+ bone marrow (BM) cells were plated in methylcellulose with the indicated concentrations of NCGC1481. Colony formation was determined after 12 days (n = 3 per condition). Values are expressed as means +/- s.e.m. from biological replicates.

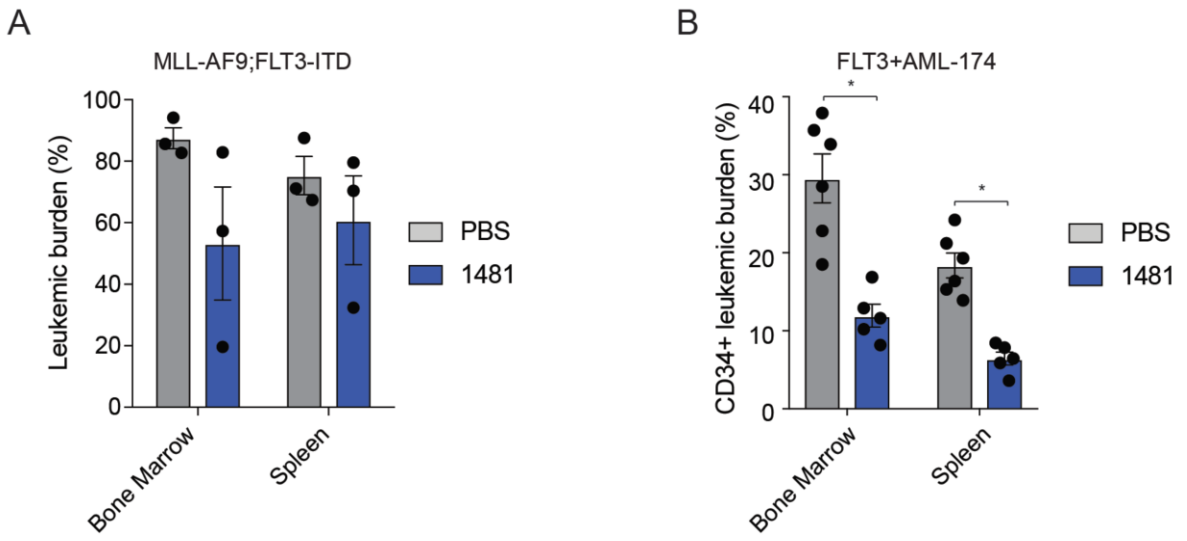

Supplemental figure 3.5. NCGC1481 reduces leukemic burden of FLT3-ITD AML. (A) Leukemic burden (%GFP+) in bone marrow (BM) and spleen at time of sacrifice in NRGS mice transplanted with MLL-AF9;FLT3-ITD cells and treated with PBS or 1481 (30 mg/kg), i.p., daily. **(B)** Leukemic burden (%CD34+) in BM and spleen at time of sacrifice in NSGS mice transplanted with FLT3+AML-174 and treated with PBS or 1481 (30 mg/kg), i.p., daily. *, $P < 0.05$. (Mark Wunderlich).

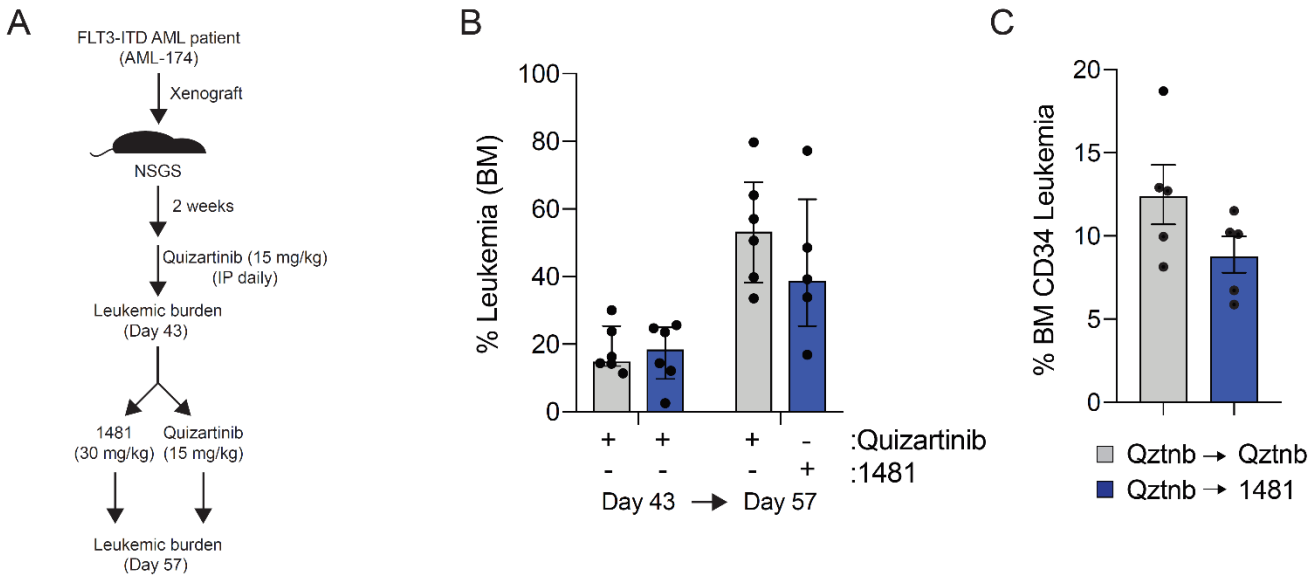

Supplemental Figure 3.6. NCGC1481 reduces the leukemic burden of FLT3-ITD AML after quizartinib treatment. (A) Overview of experimental design of xenograft studies using patient derived FLT3-ITD AML cells (AML-174). AML cells were i.v. injected into NSGS mice. Two weeks post-transplant, mice were treated with quizartinib (15 mg/kg) i.p. daily. On day 43 (after leukemic burden has been established), half of the mice were switched to daily NCGC1481 (30 mg/kg) and the other half remained on quizartinib (n = 5 mice per group). (Mark Wunderlich). **(B)** Leukemic burden (% human CD45+) in the bone marrow (BM) was determined on days 43 and 57. (Mark Wunderlich). **(C)** Leukemic stem cell burden (% human CD34+) in the BM was determined on day 57. (Mark Wunderlich)

Supplemental Tables

Supplemental Table 3.1. Reaction Biology profile of NCGC1481.

Target	IC50 (M) 1481	IC50 (M) Control Cmpd	Control Cmpd
ABL1	5.86E-10	2.95E-08	Staurosporine
ABL2/ARG	1.22E-09	1.63E-08	Staurosporine
ACK1	1.46E-07	2.63E-08	Staurosporine
AKT1	5.06E-06	4.72E-09	Staurosporine
AKT2		1.91E-08	Staurosporine
AKT3	>1.00E-05	3.07E-09	Staurosporine
ALK	3.55E-08	2.25E-09	Staurosporine
ALK1/ACVRL1	2.78E-08	1.91E-08	LDN193189
ALK2/ACVR1	6.35E-08	2.00E-08	LDN193189
ALK3/BMPR1A	7.42E-07	1.84E-08	LDN193189
ALK4/ACVR1B	4.36E-06	3.04E-07	LDN193189
ALK5/TGFBR1	9.49E-06	3.46E-07	LDN193189
ALK6/BMPR1B	2.98E-06	1.13E-08	LDN193189
ARAF		1.91E-08	GW5074
ARK5/NUAK1	8.72E-09	1.33E-09	Staurosporine
ASK1/MAP3K5		3.70E-08	Staurosporine
Aurora A	4.07E-07	1.57E-09	Staurosporine
Aurora B	2.11E-07	7.58E-09	Staurosporine
Aurora C	2.92E-07	3.92E-09	Staurosporine
AXL	2.45E-08	5.85E-09	Staurosporine
BLK	6.61E-10	1.27E-09	Staurosporine
BMPR2	9.75E-07	9.55E-07	Staurosporine
BMX/ETK	8.95E-09	5.34E-09	Staurosporine
BRAF	>1.00E-05	3.05E-08	GW5074
BRK	3.82E-08	2.38E-07	Staurosporine
BRSK1	9.49E-08	5.53E-10	Staurosporine
BRSK2	4.85E-08	1.65E-09	Staurosporine
BTK	9.22E-10	1.47E-08	Staurosporine
c-kit	2.85E-07	8.91E-08	Staurosporine
c-MER	1.63E-08	9.48E-09	Staurosporine
c-MET		8.41E-08	Staurosporine
c-Src	6.02E-10	2.65E-09	Staurosporine
CAMK1a	2.85E-06	2.05E-09	Staurosporine
CAMK1b	6.69E-06	3.10E-09	Staurosporine
CAMK1d	6.91E-07	2.12E-10	Staurosporine
CAMK1g		4.94E-09	Staurosporine
CAMK2a	4.61E-09	4.55E-12	Staurosporine
CAMK2b	1.53E-07	5.59E-11	Staurosporine
CAMK2d	2.16E-08	5.75E-11	Staurosporine
CAMK2g	1.11E-07	3.76E-10	Staurosporine
CAMK4		1.03E-07	Staurosporine
CAMKK1	2.35E-07	7.32E-08	Staurosporine
CAMKK2	7.84E-08	2.22E-08	Staurosporine
CDC7/DBF4		1.48E-08	Staurosporine
CDK1/cyclin A	1.26E-08	2.00E-09	Staurosporine
CDK1/cyclin B	1.39E-08	1.53E-09	Staurosporine
CDK1/cyclin E	3.38E-08	5.32E-09	Staurosporine
CDK14/cyclin Y (PFTK1)	9.87E-08	7.61E-08	Staurosporine
CDK16/cyclin Y (PCTAIRE)	1.43E-08	1.67E-08	Staurosporine
CDK17/cyclin Y (PCTK2)	5.66E-08	2.98E-08	Staurosporine
CDK18/cyclin Y (PCTK3)	5.04E-08	3.92E-08	Staurosporine
CDK19/cyclin C	2.17E-08	4.03E-11	Staurosporine
CDK2/cyclin A	4.79E-08	6.89E-10	Staurosporine
CDK2/Cyclin A1	1.23E-07	2.11E-09	Staurosporine
CDK2/cyclin E	1.83E-07	3.19E-09	Staurosporine
CDK2/cyclin O	7.10E-08	1.61E-09	Staurosporine
CDK3/cyclin E	4.72E-07	2.66E-09	Staurosporine
CDK4/cyclin D1	1.16E-06	2.14E-08	Staurosporine
CDK4/cyclin D3	8.44E-07	3.62E-08	Staurosporine
CDK5/p25	2.18E-07	3.00E-09	Staurosporine
CDK5/p35	8.92E-08	1.49E-09	Staurosporine
CDK6/cyclin D1	4.36E-06	8.85E-09	Staurosporine
CDK6/cyclin D3	5.58E-09	1.02E-08	Staurosporine
CDK7/cyclin H	2.24E-07	2.67E-07	Staurosporine
CDK9/cyclin K	1.20E-07	6.80E-09	Staurosporine
CDK9/cyclin T1	2.26E-07	5.01E-09	Staurosporine
CDK9/cyclin T2	9.28E-08	3.95E-09	Staurosporine
CHK1	2.63E-08	1.37E-10	Staurosporine
CHK2	5.11E-09	7.92E-09	Staurosporine
CK1a1	6.94E-06	3.40E-06	Staurosporine
CK1a1L		1.27E-06	Staurosporine
CK1d	9.79E-06	2.35E-07	D4476
CK1epsilon		3.25E-07	D4476
CK1g1	6.28E-06	7.04E-06	Staurosporine
CK1g2	5.67E-06	1.54E-06	Staurosporine
CK1g3	3.18E-06	2.44E-06	Staurosporine
CK2a		2.83E-07	GW5074
CK2a2	5.99E-06	2.39E-07	Staurosporine
CLK1	1.09E-08	5.71E-09	Staurosporine
CLK2	7.18E-09	3.55E-09	Staurosporine
CLK3	1.68E-06	1.30E-06	Staurosporine
CLK4	3.59E-08	3.19E-08	Staurosporine
COT1/MAP3K8		5.65E-06	Ro-31-8220
CSK	2.75E-09	1.29E-08	Staurosporine
CTK/MATK		3.47E-07	Staurosporine
DAPK1	9.42E-06	1.17E-08	Staurosporine
DAPK2	>1.00E-05	4.75E-09	Staurosporine
DCAMKL1	>1.00E-05	1.16E-07	Staurosporine
DCAMKL2	>1.00E-05	9.59E-08	Staurosporine
DDR1	8.50E-09	2.86E-09	Staurosporine
DDR2	2.88E-08	1.97E-09	Staurosporine
DLK/MAP3K12	5.36E-07	9.12E-08	Staurosporine
DMPK		1.08E-07	Staurosporine
DMPK2	8.73E-07	4.61E-10	Staurosporine
DRAK1/STK17A	3.26E-07	3.30E-08	Staurosporine
DYRK1/DYRK1A	5.13E-07	3.27E-09	Staurosporine
DYRK1B	1.87E-07	1.13E-09	Staurosporine
DYRK2	2.25E-06	1.04E-07	Staurosporine
DYRK3	6.81E-07	1.98E-08	Staurosporine
DYRK4		4.41E-06	GW5074
EGFR	1.33E-08	8.94E-08	Staurosporine
EPHA1	1.62E-07	1.20E-07	Staurosporine
EPHA2	3.59E-08	6.30E-08	Staurosporine
EPHA3	5.57E-08	3.49E-08	Staurosporine
EPHA4	3.74E-08	1.16E-08	Staurosporine
EPHA5	1.46E-08	1.37E-08	Staurosporine
EPHA6	1.64E-07	1.58E-08	Staurosporine
EPHA7	3.44E-07	5.47E-08	Staurosporine
EPHA8	4.04E-08	1.13E-07	Staurosporine
EPHB1	1.16E-08	3.47E-08	Staurosporine
EPHB2	1.83E-08	7.01E-08	Staurosporine
EPHB3	5.23E-07	1.33E-06	Staurosporine
EPHB4	1.47E-08	1.97E-07	Staurosporine
ERBB2/HER2	2.23E-07	1.08E-07	Staurosporine
ERBB4/HER4	8.89E-08	1.44E-07	Staurosporine
ERK1		7.10E-09	SCH772984
ERK2/MAPK1		2.23E-09	SCH772984
ERK5/MAPK7		1.61E-05	Staurosporine
ERK7/MAPK15	1.04E-08	8.40E-09	Staurosporine
ERN1/IRE1	2.87E-07	1.00E-07	Staurosporine
ERN2/IRE2	2.70E-07	3.26E-08	Staurosporine
FAK/PTK2	7.87E-08	1.03E-08	Staurosporine
FER	1.00E-08	2.43E-10	Staurosporine
FES/FPS	2.94E-07	1.36E-09	Staurosporine
FGFR1	1.50E-08	2.86E-09	Staurosporine
FGFR2	7.75E-09	1.27E-09	Staurosporine
FGFR3	3.41E-08	1.05E-08	Staurosporine
FGFR4	3.90E-07	1.25E-07	Staurosporine
FGR	<5.08E-10	8.91E-10	Staurosporine
FLT1/VEGFR1	1.58E-08	8.05E-09	Staurosporine
FLT3	8.37E-10	1.30E-09	Staurosporine

Compound was tested in 10-dose IC50 mode with 3-fold serial dilution starting at 10 µM
Control Compound, Staurosporine, was tested in 10-dose IC50 mode with 4-fold serial dilution starting at 20 µM or 100 µM
Alternate Control Compounds were tested in 10-dose IC50 mode with 3-fold or 4-fold serial dilution starting at 10 µM, 20 µM, or 100 µM
Reactions were carried out at 10 µM ATP

Data pages include raw data, % Enzyme activity (relative to DMSO controls) , and curve fits.
*Curve fits were performed where the enzyme activities at the highest concentration of compounds were less than 65%.
**An IC50 value less than 0.508 nM or higher than 10 µM is estimated based on the best curve fitting available.
RBC recommends retesting this compound with an adjusted compound concentration range in order to obtain a more definitive result.

FLT4/VEGFR3	1.01E-09	1.03E-09	Staurosporine
FMS	2.53E-08	1.40E-09	Staurosporine
FRK/PTK5	5.46E-09	1.25E-08	Staurosporine
FYN	9.57E-10	1.63E-09	Staurosporine
GCK/MAP4K2	2.82E-07	7.33E-10	Staurosporine
GLK/MAP4K3	1.36E-07	8.02E-11	Staurosporine
GRK1	2.64E-06	6.33E-08	Staurosporine
GRK2		1.15E-06	Staurosporine
GRK3		8.43E-07	Staurosporine
GRK4	1.88E-06	8.09E-08	Staurosporine
GRK5		7.21E-08	Staurosporine
GRK6	>1.00E-05	5.49E-08	Staurosporine
GRK7	2.18E-06	6.07E-09	Staurosporine
GSK3a	2.75E-06	3.57E-09	Staurosporine
GSK3b	3.33E-06	3.62E-09	Staurosporine
Haspin	7.18E-06	4.13E-08	Staurosporine
HCK	2.44E-09	2.08E-09	Staurosporine
HGK/MAP4K4	2.82E-08	4.11E-10	Staurosporine
HIPK1	2.70E-06	2.88E-07	Ro-31-8220
HIPK2	4.48E-06	5.67E-07	Staurosporine
HIPK3	4.06E-06	6.72E-07	Staurosporine
HIPK4	1.99E-07	2.41E-07	Staurosporine
HPK1/MAP4K1	1.72E-08	4.12E-08	Ro-31-8220
IGF1R	4.75E-06	2.88E-08	Staurosporine
IKKa/CHUK		1.45E-07	Staurosporine
IKKb/IKBKB		3.18E-07	Staurosporine
IKKe/IKBKE	3.28E-06	2.96E-10	Staurosporine
IR	8.14E-07	6.73E-09	Staurosporine
IRAK1	1.92E-08	3.04E-08	Staurosporine
IRAK4	2.92E-09	4.37E-09	Staurosporine
IRR/INSRR	1.03E-06	9.07E-09	Staurosporine
ITK	4.37E-09	5.40E-09	Staurosporine
JAK1	6.75E-07	5.13E-10	Staurosporine
JAK2	2.53E-07	2.05E-10	Staurosporine
JAK3	5.82E-08	8.79E-11	Staurosporine
JNK1		8.17E-07	Staurosporine
JNK2		1.71E-06	Staurosporine
JNK3		1.63E-07	JNKi VIII
KDR/VEGFR2	4.98E-09	5.76E-09	Staurosporine
KHS/MAP4K5	3.09E-08	2.60E-10	Staurosporine
KSR1		5.31E-06	Staurosporine
KSR2		4.74E-06	Staurosporine
LATS1	5.16E-07	1.33E-08	Staurosporine
LATS2	1.11E-07	4.95E-09	Staurosporine
LCK	1.61E-09	1.55E-09	Staurosporine
LCK2/ICK	3.30E-07	5.77E-08	Staurosporine
LIMK1	1.14E-08	8.27E-10	Staurosporine
LIMK2	2.59E-07	6.45E-08	Staurosporine
LKB1	2.94E-07	4.96E-08	Staurosporine
LOK/STK10	6.02E-08	6.37E-09	Staurosporine
LRRK2	6.01E-08	3.20E-09	Staurosporine
LYN	4.96E-10	6.62E-10	Staurosporine
LYN B	1.09E-09	2.40E-09	Staurosporine
MAK	1.03E-07	2.41E-08	Staurosporine
MAPKAPK2		1.47E-07	Staurosporine
MAPKAPK3		4.69E-06	Staurosporine
MAPKAPK5/PRAK	>1.00E-05	2.30E-07	Staurosporine
MARK1	2.45E-07	3.56E-10	Staurosporine
MARK2/PAR-1Ba	1.23E-07	1.64E-10	Staurosporine
MARK3	7.66E-08	4.30E-10	Staurosporine
MARK4	4.21E-08	9.42E-11	Staurosporine
MEK1	3.71E-07	1.67E-08	Staurosporine
MEK2	4.30E-07	2.75E-08	Staurosporine
MEK3	2.34E-06	5.97E-09	Staurosporine
MEK5	8.53E-08	1.90E-08	Staurosporine
MEKK1		6.23E-07	Staurosporine
MEKK2	6.80E-07	3.68E-08	Staurosporine
MEKK3	7.69E-07	2.85E-08	Staurosporine
MEKK6		1.91E-07	Staurosporine
MELK	1.26E-07	4.73E-10	Staurosporine
MINK/MINK1	4.94E-08	1.04E-09	Staurosporine
MKK4	3.13E-06	1.18E-06	Staurosporine
MKK6	4.43E-06	2.93E-09	Staurosporine
MKK7	>1.00E-05	1.50E-06	Staurosporine
MLCK/MYLK	2.65E-06	5.49E-08	Staurosporine
MLCK2/MYLK2	2.06E-07	1.25E-08	Staurosporine
MLK1/MAP3K9	1.76E-08	1.27E-09	Staurosporine
MLK2/MAP3K10	2.07E-07	2.17E-09	Staurosporine
MLK3/MAP3K11	2.47E-08	5.38E-09	Staurosporine
MLK4	1.34E-06	1.73E-06	Staurosporine
MNK1	3.39E-08	7.04E-08	Staurosporine
MNK2	2.28E-08	1.33E-08	Staurosporine
MRCKa/CDC42BPA	>1.00E-05	3.10E-09	Staurosporine
MRCKb/CDC42BPB	2.83E-06	1.69E-09	Staurosporine
MSK1/RPS6KA5	3.41E-07	3.43E-10	Staurosporine
MSK2/RPS6KA4	9.28E-07	8.27E-09	Staurosporine
MSSK1/STK23		1.66E-06	Staurosporine
MST1/STK4	4.26E-08	6.55E-10	Staurosporine
MST2/STK3	6.93E-08	4.90E-09	Staurosporine
MST3/STK24	6.65E-06	2.47E-09	Staurosporine
MST4	1.86E-06	5.57E-09	Staurosporine
MUSK	4.35E-07	8.49E-08	Staurosporine
MYLK3		1.51E-07	Staurosporine
MYLK4	1.27E-07	5.98E-08	Staurosporine
MYO3A	7.31E-07	2.55E-08	Staurosporine
MYO3b	2.56E-07	4.95E-09	Staurosporine
NEK1	6.28E-06	1.15E-08	Staurosporine
NEK11		8.72E-07	Staurosporine
NEK2	6.19E-06	3.33E-07	Staurosporine
NEK3		6.52E-05	Staurosporine
NEK4	>1.00E-05	9.90E-08	Staurosporine
NEK5		5.72E-08	Staurosporine
NEK6		3.14E-05	PKR Inhibitor
NEK7		5.53E-06	PKR Inhibitor
NEK8	1.30E-06	2.83E-08	Staurosporine
NEK9		1.10E-07	Staurosporine
NIM1		1.36E-07	Staurosporine
NLK	7.52E-07	5.48E-08	Staurosporine
OSR1/OXSR1		6.58E-08	Staurosporine
P38a/MAPK14	8.87E-06	1.97E-08	SB202190
P38b/MAPK11	3.84E-06	2.84E-08	SB202190
P38d/MAPK13	4.30E-06	1.14E-07	Staurosporine
P38g		1.84E-07	Staurosporine
p70S6K/RPS6KB1	1.08E-07	4.76E-10	Staurosporine
p70S6Kb/RPS6KB2	3.50E-07	9.37E-10	Staurosporine
PAK1	3.94E-06	3.57E-10	Staurosporine
PAK2	6.90E-06	2.59E-09	Staurosporine
PAK3	3.74E-06	3.46E-10	Staurosporine
PAK4	1.95E-06	2.52E-08	Staurosporine
PAK5	1.45E-06	3.62E-09	Staurosporine
PAK6		2.77E-08	Staurosporine
PASK	4.66E-06	8.95E-09	Staurosporine
PBK/TOPK		5.11E-08	Staurosporine
PDGFRa	1.06E-09	5.82E-10	Staurosporine
PDGFRb	9.53E-09	4.61E-09	Staurosporine
PDK1/PDPK1	1.87E-07	4.79E-10	Staurosporine
PEAK1	5.78E-10	2.92E-09	Staurosporine
PHKg1	4.60E-09	2.34E-09	Staurosporine
PHKg2	3.39E-09	5.33E-10	Staurosporine
PIM1	2.45E-06	3.90E-09	Staurosporine
PIM2		1.98E-08	Staurosporine
PIM3	3.45E-07	7.46E-11	Staurosporine
PKA	2.65E-07	9.20E-10	Staurosporine
PKAcb	6.47E-07	1.08E-09	Staurosporine

PKAcg	2.20E-06	2.79E-09	Staurosporine
PKCa	8.94E-07	3.41E-10	Staurosporine
PKCb1	1.74E-06	2.81E-09	Staurosporine
PKCb2	6.63E-07	2.07E-09	Staurosporine
PKCd	3.37E-07	1.26E-10	Staurosporine
PKCepsilon	6.57E-07	1.95E-10	Staurosporine
PKCeta	1.13E-06	3.94E-10	Staurosporine
PKCg	1.44E-06	7.43E-10	Staurosporine
PKCiota		1.56E-08	Staurosporine
PKCmu/PRKD1	1.03E-07	1.68E-09	Staurosporine
PKCnu/PRKD3	5.64E-08	1.06E-09	Staurosporine
PKCtheta	9.96E-08	1.25E-09	Staurosporine
PKCzeta		4.60E-08	Staurosporine
PKD2/PRKD2	7.72E-08	1.46E-09	Staurosporine
PKG1a	3.13E-06	1.79E-09	Staurosporine
PKG1b	3.41E-06	3.70E-09	Staurosporine
PKG2/PRKG2	>1.00E-05	2.16E-09	Staurosporine
PKN1/PRK1	2.25E-07	2.56E-09	Staurosporine
PKN2/PRK2	3.50E-06	6.51E-09	Staurosporine
PKN3/PRK3	3.84E-07	1.16E-08	Staurosporine
PLK1		1.88E-07	Staurosporine
PLK2		3.92E-07	Staurosporine
PLK3		2.04E-07	Staurosporine
PLK4/SAK	2.43E-07	7.69E-09	Staurosporine
PRKX	2.06E-08	1.44E-09	Staurosporine
PYK2	1.70E-07	9.50E-09	Staurosporine
RAF1		1.04E-08	GW5074
RET	2.07E-09	2.31E-09	Staurosporine
RIPK2	2.16E-07	2.96E-07	Staurosporine
RIPK3	3.00E-08	2.45E-06	GW5074
RIPK4	2.09E-07	4.53E-07	Staurosporine
RIPK5	3.94E-06	4.93E-08	Staurosporine
ROCK1	5.29E-07	4.96E-10	Staurosporine
ROCK2	1.24E-06	5.04E-10	Staurosporine
RON/MST1R		7.53E-08	Staurosporine
ROS/ROS1	5.98E-09	9.63E-11	Staurosporine
RSK1	7.73E-09	5.28E-11	Staurosporine
RSK2	2.11E-08	9.81E-11	Staurosporine
RSK3	8.75E-09	1.80E-10	Staurosporine
RSK4	2.95E-08	1.25E-10	Staurosporine
SBK1	7.37E-06	4.98E-08	Staurosporine
SGK1	4.05E-06	5.26E-09	Staurosporine
SGK2	>1.00E-05	2.48E-08	Staurosporine
SGK3/SGKL		7.22E-08	Staurosporine
SIK1	1.68E-09	5.02E-10	Staurosporine
SIK2	1.29E-09	3.67E-10	Staurosporine
SIK3	8.65E-08	4.68E-10	Staurosporine
SLK/STK2	3.33E-07	1.93E-08	Staurosporine
SNARK/NUAK2	1.45E-07	1.49E-09	Staurosporine
SNRK		1.38E-08	Staurosporine
SRMS	2.23E-06	5.33E-06	Staurosporine
SRPK1		3.15E-08	Staurosporine
SRPK2		1.62E-07	Staurosporine
SSTK/TSSK6		1.89E-07	Staurosporine
STK16	5.91E-06	2.16E-07	Staurosporine
STK21/CIT	>1.00E-05	1.24E-06	Staurosporine
STK22D/TSSK1	2.43E-07	4.28E-11	Staurosporine
STK25/YSK1	6.44E-06	3.08E-09	Staurosporine
STK32B/YANK2	>1.00E-05	2.72E-08	Staurosporine
STK32C/YANK3		8.91E-08	Staurosporine
STK33	1.35E-07	3.23E-08	Staurosporine
STK38/NDR1	1.58E-06	7.37E-10	Staurosporine
STK38L/NDR2	4.62E-06	2.35E-09	Staurosporine
STK39/STLK3	3.46E-07	6.28E-09	Staurosporine
SYK	1.90E-08	1.40E-10	Staurosporine
TAK1	1.33E-07	5.76E-08	Staurosporine
TAOK1	2.19E-06	1.07E-09	Staurosporine
TAOK2/TAO1	>1.00E-05	4.05E-09	Staurosporine
TAOK3/JIK	2.51E-06	1.85E-09	Staurosporine
TBK1	1.13E-06	1.34E-09	Staurosporine
TEC	4.07E-08	4.65E-08	Staurosporine
TESK1	5.58E-07	2.29E-07	Staurosporine
TESK2	4.60E-07	5.38E-06	Staurosporine
TGFBR2	7.89E-08	1.76E-07	LDN193189
TIE2/TEK	7.67E-07	4.22E-08	Staurosporine
TLK1		2.44E-08	Staurosporine
TLK2	6.50E-06	1.94E-09	Staurosporine
TNIK	4.48E-09	5.79E-10	Staurosporine
TNK1	7.32E-09	3.88E-10	Staurosporine
TRKA	1.46E-08	1.10E-09	Staurosporine
TRKB	1.75E-09	7.03E-11	Staurosporine
TRKC	7.14E-10	2.41E-10	Staurosporine
TSSK2	8.08E-06	6.00E-09	Staurosporine
TSSK3/STK22C		4.62E-09	Staurosporine
TTBK1	>1.00E-05	1.13E-04	SB202190
TTBK2	5.66E-06	7.91E-06	SB202190
TXK	6.82E-09	2.50E-08	Staurosporine
TYK1/LTK	1.03E-07	1.45E-08	Staurosporine
TYK2	7.21E-07	2.04E-10	Staurosporine
TYRO3/SKY	2.56E-07	1.60E-09	Staurosporine
ULK1	1.73E-07	9.68E-09	Staurosporine
ULK2	1.63E-07	3.41E-09	Staurosporine
ULK3	1.40E-07	3.15E-09	Staurosporine
VRK1	2.07E-05	6.70E-07	Ro-31-8220
VRK2		1.38E-05	Ro-31-8220
WEE1		7.72E-08	Wee-1 Inhibitor
WNK1		4.61E-05	Staurosporine
WNK2		1.30E-06	Staurosporine
WNK3	>1.00E-05	2.76E-06	Wee-1 Inhibitor
YES/YES1	6.94E-10	1.94E-09	Staurosporine
YSK4/MAP3K19	>1.00E-05	6.15E-09	Staurosporine
ZAK/MLTK	7.17E-08	2.24E-06	GW5074
ZAP70	>1.00E-05	8.62E-09	Staurosporine
ZIPK/DAPK3	6.03E-06	3.12E-09	Staurosporine

* Empty cells indicate no inhibition or compound activity that could not be fit to an IC50 curve

Supplemental Table 3.2. KiNativ profile of NCGC1481 in MV4;11 lysate.

Kinase	Reference	Sequence	Labeling Site	NCGC1481 10µM	NCGC1481 1µM	NCGC1481 0.1µM	IC50 (µM)
ABL, ARG	UniRef100_Q4JIM5, U	LMTGDTYTAHAGAKFPIK	Activation Loop	>99	86.3	38.1	0.16
ABL, ARG	UniRef100_Q4JIM5, U	VSLTVAVKTLKEDTMEVEEFLK	Lys1	>94	82.5	44.2	0.17
ACK	UniRef100_Q07912, U	TVSVAVKCLKPDVLSQPEAMDDF	Lys1	68.1	14.6	9.6	4.7
AKT1	UniRef100_Q01314, U	GTFGKVILVK	ATP Loop	20.2	24.2	9.6	>10
AKT2, AKT3	UniRef100_G1SD70, U	GTFGKVILVR	ATP Loop	-4.1	15.2	-8.0	>10
AMPKa1	UniRef100_F1MBG5, U	IGHYILGDTLGVGTFGKVK	ATP Loop	34.2	30.6	1.8	>10
AMPKa1, AMPKa2	UniRef100_F7HR71, U	LDKPENVLLDARMNAK	Lys2	85.6	56.5	18.9	0.61
AMPKa1, AMPKa2	UniRef100_F7HR71, U	VAVKILNR	Lys1	89.8	51.1	9.7	1.1
ARAF	UniRef100_P14056, U	DLKSNNIFLHEGLTVK	Lys2	-11.7	7.8	-5.3	>10
ATR	UniRef100_UPI00080	FYIMMCKPK	ATP	2.4	1.9	-5.1	>10
AurA	UniRef100_O14965, U	DIKPENLLLGSAGELK	Lys2	63.6	12.6	7.5	5.7
AurA	UniRef100_O14965, U	FILALKVLFK	Lys1	56.8	16.6	-12.1	7.6
AurA, AurB, AurC	UniRef100_O14965, U	GKFGNVYLAR	ATP Loop	79.5	35.1	5.2	2.2
AurB	UniRef100_Q96GB6, U	SHIFIVALKVLFK	Lys1	96.0	62.0	10.9	0.93
BARK1	UniRef100_G1T1F2, U	DLKPANILLDEHGHVR	Lys2	36.6	-0.5	7.1	>10
BRAF	UniRef100_P28028, U	DLKSNNIFLHEDLTVK	Lys2	10.4	15.0	3.0	>10
BTK	UniRef100_P35991, U	YVLDDEYTSSVGSKFPVR	Activation Loop	89.5	48.9	1.8	1.1
BTK	UniRef100_P35991, U	GQYDVAKMIK	Lys1	84.2	42.3	5.9	1.6
CaMK1a	UniRef100_UPI0001C	LVAIKCIAK	Lys1	1.1	-4.9	-4.3	>10
CaMK1d	UniRef100_UPI00048	LFAVKCIPK	Lys1	-7.0	0.4	-4.8	>10
CaMK2a, CaMK2b, CaMK2d, CaMK	UniRef100_UPI00073	DLKPENLLLASK	Lys2	80.2	19.9	0.3	6.6
CaMK2g	UniRef100_F7Y2A9, U	TSTQLYAAKIINTK	Lys1	89.8	12.7	0.6	4.5
CaMKK1	UniRef100_P97756, U	DIKPSNLLLGDDGHVK	Lys2	8.6	4.9	-13.3	>10
CaMKK2	UniRef100_Q96RR4, U	LAYNENDNTYYAMKVLSK	Lys1	85.5	69.8	17.6	1.1
CaMKK2	UniRef100_Q96RR4, U	DIKPSNLLVGEDCHIK	Lys2	75.2	66.3	14.5	1.6
CCRK	UniRef100_A6H7E6, U	DLKPSNLLISASGQLK	Lys2	14.7	-4.6	1.3	>10
CDC2	UniRef100_Q5H9N4, U	DLKPQNLLIDDK	Lys2	29.3	-1.7	12.4	>10
CDC2	UniRef100_Q5H9N4, U	DLKPQNLLIDDKGTIK	Lys2	14.1	15.8	-12.5	>10
CDC2	UniRef100_Q5H9N4, U	TTGQVVTLWYRAPK	Lys1	-10.6	1.7	-5.5	>10
CDK10	UniRef100_A0A1D5Q	DLKVSNLLMTDK	Lys2	72.0	19.0	-14.3	>10
CDK11, CDK8	UniRef100_U3KN30, U	DLKPANILVMGEGPER	Lys2	49.4	8.1	16.5	>10
CDK2	UniRef100_E7ESI2, U	DLKPQNLLINTEGAIK	Lys2	91.3	46.3	12.8	1.1
CDK2	UniRef100_E7ESI2, U	LTGEVVALKK	Lys1	93.0	48.6	9.3	1.5
CDK4	UniRef100_P11802, U	DLKPENILVTSGGTVK	Lys2	3.8	4.3	25.4	>10
CDK5	UniRef100_F8W6J7, U	DLKPQNLLINR	Lys2	26.1	8.7	-7.2	>10
CDK5	UniRef100_F8W6J7, U	NRETHEIVALKR	Lys1	25.8	9.1	12.0	>10
CDK6	UniRef100_E1BC36, U	DLKPQNILVSSQGQIK	Lys2	34.0	-10.8	-6.3	>10
CDK7	UniRef100_A0A1D5Q	DLKPNNLLLDENGVLK	Lys2	98.0	93.4	67.4	0.059
CDK7	UniRef100_A0A1D5Q	DKNTNQIVAIKK	Lys1	>99	>99	72.0	0.075
CDK9	UniRef100_G5ZKN1,	DMKAANVLITR	Lys2	73.9	31.8	-1.3	2.8
CHED	UniRef100_UPI0000D	DIKSSNLLLNNR	Lys2	9.2	9.2	-9.2	>10
CHK1	UniRef100_B4DT73, U	DIKPENLLLDER	Lys2	86.6	61.7	23.4	1.1
CHK1	UniRef100_B4DT73, U	LSKGDGLEFK	Other	14.9	9.2	-0.7	>10
CHK2	UniRef100_Q96DJ9, U	DLKPENVLLSSQEEDCLIK	Lys2	91.7	53.2	5.6	0.89
CHK2	UniRef100_Q96DJ9, U	VAPIISK	Lys1	90.5	51.6	17.8	0.99
CK1a	UniRef100_Q32LH9, U	DIKPDNFLMGIGR	Lys2	-38.2	-4.5	-2.6	>10
CK1c, CK1e	UniRef100_Q9DC28,	DVKPDNFLMGLGKK	Lys2	-17.0	-15.2	-14.6	>10
CK1g1	UniRef100_G7MXT2,	DVKPENFLIGR	Lys2	-30.7	-23.0	-38.4	>10
CK1g2	UniRef100_F7H4Z2, U	DVKPENFLVGRPGTK	Lys2	-30.5	-11.5	2.6	>10
CK2a1	UniRef100_P68400, U	GGPNIITLADIKKDPVSR	Protein Kinase Domain	-6.3	15.2	-0.6	>10
CLK3	UniRef100_Q3SX21, U	YEVVGNLGEGTTGKVVECLDHA	ATP Loop	26.5	28.5	17.5	>10
CRK7	UniRef100_UPI0008	DIKCSNILLNNEGQIK	Lys2	9.0	14.4	-2.4	>10
CSK	UniRef100_UPI00048	VSDFGLTKEASSTQDTGKLPVK	Activation Loop	85.8	36.5	2.1	1.7
CSK	UniRef100_UPI00048	VAVKCIK	Lys1	62.5	40.9	14.1	1.8
CTK	UniRef100_A0A1D5Q	VSDFGLAKAER	Activation Loop	-21.4	-4.9	0.3	>10
DGKA	UniRef100_A0JN54, U	DPVPNTHPLVFVPNPSGGK	ATP	47.2	46.8	3.3	>10
DGKH	UniRef100_F1M158, U	ATFSFCVSPLLVFVNSKSGDNQ	ATP	50.8	45.5	16.7	5.4
DNAPK	UniRef100_Q8WN22,	EHPFLVKGGEDLR	ATP	63.0	13.4	12.1	5.9
DNAPK	UniRef100_Q8WN22,	KGGSWQEINVAEK	ATP	10.8	-16.0	-1.9	>10
DYRK1A	UniRef100_F8BS57,	KFAQQMCTALLFLATPELSIIICL	Lys2	23.5	3.9	-17.7	>10
eEF2K	UniRef100_E2RIJ6, U	YIKYNSNSGFVR	ATP	-44.0	-5.7	-10.2	>10
Erk1	UniRef100_H2MWW1,	DLKPSNILINTTCDLK	Lys2	2.1	-0.8	-4.6	>10
Erk2	UniRef100_P1M27, U	DLKPSNILLNTTCDLK	Lys2	2.8	0.6	-2.7	>10
Erk5	UniRef100_UPI00022	DLKPSNLLVNENCELK	Lys2	12.7	2.3	17.8	>10
FER	UniRef100_P09760, U	QEDGGVYSSSGLKQIPIK	Activation Loop	85.2	43.9	20.1	1.0
FER	UniRef100_P09760, U	TSVAVKTCKEDLPQELK	Lys1	97.1	51.0	-0.1	1.2
FES	UniRef100_Q7PKB8,	LRADNTLVAVSQK	Lys1	0.7	2.5	0.6	>10
FGR	UniRef100_P14234, U	LIKDDEYNPCQGSKFPIK	Activation Loop	86.6	21.2	-17.2	4.4
FRAP	UniRef100_P42345, U	QSIAPSLQVITSKQRPR	ATP	-24.8	-9.6	-13.2	>10
GAK	UniRef100_O2KJH2, U	DLKVENLLLSNQGTIK	Lys2	>95	>95	76.9	0.047
GCK	UniRef100_UPI00048	DIKGANILLSTLGQDVK	Lys2	75.7	55.5	16.2	0.97
GCK	UniRef100_UPI00048	DTVTSELAAVKVK	Lys1	88.4	47.8	19.2	1.2
GCN2_Domain2 domain2	UniRef100_UPI00049	DLKPVNIFLDSDDHVK	Lys2	12.6	-2.3	-2.3	>10
GCN2_Domain2 domain2	UniRef100_UPI00049	LDGCGYAVKR	Lys1	0.0	-5.5	-13.4	>10
GSK3A	UniRef100_UPI0001C	DIKPDNLLVDKDTAVLK	Lys2	24.0	-13.1	12.3	>10
GSK3B	UniRef100_UPI00048	DIKPQNLLLDPDTAVLK	Lys2	4.7	-14.0	0.6	>10
HCK	UniRef100_G1SXU8,	VAVKTMKPGSMSVEAFLAEANV	Lys1	>83	>83	49.6	0.15
HCK	UniRef100_G1SXU8,	FCAKFPIKWTAPEAINFGSFTIK	Activation Loop	93.9	87.0	56.0	0.22
HPK1	UniRef100_A0A1D5Q	DIKVSSDLVNVLQK	Lys2	84.3	38.3	13.0	1.7
HPK1	UniRef100_A0A1D5Q	DIKGANILINDAGEVR	Lys2	73.4	38.2	3.4	2.6
IKKa	UniRef100_Q60680, U	DLKPENIVLQDVGGK	Lys2	-16.8	-19.5	8.0	>10
IKKb	UniRef100_UPI00048	DLKPENIVLQQGEGR	Lys2	-19.4	-14.8	4.3	>10
IKKb	UniRef100_UPI00048	VHNQETGEQIAKQCR	Lys1	-54.2	-14.8	-19.2	>10
IKKe, TBK1	UniRef100_UPI0001C	DIKPQNIMR	Lys2	48.2	11.5	4.7	>10
ILK	UniRef100_L8YC71, U	SMADVKFSQCPGR	Protein Kinase Domain	42.5	30.2	26.7	>10
ILK	UniRef100_L8YC71, U	WQGNDIVVKVLK	Lys1	20.0	2.2	3.3	>10
IRR	UniRef100_P51617, U	AIQFLHQDSPSLIHGDIKSSNVLL	Lys2	93.6	65.4	6.5	0.61
IRAK3	UniRef100_B3FXL5, U	SHLEHKQSCTINVTSSSSKHLWYT	Protein Kinase Domain	>96	89.9	50.2	0.11
IRAK4	UniRef100_Q1RMT8,	DIKSANILLDEAFTAK	Lys2	99.6	98.9	89.0	0.012
IRAK4	UniRef100_Q1RMT8,	GYVNNTTVAVKK	Lys1	97.1	96.4	87.3	0.025
IRE1	UniRef100_UPI00017	DLKPHNILISMPNAHGK	Lys2	3.0	11.0	3.7	>10
ITPK1	UniRef100_P0C0T1, U	ESIFFNSHNVSKPESSSVLTELDK	ATP	-09.6	-26.8	-18.2	>10
JAK1 domain1	UniRef100_P52332, U	QLASALSYLEDKDLVHGNVCTKN	Activation Loop	88.0	70.6	36.8	0.83
JAK1_Domain2 domain2	UniRef100_P52332, U	HGDFGLTKAISTDKEYYTVK	Activation Loop	1.4	3.0	-1.9	>10
JAK1_Domain2 domain2	UniRef100_P52332, U	YDPEGDNTGEQVAVKSLKPESG	Lys1	-70.1	-18.7	-10.3	>10
JNK1, JNK2, JNK3	UniRef100_G1TPJ7,	DLKPSNIVVK	Lys2	40.5	-3.2	-10.3	>10
KSR1, KSR2	UniRef100_Q6VAB6,	SKNVFYDNGK	Activation Loop	3.1	16.8	3.0	>10
LATS1	UniRef100_UPI0001C	ALYATKLPK	Lys1	23.5	5.6	-6.8	>10
LATS1	UniRef100_UPI0001C	DIKPDNILIDR	Lys2	13.2	8.1	2.5	>10
LATS2	UniRef100_UPI00048	DIKPDNILIDLDGHIK	Lys2	26.9	9.1	-1.1	>10
LKB1	UniRef100_H9ETP1, U	DIKPGNLLLTGGTLK	Lys2	68.0	37.2	10.4	1.5
LOK	UniRef100_F1NBT0, U	NKETGALAVAAKVIETK	Lys1	93.0	63.4	12.3	0.67
LOK	UniRef100_F1NBT0, U	DLKAGNVLMTLEGDIR	Lys2	84.5	28.3	0.2	4.2
LYN	UniRef100_P25911, U	VAVKTLKPGTMSVQAFLEEANLM	Lys1	>94	90.2	58.1	0.090
LYN	UniRef100_P25911, U	ESAKFPIKWTAPEAINFGCFTIK	Activation Loop	>96	93.7	50.5	0.15
MAP2K1	UniRef100_P31938, U	IMHRDVKPSNILVNSR	Lys2	39.5	18.7	-29.7	>10
MAP2K1, MAP2K2	UniRef100_J9P5W6, U	DVKPSNILVNSR	Lys2	35.7	8.8	-17.2	>10
MAP2K1, MAP2K2	UniRef100_J9P5W6, U	KLIHLEIKPAIR	Lys1	35.3	12.3	-2.9	>10
MAP2K2	UniRef100_Q1HG70,	HQIMHSDVKPSNILVNSR	Lys2	3.8	0.9	21.9	>10
MAP2K3	UniRef100_F1PXD3, U	DVKPSNVLINK	Lys2	-14.4	9.9	-7.7	>10
MAP2K3	UniRef100_F1PXD3, U	HAQSGTIMAVKR	Lys1	-47.4	3.0	0.9	>10
MAP2K4	UniRef100_P45985, U	DIKPSNILLDR	Lys2	-8.8	1.9	-0.1	>10
MAP2K4	UniRef100_P45985, U	MVHKPSGQIMAVKR	Lys1	-30.6	0.7	-4.0	>10
MAP2K5	UniRef100_Q9WV57,	DVKPSNMLVNTR	Lys2	91.9	64.7	8.3	0.71
MAP2K6	UniRef100_A0A1D5Q	HVPSGQIMAVKR	Lys1	3.2	1.4	21.9	>10
MAP2K6	UniRef100_A0A1D5Q	DVKPSNVLNALGQVK	Lys2	-3.5	-9.4	7.1	>10
MAP2K7	UniRef100_O14733, U	DVKPSNILLDER	Lys2	20.9	5.5	7.6	>10
MAP3K1	UniRef100_B7NZB6,	DVKGANLLIDSTGQR	Lys2	54.0	18.9	-12.2	8.5
MAP3K15, MAP3K5, MAP3K6	UniRef100_UPI00049	AIKEIPER	Lys1	-13.2	-5.1	2.5	>10
MAP3K2	UniRef100_Q61083,	SLAVKQVQFDPDSPETSKEVNA	Lys1	-20.7	-14.2	-5.7	>10
MAP3K2, MAP3K3	UniRef100_K7BDY8,	DIKGANILR	Lys2	23.3	24.2	9.0	>10
MAP3K3	UniRef100_F7AIB6, U	ELASKQVQFDPDSPETSKEVSAL	Lys1	-13.2	-5.9	17.9	>10
MAP3K4	UniRef100_UPI00048	DIKGANILTSSGLIK	Lys2	21.5	20.2	13.0	>10
MAP3K4	UniRef100_UPI00048	VYTCISVDTGELMAMKEIR	Lys1	13.8	4.9	13.9	>10
MAP3K5	UniRef100_D3ZZH8,	DIKGDNVLINTYSGVLK	Lys2	12.4	13.6	14.8	>10
MAP4K3	UniRef100_U3KPA8, U	NVNTGELAAIKVIK	Lys1	77.8	44.4	-5.6	2.1
MAP4K5	UniRef100_F1N2U3, U	NVHTGELAAVKIIK	Lys1	90.4	49.7	18.1	1.0
MAPKAPK3	UniRef100_Q3SZ77, U	QVLGLGVNGKVLECFHR	ATP Loop	-10.8	11.1	5.8	>10
MAPKAPK3	UniRef100_Q3SY72,	CALKLLYDSPK	Lys1	-52.4	-23.1	-9.4	>10
MARK1, MARK2	UniRef100_A0A1D5Q	EVAVKIIDK	Lys1	54.0	8.9	-2.1	8.5
MARK2	UniRef100_Q9ES12,	EVAVKIIDKTQLNSSSLQK	Lys1	54.0	9.7	-7.5	8.5
MARK3	UniRef100_P27448, U	EVAKIIDKTQLNPTSLQK	Lys1	59.8	5.6	5.9	6.8
MARK3, MARK4	UniRef100_P27448, U	EVAIKIIDK	Lys1	57.8	11.1	-0.6	7.4
MAST3	UniRef100_UPI00038	DLKPDNLLITSLGHIK	Lys2	42.4	-0.8	4.6	>10
MAST4	UniRef100_F7H355,	LYAVKVVK	Lys1	43.5	-9.7	1.3	>10
MAST4	UniRef100_F7H355,	LGAFGKVYLGQK	ATP Loop	41.2	11.7	5.3	>10
MLK3	UniRef100_Q66HA1,	DLKSNNILLQPIESDDMEHK	Lys2	93.8	73.7	19.9	0.51
MLK3	UniRef100_Q66HA1,	GELVAVKVAR	Lys1	4.5	13.0	6.2	>10
MLK4	UniRef100_Q571F9,	DLKSSNILLLK	Lys2	92.4	69.1	6.0	0.63
MLKL	UniRef100_M0RDC7,	APVAIKVFK	Lys1	-3.4	-11.5	12.4	>10
MPSK1	UniRef100_G1TXD6, U	DLKPTNILLGDEGQPVLMDLGSM	Lys2	50.3	29.1	20.5	9.9
MPSK1	UniRef100_G1TXD6, U	LCEGGFSYVDLVEGLHDGHFYA	Lys1	47.7	27.7	-19.5	>10
MSK1 domain1	UniRef100_Q5F3L1, U	DIKLENILLDSNGHVVLTDFGLSK	Lys2	16.1	-1.1	1.0	>10
MSK2 domain1	UniRef100_O75676, U	DLKLENVLLDSFGHIVLTDFGLSK	Lys2	70.8	30.9	9.0	3.2
MST1	UniRef100_Q5E9L6,	LETGQIVAIKQVPVESDLQEIIK	Lys1	89.5	54.7	2.6	1.0
MST1, MST2	UniRef100_Q5E9L6,	DIKAGNILLNTEGHAK	Lys2	92.6	50.3	27.7	0.68
MST2	UniRef100_Q13188, U	LESGQVVAIKQVPVESDLQEIIK	Lys1	91.8	61.4	5.5	0.76
MST3	UniRef100_F1PTW4,	DIKAANVLLSEHGEVK	Lys2	7.4	9.1	-18.2	>10
MST3	UniRef100_F1PTW4,	VVAKIIDLEEAEDEIEDIQQEITVL	Lys1	-22.8	-21.8	-0.7	>10
MST4	UniRef100_UPI00048	TDQVVAIKQVNLEEAEDEIEDIQQE	Lys1	12.1	-17.8	20.2	>10
MST4, YSK1	UniRef100_UPI00048	DIKAANVLLSEQGDVK	Lys2	20.9	-0.3	-0.3	>10
NDR1	UniRef100_G1TPU5,	DTGHVYAMKILR	Lys1	4.1	0.7	10.6	>10
NDR1	UniRef100_G1TPU5,	DIKPDNLLLDSK	Lys2	-20.6	-5.1	9.9	>10
NDR2	UniRef100_E2R001,	DIKPDNLLLDAK	Lys2	-19.9	-12.4	10.2	>10
NDR2	UniRef100_E2R001,	DTGHIYAMKILR	Lys1	-18.0	-5.8	-0.8	>10
NEK1	UniRef100_A0A1D5Q	DIKSQNIFLTK	Lys2	-46.3	-17.6	-8.5	>10
NEK3	UniRef100_D3ZCU1,	SKNIFLTQNGK	Activation Loop	-22.2	-2.9	1.8	>10
NEK4	UniRef100_Q9ZUJ2,	DLKTQNVFLTR	Lys2	-26.7	-1.2	-11.2	>10
NEK6, NEK7	UniRef100_A6H7J4,	DIKPANVFITATGVVK	Lys2	-26.8	3.6	-7.8	>10
NEK7	UniRef100_E1BDZ2,	AACLLDGVPVALKK	Lys1	23.3	2.3	0.8	>10

Labeling Site Key

- **Lys1:** Conserved Lysine 1
- **Lys2:** Conserved Lysine 2
- **ATP Loop:** ATP binding loop
- **Activation Loop:** Activation loop
- **ATP:** ATP site in non-canonical kinase (e.g. lipid kinase)
- **Protein Kinase Domain:** Other lysine within kinase domain, possibly not in ATP binding site
- **Other:** Labeling of residue outside of the protein kinase domain, possibly not in ATP binding site

- >90% Inhibition
- 75 - 90% Inhibition
- 50 - 75% Inhibition
- 35 - 50% Inhibition
- No change
- >100% increase in MS signal (>2 fold increase)
- ND: Not determined

Data points inhibited >35% & not considered significant are left uncolored

Note: This KiNativ dataset is the result of an analysis of duplicate treated samples and either duplicate or quadruplicate control samples. The % changes in MS signals being reported are statistically significant (Student T-test score <0.04). Additionally, the KiNativ method is performed using biological matrices (cells/tissues), which can be inherently variable, followed by a complex procedure of sample preparation and mass spec analysis. Thus, we recommend the use of independent, biological replicates to determine the inter-sample variability of the dataset (i.e., repeating the experimental conditions more than one time and with an independent sample of the biological matrix in order to validate the dataset). In addition, we strongly recommend that customers obtain supporting data through additional independent KiNativ studies or through orthogonal approaches prior to making critical project decisions.

The data reported was performed in a non-GLP manner and was not intended for regulatory submission. It was generated to provide scientific data for informational purposes only.

KiNativ project managers are available to discuss the results and assist customers in understanding the strengths and limitations of this KiNativ dataset. ActivX Biosciences, Inc. bears no responsibility for decisions made by customers based on this KiNativ dataset or for any experimental suggestions offered by KiNativ project managers.

NEK9	UniRef100_E2QYP0, U	RTEDDSLVVWKEVDLTR	Lys1	-14.1	-4.0	-17.6	>10
NEK9	UniRef100_E2QYP0, U	DIKTLNIFLTK	Lys2	-59.8	-17.6	-15.1	>10
OSR1	UniRef100_F6SQU7, U	DVKAGNILLGEDGSVQIADFGVS	Lys2	-1.6	17.7	3.6	>10
p38a	UniRef100_UPI0001C	DLKPSNLAVNEDCELK	Lys2	7.4	-6.9	9.3	>10
p38a	UniRef100_UPI0001C	QELNKTIWEVPER	Other	-2.6	-1.4	-4.1	>10
p38b	UniRef100_UPI0003A	QELNKTVWEVPQR	Other	9.9	8.1	2.0	>10
p38d, p38g	UniRef100_A0A1D5R	DLKPGNLAVNEDCELK	Lys2	-15.7	-16.5	6.8	>10
p70S6K	UniRef100_P18652, U	DLKPENIMLNHQGHVK	Lys2	21.3	0.4	21.3	>10
p70S6K, p70S6Kb	UniRef100_P18652, U	GGYGKVFQVR	ATP Loop	29.2	-11.4	-17.4	>10
p70S6Kb	UniRef100_E1BLQ5, U	DLKPENIMLSSQGHIK	Lys2	-27.6	10.7	-5.8	>10
PAK2	UniRef100_E2RJA0, U	IGQGASGTVFTATDVALGQEVA	Lys1	-20.5	-17.7	-11.9	>10
PAN3	UniRef100_G1U195, U	VMDPTKILITGK	ATP	17.1	16.4	10.8	>10
PCTAIRE1	UniRef100_UPI000225	SKLTDNLVALKEIR	Lys1	>96	>96	68.8	0.044
PCTAIRE1, PCTAIRE3	UniRef100_UPI000225	DLKPQNLLINER	Lys2	>98	95.5	66.7	0.049
PCTAIRE2	UniRef100_F1MN42, U	DLKPQNLLINEK	Lys2	>94	92.5	40.5	0.11
PEK	UniRef100_E2QWG6, U	DLKPSNIFFTMDDVVK	Lys2	-15.6	-4.3	-1.6	>10
PFTAIRE1	UniRef100_G1TVZ7, U	LVALKVIR	Lys1	91.2	58.4	9.4	0.84
PHKg2	UniRef100_P31325, U	ATGHEFAVKIMEVTAER	Lys1	76.3	41.1	3.2	2.3
PHKg2	UniRef100_P31325, U	DLKPENILLDDNMQIR	Lys2	65.8	35.4	13.4	3.5
PI4KA, PI4KAP2	UniRef100_F1LRW9,	SGTPMQSAAKAPYLAK	ATP	15.4	-12.6	-0.2	>10
PI4KB	UniRef100_O08561, U	VPHTQAVVLNSKDK	ATP	19.7	9.9	9.3	>10
PI4KB	UniRef100_O08561, U	LLSVIVKCGDDLRQELLAFQVLK	ATP	-479.4	-72.0	-11.8	>10
PIK3C2B	UniRef100_UPI00005(	VIFKCGDDLRQDMLTLQMIR	ATP	50.3	23.0	-10.4	9.9
PIK3C3	UniRef100_G7NKM7,	TEDGGKYPVIFKHGDDLR	ATP	-0.3	-1.8	3.8	>10
PIK3C3	UniRef100_G7NKM7,	TEDGGKYPVIFKHGDDLRQDQL	ATP	-10.9	-22.0	-2.6	>10
PIK3CB	UniRef100_Q8BTI9, U	VFGEDSVGVIFKNGDDLRQDML	ATP	6.0	11.3	-1.4	>10
PIK3CD	UniRef100_F1NHX1,	VNWLAHNVSKDNRQ	ATP	20.8	2.3	-6.2	>10
PIK3CD	UniRef100_F1NHX1,	TKVNWLAHNVSKDNRQ	ATP	2.1	9.5	-3.1	>10
PIK3CG	UniRef100_D3ZFJ0, U	KKPLWLEFK	ATP	-8.6	-2.1	-1.1	>10
PIP4K2A	UniRef100_O70172, U	ELPTLKDNDFINEGQK	ATP	-3.9	-5.5	9.7	>10
PIP4K2B	UniRef100_Q80XI4, U	AKDLPTFKDNDFLNEGQK	ATP	-5.4	7.0	2.0	>10
PIP4K2C	UniRef100_Q8TBX8, U	TLVIKEVSSEDIADMHSNLSNYH(	ATP	13.3	7.6	3.2	>10
PIP4K2C	UniRef100_Q8TBX8, U	VKELPTLKDMDFLNK	ATP	7.4	8.1	0.3	>10
PIP5K3	UniRef100_D3ZT14, U	GGKSGAAFYATEDDRFILK	ATP	5.4	-1.2	-4.7	>10
PITSLRE	UniRef100_P24788, U	DLKTSNLLLSHAGILK	Lys2	-51.5	-24.9	-14.4	>10
PKCa, PKCb	UniRef100_P05696, U	DLKLDNVMLDSEGHIK	Lys2	40.5	18.8	4.9	>10
PKD1, PKD2	UniRef100_E2RR18, U	NIVHCDLKPENVLLASADPFPQV	Lys2	61.0	9.1	11.4	6.4
PKD2	UniRef100_E2RR18, U	DVAVKVIDK	Lys1	60.1	8.7	-20.7	6.6
PKD3	UniRef100_E2R428, U	NIVHCDLKPENVLLASAEPFPQV	Lys2	83.8	28.1	11.6	2.2
PKD3	UniRef100_E2R428, U	DVAIKVIDK	Lys1	75.3	27.6	9.6	2.9
PKN1	UniRef100_Q16512, U	DLKLDNLLLDTEGYVK	Lys2	46.8	19.9	-4.8	>10
PKN1	UniRef100_Q16512, U	VLLSEFRPSGELFAIKALK	Lys1	40.8	20.0	-12.3	>10
PKN2	UniRef100_Q8BWW9	DLKLDNLLLDTEGFVK	Lys2	-36.4	-27.1	-18.4	>10
PKR	UniRef100_G1SSL4, U	DLKPSNIFLVDTK	Lys2	3.7	10.7	15.1	>10
PKR	UniRef100_G1SSL4, U	IGDFGLVTSLKNDGKR	Activation Loop	-11.5	-3.6	-5.9	>10
PLK1	UniRef100_P53350, U	CFEISDADTKEVFAGKIVPK	Lys1	-7.5	0.4	-3.2	>10
PLK1	UniRef100_P53350, U	DLKLGNLFLNEDLEVK	Lys2	-8.9	10.6	-1.3	>10
PRP4	UniRef100_G1SD98, U	CNILHADIKPDNILVNESK	Lys2	-18.6	-7.8	6.5	>10
PRP4	UniRef100_G1SD98, U	AAGIGKDFKENPNLR	Other	-31.4	-9.3	-5.1	>10
PRPK	UniRef100_Q96S44, U	FLSGLELVKQGAEAR	ATP Loop	-48.3	-26.3	-7.5	>10
PYK2	UniRef100_Q9QVP9,	INVAVKTCK	Lys1	90.7	63.1	12.7	0.80
PYK2	UniRef100_Q9QVP9,	YIEDEDYYKASVTR	Activation Loop	84.8	49.3	-1.0	1.4
RAF1	UniRef100_Q99N57, U	DMKSNNIFLHEGLTVK	Lys2	0.5	1.1	2.7	>10
RIPK3	UniRef100_Q9Z2P5, U	DLKPSNVLLDPELHVK	Lys2	86.1	23.4	-56.5	2.4
ROCK1	UniRef100_A0A1D5R(	KLQLELNQER	Other	-49.9	-16.4	1.8	>10
ROCK1, ROCK2	UniRef100_A0A1D5R(	DVKPDNMLLDK	Lys2	-15.2	-10.5	5.2	>10
ROCK2	UniRef100_O75116, U	KLHMELK	Protein Kinase Domain	9.6	-4.2	17.7	>10
RSK1 domain1	UniRef100_P18653, U	LTDFGLSKEAIDHEKK	Activation Loop	83.8	35.3	21.7	1.4
RSK1 domain1, RSK2 domain1, RSI	UniRef100_P18653, U	DLKPENILLDEEGHIK	Lys2	80.5	35.6	7.7	2.1
RSK1_Domain2 domain2	UniRef100_P18653, U	DLKPSNILYVDESGNPECLR	Lys2	65.0	14.0	-7.1	5.4
RSK2 domain1	UniRef100_Q9TSC3,	LTDFGLSKESIDHEKK	Activation Loop	81.5	23.8	19.8	2.7
RSK2 domain1	UniRef100_Q9TSC3,	VLGQGSFGKVFLVK	ATP Loop	59.5	27.9	-2.0	4.7
RSK2_Domain2 domain2	UniRef100_Q9TSC3,	DLKPSNILYVDESGNPESIR	Lys2	3.6	-14.1	-11.0	>10
RSKL1	UniRef100_D3Z991, U	VLGVIDKVLLVMDTR	ATP	-5.1	8.3	1.6	>10
SGK3	UniRef100_Q96BR1,	FYAVKVLQK	Lys1	7.0	-6.4	0.4	>10
SGK3	UniRef100_Q96BR1,	IVYRDLKPENILLDSVGHVVLTDF	Lys2	-15.4	-3.0	-20.6	>10
SLK	UniRef100_UPI0001C	AQNKETSVLAAAKVIDTK	Lys1	89.6	56.9	-3.6	0.96
SLK	UniRef100_UPI0001C	DLKAGNILFTLDGDIK	Lys2	57.7	32.4	10.4	4.7
SMG1	UniRef100_A0A1D5P8	SYPYLFKGLEDLHLDER	ATP	78.7	45.6	-1.0	2.0
SMG1	UniRef100_A0A1D5P8	DTVTIHSVGGTITILPTKTKPK	ATP	78.6	23.2	-1.0	3.0
SNRK	UniRef100_G1TXD8,	DLKPENVVFFEK	Lys2	-0.3	0.5	5.0	>10
SRPK1	UniRef100_Q4KLN3,	IIHTDIKPENILLSVNEQYIR	Lys2	-27.6	-17.5	1.3	>10
STLK3	UniRef100_UPI0003A	DLKAGNILLGEDGSVQIADFGVS	Lys2	11.2	33.7	26.5	>10
STLK5	UniRef100_Q7RTN6,	SVKASHILISVDGK	Lys2	13.7	21.5	-11.7	>10
STLK5	UniRef100_Q7RTN6,	YSVKVLPWLSPEVLQQNLQGYD	Activation Loop	-4.6	3.5	-0.7	>10
STLK6	UniRef100_F1MB87, U	SIKASHILISGDGLVTLSGLSHLH	Lys2	-13.5	0.9	2.7	>10
SYK	UniRef100_F1PSC8, U	ISDFGLSKALR	Activation Loop	54.4	20.6	-12.0	6.1
SYK	UniRef100_F1PSC8, U	TVAVKILK	Lys1	61.6	0.0	8.6	6.2
TAK1	UniRef100_G1SFY3, U	DLKPPNLLLVAGGTVLK	Lys2	77.3	59.8	6.2	1.8
TAO1, TAO3	UniRef100_O88664, U	DIKAGNILLTEPGQVK	Lys2	-8.1	6.8	-12.6	>10
TAO2	UniRef100_Q9JLS3, U	DVKAGNILLSEPGLVK	Lys2	-8.5	5.8	4.9	>10
TBK1	UniRef100_E1BKP4, U	TGDLFAIKVFNNISFLRPVDVQM	Lys1	43.3	1.6	-3.4	>10
TEC	UniRef100_UPI0001C	VAIKAIR	Lys1	62.4	-18.9	-49.6	6.0
TEC	UniRef100_UPI0001C	YVLDDQYTSSSGAKFPVK	Activation Loop	37.5	-25.7	-8.0	>10
TLK1	UniRef100_D3ZXW7,	YLNEIKPPIIHYDLKPGNILLVDGT	Lys2	-9.0	-14.6	-11.0	>10
TLK1	UniRef100_D3ZXW7,	YAAVKIHQLNK	Lys1	-43.1	-16.1	-10.2	>10
TLK2	UniRef100_G1SQ97,	YVAVKIHQLNK	Lys1	1.8	-16.8	-21.4	>10
TLK2	UniRef100_G1SQ97,	YLNEIKPPIIHYDLKPGNILLVNGT	Lys2	-2.6	-15.0	4.5	>10
TYK2_Domain2 domain2	UniRef100_F1PBD0, U	IGDFGLAKAVPEGHEYYR	Activation Loop	-4.7	-4.6	0.5	>10
ULK1	UniRef100_O70405, U	DLKPQNILLSNPAGR	Lys2	-1.6	4.2	-1.3	>10
ULK3	UniRef100_F1P6D2, U	EVVAIKCVAK	Lys1	75.2	30.6	-5.5	2.8
ULK3	UniRef100_F1P6D2, U	NISHLDLKPQNILLSSLEKPHLK	Lys2	63.0	18.5	6.9	5.9
VRK2	UniRef100_J9PA85, U	MLDVLEYIHENEYVHGDIKAANLL	Lys2	-39.4	-14.2	-0.4	>10
Wee1	UniRef100_Q63802, U	YIHSMSLVHMDIKPSNIFISR	Lys2	-30.1	-5.0	22.7	>10
Wnk1, Wnk2, Wnk3	UniRef100_Q9Y3S1,	DLKCDNIFITGPTGSVK	Lys2	-5.5	2.7	8.2	>10
Wnk1, Wnk2, Wnk4	UniRef100_Q9Y3S1,	IGDLGLATLKR	Activation Loop	-24.3	5.8	-7.1	>10
YANK3	UniRef100_Q8QZV4,	DVKPDNILLDER	Lys2	-44.9	-9.5	-8.1	>10
ZAK	UniRef100_E2REE9, U	WISQDKEVAVKK	Lys1	90.7	69.7	25.5	0.59
ZC1/HGK, ZC2/TNIK, ZC3/MINK	UniRef100_UPI00048(	DIKGQNVLLTENAEVK	Lys2	97.0	90.7	61.0	0.083

Supplemental Table 3.3. AML patient characteristics.

Patient ID	WHO Classification	Cytogenetics
AML-1	AML with t(8;21)(q22;q22.1)	46,XX,t(9;11)(p22;q23)[4]/47,idem,+21[14]/46,XX[2]
AML-2	Acute monoblastic/monocytic leukemia	46,XY,add(6)(q27),del(11)(q23)[15]/47,idem,+14[3]/46,XY[2]
AML-3	Acute monoblastic/monocytic leukemia	46,XY,der(10)?add(10)(p13)ins(10;11)(p12;q?23q?21),?add(10)(p12),del(11)(q21q23)[14]/47,sl,+8[6]
AML-4	Therapy-related AML	46,XX,der(10)t(10;11)(p11.2;q23)
AML-5	Acute monoblastic/monocytic leukemia	50,XX,+der(6)t(6;11)(q27;q23)[19],t(6;11)(q27;q23),+8[19],+8[19],+19[19][cp20]
AML-6	Acute monoblastic/monocytic leukemia	46,XY,inv(11)(p11.2q23)[2]/46,sl,add(20)(q13.1)[13]/46,sdl1,t(6;7)(p21;q36)[4]/46,XY[1]
AML-7	Therapy-related AML	44,XY,i(5)(p10),add(7)(q22),-15,-17,del(20)(q11.2q13.3),-21,+mar[2]/45,idem,+r18]
AML-8	AML-NOS	48,XX,der(7)ins(7)(q11.2q22q36)t(7;12)(q36;p13),+8,der(12)t(7;12)(q36;p13),+19[19]//46,XY[1]
AML-9	AML with inv(3)(q21.3q26.2)	45,XY,inv(3)(q21q26.2),-7[15]/45,idem,t(5;8;21)(q22;q24;q11.2)[5]
AML-10	AML with t(8;21)(q22;q22.1)	45,X,-Y,t(8;21)(q21.3;q22)[20]
AML-11	AML with t(8;21)(q22;q22.1)	46,XX,t(8;21)(q21.3;q22)[19]/46,XX[1]
AML-12	Acute monoblastic/monocytic leukemia	46,XX,t(1;8)(p13;q13),der(11)t(1;11)(q21;p15),r(12)(p13q24.1)[8]/47,idem,-der(1)t(1;8)(p13;q13),+der
AML-13	Acute megakaryoblastic leukemia	46,XX,inv(7)(p13q36)[cp19]/46,XX[1]
AML-019	Acute myelomonocytic/monocytic leukemia	47,X,-Y,del(6)(q15q21),+8,+14,del(15)(q12q15)[17]/47,idem,der(1)t(1;1)(p36.1q44)[2]/47,idem,t(1;9)(q23;q34)[1]
AML-174	AML	DNMT3A R882C FLT3 L576_Q577insQMVQVTGSSDNEYFYVD PTPN11 D61Y WT1 A382fs*11, A382fs*4
AML-11-02	De Novo AML, FAB M2	FLT3 FLT3-ITD (V615_L616ins34); MYC duplication; NSD1 NUP98-NSD1 fusion

Supplemental Table 3.4. Peptide phosphorylation in the PamChip Serine/Threonine in-cell kinase array with NCGC1481 treatment.

MLL-AF9;FLT3-ITD + NCGC1481 (0.1 nM) Log2 FC				
	6hr Replicate 1	6hr Replicate 2	12hr Replicate 1	12hr Replicate 2
ACM1_421_433	-0.10826874	-0.40524197	0.11344528	-0.40072298
ACM1_444_456	0.10704994	-0.0879	0.36934567	0.00384
ACM4_456_468	-0.25490379	-0.23824644	0.3059144	0.12533379
ACM5_494_506	-0.15217209	-0.15392971	0.11492729	0.23131275
ACM5_498_510	0.00104	-0.0467	0.00826	0.0922
ADDB_696_708	-0.16080284	-0.39557934	0.0442	-0.13157272
ADDB_706_718	-0.0676	-0.21958065	0.0391	-0.0303
ADRB2_338_350	-0.11982727	-0.28458023	-0.1	-0.0537
ANDR_785_797	-0.1751914	-0.34004927	0.0866	-0.0954
ANXA1_209_221	-0.58775139	-0.34327316	0.0974	0.0104
ART_025_CXGLRRWSLGGLRRWSL	0.0689	-0.3562212	-0.00949	-0.10269594
BAD_112_124	-0.0584	0.00998	0.4749012	0.21482658
BAD_69_81	0.18568611	-0.0903	0.20218897	0.24398089
BAD_93_105	0.00742	-0.072	-0.00862	0.078
BCKD_45_57	0.20790625	-0.10198402	0.0506	0.1658349
CA2D1_494_506	-0.20555306	-0.27677107	0.10713911	0.1930337
CAC1C_1974_1986	-0.00827	-0.29054737	0.0321	0.0388
CD27_212_224	-0.48242664	0.21833468	0.36491919	-0.1279974
CDC2_154_169	-0.47798896	-0.14368796	-0.14549875	0.31961775
CDK7_163_175	0.5614078	0.57502747	0.64107013	-0.29643059
CDN1A_139_151	0.0552	0.026	0.0767	-0.0678
CENPA_1_14	0.2165556	-0.16449356	0.0908	-0.19587898
CFTR_730_742	-0.0769	-0.35110283	0.11704588	0.00299
CFTR_761_773	-0.11872101	-0.18506241	0.0252	0.0472
CGHB_109_121	-0.25234079	0.00136	-0.6914134	0.14057875
CREB1_126_138	-0.13040447	-0.37913799	-0.0216	-0.21422768
CSF1R_701_713	-0.0187	-0.17639351	0.0535	-0.17843437
DCX_49_61	0.0622	-0.22672081	-0.0436	-0.56027579
DESP_2842_2854	-0.21016216	-0.58347273	0.55071116	-0.0606
E1A_ADE05_212_224	-0.3362217	-0.67150927	-0.0876	-0.0399
EPB42_241_253	-0.26860333	-0.39986086	-0.24814272	0.0921
ERBB2_679_691	-0.0649	-0.26422501	-0.12197495	-0.1107769
ESR1_160_172	-0.26135254	-0.55164051	-0.11728621	-0.21304798
F263_454_466	-0.14481449	-0.30047989	0.0369	0.0968
FIBA_569_581	-0.15789795	0.60535097	0.849545	-0.18590713
FOXO3_25_37	-0.0565	0.13150215	0.033	-0.18209457
FRAP_2443_2455	0.28679514	0.13306475	0.36899996	-0.27008915
GBRB2_427_439	-0.11397457	-0.36040402	-0.15326977	-0.10653496
GPR6_349_361	0.0162	-0.091	-0.0867	-0.31696129
GPSM2_394_406	0.25891161	-0.31403971	-0.25588465	-0.36399698
GRIK2_708_720	-0.0705	-0.25255299	0.0944	0.0511
GSUB_61_73	-0.23232555	0.0321	-0.44156313	-0.1719842
GYS2_1_13	-0.25240898	-0.0238	-0.49770927	0.0898
H2B1B_27_40	-0.13661051	-0.11694574	-0.32170439	-0.46190786
H32_3_18	-0.18583441	-0.23373938	-0.0141	-0.20748234
IF4E_203_215	-0.35267162	-0.14540601	-1.13897634	-0.00723
K6PL_766_778	-0.0285	-0.14996624	0.0513	-0.15354252
KAP2_92_104	-0.12350273	-0.19911099	-0.0105	0.0204
KAP3_107_119	-0.16541481	-0.22109222	-0.0242	0.10908413
KAPCG_192_206	0.2044239	0.0266	-0.22728777	-0.16297197
KCC2G_278_289	0.73413897	-0.1487236	0.53043079	-0.32248592
KCNA1_438_450	0.0696	-0.56559706	-0.38385201	-0.29798555
KCNA2_442_454	0.0681	-0.0887	-0.2155118	-0.34123993
KCNA3_461_473	0.15659523	-0.17971993	-0.0417	-0.47733641
KCNA6_504_516	-0.16359139	-0.31090641	0.0211	0.16789722
KIF2C_105_118_S106G	-0.1688509	-0.17427445	-0.38584995	-0.27008724
KPB1_1011_1023	-0.0774	-0.25309944	0.20937061	-0.00431
KPCB_19_31_A25S	0.0114	-0.0483	-0.24130821	-0.34244156
KS6A1_374_386	-0.39452457	0.0526	-0.38095427	-0.25551987
LIPS_944_956	0.33844948	-0.14823771	0.1788969	-0.23310566
LMNB1_16_28	0.46389127	-0.43255162	0.0225	-0.6421442
MARCS_152_164	-0.0749	-0.0364	-0.31711912	-0.17656374
MARCS_160_172	0.0125	-0.0189	1.32962894	-0.22192907
MBP_222_234	0.0399	-0.24583626	-4.38582182	-0.13633299
MP2K1_287_299	-0.049	-0.21258497	0.3506093	-0.24818659
MPIP1_172_184	-0.20105457	-0.25726795	-0.24376392	-0.1878705
MYPC3_268_280	-0.0923	-0.32916832	0.10748196	0.0669
NCF1_296_308	-0.022	-0.46823502	-0.0892	-0.33484745
NCF1_321_333	-0.0305	-0.34931469	-0.14310551	-0.098
NEK2_172_184	0.22519732	-0.29643297	-0.0196	-0.42799997
NEK3_158_170	0.27563429	-0.21406627	-0.44173241	-0.66097593
NFKB1_330_342	-0.28422022	-0.15769863	0.0709	0.0714
NMDZ1_890_902	-0.0359	-0.30175114	-0.20586968	-0.4483738
NOS3_1171_1183	-0.0481	-0.0875	-0.23232746	-0.33998394
NR4A1_344_356	-0.099	-0.14154911	0.0471	-0.55368424
P53_308_323	-0.58313036	-0.4055357	-0.4551754	-0.49957085

MV4-11 + NCGC1481 (0.1 nM) Log2 FC				
	6hr Replicate 1	6hr Replicate 2	12hr Replicate 1	12hr Replicate 2
ACM1_421_433	0.12820768	0.0193	-0.2952895	-0.2271876
ACM1_444_456	0.26071644	0.18684197	-0.1180835	0.0422
ACM4_456_468	0.13948107	0.0193	0.0659	0.12779379
ACM5_494_506	0.0697	0.24728346	0.0842	0.00435
ACM5_498_510	0.13873959	0.15473747	-0.0142	0.0278
ADDB_696_708	0.22362614	0.17718315	0.0479	0.37502289
ADDB_706_718	0.35137081	0.4248395	-0.00256	0.0141
ADRB2_338_350	0.25703669	0.19050932	-0.1872268	-0.0117
ANDR_785_797	-0.0986	0.30822897	-0.1352	0.0312
ANXA1_209_221	0.0451	0.3039856	-0.0485	-0.0855
ART_025_CXGLRRWSLGGLRRWSL	0.0567	0.3558526	-0.2158899	-0.159699
BAD_112_124	0.46835995	0.84733486	0.0686	0.34206009
BAD_69_81	0.34450197	0.48379183	-0.4198918	-0.00645
BAD_93_105	0.0966	0.40223265	-0.1519718	-0.1645374
BCKD_45_57	1.30943537	0.1961112	-0.399096	-0.0269
CA2D1_494_506	0.45267296	0.68514919	0.2486186	-0.0433
CAC1C_1974_1986	0.0585	0.22129345	-0.0595	-0.0324
CD27_212_224	0.0988	0.48586559	-0.664268	-0.196775
CDC2_154_169	0.2959137	0.45260239	0.0791	0.11231256
CDK7_163_175	-0.157445	0.2957387	-0.2967176	0.12778616
CDN1A_139_151	0.096	0.41729736	-0.2242413	-0.0142
CENPA_1_14	0.0676	0.63525677	-0.1408548	0.0972
CFTR_730_742	0.18267441	0.25310803	-0.2110853	0.10877419
CFTR_761_773	0.047	0.0242	-0.1048756	-0.00814
CGHB_109_121	0.48920393	0.0686	-0.3705444	-0.2599611
CREB1_126_138	-0.1147537	0.098	-0.238452	-0.2030764
CSF1R_701_713	0.0791	0.66742897	-0.1975107	0.19717264
DCX_49_61	0.0651	1.26862979	-0.7397969	0.15799403
DESP_2842_2854	0.0533	0.739048	-0.2702551	-0.2388587
E1A_ADE05_212_224	-0.1355786	0.12323141	-0.1051497	-0.2176404
EPB42_241_253	0.12577534	0.42459726	-0.0817	0.0121
ERBB2_679_691	0.0221	0.65691662	-0.00145	-0.0567
ESR1_160_172	-0.1241126	0.70757484	-0.1358151	0.20037174
F263_454_466	-0.0162	0.0414	-0.1086969	0.00768
FIBA_569_581	-0.2157288	-0.2223923	0.0277	-0.4493518
FOXO3_25_37	0.24857473	0.70933056	-0.2211366	-0.0325
FRAP_2443_2455	0.0172	0.74165916	-0.2610583	-0.078
GBRB2_427_439	-0.0944	0.0804	-0.1475754	-0.1308136
GPR6_349_361	0.092	0.70026588	-0.3090987	-0.0932
GPSM2_394_406	-0.2417221	0.86050081	-0.2641206	0.15676928
GRIK2_708_720	0.23253822	0.0231	-0.1863441	-0.0504
GSUB_61_73	0.23100805	0.68484736	-0.250411	0.0177
GYS2_1_13	0.23508453	0.80969048	-0.0628	0.0378
H2B1B_27_40	0.37079239	0.64061117	-0.0788	-0.2398
H32_3_18	0.22104168	0.66908789	-0.0464	0.00346
IF4E_203_215	0.74658489	1.48304915	-0.144712	0.48914671
K6PL_766_778	0.1854682	0.63229656	-0.2566333	0.17696381
KAP2_92_104	0.29921722	0.0462	-0.0846	-0.1199503
KAP3_107_119	0.0833	0.13310146	-0.0962	-0.0146
KAPCG_192_206	0.0882	0.74066019	-0.0373	-0.10116
KCC2G_278_289	-0.0229	0.25074673	-0.1643977	-0.2061076
KCNA1_438_450	-0.475338	0.0961	-0.1235847	-0.0646
KCNA2_442_454	-0.1215444	0.84233093	-0.3177276	0.0773
KCNA3_461_473	-0.5693207	0.72036982	-0.2851009	0.1537199
KCNA6_504_516	0.0608	0.0391	-0.1203909	-0.0305
KIF2C_105_118_S106G	0.0504	0.70845985	-0.1921949	0.0571
KPB1_1011_1023	0.0694	0.2923584	-0.1709213	0.15631676
KPCB_19_31_A25S	0.12730598	0.67988682	-0.0449	-0.0634
KS6A1_374_386	0.23362637	0.58058882	0.0936	-0.0802
LIPS_944_956	0.0303	0.72142696	-0.2575464	0.15512705
LMNB1_16_28	-0.0965	0.18501473	-0.5225835	-0.2784133
MARCS_152_164	0.17694426	0.6707716	-0.3431835	-0.0466
MARCS_160_172	0.2239604	-0.1656914	0.19124985	-0.1360321
MBP_222_234	0.0668	-0.170126	-0.0358	-0.2713351
MP2K1_287_299	-0.029	0.60576868	-0.6908312	-0.3332553
MPIP1_172_184	0.13990974	0.6943779	-0.1858029	-0.0208
MYPC3_268_280	0.11872387	0.15591812	-0.1203012	0.0566
NCF1_296_308	-0.1886606	0.19636917	-0.2542982	-0.0643
NCF1_321_333	-0.1158953	0.12217617	-0.145009	-0.0593
NEK2_172_184	0.13204908	0.14207315	-0.0676	0.0824
NEK3_158_170	0.54903245	0.33188629	0.17416668	0.34475088
NFKB1_330_342	0.0383	0.14990759	-0.069	0.019
NMDZ1_890_902	0.0804	0.56337452	-0.1335258	-0.0321
NOS3_1171_1183	0.0138	0.45212555	-0.1992722	-0.2971067
NR4A1_344_356	0.34841776	0.41934872	-0.2300572	-0.2665663
P53_308_323	0.0396	0.42951775	-0.4972758	-0.0863

PLEK_106_118	0.13957882	-0.0444	0.0951	-0.32638264
PLM_76_88	-1.31494141	0.96523452	-0.22870064	0.11228371
PP2AB_297_309	-0.18306613	0.0786	-0.29828525	-0.1080277
PPR1A_28_40	-0.00866	-0.0374	-0.21283627	-0.23391628
PRKDC_2618_2630	0.3712306	-0.294034	-0.39592862	-0.92748761
PTK6_436_448	-0.15716457	-0.20697498	-0.00197	-0.24238586
PTN12_32_44	-0.13795662	-0.42022133	-0.16967964	-0.11228848
PYGL_8_20	-2.96207762	3.24362302	-1.84178841	3.61637545
RADI_559_569	1.98281336	0.95036924	0.23029763	1.04551458
RAF1_253_265	0.10816479	-0.33619356	-0.23814297	-0.31332922
RAP1B_172_184	-0.18397188	-0.29198456	-0.17353582	-0.25905371
RBL2_655_667	0.0613	-0.10801315	0.00987	-0.29373694
RB_242_254	-0.27081871	-0.36152554	-0.0593	-0.17012358
RB_350_362	-4.12694788	-0.38235807	0.12909007	0.56341982
RB_803_815	-0.19531822	-0.000517	-0.41438961	0.0959
REL_260_272	0.0455	-0.4372201	-0.000779	-0.0698
RS6_228_240	-0.0611	-0.19621563	0.13828087	-0.0828
RYR1_4317_4329	-0.153512	-0.32408714	-0.0522	-0.19150066
SCN7A_898_910	0.0438	-0.31005621	0.28070116	0.0855
STK6_283_295	-0.2581234	-0.10778141	-0.10184574	0.14477634
STMN2_90_102	-0.43558478	-0.90140319	0.12764788	-0.0487
TOP2A_1463_1475	-0.22251988	-0.31197166	-0.23500633	-0.0971
TY3H_65_77	-0.20502472	-0.30412388	0.0333	0.0555
VASP_150_162	-0.0327	-0.42125607	-0.17118835	0.064
VASP_271_283	-0.17822838	-0.34823895	-0.11210632	-0.14657497
VTNC_390_402	-0.13223934	-0.26059914	0.0997	-0.012

PLEK_106_118	0.0779	0.27259827	-0.2422056	-0.1626492
PLM_76_88	-0.4859052	0.17642641	-0.3757043	-0.4689512
PP2AB_297_309	0.68379688	0.40942407	-0.279604	0.13725185
PPR1A_28_40	0.0921	0.25848103	-0.2993574	-0.2346258
PRKDC_2618_2630	0.72185564	0.72843623	-0.4881907	0.54516149
PTK6_436_448	0.0504	0.29331589	-0.1610212	0.1094656
PTN12_32_44	-0.2908087	0.1993866	-0.2796249	-0.1027508
PYGL_8_20	-1.0930171	-0.1702387	2.0657239	0.0919
RADI_559_569	0.4344027	-0.0603	1.34665036	-0.2455471
RAF1_253_265	0.12623978	0.21874714	-0.3535285	0.0463
RAP1B_172_184	0.16301107	0.31465006	-0.1882057	-0.09
RBL2_655_667	-0.0999	0.18163157	-0.2755423	-0.2090402
RB_242_254	0.13987255	0.38706923	-0.2823682	0.0292
RB_350_362	0.21439362	-0.3299599	-0.1127362	-0.1674051
RB_803_815	0.19199181	0.29471731	-0.1045046	0.0746
REL_260_272	0.0817	0.25196886	-0.3421278	0.0388
RS6_228_240	-0.0336	0.11476708	-0.3241615	-0.1246843
RYR1_4317_4329	-0.388649	-0.0414	-0.3885784	-0.2867794
SCN7A_898_910	0.0177	0.22122908	-0.1872759	0.0641
STK6_283_295	0.26796913	0.19301415	-0.0429	-0.1045198
STMN2_90_102	0.00436	0.0737	-0.1026402	-0.2791643
TOP2A_1463_1475	-0.1242237	0.0514	-0.2979574	-0.1403522
TY3H_65_77	0.0157	0.22985077	-0.0929	0.0461
VASP_150_162	-0.2242074	0.27667904	-0.2746878	-0.1100101
VASP_271_283	-0.2998734	0.07	-0.3349872	-0.2573557
VTNC_390_402	0.0705	0.19824505	-0.042	0.00929

Supplemental Table 3.5. Gene expression analysis of FLT3-ITD AML treated with NCGC1481.

RNA-seq: MLL-AF9;FLT3-ITD + 1481 (0.1 nM, 6 hr) - Log FC>±2 (P < 0.05)						
Gene	LogFC	AveExpr	t	P.Value	Adj.P.Val	B
LOC645405	2.43809	-4.02322	4.017478	0.000661	0.046391	-4.26536
TAS2R60	2.43809	-4.02322	4.017478	0.000661	0.046391	-4.26536
PLSCR3	2.314294	-3.30531	3.703171	0.001382	0.064688	-4.24882
TMEM191B	2.310621	-3.30531	3.711583	0.001355	0.064499	-4.24774
ABCG2	2.27492	-4.10412	3.747337	0.001247	0.062131	-4.29934
HNRNPCL1	2.229605	-3.61772	3.489115	0.002278	0.082148	-4.30195
DNAJC22	2.198797	-4.14605	3.47673	0.002345	0.082148	-4.33138
SNORD121B	2.188112	-4.14605	3.417709	0.002689	0.088424	-4.33794
FMR1-AS1	2.18257	-4.14605	3.391786	0.002856	0.09118	-4.34084
LGALS2	2.148065	-2.63806	3.497204	0.002236	0.081683	-4.20554
TTC3P1	2.076788	-3.15647	3.308741	0.00346	0.10117	-4.28571
SLAMF7	2.069431	-3.69863	3.196516	0.004479	0.114521	-4.34279
ALG1L	2.058909	-2.8923	3.626562	0.001654	0.070577	-4.21364
CACNA1H	2.035563	-4.22695	3.260176	0.00387	0.106882	-4.35986
CMTM2	2.035563	-4.22695	3.260176	0.00387	0.106882	-4.35986
ZACN	2.024134	-3.69863	3.215573	0.004288	0.111914	-4.34042
EPHX3	-2.06736	-3.4949	-2.92694	0.00826	0.153199	-4.36358
USH1G	-2.10531	-4.22695	-3.31181	0.003436	0.10077	-4.35401
ARL13A	-2.13145	-4.22695	-3.4503	0.002494	0.084657	-4.33877
TMC2	-2.13145	-4.22695	-3.4503	0.002494	0.084657	-4.33877
LOC1005068	-2.13793	-3.69863	-3.36506	0.003038	0.093959	-4.32206
PLEKHA4	-2.22124	-2.58515	-4.18481	0.000446	0.039414	-4.09187
AIF1L	-2.22272	-3.63187	-3.16903	0.00477	0.117696	-4.3427
RORA	-2.25561	-4.14605	-3.46006	0.002438	0.083637	-4.33311
TIGD4	-2.27196	-4.14605	-3.53626	0.002042	0.078084	-4.3247
RPH3A	-2.29847	-4.14605	-3.6885	0.001431	0.065879	-4.30816
MIR635	-2.31572	-3.36574	-3.595	0.00178	0.07292	-4.26715
FAM166A	-2.36007	-4.10412	-3.8821	0.000909	0.053885	-4.28489
FOXH1	-2.42501	-4.06514	-3.71737	0.001337	0.064499	-4.29998
LOC1005063	-2.47793	-3.25763	-3.62777	0.001649	0.070577	-4.25539
ARHGEF38	-2.51527	-3.50904	-4.08399	0.000565	0.043411	-4.22412
TBC1D26	-2.6234	-3.95646	-3.80381	0.001092	0.058142	-4.28363
LOC1005058	-2.68217	-3.40437	-3.87768	0.000918	0.053936	-4.24067
LOC388906	-2.91563	-3.82146	-4.71595	0.000128	0.021546	-4.1803

RNA-seq: MLL-AF9;FLT3-ITD + 1481 (0.1 nM) 12 hr - LogFC >±2 (P<0.05)						
Gene	logFC	AveExpr	t	P.Value	adj.P.Val	B
HBB	11.32923	0.422654	22.7847	1.83E-13	3.45E-09	2.484839
HBA2	8.134667	-1.17354	14.43542	1.74E-10	1.64E-06	1.915767
HBA1	5.669539	-1.36947	9.756144	4.54E-08	0.000285	1.69225
LOC100506679	2.203404	-3.63148	3.628192	0.002318	0.186528	-2.62686
SNORD116-24	2.124535	-4.17831	3.637681	0.002272	0.185764	-2.72836
SLC5A4	2.120473	-4.17831	3.607304	0.002421	0.190002	-2.75152
CD8A	2.09909	-3.66413	3.446608	0.003391	0.216471	-2.78309
ALG1L	2.064357	-2.89016	3.746782	0.001808	0.168653	-2.29453
EN2	2.006523	-4.24071	3.160302	0.00617	0.258793	-3.11273
LOC285696	-2.03746	-3.80547	-2.93881	0.009773	0.299745	-3.22569
MIR4712	-2.04154	-4.5653	-2.58321	0.020217	0.367844	-3.61465
NACA2	-2.04886	-3.48263	-2.53662	0.022204	0.377111	-3.52866
LRGUK	-2.06341	-3.11534	-3.28363	0.00477	0.245413	-2.76417
LOC727805	-2.06754	-4.03697	-3.31344	0.004481	0.236724	-2.9658
C17orf106-CDK3	-2.07513	-2.76909	-2.70459	0.015806	0.343398	-3.26535
RGMB	-2.11521	-4.5653	-2.89184	0.010768	0.30585	-3.3757
BTLA	-2.12831	-3.99505	-3.50766	0.002984	0.206061	-2.80287
LOC441528	-2.15719	-3.99505	-3.46211	0.003283	0.213903	-2.83882
SNORA15	-2.161	-3.72456	-2.9905	0.008782	0.292183	-3.16845
ODZ4	-2.18671	-4.50487	-3.59906	0.002464	0.190145	-2.83085
FOXI1	-2.35343	-4.42396	-3.75008	0.001796	0.168653	-2.70196
SMAD5-AS1	-2.4161	-3.60174	-3.67136	0.002117	0.18207	-2.56758
EGR3	-2.42708	-3.83521	-3.49448	0.003067	0.20945	-2.77887
LOC100506880	-2.4507	-3.85372	-3.90631	0.001295	0.156071	-2.46022
MYCBPAP	-2.46325	-3.83324	-3.9762	0.001119	0.142171	-2.40196
AXDND1	-2.47399	-3.58956	-3.65427	0.002194	0.182919	-2.57885
COL4A5	-2.48159	-4.36353	-3.81984	0.001552	0.160904	-2.63663
C12orf69	-2.57524	-3.77281	-4.0641	0.000932	0.134442	-2.31971
RPH3A	-2.60847	-4.30114	-4.34642	0.00052	0.107073	-2.25439
SETP20	-2.67999	-4.24071	-4.03724	0.000986	0.13751	-2.44934
GGTLC1	-2.93274	-4.11788	-4.75946	0.000224	0.073473	-1.92912

Materials and Methods

Study design

The first objective of this study was to find target-independent mechanisms of resistance, such as alternate activation of survival and proliferation pathways (adaptive resistance), to FLT3 inhibition in FLT3-mutant AML by performing an integrative in-cell kinase (PamChip kinase array) and gene regulatory network (RNA-seq) analysis. The second objective was to identify an inhibitor with the potential of suppressing FLT3-ITD as well the pathway contributing to adaptive resistance in FLT3-mutant AML. To overcome adaptive resistance to FLT3 inhibition, we synthesized a series of small molecules to inhibit the compensatory pathway activation contributing to adaptive resistance (via IRAK1/4) and FLT3 in FLT3-mutant AML. The chemical starting points for optimization of IRAK1/4 and FLT3 small molecule inhibitors was based on the 3-(pyridin-2-yl)imidazo[1,2-a]pyridines that were previously reported as selective IRAK4 inhibitors. The potency and selectivity of the inhibitors was determined by biochemical binding and inhibitory assays, and in situ kinase profiling. The optimized small molecule inhibitor (NCGC1481) was confirmed by co-crystallography to bind IRAK4 in an inactive confirmation. In-cell kinase (PamChip kinase array) assays, immunoblotting, and gene expression profiling confirmed that NCGC1481 simultaneously suppresses FLT3 and IRAK1/4 in FLT3-mutant AML. The therapeutic benefit of targeting IRAK1/4 and FLT3 in FLT3-mutant AML with NCGC1481 as compared to a selective FLT3 inhibitor was confirmed in human cell lines and patient-derived samples in vitro and in vivo. All normal human derived samples were obtained from the Translational Research Development Support Laboratory of CCHMC under an approved Institutional Review Board protocol. AML primary patient samples were obtained with written informed consent and approved by the institutional review board of Cincinnati Children's Hospital Medical Center. These samples had been obtained within the framework of routine diagnostic BM aspirations after written informed consent in accordance with the Declaration of Helsinki. Existing de-identified cryopreserved samples were used for the study without age or gender preferences. Investigators

and data analyzers were blinded for the evaluation of NCGC1481 in primary patient-derived AML samples in vitro. Mouse experiments have been planned in an effort to provide 60%-80% power for a target effect size of 1.2-1.5 (effect size=|mean difference|/SD). All mice were randomly allocated into experimental groups. For all other experiments, at least 2 independent biological replicates were performed/utilized in the sample calculation. No data was excluded from the studies. STR loci analysis was performed on all cell lines when received and after experimentation was complete. All cell lines are routinely tested and are confirmed to be negative for mycoplasma.

Cell lines, patient samples, and culture conditions

MLL-AF9 FLT3-ITD and MLL-AF9 $NRAS^{G12D}$ cell lines, provided by Dr. James Mulloy (Cincinnati Children's Hospital Medical Center, Cincinnati, OH) were cultured in Isocov's DMEM medium (Corning Cell Grow, Cat#10-016-CV) with 20% Fetal Bovine Serum (FBS) (Atlanta Biologicals, Cat#S11550) and 1% penicillin-streptomycin (P/S) (HyClone, Cat#SV30010) (*45*). MV4;11 cell line was provided by Dr. Lee Grimes (CCHMC, Cincinnati, OH) and purchased from ATCC (Cat#CRL-9591). They were cultured in RPMI 1640 medium with 10% FBS and 1% (P/S). MOLM13 cell line, purchased from AddexBio (Cat#C0003003), was cultured in RPMI 1640 medium (HyClone, Cat#SH30027.01) with 20% FBS and 1% P/S. THP1-Blue™ NF-κB were obtained from InvivoGen (Cat#thp-nfkb) and grown according to manufacturer instructions. BaF3 cells were provided by Dr. Mohammed Azam (CCHMC, Cincinnati, OH) and purchased from ATCC (Cat#HB-283). They were cultured in RMPI 1640 medium with 10% FBS, 1% P/S, and recombinant murine interleukin-3 at 10 ng/mL (PeproTech, Cat#213-12-50UG). Human CD34+ umbilical cord blood, human CD34+ bone marrow, and human normal whole bone marrow were obtained from the Translational Research Development Support Laboratory of Cincinnati Children's Hospital under an approved Institutional Review Board protocol. These cells were maintained in StemSpan Serum-Free Expansion Media (Stemcell Techologies, Cat#09650) supplemented with 10 ng/mL of recombinant human stem cell factor (SCF) (PeproTech, Cat#300-

07-50UG), recombinant human thrombopoietin (TPO) (PeproTech, Cat#300-18-50UG), recombinant human FLT3 ligand (FLT3L) (PeproTech, Cat#300-19-50UG), recombinant human interleukin-3 (IL-3) (PeproTech, Cat#200-03-50UG), and recombinant human interleukin-6 (IL-6) (PeproTech, Cat#200-06-50UG). AML primary patient samples were obtained with written informed consent and approved by the institutional review board of Cincinnati Children's Hospital Medical Center. These samples had been obtained within the framework of routine diagnostic BM aspirations after written informed consent in accordance with the Declaration of Helsinki. AML-019 was purchased from the Public Repository of Xenografts (PRoXe) (Cat#DFAM-16835-V1).

Reagents

IRAK1/4 inhibitor (Amgen Inc.) was purchased from Sigma-Aldrich (Cat#I5409). Quizartinib was purchased from Selleckchem (Cat#S1526). IKK7 was purchased from Selleckchem (Cat#S2882). Gilteritinib was purchased from Chemietik (Cat#CT-GILT). ODN-INH-18 was purchased from invivogen (Cat#tlrl-inh18). PF06650833 (PF066) was purchased from Sigma-Aldrich (PZ0327-5MG). The TLR9 antagonist, ODN-INH-18 was purchased from InvivoGen (Cat#tlrl-inh18).

Immunoblotting

Protein lysates were made by lysing cells in cold RIPA lysis buffer (50 mM Tris-HCl, 150 mM NaCl, 1 mM EDTA, 1% Titon X-100, and 0.1% SDS), in the presence of sodium orthovanadate, PMSF, and protease and phosphatase inhibitors. Protein concentration was quantified using BCA assay (Pierce, Cat#23225). Protein lysates were separated by SDS-polyacrylamide gel electrophoresis (BIO-RAD), transferred to nitrocellulose membranes (BIO-RAD, Cat#1620112), and immunoblotted. The following antibodies were used for western blot analysis: GAPDH (Cell Signaling, Cat#D16H11, 1:1000 milk), FLT3 (Cell Signaling, Cat#3462, 1:500 BSA), phospho-FLT3 (Tyr591) (Cell Signaling, Cat#3461, 1:500 BSA), IRAK4 (Cell Signaling, Cat#4363, 1:1000 BSA), phospho-IRAK4 (Thr345/Ser346) (Cell Signaling, Cat#11927, 1:500 BSA), IRAK1 (H-273) (Santa Cruz, Cat#sc-7883, 1:1000 milk), phospho-IRAK1 (T209) (Assay Biotech, Cat#A1074, 1:500 BSA), JNK2 (Cell Signaling, Cat#9258, 1:1000 BSA), phospho-SAPK/JNK (Thr183/Tyr185)

(Cell Signaling, Cat#4668, 1:500 BSA), p38 MAPK (Cell Signaling, Cat#9212, 1:1000 BSA), phospho-p38 MAPK (Thr180/Tyr182) (Cell Signaling, Cat#4631, 1:500 BSA), STAT5 (Cell Signaling, Cat#9363, 1:1000 BSA), phospho-STAT5 (Cell Signaling, Cat#9351, 1:1000 BSA), phospho-Src Family (Tyr416) (Cell Signaling, Cat#2101, 1:1000 BSA), Src (Cell Signaling, Cat#2108, 1:1000 BSA), TLR9 (Cell Signaling, Cat#2254, 1:1000 BSA), peroxidase-conjugated AffiniPure Goat Anti-rabbit IgG (Jackson ImmunoResearch Laboratories, Inc., Cat#111-035-003, 1:10000 milk). Blots were visualized using ECL Western Blotting Substrate (Pierce, Cat#32106) and imaged on autoradiography film (HyBlot CL) or BIO-RAD ChemiDoc Touch Imaging system.

DNA sequencing

To isolate whole genomic DNA, cell pellets were resuspended in NaOH (50 mM) and incubated at 95° C for 1 hour. Samples were spun down and the supernatant pH was neutralized with Tris-HCl (1 M). The FLT3 kinase domain was amplified by PCR from whole genomic DNA using GeneAmp Fast PCR Mastermix (Applied Biosystems, Cat#28796). The PCR product was extracted using QIAquick Gel Extraction Kit (Qiagen, Cat#28706). For amplification and bidirectional sequencing of the F691 locus, the following primers were used: Forward - 5'-GAGAGGCACTCATGTCAGAACTCA-3', reverse - 5'-AGTCCTCCTCTTCTTCCAGCCTTT-3' (*21*). For the D835 locus, the following primers were used: Forward - 5'-TGTGTTCACAGAGACCTGGC-3', reverse - 5'-TTTACAGGCAGACGGGCATT-3'. For the NRAS G12/13 locus, the following primers were used: Forward – 5'-ATTAATCCGGTGTTTTTGCGTTCT-3', reverse – 5'- CATCTCTGAATCCTTTATCTCCAT-3' (*82*).

In vitro cellular studies

For colony formation, cells were suspended at 1000 cells/mL in methylcellulose (MethylCult H4434 Classic, Cat#04434). Colonies were counted 7-10 days after plating. AnnexinV viability staining was carried out according to manufacture instructions (AnnexinV Binding Buffer:

Invitrogen, Cat#00-0055-56; AnnexinV-APC conjugated antibody: 1:100, eBioscience, Cat#88-8007). Analysis was performed using BD FACSCanto flow cytometer with Diva software. Trypan Blue (Invitrogen, Cat#T10282) exclusion was done using an automated cell counter (BioRad TC10). CellTiter Glo Luminescent Viability Assay (Promega, Cat#G7572) was performed according to manufacturer protocol. Analysis was performed using GloMax 96 microplate Luminometer (Promega) with GloMax Software.

Lenti- and retroviral Infections

The pLKO.1 (OpenBiosystems) constructs were obtained from the Viral Vector Core at CCHMC and used to express shCTL, and shIRAK4 (TRCN0000002065). Puromycin resistance gene was replaced by green fluorescent protein (GFP). The pGreenFire1-NF-κB (EF1α-puro) lentivector was purchased from System Biosciences (Cat#TR012VA-P). Flag-IRAK4 in pMSCV-pGK-GFP was designed as previously described (*81*). Cells were transduced as previously described (*83*).

NF-κB activation reporter

THP1-Blue NF-κB SEAP reporter cells were grown in a 96 well plate in triplicate with the indicated inhibitor for 24 hours. In a new 96 well plate, 20 µL of cell supernatant was added to 180 µL of warmed QuantiBlue Reagent (Invivogen, Cat#rep-qbs2) and incubated at 37 °C for 30 minutes. Absorbance was read at 630 nm.

RNA-Sequencing

RNA was isolated using Quick-RNA MiniPrep (Zymo Research, Cat#R1055) from MLL-AF9;FLT-ITD cells treated with DMSO, quizartinib (0.3 nM), or NCGC1481 (0.1 nM) for 6 and 12 hours in biological triplicates. RNA libraries were prepared according to the Illumina TruSeq Stranded mRNA (polyA capture) library protocol by the DNA Sequencing and Genotyping Core at CCHMC. The data discussed in this publication have been deposited in NCBI's Gene Expression Omnibus and are accessible through GEO Series accession number GSE121272. (https://www.ncbi.nlm.nih.gov/geo/query/acc.cgi?acc=GSE121272)

Chemical characterization

NCGC1481: 6-(7-methoxy-6-(1-methyl-1H-pyrazol-4-yl)imidazo[1,2-a]pyridin-3-yl)-N-(pyrrolidin-3-yl)pyridin-2-amine: ^{1}H NMR (400 MHz, DMSO-d_6) δ 9.88 (s, 1H), 8.90 (br.s, 1H), 8.78 (br.s, 1H), 8.44 (s, 1H), 8.22 (s, 1H), 7.90 (d, *J* = 0.8 Hz, 1H), 7.62 (dd, *J* = 8.4, 7.4 Hz, 1H), 7.36 (s, 1H), 7.22 – 7.17 (m, 2H), 6.56 (d, *J* = 8.3 Hz, 1H), 4.59 – 4.55 (m, 1H), 4.08 (s, 3H), 3.91 (s, 3H), 3.25 – 3.17 (m, 2H), 2.20 – 2.11 (m, 1H), 2.08 – 1.99 (m, 1H). HRMS: *m/z* $(M+H)^+$ = 389.1964 (Calculated for $C_{21}H_{23}N_7O$ = 389.1964).

qHTS Drug Screening

MLL-AF9.3 cells were grown in Iscove's Modified Dulbecco's Medium (IMDM) (ThermoFisher Scientific #12440-061) supplemented with 20% FBS (StemCell Technologies #06100), 1% penicillin/streptomycin (ThermoFisher Scientific #15140122) 10ng/mL of the following human growth factors: recombinant human stem cell factor (SCF) (PeproTech, Cat#300-07-50UG), recombinant human thrombopoietin (TPO) (PeproTech, Cat#300-18-50UG), recombinant human FLT3 ligand (FLT3L) (PeproTech, Cat#300-19-50UG), recombinant human interleukin-3 (IL-3) (PeproTech, Cat#200-03-50UG), and recombinant human interleukin-6 (IL-6) (PeproTech, Cat#200-06-50UG). MLL-AF9.3-FLT3ITD cells were maintained in IMDM supplemented with 20% FBS and no growth factors. Cells were plated at a density of 500 cells/well in 5μL of complete growth media in 1536 well white tissue cultured assay plates (Greiner). 23nL of compounds were then added to each assay plate using a Pintool dispenser (Kalypsys). Plates were then covered with a stainless steel gasketed lid and placed into an incubator with standard humidity, temperature, CO_2 settings for 48 hours. After this incubation, 3μL of CellTiter-Glo reagent was added to each well then incubated for 15 minutes at room temperature. Luminescence readings were taken using a ViewLux (PerkinElmer) with clear filter and a 2 second exposure time. Curve fitting was done using a 4-parameter Hill slope equation.

IRAK4 crystalography

We expressed $IRAK4_{160-460}$ with the addition of a TEV-cleavable octa-histidine tag at the N-terminus in Sf9 insect cells. The protein was purified by nickel affinity chromatography then the histidine tag was removed by cleavage with TEV protease and the protein was subjected to a second nickel affinity chromatography step. The flow-through from the second Ni affinity step was further purified by size-exclusion chromatography in 20 mM Tris-HCl, pH 8.0, 1 mM DTT. The protein was concentrated to 9.5 mg/ml for crystallization. Crystals were grown in the MCSG1 screen, condition E10: 0.2 M Ammonium Tartrate Dibasic, 20% (*w/v*) PEG3350 with 1 mM NCGC00371481 and cryopreserved in 20% (*v/v*) ethylene glycol with 1 mM NCGC00371481. The crystals grew in 13 days at 14ºC. The IRAK4-NCGC00371481 structure crystallized in the C*2* space group, with unit cell dimensions *a*=138.29 Å, *b*=141.91 Å, *c*= 87.89 Å, β = 126.22º. We collected X-ray data in-house at Beryllium using a Rigaku SuperBright FR-E+ X-ray generator with Osmic VariMax HF optics and a Saturn 944+ CCD detector.

Synergy matrix analysis

The compound synergy analysis and calculations have been previously described (*84*). Briefly, MA9 FLT3-ITD cells were treated with 10 doses of quizaritinib and 10 doses of IRAK-Inh in a 10 x 10 combination matrix for 48 hours. Viability was assessed using CellTiter-Glo and then a delta Bliss score was calculated for each drug combination using the Bliss independence model.

Serine-threonine kinase array and analysis

MLL-AF9 FLT3-ITD or MV4-11 cells were treated for 6 or 12 hours with quizartinib (0.3 nM), NCGC-1481 (0.1 nM), or DMSO. Whole cell lysates were prepared according to PamGene instructions (Protocol 1160). PamChip serine-threonine kinase array was performed by PamGene. From 144 non-redundant peptides, individual peptide phosphorylation intensities were normalized to DMSO control and log-transformed. Peptides determined to have significant increased or decreased phosphorylation ($P<0.05$) were used to infer active serine/threonine kinases (STK). The database of potential upstream STKs was downloaded from PhosphoNet

(https://www.phosphonet.ca). A given STK-substrate pair was considered highly probable if its Kinexus predictor score (v2) was greater than 300. The PamChip peptide data was integrated with the PhosphoNet kinase-substrate network to calculate kinase specificity scores (using 2000 permutations across target peptides) and the kinase significance scores (using 2000 permutations across sample labels). The kinases were then prioritized based on the sum of the two scores. Pathway and network analyses: Of the inferred kinases showing increased activity in the PamGene assay in AC200 relative to DMSO, 46 were found to be common to both the MLL-AF9;FLT3-ITD and MV4-11 cells lines at both 6 and 12 hours. These kinases were analyzed using ToppFun in the ToppGene Suite (toppgene.cchmc.org) to determine enriched signaling pathways. ClueGo (v2.5.1) was used to create the network map (Ontology = GO Biological Processes, $P<0.05$, Network Specificity = medium).

Quantitative analysis of quizartinib and NCGC1481 in mouse plasma

Ultra-performance liquid chromatography-tandem mass spectrometry (UPLC-MS/MS) methods were developed to determine quizartinib and NCGC1481 concentrations in mouse plasma samples. Mass spectrometric analysis was performed on a Waters Xevo TQ-S triple quadrupole instrument using electrospray ionization in positive mode with the selected reaction monitoring. The separation of test compounds from endogenous components was performed on an Acquity BEH C18 column (50 x 2.1 mm, 1.7 µ) using a Waters Acquity UPLC system with 0.6 mL/min flow rate and gradient elution. The mobile phases were 0.1%formic acid in water and 0.1% formic acid in acetonitrile. The calibration standards and quality control samples were prepared in the blank mouse plasma. Aliquots of 10 µL plasma samples were mixed with 200 µL internal standard in acetonitrile to precipitate proteins in a 96-well plate. 0.5 µL supernatant was injected for the UPLC-MS/MS analysis. Data were analyzed using MassLynx V4.1 (Waters Corp., Milford, MA). Adult male NRG/NRGS mice (n=3/sampling time point) were obtained from Jackson Laboratory (Bar Harbor, ME). All experimental procedures were approved by the Animal Care and Use Committee (ACUC) of the NIH Division of Veterinary Resources (DVR). A single dose of 30 mg/kg

was administered through intraperitoneal (IP) route of administration. Dosing solutions were freshly prepared on the day of administration in saline. The blood samples (~ 80 µL) were collected in K2EDTA tubes at 0.083, 0.25, 0.5, 1, 2, 4, 7 and 24 hr after drug administration, and plasma (~ 30 µL) was harvested after centrifugation at 3000 rpm for 10 min. All plasma samples were stored at -80°C until analysis. The pharmacokinetic parameters were calculated using the non-compartmental approach (Model 200) of the pharmacokinetic software Phoenix WinNonlin, version 6.2 (Certara, St. Louis, MO). The area under the plasma concentration versus time curve (AUC) was calculated using the linear trapezoidal method. The slope of the apparent terminal phase was estimated by log linear regression using at least 3 data points and the terminal rate constant (λ) was derived from the slope. $AUC_{0-\infty}$ was estimated as the sum of the AUC_{0-t} (where t is the time of the last measurable concentration) and Ct/λ. The apparent terminal half-life ($t_{½}$) was calculated as $0.693/\lambda$.

Kinome screens

Dissociation constants (Kd) were measured at DiscoverX using the KINOME*scan*™ Profiling Service. Kinase inhibition (IC50s) was measured at Reaction Biology using the Kinase Assay service.

Xenografts

NRGS (NOD.Rag$^{-/-}$;yc^{null}; hIL-3, hGM-CSF, hSF) mice were provided by Dr. James Mulloy (Cincinnati Children's Hospital Medical Center, Cincinnati, OH) (*85*). NSGS mice were purchased from the CCHMC Comprehensive Mouse and Cancer Core. For xenotransplantation, MLL-AF9;FLT3-ITD CD34+ cells ($2x10^5$ per mouse) or AML patient cells ($2x10^6$ per mouse) were intravenously injected into the tail veins of NRGS or NSGS animals. Mice were monitored by BM aspirate and physical attributes of disease, such as limb paralysis, fatigue, and rough fur. NCGC-1481 and quizartinib were prepared in DMSO and further dissolved in sterile phosphate buffered saline (PBS). Animals were injected i.p. with 30 mg/kg NCGC-1481 or 15 mg/kg quizartinib 5x

weekly. All mice were bred, housed and handled in the Association for Assessment and Accreditation of Laboratory Animal Care-accredited animal facility of Cincinnati Children's Hospital Medical Center. The study is compliant with all relevant ethical regulations regarding animal research.

Statistical Analysis

The number of animals, cells, and experimental replicates can be found in the figure legends. Differences among multiple groups were assessed by one-way ANOVA followed by Tukey's multiple comparison post test for all possible comparisons. Comparison of two groups was performed using an unpaired Student's *t* test (unpaired, two-tailed) or Mann-Whitney when sample size allowed. Significance was set at $P < 0.05$. Unless otherwise specified, results are depicted as the mean ± SEM. For Kaplan-Meier analysis, Mantel-Cox test was used. Data were analyzed and plotted using GraphPad Prism 7 software.

Acknowledgments

We thank Jeff Bailey and Victoria Summey for assistance with transplantations (Comprehensive Mouse and Cancer Core at CCHMC). We thank the Viral Vector Core and DNA sequencing and Genotyping Core at CCHMC for their assistance. We thank Garrett Rhyasen for his contributions to pilot experiments at the start of this project.

Funding

This work was supported by Cincinnati Children's Hospital Research Foundation, Cancer Free Kids, Leukemia Lymphoma Society, and National Institute of Health (R35HL135787, RO1DK102759, RO1DK113639) grants to D.T.S, and the intramural research programs of the National Center for Advancing Translational Sciences and the National Cancer Institute to C.J.T.. D.T.S. is a Leukemia Lymphoma Society Scholar. K.M. is supported by a National Institute of Health Research Training and Career Development Grant (F31CA217140).

Author Contributions

C.J.T. and D.T.S. conceived and joint-supervised the study. K.M., C.J.T., and D.T.S. conceived the experiments and wrote the manuscript. K.M., L.M.W., L.C.B., M.W., K.W., X.Z., E.O., and K.H. performed experiments and analyzed data related to the in vitro AML studies. M.W., J.C.M., and K.H. performed experiments and analyzed data related to the animal studies. K.C. contributed to the RNA-seq and Pamgene kinase data processing, quality check, expression analysis, and generation of figures and tables. M.W., J-K. J., S.B.H., P.S., performed experiments and analyzed data related to the chemical synthesis of the compounds. A.W. and X.X. performed pharmacokinetic analyses. D.L and J.A. performed experiments and analysis of NCGC-1481/IRAK4 co-crystal structures. G.T. performed analyses of the NCGC-1481/IRAK4 co-crystal structure. J.P.P. provided patient-derived samples and helped interpret data. R.L.L., C.F., and E.B., conducted the gilternitib clinical trial, provided samples, and analyzed data.

Competing interests

C.J.T., K.M., M.W., J-K. J. and D.T.S. are inventors of the following patent: PCT/US2017/047088. D.T.S. has received support from Celegene, and honoraria from Curis Inc. R.L.L. is on the supervisory board of Qiagen and is a scientific advisor to Loxo, Imago, C4 Therapeutics and Isoplexis, which each include an equity interest. He receives research support from and consulted for Celgene and Roche, he has received research support from Prelude Therapeutics, and he has consulted for Incyte, Novartis, Morphosys and Janssen. He has received honoraria from Lilly and Amgen for invited lectures and from Gilead for grant reviews.

Data and materials availability

All data associated with this study are present in the paper or supplementary materials. The RNA-sequencing data discussed in this publication have been deposited in NCBI's Gene Expression Omnibus and are accessible through GEO Series accession number GSE121272. (https://www.ncbi.nlm.nih.gov/geo/query/acc.cgi?acc=GSE121272). NCGC1481 is available upon request from the corresponding authors.

References

1. S. H. Chu, D. Small, Mechanisms of resistance to FLT3 inhibitors. *Drug Resist Updat* **12**, 8-16 (2009).
2. M. Larrosa-Garcia, M. R. Baer, FLT3 Inhibitors in Acute Myeloid Leukemia: Current Status and Future Directions. *Mol Cancer Ther* **16**, 991-1001 (2017).
3. J. Griffith *et al.*, The structural basis for autoinhibition of FLT3 by the juxtamembrane domain. *Mol Cell* **13**, 169-178 (2004).
4. D. G. Gilliland, J. D. Griffin, The roles of FLT3 in hematopoiesis and leukemia. *Blood* **100**, 1532-1542 (2002).
5. T. Grafone, M. Palmisano, C. Nicci, S. Storti, An overview on the role of FLT3-tyrosine kinase receptor in acute myeloid leukemia: biology and treatment. *Oncol Rev* **6**, e8 (2012).
6. H. G. Drexler, H. Quentmeier, FLT3: Receptor and ligand. *Growth Factors* **22**, 71-73 (2004).
7. P. D. Kottaridis *et al.*, The presence of a FLT3 internal tandem duplication in patients with acute myeloid leukemia (AML) adds important prognostic information to cytogenetic risk group and response to the first cycle of chemotherapy: analysis of 854 patients from the United Kingdom Medical Research Council AML 10 and 12 trials. *Blood* **98**, 1752-1759 (2001).
8. C. Thiede *et al.*, Analysis of FLT3-activating mutations in 979 patients with acute myelogenous leukemia: association with FAB subtypes and identification of subgroups with poor prognosis. *Blood* **99**, 4326-4335 (2002).
9. S. P. Whitman *et al.*, Absence of the wild-type allele predicts poor prognosis in adult de novo acute myeloid leukemia with normal cytogenetics and the internal tandem duplication of FLT3: a cancer and leukemia group B study. *Cancer Res* **61**, 7233-7239 (2001).
10. N. Boissel *et al.*, Prognostic significance of FLT3 internal tandem repeat in patients with de novo acute myeloid leukemia treated with reinforced courses of chemotherapy. *Leukemia* **16**, 1699-1704 (2002).
11. J. Cortes *et al.*, Quizartinib, an FLT3 inhibitor, as monotherapy in patients with relapsed or refractory acute myeloid leukaemia: an open-label, multicentre, single-arm, phase 2 trial. *Lancet Oncol* **19**, 889-903 (2018).
12. J. E. Cortes *et al.*, Phase I study of quizartinib administered daily to patients with relapsed or refractory acute myeloid leukemia irrespective of FMS-like tyrosine kinase 3-internal tandem duplication status. *J Clin Oncol* **31**, 3681-3687 (2013).
13. J. E. Cortes *et al.*, Phase 2b study of 2 dosing regimens of quizartinib monotherapy in FLT3-ITD-mutated, relapsed or refractory AML. *Blood* **132**, 598-607 (2018).
14. W. Fiedler *et al.*, A phase I/II study of sunitinib and intensive chemotherapy in patients over 60 years of age with acute myeloid leukaemia and activating FLT3 mutations. *Br J Haematol* **169**, 694-700 (2015).
15. W. Fiedler *et al.*, A phase 1 study of SU11248 in the treatment of patients with refractory or resistant acute myeloid leukemia (AML) or not amenable to conventional therapy for the disease. *Blood* **105**, 986-993 (2005).
16. T. Fischer *et al.*, Phase IIB trial of oral Midostaurin (PKC412), the FMS-like tyrosine kinase 3 receptor (FLT3) and multi-targeted kinase inhibitor, in patients with acute myeloid leukemia and high-risk myelodysplastic syndrome with either wild-type or mutated FLT3. *J Clin Oncol* **28**, 4339-4345 (2010).

17. C. H. Man *et al.*, Sorafenib treatment of FLT3-ITD(+) acute myeloid leukemia: favorable initial outcome and mechanisms of subsequent nonresponsiveness associated with the emergence of a D835 mutation. *Blood* **119**, 5133-5143 (2012).
18. A. E. Perl *et al.*, Selective inhibition of FLT3 by gilteritinib in relapsed or refractory acute myeloid leukaemia: a multicentre, first-in-human, open-label, phase 1-2 study. *Lancet Oncol* **18**, 1061-1075 (2017).
19. R. M. Stone *et al.*, Patients with acute myeloid leukemia and an activating mutation in FLT3 respond to a small-molecule FLT3 tyrosine kinase inhibitor, PKC412. *Blood* **105**, 54-60 (2005).
20. R. M. Stone *et al.*, Midostaurin plus Chemotherapy for Acute Myeloid Leukemia with a FLT3 Mutation. *N Engl J Med* **377**, 454-464 (2017).
21. C. C. Smith *et al.*, Validation of ITD mutations in FLT3 as a therapeutic target in human acute myeloid leukaemia. *Nature* **485**, 260-263 (2012).
22. Y. Alvarado *et al.*, Treatment with FLT3 inhibitor in patients with FLT3-mutated acute myeloid leukemia is associated with development of secondary FLT3-tyrosine kinase domain mutations. *Cancer* **120**, 2142-2149 (2014).
23. C. C. Smith *et al.*, Heterogeneous resistance to quizartinib in acute myeloid leukemia revealed by single-cell analysis. *Blood* **130**, 48-58 (2017).
24. O. Piloto *et al.*, Prolonged exposure to FLT3 inhibitors leads to resistance via activation of parallel signaling pathways. *Blood* **109**, 1643-1652 (2007).
25. E. Siendones *et al.*, Inhibition of Flt3-activating mutations does not prevent constitutive activation of ERK/Akt/STAT pathways in some AML cells: a possible cause for the limited effectiveness of monotherapy with small-molecule inhibitors. *Hematol Oncol* **25**, 30-37 (2007).
26. J. K. Bruner *et al.*, Adaptation to TKI Treatment Reactivates ERK Signaling in Tyrosine Kinase-Driven Leukemias and Other Malignancies. *Cancer Res* **77**, 5554-5563 (2017).
27. S. Chandarlapaty, Negative feedback and adaptive resistance to the targeted therapy of cancer. *Cancer Discov* **2**, 311-319 (2012).
28. J. G. van Oosterwijk *et al.*, Hypoxia-induced upregulation of BMX kinase mediates therapeutic resistance in acute myeloid leukemia. *J Clin Invest* **128**, 369-380 (2018).
29. O. Lindblad *et al.*, Aberrant activation of the PI3K/mTOR pathway promotes resistance to sorafenib in AML. *Oncogene* **35**, 5119-5131 (2016).
30. A. S. Green *et al.*, Pim kinases modulate resistance to FLT3 tyrosine kinase inhibitors in FLT3-ITD acute myeloid leukemia. *Sci Adv* **1**, e1500221 (2015).
31. C. Nishioka *et al.*, Blockade of MEK/ERK signaling enhances sunitinib-induced growth inhibition and apoptosis of leukemia cells possessing activating mutations of the FLT3 gene. *Leuk Res* **32**, 865-872 (2008).
32. W. Zhang *et al.*, The Dual MEK/FLT3 Inhibitor E6201 Exerts Cytotoxic Activity against Acute Myeloid Leukemia Cells Harboring Resistance-Conferring FLT3 Mutations. *Cancer Res* **76**, 1528-1537 (2016).
33. E. Griessinger *et al.*, Preclinical targeting of NF-kappaB and FLT3 pathways in AML cells. *Leukemia* **22**, 1466-1469 (2008).
34. L. P. Jordheim *et al.*, Sensitivity and gene expression profile of fresh human acute myeloid leukemia cells exposed ex vivo to AS602868. *Cancer Chemother Pharmacol* **68**, 97-105 (2011).
35. F. Wang *et al.*, Metformin synergistically sensitizes FLT3-ITD-positive acute myeloid leukemia to sorafenib by promoting mTOR-mediated apoptosis and autophagy. *Leuk Res* **39**, 1421-1427 (2015).
36. K. A. Minson *et al.*, The MERTK/FLT3 inhibitor MRX-2843 overcomes resistance-conferring FLT3 mutations in acute myeloid leukemia. *JCI Insight* **1**, e85630 (2016).

37. K. Keegan *et al.*, Preclinical evaluation of AMG 925, a FLT3/CDK4 dual kinase inhibitor for treating acute myeloid leukemia. *Mol Cancer Ther* **13**, 880-889 (2014).
38. S. Ma *et al.*, SKLB-677, an FLT3 and Wnt/beta-catenin signaling inhibitor, displays potent activity in models of FLT3-driven AML. *Sci Rep* **5**, 15646 (2015).
39. E. A. Nelson *et al.*, The STAT5 Inhibitor Pimozide Displays Efficacy in Models of Acute Myelogenous Leukemia Driven by FLT3 Mutations. *Genes Cancer* **3**, 503-511 (2012).
40. K. Natarajan *et al.*, Pim-1 kinase phosphorylates and stabilizes 130 kDa FLT3 and promotes aberrant STAT5 signaling in acute myeloid leukemia with FLT3 internal tandem duplication. *PLoS One* **8**, e74653 (2013).
41. M. G. Mohi *et al.*, Combination of rapamycin and protein tyrosine kinase (PTK) inhibitors for the treatment of leukemias caused by oncogenic PTKs. *Proc Natl Acad Sci U S A* **101**, 3130-3135 (2004).
42. E. Weisberg *et al.*, Selective Akt inhibitors synergize with tyrosine kinase inhibitors and effectively override stroma-associated cytoprotection of mutant FLT3-positive AML cells. *PLoS One* **8**, e56473 (2013).
43. J. S. Lopez, U. Banerji, Combine and conquer: challenges for targeted therapy combinations in early phase trials. *Nat Rev Clin Oncol* **14**, 57-66 (2017).
44. T. Ueda *et al.*, Expansion of human NOD/SCID-repopulating cells by stem cell factor, Flk2/Flt3 ligand, thrombopoietin, IL-6, and soluble IL-6 receptor. *J Clin Invest* **105**, 1013-1021 (2000).
45. M. Wunderlich, J. C. Mulloy, Model systems for examining effects of leukemia-associated oncogenes in primary human CD34+ cells via retroviral transduction. *Methods Mol Biol* **538**, 263-285 (2009).
46. A. Colmone *et al.*, Leukemic cells create bone marrow niches that disrupt the behavior of normal hematopoietic progenitor cells. *Science* **322**, 1861-1865 (2008).
47. F. Corazza *et al.*, Circulating thrombopoietin as an in vivo growth factor for blast cells in acute myeloid leukemia. *Blood* **107**, 2525-2530 (2006).
48. M. De Waele *et al.*, Growth factor receptor profile of CD34+ cells in AML and B-lineage ALL and in their normal bone marrow counterparts. *Eur J Haematol* **66**, 178-187 (2001).
49. Z. Dong-Feng *et al.*, The TPO/c-MPL pathway in the bone marrow may protect leukemia cells from chemotherapy in AML Patients. *Pathol Oncol Res* **20**, 309-317 (2014).
50. H. G. Drexler, Expression of FLT3 receptor and response to FLT3 ligand by leukemic cells. *Leukemia* **10**, 588-599 (1996).
51. M. Lisovsky *et al.*, Flt3 ligand stimulates proliferation and inhibits apoptosis of acute myeloid leukemia cells: regulation of Bcl-2 and Bax. *Blood* **88**, 3987-3997 (1996).
52. B. Sanchez-Correa *et al.*, Cytokine profiles in acute myeloid leukemia patients at diagnosis: survival is inversely correlated with IL-6 and directly correlated with IL-10 levels. *Cytokine* **61**, 885-891 (2013).
53. M. Tao *et al.*, SCF, IL-1beta, IL-1ra and GM-CSF in the bone marrow and serum of normal individuals and of AML and CML patients. *Cytokine* **12**, 699-707 (2000).
54. C. H. Man *et al.*, A novel tescalcin-sodium/hydrogen exchange axis underlying sorafenib resistance in FLT3-ITD+ AML. *Blood* **123**, 2530-2539 (2014).
55. C. C. Smith *et al.*, Activity of ponatinib against clinically-relevant AC220-resistant kinase domain mutants of FLT3-ITD. *Blood* **121**, 3165-3171 (2013).
56. W. Zhang *et al.*, Reversal of acquired drug resistance in FLT3-mutated acute myeloid leukemia cells via distinct drug combination strategies. *Clin Cancer Res* **20**, 2363-2374 (2014).
57. A. L. Boyd *et al.*, Identification of Chemotherapy-Induced Leukemic-Regenerating Cells Reveals a Transient Vulnerability of Human AML Recurrence. *Cancer Cell* **34**, 483-498 e485 (2018).
58. S. Akira, K. Takeda, Toll-like receptor signalling. *Nat Rev Immunol* **4**, 499-511 (2004).

59. L. J. Beverly, D. T. Starczynowski, IRAK1: oncotarget in MDS and AML. *Oncotarget* **5**, 1699-1700 (2014).
60. J. Brown, H. Wang, G. N. Hajishengallis, M. Martin, TLR-signaling networks: an integration of adaptor molecules, kinases, and cross-talk. *J Dent Res* **90**, 417-427 (2011).
61. D. Chaudhary, S. Robinson, D. L. Romero, Recent advances in the discovery of small molecule inhibitors of interleukin-1 receptor-associated kinase 4 (IRAK4) as a therapeutic target for inflammation and oncology disorders. *J Med Chem* **58**, 96-110 (2015).
62. C. Dussiau *et al.*, Targeting IRAK1 in T-cell acute lymphoblastic leukemia. *Oncotarget* **6**, 18956-18965 (2015).
63. S. Flannery, A. G. Bowie, The interleukin-1 receptor-associated kinases: critical regulators of innate immune signalling. *Biochem Pharmacol* **80**, 1981-1991 (2010).
64. M. M. Hosseini *et al.*, Inhibition of interleukin-1 receptor-associated kinase-1 is a therapeutic strategy for acute myeloid leukemia subtypes. *Leukemia*, (2018).
65. S. Janssens, R. Beyaert, Functional diversity and regulation of different interleukin-1 receptor-associated kinase (IRAK) family members. *Mol Cell* **11**, 293-302 (2003).
66. Z. Li *et al.*, Inhibition of IRAK1/4 sensitizes T cell acute lymphoblastic leukemia to chemotherapies. *J Clin Invest* **125**, 1081-1097 (2015).
67. E. M. Moresco, D. LaVine, B. Beutler, Toll-like receptors. *Curr Biol* **21**, R488-493 (2011).
68. M. C. Patra, S. Choi, Recent Progress in the Molecular Recognition and Therapeutic Importance of Interleukin-1 Receptor-Associated Kinase 4. *Molecules* **21**, (2016).
69. G. W. Rhyasen *et al.*, Targeting IRAK1 as a therapeutic approach for myelodysplastic syndrome. *Cancer Cell* **24**, 90-104 (2013).
70. S. E. Ewald *et al.*, The ectodomain of Toll-like receptor 9 is cleaved to generate a functional receptor. *Nature* **456**, 658-662 (2008).
71. T. Guerrier *et al.*, TLR9 expressed on plasma membrane acts as a negative regulator of human B cell response. *J Autoimmun* **51**, 23-29 (2014).
72. J. P. Powers *et al.*, Discovery and initial SAR of inhibitors of interleukin-1 receptor-associated kinase-4. *Bioorg Med Chem Lett* **16**, 2842-2845 (2006).
73. J. W. Singer *et al.*, Inhibition of interleukin-1 receptor-associated kinase 1 (IRAK1) as a therapeutic strategy. *Oncotarget* **9**, 33416-33439 (2018).
74. G. M. Buckley *et al.*, IRAK-4 inhibitors. Part III: a series of imidazo[1,2-a]pyridines. *Bioorg Med Chem Lett* **18**, 3656-3660 (2008).
75. L. M. Graves, D. W. Litchfield, "Going KiNativ": probing the Native Kinome. *Chem Biol* **18**, 683-684 (2011).
76. M. Wunderlich *et al.*, AML xenograft efficiency is significantly improved in NOD/SCID-IL2RG mice constitutively expressing human SCF, GM-CSF and IL-3. *Leukemia* **24**, 1785-1788 (2010).
77. M. Wunderlich *et al.*, AML cells are differentially sensitive to chemotherapy treatment in a human xenograft model. *Blood* **121**, e90-97 (2013).
78. J. Zhang, L. Li, A. Friedman, D. Small, I. Paz-Priel, Canonical NF-kB Signalling Is a Potential Target in FLT3/ITD AML. *Blood* **120**, 2447 (2012).
79. S. Muralidharan, P. Mandrekar, Cellular stress response and innate immune signaling: integrating pathways in host defense and inflammation. *J Leukoc Biol* **94**, 1167-1184 (2013).
80. M. A. Gregory *et al.*, ATM/G6PD-driven redox metabolism promotes FLT3 inhibitor resistance in acute myeloid leukemia. *Proc Natl Acad Sci U S A* **113**, E6669-E6678 (2016).
81. A. Huang *et al.*, Metabolic alterations and drug sensitivity of tyrosine kinase inhibitor resistant leukemia cells with a FLT3/ITD mutation. *Cancer Lett* **377**, 149-157 (2016).

82. K. J. Ishii, S. Akira, Innate immune recognition of, and regulation by, DNA. *Trends Immunol* **27**, 525-532 (2006).
83. S. Janssens, B. Pulendran, B. N. Lambrecht, Emerging functions of the unfolded protein response in immunity. *Nat Immunol* **15**, 910-919 (2014).
84. M. Levis *et al.*, A FLT3-targeted tyrosine kinase inhibitor is cytotoxic to leukemia cells in vitro and in vivo. *Blood* **99**, 3885-3891 (2002).
85. D. Menendez *et al.*, The Toll-like receptor gene family is integrated into human DNA damage and p53 networks. *PLoS Genet* **7**, e1001360 (2011).
86. L. Schaefer, Complexity of danger: the diverse nature of damage-associated molecular patterns. *J Biol Chem* **289**, 35237-35245 (2014).
87. P. P. Zarrinkar *et al.*, AC220 is a uniquely potent and selective inhibitor of FLT3 for the treatment of acute myeloid leukemia (AML). *Blood* **114**, 2984-2992 (2009).
88. A. Wang *et al.*, Dual inhibition of AKT/FLT3-ITD by A674563 overcomes FLT3 ligand-induced drug resistance in FLT3-ITD positive AML. *Oncotarget* **7**, 29131-29142 (2016).
89. P. N. Kelly *et al.*, Selective interleukin-1 receptor-associated kinase 4 inhibitors for the treatment of autoimmune disorders and lymphoid malignancy. *J Exp Med* **212**, 2189-2201 (2015).
90. M. A. Smith *et al.*, U2AF1 mutations induce oncogenic IRAK4 isoforms and activate innate immune pathways in myeloid malignancies. *Nat Cell Biol* **21**, 640-650 (2019).
91. J. Fang *et al.*, Cytotoxic effects of bortezomib in myelodysplastic syndrome/acute myeloid leukemia depend on autophagy-mediated lysosomal degradation of TRAF6 and repression of PSMA1. *Blood* **120**, 858-867 (2012).
92. S. Goyama, M. Wunderlich, J. C. Mulloy, Xenograft models for normal and malignant stem cells. *Blood* **125**, 2630-2640 (2015).

Chapter 4: Discussion, Implications, and Future Directions

Summary

Development of targeted therapies presents an attractive treatment strategy in AML to overcome the high rate of relapse and adverse events associated with chemotherapy and radiation. However, it is often difficult find a selective target for AML cells that spares healthy hematopoietic cells and also is amenable to small-molecule inhibition. With the high incidence of FLT3 mutations in AML as well as being a druggable tyrosine kinase, FLT3 is a prime candidate for targeted inhibition. Indeed, many FLT3 inhibitors have been developed in the last decade and two, midostaurin and gilteritinib, have been recently FDA approved in AML. Although these compounds have been able to extend survival for a few months, which is certainly a meaningful amount of time for a patient and their family, FLT3 inhibition has not proven to be a curative therapy. A variety of resistance mechanisms have been identified that contribute to relapse, the most common being acquired TK mutations and activation of parallel signaling pathways (adaptive resistance). Several candidates for players in adaptive resistance have been suggested, such as PI3K signaling and MAPK signaling; however, although these pathways are downstream of FLT3, they can also be activated by many other receptors and a broader look a what other upstream signaling changes occur in FLT3-inhibitor-treated cells has not been published. In Chapter 2, we showed, using RNA-sequencing and kinome profiling, that innate immune pathways were upregulated upon FLT3-inhibitor treatment. Furthermore, we showed that targeting innate immune signaling through genetic or pharmacologic inhibition of IRAK1/4 sensitized cells to FLT3-inhibition and reduced capacity for resistance. These results led to the development of a novel series of FLT3-IRAK1/4 inhibitors, with lead compound NCGC1481. In Chapter 3, we showed that although these compounds are able to inhibit multiple kinases, SAR analysis revealed that IRAK1/4 inhibition was correlated with cytotoxicity in FLT3-mutant cell lines. Furthermore, we showed that NCGC1481 prevented the upregulation of innate immune

pathways seen with FLT3 inhibitors. Importantly, NCGC1481 was well tolerated by mice and had minimal effects in vitro on normal human hematopoietic cells suggesting that NCGC1481 has potential for a therapeutic window in humans. Additionally, NCGC1481 reduced survival in quizartinib-resistant cell lines and patient samples in vitro and significantly extended survival in mouse xenografts of AML patient samples. Taken together, these data support the hypothesis that innate immune signaling provides an adaptive resistance mechanism to FLT3-inhibition in AML and that our FLT3-IRAK1/4 inhibitor, NCGC1481, represents a novel class of inhibitors that has the potential to make a significant impact in the treatment of FLT3-mutant AML.

Polypharmacology

There is an ongoing effort to make drugs that are more and more selective in order to mitigate off-target effects and toxicity. However, there can also be value in embracing pharmacologic promiscuity. Often, cancers harbor more than one driving mutation and they also have the potential to activate resistance mechanisms as discussed earlier. Therefore, the ability to target more than one pathway would be a useful strategy in overcoming resistance. Inhibiting multiple pathways through the combination of selective inhibitors is one way to approach this. A few drug “cocktails” have been approved for use and have shown promising results *(1)*. However, there are many disadvantages in using multiple compounds such as increased costs, the potential for drug-drug interactions, and the combination and potential amplification of toxicity. There is also the issue of optimizing timing and doses of multiple drugs to make sure that each drug gets to the appropriate tissue at the right time. Furthermore, there is the added obstacle of decreased patient compliance when treatment schedules get too complicated.

These issues can be alleviated by polypharmacology, i.e. using a single compound to hit multiple targets. So far, there are few rationally designed polypharmacologic inhibitors; what is more common is repurposing “off-target” effects of already published inhibitors. One example of this is midostaurin. As discussed earlier, midostaurin was recently approved as a FLT3-inhibitor

in FLT3-mutant AML. However, midostaurin was originally developed as a protein kinase C (PKC) inhibitor and was also found to inhibit a wide range of other kinases such as vascular endothelial growth factor (VEGF) and KIT. Midostaurin's ability to inhibit multiple kinases likely contributes to its efficacy in FLT3-mutant AML. Additionally, the FLT3-inhibitor gilteritinib can also inhibit AXL which has been implicated as a driver in AML as well as FLT3-inhibitor resistance *(2, 3)*. Like midostaurin, gilteritinib's affinity for multiple key kinases likely contribute to its clinical efficacy and recent FDA approval.

Of course, polypharmacology is not without its limitations. It may be physically or chemically impossible to hit certain targets with a single compound. Alternatively, it may be impossible to hit a target-of-interest without also hitting a homologous protein that would be detrimental to inhibit. Additionally, with the complexity of cancer genetics, using multiple selective agents allows physicians to "mix-and-match" based on a patient's individual genetic profile rather than depending on finding a single drug that fits the patient's individual needs. Despite these limitations, further investigation of potential new polypharmacologic targets presents an exciting prospect for future cancer therapy.

Our novel FLT3-IRAK1/4 inhibitor, NCGC1481 takes advantage of these principles of polypharmacology to inhibit both a driver of AML (FLT3) as well as a resistance mechanism (innate immune signaling) to provide a novel strategy for overcoming inhibitor resistance.

Future directions

One question that begs to be answered is why does FLT3 inhibition cause increased innate immune signaling? We posit in the end of Chapter 2 that the innate immune response may be activated as a result of cellular stress. TLRs and inflammatory cytokines were shown to have increased gene expression in our RNA-seq analysis of FLT3-inhibitor-treated cells. One hypothesis is that FLT3-inhibition causes intrinsic cell stress, in addition to cell death of sensitive

cells, which results in release of inflammatory cytokines and TLR ligands. These then can induce innate immune activation through paracrine and/or autocrine signaling.

This hypothesis also opens up the possibility of innate immune signaling playing a role in resistance to other anti-cancer agents and other cancers beyond AML or hematopoietic malignancies. A handful of studies have shown that IRAK1 and/or IRAK4 have increased expression in a variety other cancers, including breast, head and neck, and pancreatic cancer *(4–6)*. Furthermore, IRAK1/4 activity has been shown to play a role in chemoresistance or radioresistance in some cancers. Zhang et al (2017) found that in pancreatic ductal carcinoma patient samples, increased phosphorylation of IRAK4 was correlated with poorer response to chemotherapy and worse overall survival *(6)*. Furthermore, they showed that genetic or pharmacologic inhibition of IRAK4 sensitized the cells to chemotherapy in vitro, suggesting that innate immune signaling may play a role in chemoresistance. Most of these studies have looked at baseline IRAK1/4 activity rather than induction of innate of signaling after exposure to therapy. Interestingly, Wee et al (2015) found that IRAK1 phosphorylation was induced by paclitaxel treatment in breast cancer cells and that IRAK1 inhibition sensitized the cells to paclitaxel *(4)*. Additionally, a recent paper found that radiation induced IRAK1 signaling in a zebrafish tumor model *(7)*. These studies echo our findings in which baseline innate immune signaling is somewhat dispensable, i.e. the cancer cells are not sensitive to IRAK1/4 inhibition alone, but this pathway becomes crucial for survival upon cell stress. One potential implication for these findings is the widespread use of IRAK1/4 inhibitors in combination with chemotherapy or targeted agents in potentially any cancer. Inhibiting innate immune signaling could become the next broadly used treatment strategy in cancer.

References

1. B. Al-Lazikani, U. Banerji, P. Workman, Combinatorial drug therapy for cancer in the post-genomic era, *Nat. Biotechnol.* **30**, 679–692 (2012).
2. M. Mori, N. Kaneko, Y. Ueno, M. Yamada, R. Tanaka, R. Saito, I. Shimada, K. Mori, S. Kuromitsu, Gilteritinib, a FLT3/AXL inhibitor, shows antileukemic activity in mouse models of FLT3 mutated acute myeloid leukemia, *Invest. New Drugs* **35**, 556–565 (2017).
3. I. K. Park, B. Mundy-Bosse, S. P. Whitman, X. Zhang, S. L. Warner, D. J. Bearss, W. Blum, G. Marcucci, M. A. Caligiuri, Receptor tyrosine kinase Axl is required for resistance of leukemic cells to FLT3-targeted therapy in acute myeloid leukemia, *Leukemia* **29**, 2382–2389 (2015).
4. Z. N. Wee, S. M. J. M. Yatim, V. K. Kohlbauer, M. Feng, J. Y. Goh, B. Yi, P. L. Lee, S. Zhang, P. P. Wang, E. Lim, W. L. Tam, Y. Cai, H. J. Ditzel, D. S. B. Hoon, E. Y. Tan, Q. Yu, IRAK1 is a therapeutic target that drives breast cancer metastasis and resistance to paclitaxel, *Nat. Commun.* **6**, 1–15 (2015).
5. A. K. Adams, L. C. Bolanos, P. J. Dexheimer, R. A. Karns, B. J. Aronow, K. Komurov, A. G. Jegga, K. A. Casper, Y. J. Patil, K. M. Wilson, D. T. Starczynowski, S. I. Wells, IRAK1 is a novel DEK transcriptional target and is essential for head and neck cancer cell survival, *Oncotarget* **6**, 43395–43407 (2015).
6. D. Zhang, L. Li, H. Jiang, B. L. Knolhoff, A. C. Lockhart, A. Wang-Gillam, D. G. DeNardo, M. B. Ruzinova, K. H. Lim, Constitutive IRAK4 activation underlies poor prognosis and chemoresistance in pancreatic ductal adenocarcinoma, *Clin. Cancer Res.* **23**, 1748–1759 (2017).
7. P. H. Liu, R. B. Shah, Y. Li, A. Arora, P. M. U. Ung, R. Raman, A. Gorbatenko, S. Kozono, X. Z. Zhou, V. Brechin, J. M. Barbaro, R. Thompson, R. M. White, J. A. Aguirre-Ghiso, J. V. Heymach, K. P. Lu, J. M. Silva, K. S. Panageas, A. Schlessinger, R. G. Maki, H. D. Skinner, E. de Stanchina, S. Sidi, An IRAK1–PIN1 signalling axis drives intrinsic tumour resistance to radiation therapy, *Nat. Cell Biol.* **21**, 203–213 (2019).